Flood Damage Assessment: A Case Study in Bakan and Phnom Kravanh Districts, Pursat Province, Cambodia

Mr. Chhunleang Rorm

A Thesis Submitted in Partial Fulfillment of the Requirements
for the Degree of Master of Engineering in Water Resources Engineering
Department of Water Resources Engineering
Faculty of Engineering
Chulalongkorn University
Academic Year 2018

การประเมินความเสียหายจากน้ำท่วม, กรณีศึกษาในเขต Bakan และ Phnom Kravanh จังหวัด Pursat, ประเทศกัมพูชา

นายชุนเลียง รอม

วิทยานิพนธ์นี้เป็นส่วนหนึ่งของการศึกษาตามหลักสูตรปริญญาวิศวกรรมศาสตรมหาบัณฑิต
สาขาวิชาวิศวกรรมแหล่งน้ำ ภาควิชาวิศวกรรมแหล่งน้ำ
คณะวิศวกรรมศาสตร์ จุฬาลงกรณ์มหาวิทยาลัย
ปีการศึกษา 2561

Thesis Title	Flood Damage Assessment: A Case Study in Bakan and Phnom Kravanh Districts, Pursat Province, Cambodia
By	Mr. Chhunleang Rorm
Field of Study	Water Resources Engineering
Thesis Advisor	Dr. PONGSAK SUTTINON
Thesis Co Advisor	Dr. Sokchhay Heng

Accepted by the Faculty of Engineering, Chulalongkorn University in Partial Fulfillment of the Requirement for the Master of Engineering

.... Dean of the Faculty of Engineering
(Associate Professor SUPOT TEACHAVORASINSKUN, D.Eng.)

THESIS COMMITTEE

.... Chairman
(Assistant Professor Anurak Sriariyawat, Ph.D.)

.... Thesis Advisor
(Dr. PONGSAK SUTTINON)

.... Thesis Co-Advisor
(Dr. Sokchhay Heng)

.... Examiner
(Associate Professor TUANTAN KITPAISALSAKUL, D.Eng.)

.... External Examiner
(Assistant Professor Nattapong Puttanapong, Ph.D.)

ชุนเลียง รอม : การประเมินความเสียหายจากน้ำท่วม, กรณีศึกษาในเขต Bakan และ Phnom Kravanh จังหวัด Pursat, ประเทศกัมพูชา. (Flood Damage Assessment: A Case Study in Bakan and Phnom Kravanh Districts, Pursat Province, Cambodia) อ.ที่ปรึกษาหลัก : อ.ดร.พงษ์ศักดิ์ สุทธินนท์, อ.ที่ปรึกษาร่วม : อ.ดร.ซกเชย์ เฮง

อุทกภัยเป็นภัยธรรมชาติหลักของจังหวัดปูสาท (Pursat) ซึ่งเป็นแหล่งเกษตรกรรมที่สำคัญของประเทศกัมพูชา นอกจากนี้อุทกภัยยังส่งผลกระทบต่อปัญหาด้านสังคม เช่น ความยากจน ความไม่มั่นคงด้านอาหาร และปัญหาด้านสุขภาพ ซึ่งจะส่งผลกระทบทางอ้อมต่อเศรษฐกิจของประเทศ จากปัญหาดังกล่าวการประเมินความเสียหายจากอุทกภัยจึงเป็นขั้นตอนเบื้องต้นที่สำคัญเพื่อที่จะเสนอมาตรการในการลดความเสียหายจากอุทกภัยที่เหมาะสม

วัตถุประสงค์ของการวิจัยนี้คือ (1) เพื่อประเมินความเสียหายจากอุทกภัยในภาคเกษตรและภาคประชาชนที่ได้รับผลกระทบในอำเภอบากาน (Bakan) และอำเภอพนมกาวาย (Phnom Kravanh) ในจังหวัดปูสาทช่วงปี ค.ศ. 2000 ถึง 2014 (2) เพื่อสร้างกราฟความน่าจะเป็นของความเสียหายจากอุทกภัยในปี ค.ศ. 2014 และ (3) เพื่อประเมินความเสียหายจากอุทกภัยภายใต้การพัฒนาเศรษฐกิจและสังคมในอนาคตในปี ค.ศ. 2030 และ 2050 การศึกษาครั้งนี้ถูกแบ่งออกเป็นสามส่วน คือ (1) การประเมินความเสียหายจากอุทกภัยโดยใช้ภาพถ่ายทางอากาศจาก Google Earth Engine (2) การวิเคราะห์ทางอุทกศาสตร์และเศรษฐศาสตร์ และ (3) แผนการบรรเทาน้ำท่วม

ผลการศึกษาสามารถแสดงความสัมพันธ์ระหว่างอัตราการไหลสูงสุดรายเดือนและขอบเขตน้ำท่วมสูงสุดรายเดือน (R^2 = 0.59) ในอำเภอบากานและอำเภอพนมกาวายในจังหวัดปูสาทช่วงปี ค.ศ. 2000 ถึง 2014 โดยค่าความเสียหายเฉลี่ยรายปีในทุกภาคส่วนในปี ค.ศ. 2014 เท่ากับ 1.66 ล้านดอลลาร์สหรัฐ (USD) โดยแบ่งเป็นความเสียหายภาคเกษตรร้อยละ 90 และความเสียหายภาคประชาชนในพื้นที่ที่ได้รับผลกระทบโดยเฉพาะในชนบทอีกร้อยละ 10 ค่าความเสียหายเฉลี่ยรายปีในทุกภาคส่วนใน ปี ค.ศ. 2030 และ 2050 คือ 3.55 และ 8.99 ล้านดอลลาร์สหรัฐ (USD) ตามลำดับ อย่างไรก็ตามหากมีการใช้มาตรการบรรเทาอุทกภัยแล้วจะสามารถลดความเสียหายได้ถึงร้อยละ 36 จากผลการศึกษานี้ผู้กำหนดนโยบายสามารถใช้ข้อมูลดังกล่าวในการสนับสนุนการตัดสินใจนโยบายภาครัฐสำหรับแผนการบรรเทาอุทกภัยเพื่อที่จะลดความเสียหายในอนาคต

สาขาวิชา	วิศวกรรมแหล่งน้ำ	ลายมือชื่อนิสิต ....
ปีการศึกษา	2561	ลายมือชื่อ อ.ที่ปรึกษาหลัก ....
		ลายมือชื่อ อ.ที่ปรึกษาร่วม ....

6070404021 : MAJOR WATER RESOURCES ENGINEERING
KEYWORD: Flood Damage Assessment, Google Earth Engine, Pursat Province, Cambodia

Chhunleang Rorm : Flood Damage Assessment: A Case Study in Bakan and Phnom Kravanh Districts, Pursat Province, Cambodia. Advisor: Dr. PONGSAK SUTTINON Co-advisor: Dr. Sokchhay Heng

Flood is still a major climate hazard in Pursat province, a potential province for agricultural development in Cambodia. The consequences of this water-related disaster are social problems such as poverty, food insecurity and health problems, which indirectly prolong the growth of the country's economy. To propose a proper flood mitigation measure, flood damage assessment is considered as a fundamental step to implement so that the value of elements at risk is initially evaluated. The objectives of this research are to assess flood damage in agriculture and affected people in Bakan and Phnom Kravanh districts, Pursat province from 2000 to 2014, to develop flood damage probability curve in 2014 and to estimate potential flood damage in 2030 and 2050 associated with socio-economic development. The study is divided into three parts 1) flood damage assessment using satellite datasets in Google Earth Engine (GEE); 2) hydrological and economic analysis; and 3) flood mitigation plans. The study shows a better correlation between maximum monthly observed discharge and maximum monthly water extent from GEE ($R^2 = 0.59$) in Bakan and Phnom Kravanh districts from 2000 to 2014. The annual average damage in all sectors in 2014 is estimated to be 1.66 million USD in which around 90% is in Agriculture and 10% is on the affected people meaning that the affected area is in the rural area. The annual average damage in all sectors in 2030 and 2050 in the second scenario is estimated to be 3.55 and 8.99 million USD respectively, while the proposed mitigation plan can reduce around 36% of the total damages in both years. This result can be used as the basic information to support the government policy in the future regarding the mitigation plans to reduce flood damages.

Field of Study:	Water Resources Engineering	Student's Signature ....
Academic Year:	2018	Advisor's Signature ....
		Co-advisor's Signature ....

ACKNOWLEDGEMENTS

First of all, I would like to express my sincere gratitude to my advisor Dr. Pongsak Suttinon for his support, patience, motivation, enthusiasm, and immense knowledge and advice during my master study and research in Chulalongkorn University.

Besides, I would like to thank my thesis co-advisor Dr. Sokchhay Heng for his continuous support and encouragement since my undergraduate study in Cambodia until my master degree in Thailand.

I would like to thank my thesis external examiner Asst. Prof. Dr. Nattapong Puttanapong for his constructive and innovative idea to improve this research since the beginning of my work. Moreover, I would like to thank the chairman of my thesis committee Asst. Prof. Dr. Anurak Sriariyawat and internal examiner Assoc. Prof. Dr. Tuantan Kitpaisalsakul for their encouragement, and constructive comments.

I would like to thank Chulalongkorn University for providing me a great opportunity and support during my master degree through the Scholarship Program for ASEAN Countries. Furthermore, I would like to thank all lecturers and staffs in the Department of Water Resources Engineering for their wonderful lectures and their assistance and helpfulness.

Last, I also would like to express high gratitude to the Community Based Disaster Risk Management (CBDRM) and Farmer Water Users Community (FWUC) Project of which some socio-economic development data were extracted for the analysis in this study.

Chhunleang Rorm

TABLE OF CONTENTS

Page

LIST OF TABLES

Page

LIST OF FIGURES

Page

CHAPTER 1
INTRODUCTION

1.1 Background

Cambodia successfully overcame the low-income country trap to be a lower middle-income country in 2014 due to the increase of real national Growth Domestic Product (GDP) around 7% every year within the last two decades with GDP per capita about 1580 USD in 2018 (RGC 2014). In 2017, three main sectors that led the country economy were service (39.67%), industry (30.88%) and agriculture (23.38%). Even though agriculture now shares the small portion of country GDP, still this sector provides a lot of works for Cambodian people since 78% of the Cambodian people resides in the rural areas, and around 45% of the total labor force directly engaged in the agricultural sector, implying that The Royal Government of Cambodia (RGC) needs to make a good strategic management plan in this sector in order to lift the country out of poverty. In 2015, the Cambodian government set a goal of exporting one million tons of milled rice to the international market in the purpose of enhancing this sector to be more productive as well as creating more jobs for Cambodia farmers; however, the actual exports totaled only at 538,396 tons. In 2016, 542,144 tons of milled rice was exported, showing that yet the target has not been reached. The challenges in this aspect have been raised up, for instance, water supply for agriculture-related with water and disaster management, agricultural machinery, farm technics, packaging, and international market penetration.

In terms of water and disaster management, the RGC agencies, especially the Ministry of Water Resources and Meteorology (MOWRAM) has been trying to enlarge arable land by providing irrigation system in the rural area. Within the last decade, around 200,000 hectares of arable have been increased from 4.8 in 2014 to 5.6 million hectares in 2018 (RGC 2014). However, climate hazards, especially floods and drought, frequently happen almost every part of the country making the crop productivity low both quantity and quality. For flood, not only agriculture but also housing, and infrastructure, are considered as elements at risk once this kind of climate hazard occurred. According to the National Committee for Disaster

Management (NCDM) flood have destroyed assets and livelihoods in many provinces every year. This situation tended to push people into poverty due to the direct and cascade effects of flood and flash flood.

Pursat Province, the potential province for agricultural development, is prone to natural disasters, including floods, drought, and typhoon. Almost every year during the monsoon season, flooding and flash floods cause significant damages and losses to lives, injury, loss of livestock, and damages to housing, crop and community infrastructures. The most vulnerable group during the disaster occurrence includes the poor, women-headed households, children, old people, and the disables. Remarkable flood damages in the province were in 1996, 2000, 2011 and 2013, which normally shoved the locale people into poverty, food insecurity and health problems. Moreover, flood recovery, for a developing country like Cambodia, always takes time and good budget allocation, which directly or indirectly prolongs the growth of the country economy.

On the other hand, the RGC plans to develop Cambodia to be an upper-middle-income country in 2030 and a high-income country in 2050. In order to reach this target, many strategic plans have been set up including the disaster management plan both national and local level to help to improve the quality of life of local people to be resilient with the flood as well as other disasters. To implement this strategic plan, flood damage assessment is a very essential step for flood risk management (Merz, Hall et al. 2010). Flood damage assessment is not the desired end goal; however, it is conducted because of the need to obtain a disaster risk profile of the community and based on this, formulate and implement a proper-disaster preparedness and mitigation plan for the community (Moser 1994).

To assess flood damages, the reliable and long-term ground observation data (empirical database) is normally considered as an important initial input for analysis. However, this requirement is not applicable in some parts of the developing countries such as Cambodia due to the low quality of flood damage records and the limitation of the number of meteorological and hydrological stations in operation and the assessable land at the upper parts of the river basins. In this aspect, remote-sensing data have been recently used to support the methodological framework such as satellite rainfall data or satellite image of flood extent.

Since Google Earth Engine (GEE), a cloud-based geospatial processing platform, was launched, many datasets were derived and made them available on the Google Earth Engine server (Gorelick, Hancher et al. 2017). Global Surface Water (GSW) is one of those available datasets that provides better understanding on long-term change of global surface water with high resolution (Pekel, Cottam et al. 2016). According to the possibilities provided by Google Earth Engine, flood inundation map can be developed in Earth Engine server by using global surface water dataset with some Earth Engine APIs.

1.2 Statement of Problem

As indicated that flooding and flash floods have annually affected and devastated agricultural productivity, housing, and infrastructure in rural areas, the methodological framework as developed in this research is served as a guideline to assess flood damages in Bakan and Phnom Kravanh districts, Pursat province. The following questions will be worked out:

1) Can Google Earth Engine be used to identify flood and its impacts?
2) What is the relationship between water-related disaster and socio-economic development?
3) What is the potential damage if the same flood happens at the same location, where the socio-economic has been improved?

The rationale to develop the methodological framework comes from 3 main reasons:

1) The constrains of the boundary condition especially the unavailability of data at the upstream part of the catchment makes it difficult for using hydrodynamic model to assess flood characteristics in the study area.
2) Flood damages are obvious. It is still an issue obstructing the growth of the country’s economy, especially in the countryside.
3) There is no combination methodological framework between flood damages and socio-economic development to make better understand on the effect of flood on economic development in the future.

1.3 Objective

The three main objectives of this research are:

1) To assess the actual flood damages to Agriculture and Affected people from 2000 to 2014 by using Google Earth Engine.
2) To develop flood damage probability curve between 2000 and 2014 in each sector.
3) To estimate potential flood damages in 2030 and 2050 associated with socio-economic development including mitigation plan.

1.4 Scopes and Limitations

In order to implement this methodological framework, this research tries to use both quantitative and qualitative types of research in the sense that quantitative research facilitates qualitative research in terms of understanding of fundamental facts, opinions, and inspiration from local people through answers from questionnaire survey in the study area. However, there are still some scopes and limitations in the study as below:

1.4.1 Scopes

1) In this study, flood damage is assessed only in Bakan and Phnom Kravanh districts, Pursat province, Cambodia.
2) Only direct and indirect tangible flood damages, specifically agriculture and affected people are assessed, where the majority of the physical flood damages consists.
3) Year 2030 and year 2050 are the events in the future due to the strategic development plan of the Royal Government of Cambodia (RGC).
4) There are three main sources of flood in Bakan and Phnom Kravanh districts, which are the upstream flow, rainfall in the Pursat River Basin and back water effect from the Tonle Sap Lake; however, in this study only flood caused by the upstream flow represented by the recorded flow at Bak Trakoun flow station is taken into account due to the limitation of data.

1.4.2 Limitations

1) The actual flood damage assessment is considered between 2000 and 2014 due to the available flood extent map in GEE.
2) No climate change scenarios are adopted; this is because the impact of climate change on flood intensity is still uncertain (Vu and Ranzi 2017).
3) Flow data at Bak Trakoun flow station from 1994 to 2018 is used for flood frequency analysis.
4) The affected area of NDVI in agriculture by flood is considered as damage area in Agriculture.
5) The average value of the price of rice and cassava from 2016 to 2019 applied to the case study between 2000 and 2014.
6) The national growth rate and national GDP per capita in 2030 and 2050 are applied for Bakan and Phnom Kravanh districts in the assumption that the growth rate and the GDP per capita is well-distributed over the country.
7) The interruption of business activities by flood to the people is considered to be one month based on the experience of previous floods.

1.5 Research Procedure

The overall methodological framework in this research indicated in Figure 1.1 consists of four main steps:

1) Data collection and analysis
2) Flood damage assessment using GEE
3) Flood damage analysis: 2000 to 2014 (Real data)
4) Flood damage estimation and mitigation plan: 2030 and 2050 (Project life)

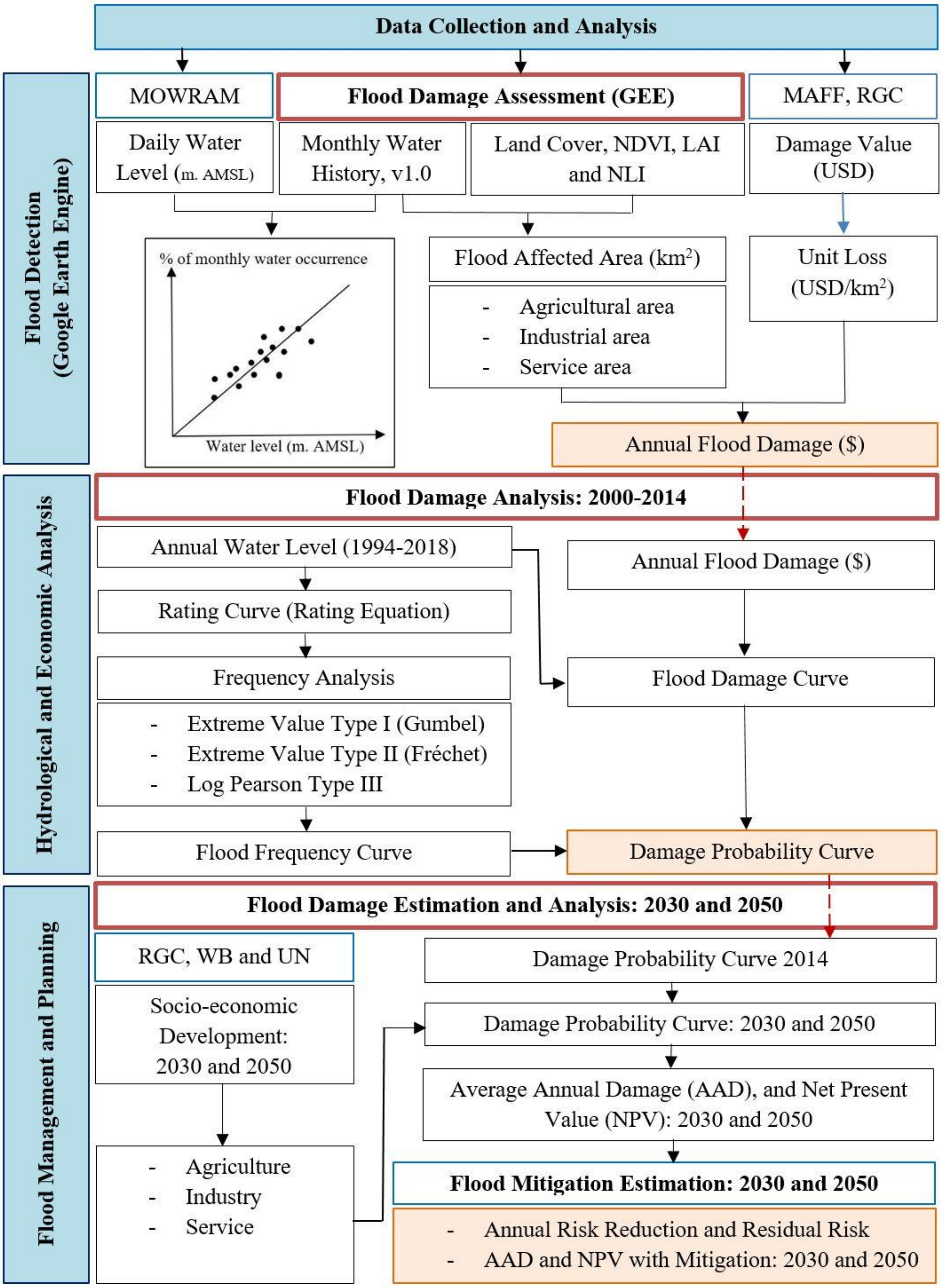

Figure 1.1: Methodological framework of the research

1.5.1 Data Collection and Analysis:

All data used in this study are collected from some important sources as shown in Table 1-1.

Table 1-1: Data collection

N	Name of Data	Availability				Period	Source
		Daily	**Weekly**	**Monthly**	**Annually**		
1	HVCA (Survey in Pursat Province)					2016	MOWRAM
2	Water Level/Discharge	√				1994 - 2018	MOWRAM
3	Monthly Water History, v1.0			√		1984 - 2015	Google Earth Engine
4	Land Cover Type				√	1987 - Present	Land Cover Portal (GEE)
5	Normalized Different Vegetation Index		√			2000 - Present	Google Earth Engine
6	Night Time Light Index				√	1992 - Present	Google Earth Engine
7	Leaf Area Index	4 days				2002 - Present	Google Earth Engine
8	Socio-Economic Development				√	2000 - Present	RGC, ADB, World Bank, UN
9	Crop yield and price			√	√		MAFF, Ricepedia

1.5.2 Flood Damage Assessment using Google Earth Engine:

Flood damage assessment using Google Earth Engine is shown in the first part of Figure 1.1, which is flood detection using Google Earth Engine. The detail of the process is indicated as below:

- The dry and wet months in each year are differentiated based on monthly water level in Bak Trakoun hydrological station.
- Water extent in Bakan and Phnom Kravanh districts in each wet month is captured by Monthly Water History, v1.0 by using Google Earth Engine.
- The relationship between water level of wet months and monthly water occurrence of Monthly Water History, v1.0 is also derived.
- According to the Ministry of Water Resources and Meteorology (MOWRAM), the threshold discharge at Bak Trakoun flow station considered to be warned for flood preparation and mitigation is 800 m^3/s. Hence, flood year is the year existing the annual maximum discharge equal or greater than 800 m^3/s.
- By overlapping MCD12Q1.006 MODIS Land Cover Yearly Global 500m and Land Use map from the Mekong River Commission (MRC) with flood inundation map derived from Monthly Water History, v1.0 (GEE), the affected area in Agriculture, and Affected people is identified.
- Normalized Difference Vegetation Index (NDVI) and Leaf Area Index (LAI) and Nighttime Light Index are used to confirm the damage in the affected area for Agriculture and Affected people respectively.
- Finally, unit loss approach is used in order to assess the damage value in monetary terms based on:
    - Agriculture: the crops price at farm gate value (FGV) recorded by the Ministry of Agriculture, Forestry and Fisheries (MAFF).
    - Affected people: the GDP per capita recorded by the Royal Government of Cambodia.

1.5.3 Flood Damage Analysis: 2000 to 2014

- Flood frequency curve is developed based on annual maximum discharges from 1994 to 2018. One of the following extreme value distributions will be used to represent the observed annual maximum discharges based on the goodness of fit (Chi-square method).
  - Extreme value type I (Gumbel)
  - Extreme value type II (Fréchet)
  - Log-Pearson Type III
- Flood damage curves in each sector are developed based on annual maximum water level and annual flood damages.
- Damage probability curves are derived due to the information from flood frequency curve and flood damage curves. This information will be used as an input for the calculation of Average Annual Damage (ADD) and Net Present Value (NPV) of flood damage in 2030 and 2050.

1.5.4 Flood Damage Estimation and Mitigation Plan: 2030 and 2050

- Socio-economic development in 2030 and 2050 in Agriculture and Affected people in Bakan and Phnom Kravanh districts is estimated based on three means, which are the government policy, the perception of local experts and the trend of the development in the last two decades.
- Damage probability curve in 2030 and 2050 is developed based on the damage probability curves in 2014 with the different scenarios of socioeconomic development in each sector in 2030 and 2050.
- Based on the information of damage probability curve in 2030 and 2050, the Average Annual Damage (AAD) and Net Present Value (NPV) of flood damages in 2030 and 2050 are derived.
- Flood mitigation in 2030 and 2050 is implemented with the assumption that the damages caused by flood in the corresponding return period have been partially removed due to flood mitigation measures for reasons.
- Finally, the NPV of annual flood risk reduction and residual risk after flood mitigation is determined.

1.6 Thesis Outline

The outline of the thesis consists of eight main chapters:

1) Chapter 1: Introduction which describes about the rationale of the thesis, problem statement, objective, research procedure, and thesis outline.
2) Chapter 2: Review of literature focusing on the previous researches related to flood in Cambodia, methods for flood damage assessment and GEE.
3) Chapter 3: Study area description, mainly indicating about the characteristics of the study area such as the climate hazards frequently happened, the geographical, hydrological and meteorological condition, as well as the socio-economic development in the study area.
4) Chapter 4: Methodology selected to implement in this research starting from data collection and extraction by GEE to the flood risk reduction.
5) Chapter 5: Result and Discussion indicating the series of finding from the applied methodology and discussing in detail for reasons to support whether the results response to the objectives.
6) Chapter 6: Conclusion and Recommendation illustrating the summarized results corresponding to each objective and expressing the measures should be taken or further works that would be implemented to improve the research based on the findings of the research.

CHAPTER 2
REVIEW OF LITERATURE

2.1 Flood in a River Basin

The definition of flood can be classified based on the causes and consequences of the flood event. According to (Handmer, Abrahams et al. 2005), flood is an overflow of the water from water bodies such as a stream, river or lake onto the nearby area where the normal condition is usually dry since its elevation is higher than water level. This situation happens when the discharge of the water exceeds the water bodies' capacity due to a heavy rainfall in a particular time in the catchment or the influence of the massive water discharge from the upstream into the catchment. However, the geographical characteristics of the area also potentially creates flood beyond the water bodies whenever a big storm coming within a short period of time on the saturated soil or poor-absorption-ability dry soil. This phenomenon can be found in the mountainous area where steep slope meets the flat land as well as in an urban area where the land is covered by impervious material (Suriya and Mudgal 2012). Beside natural phenomena, human activities are also considered the causes boosting the flood; for example, deforestation in the catchment (Reinhardt-Imjela, Imjela et al. 2018), water structure failure such as dam break (Prakash, Rothauge et al. 2014) and poor water management. Once flood occurs, the significant damages and losses due to this catastrophe have been evaluated according to some important flood parameters such as flood duration, flood depth, flood velocity, and flood warning system (Romali, Sulaiman et al. 2015). According to (Dutta, Herath et al. 2003) all factors can be the important flood parameters that influence flood damages; however most of the time, only flood depth have been selected as flood parameter for previous flood damage assessments.

2.2 Historical Flood in Cambodia

Cambodia is one of the countries which have a high economic risk from natural hazards, resulted in affect people and their assets every year. The main natural hazard that Cambodia exposed is floods followed by drought, occasional epidemics, and storms. In the last quarter of 2011 and 2013, a combination of successive typhoons and torrential rains caused large-scale flooding across the country (ROS Bansok, Phirun et al. 2011). It makes a large portion of the country naturally susceptible to annual flooding, particularly along the Tonle Sap and Mekong River watersheds. The flood event has both beneficial and harmful consequences. They have a favorable impact on agro-based livelihoods (e.g. Improve soil moisture, fertility for agriculture, ground and surface water recharge and provide ecological benefits for fisheries). However, the event also become excessive and result in the loss of human life, destruction of crops and livestock, and damaged homes and infrastructures (e.g. school, health centers, irrigation canals, local roads and bridge).

Figure 2.1: Flood in Cambodia in 2011 (An 2014)

There are two major flood types in previous year in Cambodia; major flooding events affecting a significant have been occurring in the last 52 years approximately every five years, namely in: 1961, 1966, 1978, 1984, 1991, 1996, 2000, 2001, 2002, 2011 and 2013. In the year 2000, one of the worst floods in the country's history occurred, where the NCDM reported that an estimated 750,618 families representing 3,448,624 people were evacuated from their homes and villages (Thomas, Ponlok et al. 2013). There were 347 deaths, 80% of whom were children, and total physical damages was estimated US$150 million. The flood in 2011 affected 350,000 households (over 1.5 million people) with 52,000 homes being evacuated. The 2011 floods caused an estimated loss at US$ 630 million. The flood in 2013 affected 20 of 24 provinces, 377,354 households, claimed 168 lives and forced 31,314 households to evacuate to safe areas. The number of affected provinces by flood year is shown in Figure 2.2.

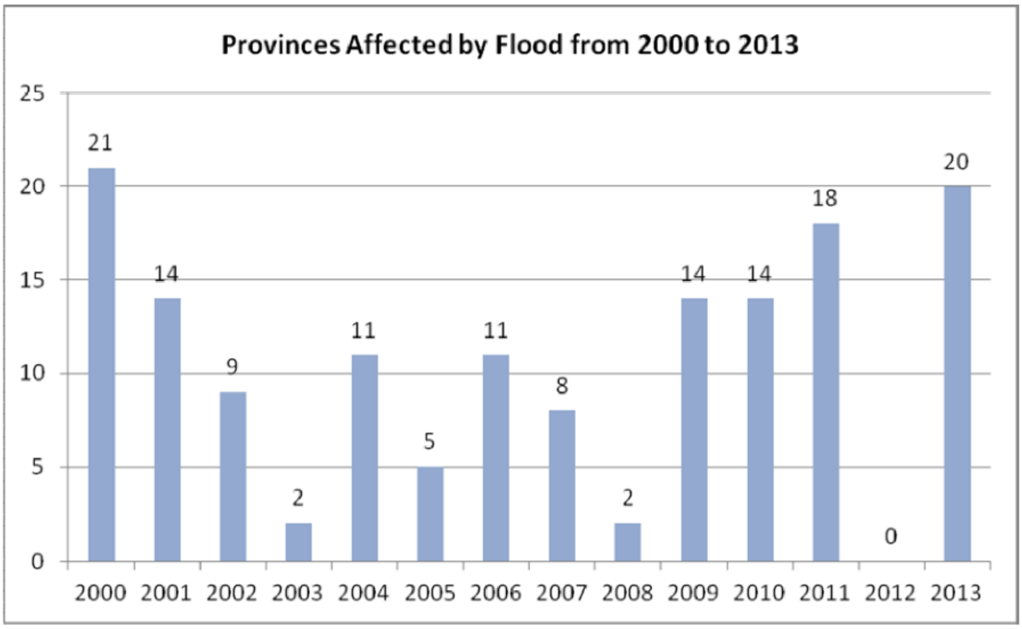

Figure 2.2: Number of provinces affected by flood from 2000 to 2013 (NCDM)

2.3 Flood Inundation Map Using Satellite Image

As mentioned in section 2.2, flood is the most significant climate hazard, which causes damages and difficulties for socio-economic development. Therefore, understanding the current status of flood inundation in time and space is important in evaluating the relationships between variations in the water regime, and local agricultural activity. However, many places around the globe such as some parts of Cambodia are struggling with ground-based observation data to perform a high accuracy hydro-dynamical model in order to understand flood characteristics. Based on this constraint, other measures such as using satellite remote sensing data are considered as a possible way to study flood inundation characteristic.

Satellite remote sensing is expected to provide powerful techniques for objectively detecting inundated area. Flood detection is one of the classical themes of remote sensing, and many studies have been undertaken in this field for a variety of purposes, including studies of paddy field as crop production areas, analyses of wetlands as a source of greenhouse gas and a habitat for aquatic life and birds, and studies of flooded districts.

Flood inundated area estimated from MODIS was compared with that from flood inundation maps produced by Mekong River Commission (MRC), which was derived from RADARSAT combining with Digital Elevation Model (DEM) data and hydrological data as illustrated in Figure 2.3. The result showed that the Wavelet-based Filter for detecting spatio-temporal changes in Flood Inundation (WFFI) or MODIS products as indicated in Figure 2.4 enable an understanding of seasonal and annual changes in the water distribution and environment of Cambodia and the VMD from a global viewpoint.

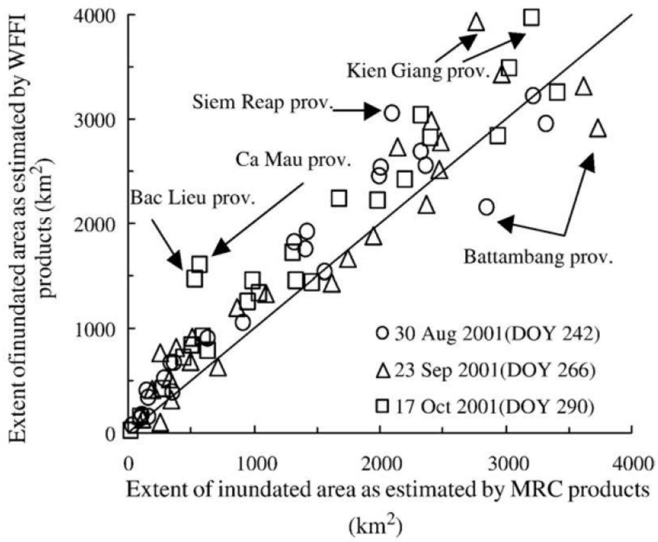

Figure 2.3: Comparison of inundated areas predicted by WFFI and MRC products at the province level (Sakamoto, Van Nguyen et al. 2007)

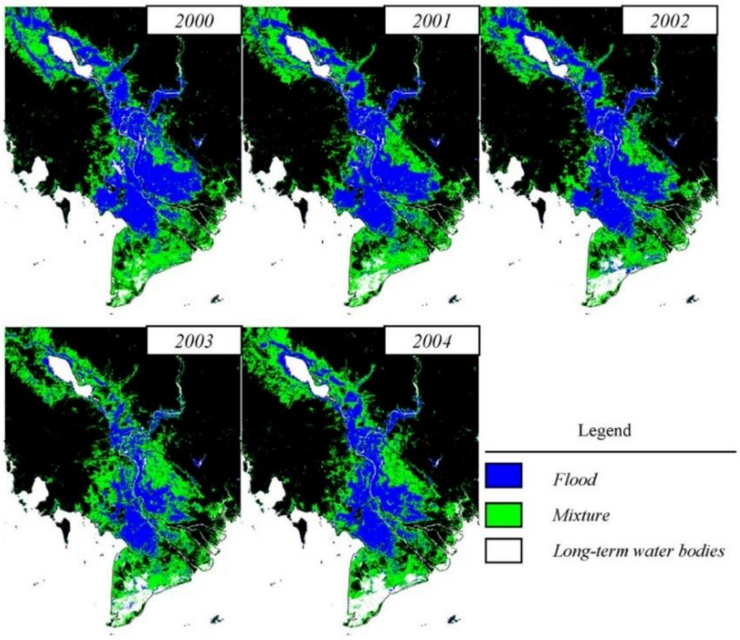

Figure 2.4: Maximum estimated extent of the floodplain over the period 2000 to 2004 (Sakamoto, Van Nguyen et al. 2007)

2.4 Google Earth Engine and Its Application

As mentioned in Flood Inundation Map Using Satellite Image, the process was implemented by extract the satellite images from particular source, and then visualized and analyzed in other software such as Geographic Information System (GIS), or Quantum GIS (QGIS). It requires big data storage and strong computer to compute and analyze those data; more importantly, time consuming to integrate that information to get one particular purpose is also a challenging.

2.4.1 Google Earth Engine

Google Earth Engine is a platform for scientific analysis and visualization of geospatial datasets, for academic, non-profit, business and government users. Earth Engine hosts satellite imagery and stores it in a public data archive that includes historical earth images going back more that forty years. Because it is a cloud-based geospatial processing platform, all analysis and visualization can be carried out on the server side, which is called cloud computing by applied the Earth Engine Application Programming Interface (Earth Engine API). The purpose of Earth Engine is to:

- Perform highly-interactive algorithm development at global scale
- Push the edge of the envelope for big data in remote sensing
- Enable high-impact, data-driven science
- Make substantive progress on global challenges that involve large geospatial datasets

The main components of Earth Engine are:

- **Datasets**: A petabyte-scale archive of publicly available remotely sensed imagery and other data as shown in Figure 2.5.

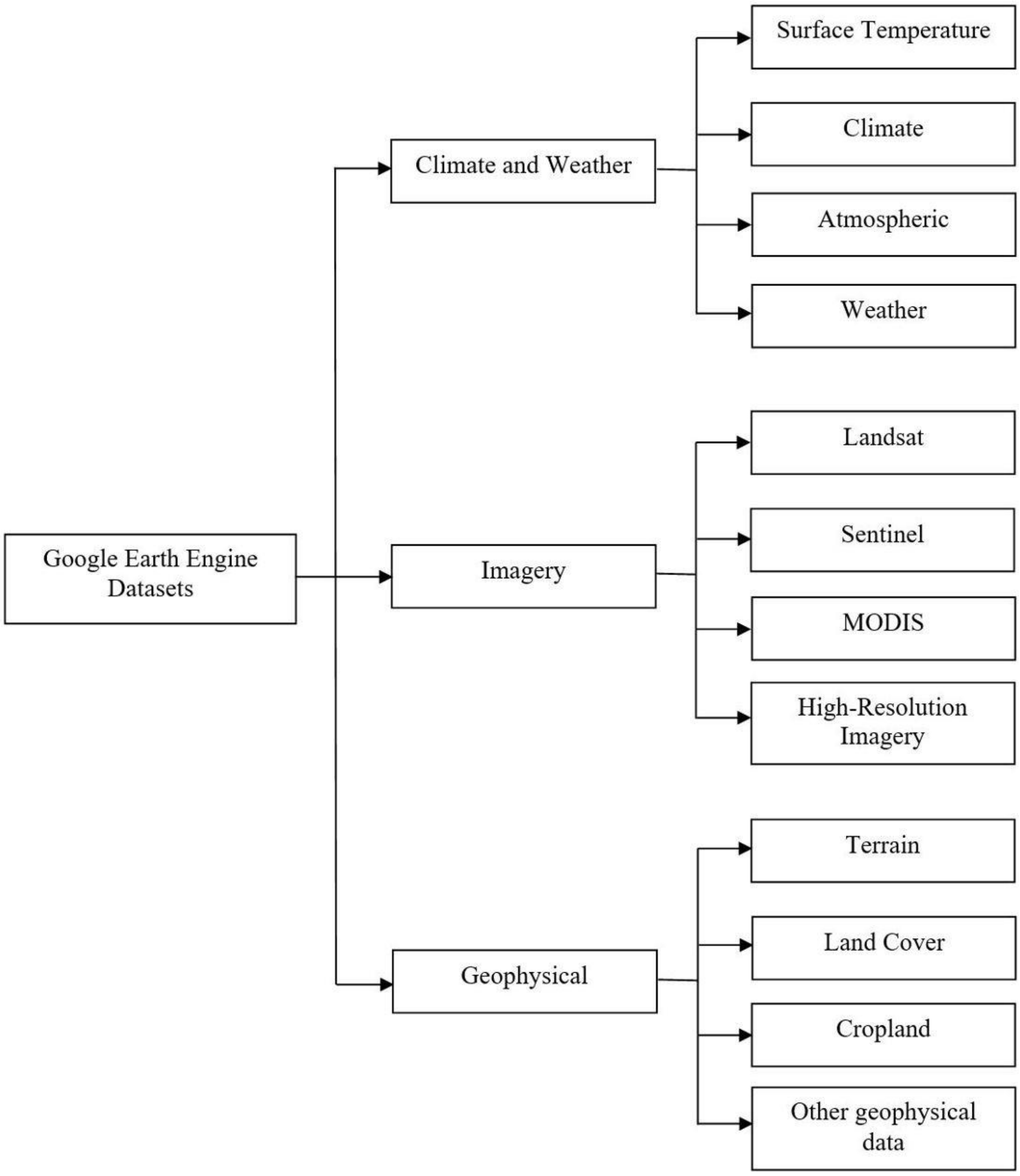

Figure 2.5: Google Earth Engine dataset in Earth Engine Data Catalogue

- **Compute power**: Google's computational infrastructure optimized for parallel processing of geospatial data (Gorelick et al., 2017).
- **APIs**: APIs for JavaScript and Python for making requests to the Earth Engine servers. Both JavaScript and Python are available, however, JavaScript are strongly recommended.
- **Code Editor**: An online Integrated Development Environment (IDE) for rapid prototyping and visualization of complex spatial analyses using the JavaScript API. The Code Editor has the following elements as indicated in Figure 2.6:

- JavaScript code editor
- Map display for visualizing geospatial datasets
- API reference documentation (Doc tab)
- Git-based script manager (Scripts tab)
- Console output (Tasks tab) to handle long-running queries
- Interactive map query (Inspector tab)
- Search of the data achieve or saved scripts
- Geometry drawing tools

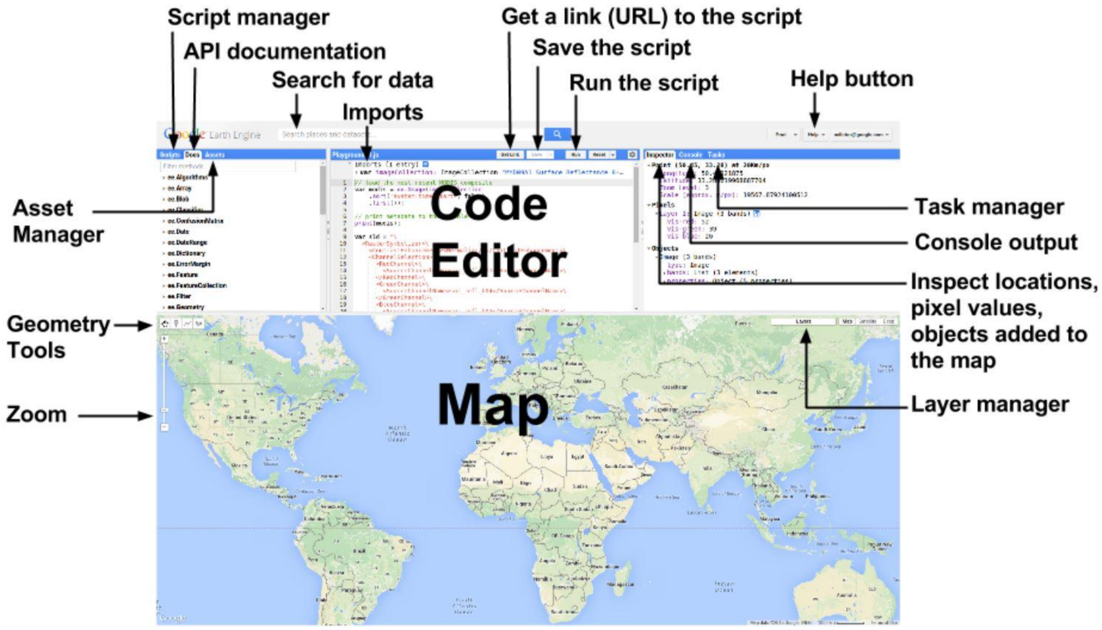

Figure 2.6: Diagram of components of the Earth Engine Code Editor (Source: https://code.earthengine.google.com/)

2.4.2 Case Study Using Google Earth Engine

Hansen, Potapov et al. (2013) used Earth Engine to survey over a decade of global tree cover extent loss, and gain. The study analyzed nearly all global land, excluding only Antarctica and some Arctic islands. The total area of the study is about 128.8 million km^2, which is equivalent of 143 billion pixels of Landsat data at a 30-m spatial resolution. The computation required thousands of machines working in parallel, as well as automatically managed data format conversion, re-projection and resampling.

Another case study using GEE was conducted by Joshi, Dinerstein et al. (2016). They are a research team led by University of Minnesota's Anup Joshi developing a satellite-based monitoring system to track changes and prevent loss to critical endangered wild tiger habitats. Using GEE, forest loss data generated by Dr. Matt Hansen (Hansen, Potapov et al. 2013) and Google, and other data available at Global Forest Watch, the team assessed the changes to all critical tiger habitats over a 14 year period.

Another study called "Global Surface Water" was conducted by The European Commission's Joint Research Centre (JRC) using the Earth Engine to develop high-resolution maps of global surface water occurrence, change, seasonality, recurrence, and transitions (Pekel, Cottam et al. 2016). The Landsat images were collected over the past three decades to identify both permanent and seasonal water bodies. Understanding these changes is vital for ensuring the security of our global water supply for agriculture, industry, and human consumption; for assessing water-related disaster reduction and recovery; and for the study of waterborne pollution and the spread of disease.

The data of global surface water is available in Other Geophysical Data of Figure 2.5. There are five derived datasets of global surface water such as Global surface water mapping layer, v1.0, Global surface water metadata, v1.0, Monthly water history, v1.0, Monthly water recurrence, v1.0 and Yearly water history, v1.0. Moreover, Global surface water mapping layer, v1.0 is divided into many types of water datasets following the specific objective of the discrimination as shown in Figure 2.7. Figure 2.8 indicates the changes of surface water in Myanmar before, during and after building a dam by using the combination of Monthly Water Recurrence, Water History and Monthly Water Presence. The pattern of surface water changes in the past can be characterized by just analyzing these derived datasets.

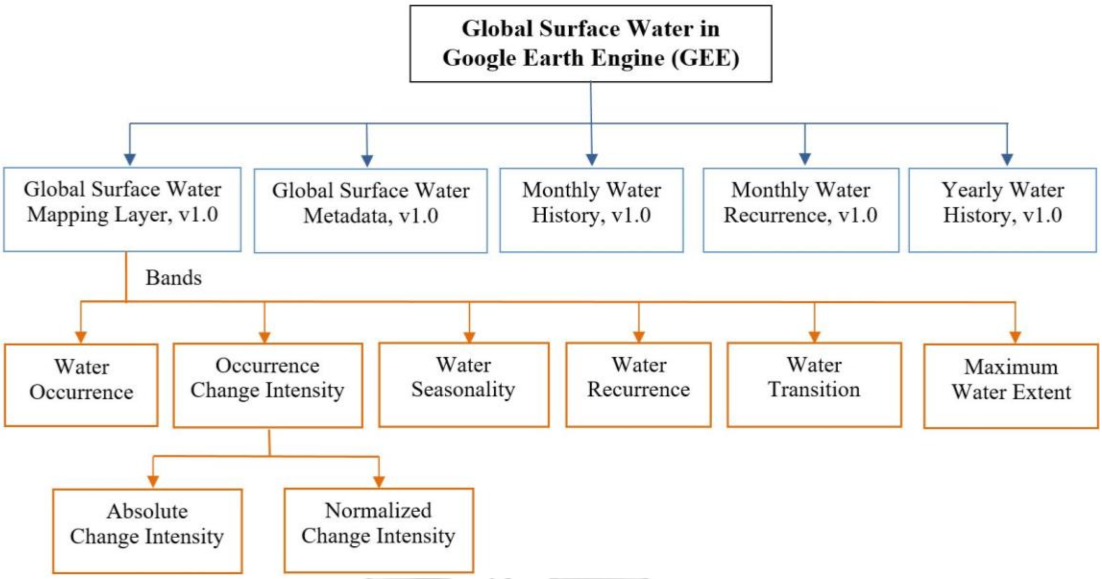

Figure 2.7: Global surface water in Google Earth Engine (Pekel, Cottam et al. 2016)

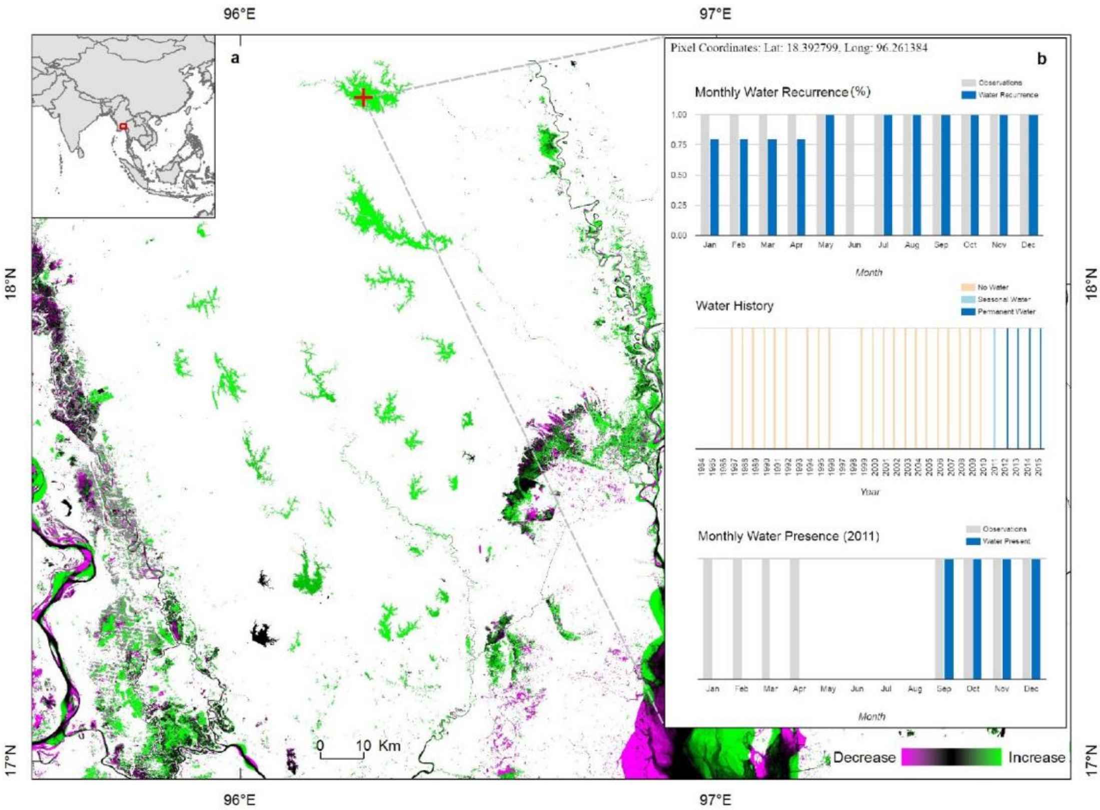

Figure 2.8: Mapping the history of surface water occurrence in Myanmar (Location: latitude 18.3928°, Longitude 96.2633°) (Pekel, Cottam et al. 2016)

2.5 Flood Damage Assessment

This section covers the previous studies and methods used to assess flood damages. Those methods consist of empirical method, in which the hydrological and hydraulic observation data have been used to combine with observed damage data to analyze the cost of the damage as well as using hydrodynamic models to predict in-stream and floodplain variables and then followed by unit cost average estimation of the flood damages in each flood event.

2.5.1 Need for Flood Damage Assessment

Flood damage assessment is very essential for flood risk management (Merz, Kreibich et al. 2010). It can be said that flood damage assessment is the fundamental step to assess the loss value of elements at risk, which allows further studies for flood mitigation measures either structural or non-structural measures, or the combination of both measures. Furthermore, flood risk assessments are even more important within the related context of decision-making in flood risk management. They are requested for:

- **Flood vulnerability assessment**: this includes all elements at risk in the flood prone area; for example, households, crop fields, infrastructures in the community, which are differently vulnerable to floods. For instance, communities, which experienced flood more or less, have better coping capacity for such events than that of communities, which are not flood experienced (Thieken, Kreibich et al. 2007, Kreibich and Thieken 2008). Therefore, high vulnerability mostly happens in non-flood-experienced communities since they often neglect risk mitigation. The information about vulnerability of elements at risk is very essential for appropriate flood mitigation measures; for example, development for emergency plans or long-term plans.
- **Flood risk mapping**: flood risk mapping is an essential component of flood risk management and risk communication. In many countries flood risk mapping is regulated by law. Even though flood mapping is often focused on mapping the flood hazard, there is also discussion about flood risk mapping,

including the potential effects on asset value, people and environment (H. de Moel, van Alphen2 et al. 2009).

- **Comparative risk analysis**: one single element at risk is possible to be vulnerable to more than one potential hazard. In this aspect, damage caused by each hazard need to be evaluated and compared whether what kind of risk should be minimized by risk reduction measures. Grünthal, Thieken et al. (2006) have discussed the comparative risk analysis between flood, windstorm and earthquake. This situation mostly happens when the budget allocation is limited for disaster risk reduction; therefore, specific risk reduction needs to be prioritized.
- **Financial appraisal for insurance sector**: in order to determine the amount of money for insurance compensation and to guarantee solvency, the expected annual damage and the probability of maximum damage to the natural disaster need to be assessed.
- **Financial assessment during and immediately after floods**: if flood occurs in a particular area, the government or NGOs need to assess the damage caused by flood in order to decide the budget for damage compensation. It is the same case as flood event in Cambodia and Thailand in 2011; the damages in all sectors were evaluated immediately after the flood (Bank 2012).

2.5.2 Types of Flood Damage

There are two main types of flood damages: tangible damages and intangible damages. Tangible damage is the damage that can be easily assessed in monitory terms, whereas intangible damage (non-marketable damage) is the damage which are not traded in the market and are difficult to convert into money. Each type of these damages is divided into two subtypes, direct and indirect damages (Markantonis, Meyer et al. 2012). Direct damage is the damage caused to humans, properties and other objects by physical contact with the submersion of the water while indirect damage is the damage caused by the interruption of physical and economic network during and after the flood event; for example, the interruption of traffic and production line, loss of income and trust (Shrestha and Lohpaisankrit 2017). Some examples of flood damages are shown in Table 2-1.

Table 2-1: Classification of flood damages (Merz, Kreibich et al. 2010)

	Direct damage	**Indirect damage**
Tangible	Structural damage Cars Infrastructure Livestock Crops Evacuation and rescue operation Clean up cost	Disruption to transport Business interruption Temporary Affected people for evacuees Loss of industrial production
Intangible	Lives and injuries Diseases Loss of memorabilia and pets Damage to cultural and heritage size Ecological damage Inconvenience	Stress and anxiety Disruption of living Loss of community Reduced land values Undermined trust in public authorities;

2.5.3 Direct Tangible Damage

As mentioned in the previous section, direct tangible damage covers the majority of the insurable objects, which are directly destroyed or disturbed by water during flooding; therefore, this type of damage is always either partly or fully comprised in the assessment of the damages. Another unavoidable reason is that direct tangible damage is easy to understand and assess comparing with other types of damage (Handmer, Abrahams et al. 2005).

The degree of direct tangible damage can be identified based on flood impact parameters and resistance parameters of elements at risk (Thieken, Müller et al. 2005). Flood impact parameters refer to the characteristic of a flood; whereas the resistance parameters reflect the characteristics of the object in the flood prone area. The example of flood impact parameters:

- **Flood area**: the bigger flood extent area, the greater losses and damages are likely to occur.
- **Flood depth**: the higher flood depth, the greater damages to building and other inventories obtained and the stronger the buoyancy force (Büchele, Kreibich et al. 2006).

- **Flood duration**: the longer duration of flood, the greater the saturation of structure and contents, the more severe the anoxia of crops, increasing the probability of damage (Forster, Kuhlmann et al. 2008).
- **Flood Velocity**: the greater the flood velocity, the greater the structural building damage due to the water force (Pistrika and Jonkman 2010).

2.5.4 Method of Cost Estimate

Various methods have been applied to assess the damage; however, the three most-used methods for quantification of direct tangible damages observed in the previous studies of flood damage assessment are:

- **Damage assessment through insurance data**: the previous flood insurance data have often been used for the direct tangible damage studies when intangible and indirect damages have not been included. The insurance payout is utilized as the indicator or cost of the physical damages created by flood. This cost represents the replacement cost; therefore, it can be very necessary to depreciate the insurance payout in order to get more appropriate value of the damages and losses.
- **The unit cost (or average) method**: unit cost estimation is the process of applying the average loss value to the individual damage element within the same type. It is possible to have many types of damage subcategory so that the average loss value of each type is even more accurate. The average loss value can also be estimated by using, for example, the insurance payout or it can be based on the expert knowledge or previous flood experience. The total cost of each type of the damage can be computed by using the average loss value of single damage type multiplying by a number of unit cost estimation.
- **Stage-damage function curve**: Stage-damage functions are important elements for flood damage estimation model. Normally, the stage-damage curves were generated to estimate the flood losses, and this is the first important step in flood losses assessment. The curves graphically represent the relationship between the expected damages/losses and the varying inundation water depth from which the average annual damage can be further derived (Smith 1994). The stage-damage curve can be developed from the two most

common used methods either using the damage data of previous flood or utilizing the hypothetical analyzing known as synthetic stage-damage function depending mainly on land use patterns, and type of elements at risk (Handmer, Abrahams et al. 2005).

2.5.5 Flood Mitigation Measures

Flood risk can be mitigated by using the mitigation measures such as structural measures and non-structural measures.

Structural Measures

Structural measures are mostly constructed to modify the flood parameters such as flood depth, duration, velocity and/or frequency of the flood in the area. There are many types of structural flood mitigation measures; however, in the developing countries such as Cambodia, the most common structural measures that are frequently seen are traditional measures such as reservoirs, dams, dikes, levees and channels.

Reservoirs

Reservoir is considered as a structural mitigation measure since it is built to store water during the high flows, which can reduce the downstream floods. Once the downstream flow decreases, the water is released from reservoirs so that the capacity of the reservoir is free for the next flood. Reservoir can be built with a single purpose or multiple purpose. In purpose of flood mitigation measure, the reservoir is named as "flood control reservoir". The reservoir can reduce flood damage by shifting the area of damage probability curve at the downstream smaller, and thus decreasing the average annual flood damage.

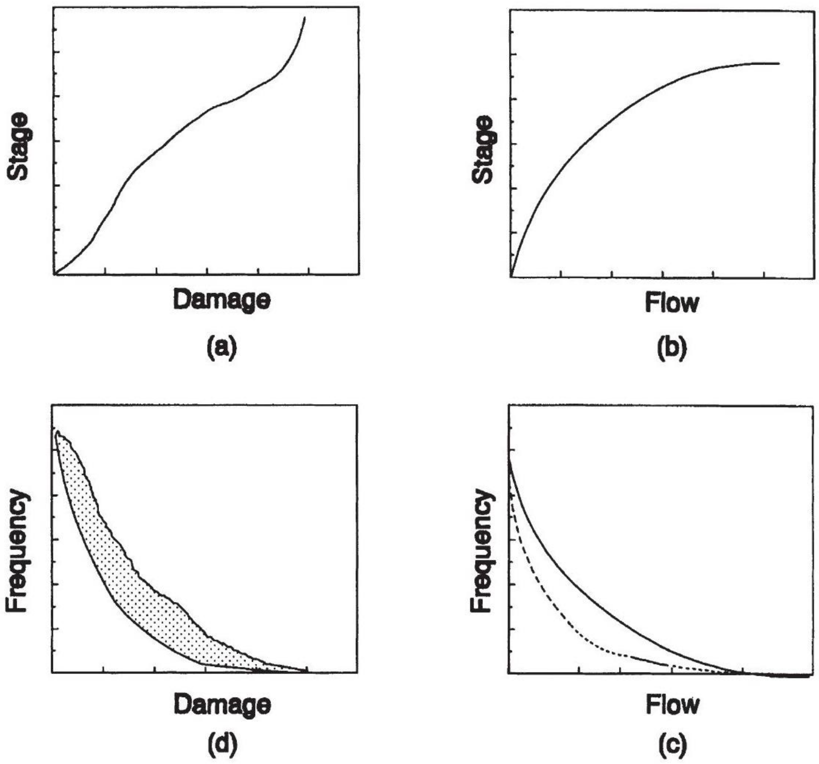

Figure 2.9: Effect of reservoir on flood damage

Levees, dikes and floodwalls

Levees, and floodwalls are frequently used structural mitigation measures specially to protect the urban areas from river floods, while the dikes are normally used to protect the village and agriculture. The dike is mostly seen as the small road in rural area to prevent the specific area from flood. Levees, dikes and floodwalls can only protect the area facing with specific magnitude of the flood. If the flow exceeds the capacity of the structures, the damage will be the same as if there is no structure. The levees, dikes and floodwalls can reduce flood damages by shifting up flood damage curve since it reduces the cross section of the floodways and makes the flood depth higher in the structure. If the level of protection is not appropriately calculated, the damage could be greater than that without the structures if the flow overtops the levees, dikes and floodwalls.

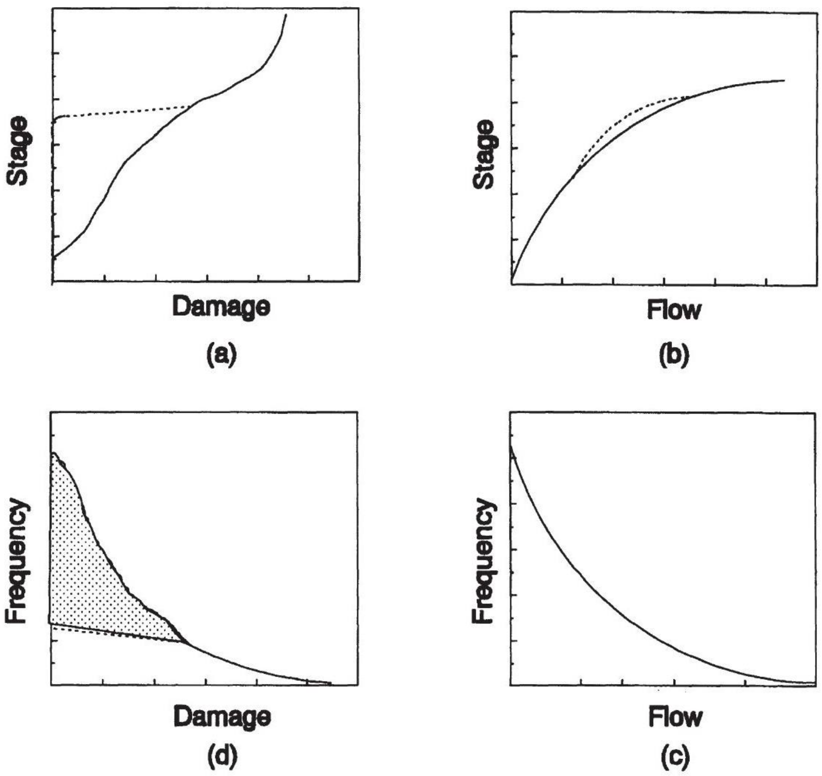

Figure 2.10: Effect of floodwall, levee and dike on flood damage

Channelization

Channelization is another type of structural flood mitigation measure. It reduces the damage by reducing the depth of flood meaning that if the flow is the same, channelization will reduce the water depth in the channel due to the its increasing cross section. Since the rating curve is decreased by channelization, the damage probability curve is also decreased resulted in reducing average annual flood damage as shown in Figure 2.11.

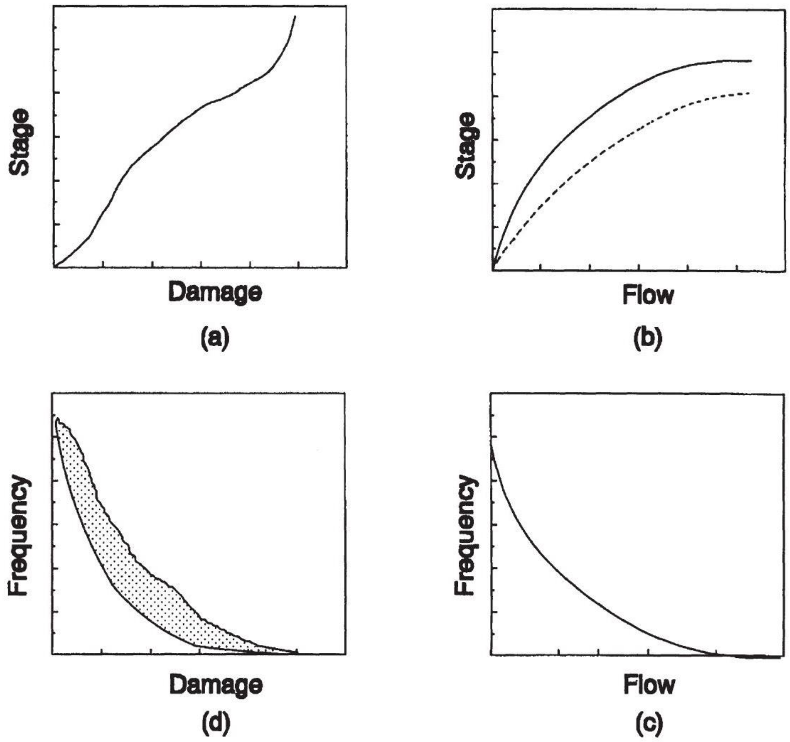

Figure 2.11: Effect of channelization on flood damage

Non-Structural Measures

Non-structural measure is carried out in the same purpose as structural measures, which is to reduce the flood risk or flood damage. However, the implementation of non-structural measures tends to modify the susceptibility of elements at risk rather than controlling the nature of flood for example flood warning and evacuation systems, flood proofing and permanent relocation from the flood prone area.

2.6 Conclusion

After doing a review of literature, we can conclude that flood is still the main climate hazard in Cambodia, where the flood damages were very obvious. Flood damage assessment is very important for flood management process because it is a very beginning step allowing further studies. Empirical method and hydrodynamic model are often used to assess flood parameters; nonetheless, empirical method (basically the observation data) is allowed to represent flood parameters in case that there is no climate change scenario prediction in the study. Since Google Earth Engine (GEE) is launched, there is one more possible way to produce flood map using

Earth Engine products and APIs. However, this method requires more understanding on computer languages. There are many methods used to assess flood damages; however, stage-damage function curve is very suitable for the condition where previous flood damages are well-recorded. The stage-damage function curve can be different from sector to sector due to the resistant parameter of element at risk of each sector. Hence, well-classified flood damage is very essential for future flood damage prediction if those sectors are developed. From this conclusion, flood damage can be assessed using empirical method or hydrodynamic model as well as remote sensing data in Google Earth Engine (GEE). Moreover, the empirical method can be used to support other methods in the way to improve the confidential level of the result.

CHAPTER 3
STUDY AREA

3.1 Pursat Province

Pursat is the fourth biggest province in Cambodia situated in the western part of the country and shared the border with Battambang Province in the north, Tonle Sap Lake in the east, Kompong Chhnang, Kompong Speu, Koh Kong Province in the south, and Trang Province, Thailand in the west, with a total area of 12,692 km^2 (Figure 3.1). It is located in latitude 12°32'N and longitude 103°55'E. The whole province is divided into 6 districts: Bakan, Kandieng, Krakor, Phnom Kravanh, Krong Pursat, and Veal Veng district with the total population 397,107 heads in 2008.

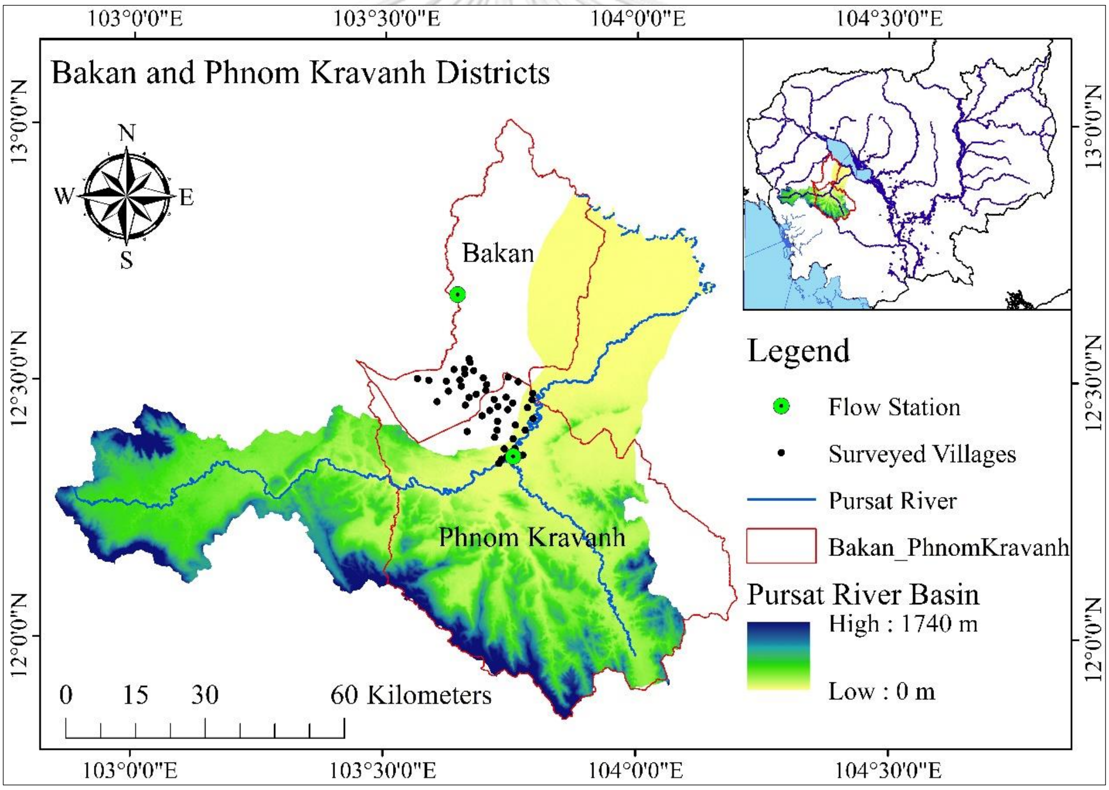

Figure 3.1: Bakan and Phnom Kravanh districts, Pursat province

Pursat Province, the potential province for agricultural development, is prone to natural and human-made disasters, including floods, drought, typhoon, lightning, river bank erosion, fire and epidemics, landslides, forest fires, animal and insect infection, and unexploded ordinance (UXO) remaining landmines. Climate hazards such as floods and drought most frequently occur in many parts of the province.

Almost every year during the monsoon season, flooding and flash floods cause significant damages and losses to lives, injury, loss of livestock, and damages to housing, crop and community infrastructures. The most vulnerable during the disaster occurrence includes the poor, women headed households, children, old people, and the disables. The damages caused by flood in the province.

3.2 Pursat River Basin

The entire Stung Pursat River Basin is located in Pursat Province and shared by six districts, from upstream to downstream: Veal Veng, Phnom Kravanh, Sampov Meas (Krong Pursat), Bakan, Krakor, and Kandieng. The total drainage area at the river mouth in the Tonle Sap Lake amounts to 5,955 km^2. The river originates in the eastern slope of the Cardamom Mountains starting at an elevation of around 1700 m AMSL (Above Mean Sea Level) and flows for approximately 150 km first easterly and when entering the Tonle Sap plain almost northwards. At the river mouth the elevation is in the range of 2 to 9 m AMSL (depending on the water level in the Tonle Sap Lake). The Pursat River has two main tributaries, the (a) Stung Peam and (b) Stung Santre (Prey Khong) rivers, both flow in a northerly direction and meet the Pursat River just above the Bak Trakuon hydrological station. From Bak Trakuon, the river enters into the flood plains meandering within an alluvial plain of about 5 km width. More than 75% of the catchment is surrounded hilly terrain, with an elevation greater than 30 m AMSL, and is covered by forested land of varying density (JICA 2011).

3.2.1 Meteorological and Hydrological Data

Since the study area is a part of the Pursat River Basin, understanding the hydrological and meteorological characteristics of the whole catchment is very important for any further studies related to hydrological and meteorological characteristics of the study area. There are 14 rainfall stations in Pursat River Basin, however, not all of them have been operated and some stations are located far away downstream from the study area which cannot be used to analyze the peak discharge in the study catchment. Therefore, eight rainfall stations in the catchment have been selected to analyze the characteristics of rainfall distribution each year in the basin before selecting the appropriate stations to represent the rainfall distribution and water level in the study area as shown in Table 3-1.

On the Pursat River, several hydrological stations are located or were in operation for some time. All stations including their status are listed in Table 3-1. Among all the hydrological stations, the Bak Trakoun hydrological station (ID: 580103) is the station with the longest period of collected data, spanning from 1994 to 2014. Additionally, records on frequent discharge measurements and developed rating curves are available for this site. More importantly, the location of the Bak Trakoun station is just downstream close to the study area, which is very suitable for the selected water level station in this study. The location of Bak Trakoun hydrological station are shown in Figure 3.1.

Table 3-1: Meteorological and hydrological stations in Pursat River Basin (MOWRAM)

Data	**Station ID**	**Station Name**	**WGS 1984 Zone 48N**		**Gauge**	**Data Availability**
			X	**Y**	**(m. MSL)**	
Precipitation	120304	Dap Bat	372284	1369963		2000 - 2010
	120312	Kravanh	365457	1364266		2000 - 2011
	120313	Peam	360323	1356910		2000 - 2010
	120324	Phteah Rung	361016	1369771		2000 - 2011
	210325	Rovieng	341978	1362267		2000 - 2011
	120328	Santre	372359	1355370		2000 - 2011
	120309	Talo	353459	1383184		2000 - 2010
	210326	Tanlouch	352449	1362466		2000 - 2011
Water level	580103	Bac Trakoun	364762	1366148	20.758	1994 - 2014
	580104	Santre	383203	1339868		2000 - 2010
	580201	Peam	365664	1363521		2000 - 2010

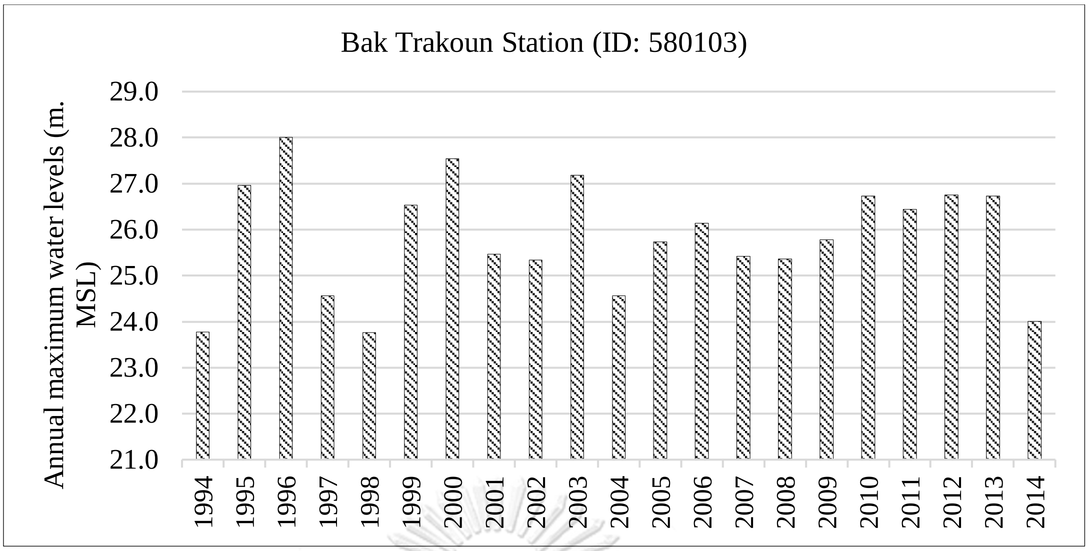

Figure 3.2: Annual maximum water level at Bak Trakoun flow Station (MOWRAM)

The maximum water level at Bak Trakoun station from 1994 to 2014 are shown in Figure 3.2. However, since water levels have been generally recorded every morning at 7:00 am, the instantaneous peak water levels during a flood event are not available. This has an influence on the estimation of the peak discharge, hence, the calculated flood frequency.

There is a very high probability that the annual flood occurs in October (65% in the past 20 years). However, floods were observed as early as May and as late as November.

3.2.2 Rating Curve Development for Bak Trakoun

Stage-discharge rating curves are used to convert water level data recorded by the hydrometric monitoring stations into a discharge time-series (hydrograph). Rating curves were derived for the Bak Trakoun station on the Pursat River for the period before 2010 and after 2010. During the field visit to the site, it was confirmed that there are no backwater effects and hence no corrective measures need to be taken.

A list of discharge measurements and developed rating curve were provided by the Department of Hydrology and River Works (DHRW) of Ministry of Water Resources and Meteorology (MOWRAM). The discharge measurements span the period 2010 to early 2013, containing 68 pairs with a water level range of 0.9 m to 5.96 and discharges between 0.35 m^3/s and 1101 m^3/s.

The observed range of water levels from 1994 to 2014 at Bak Trakoun is between an absolute minimum of 0.05m and the peak flood of 7.31m; hence, the measurement pairs are covering most of the range.

Based on the available discharge measurement data rating curves were developed and the resulting hydrographs compared. Generally, power function of the form $Q = a \times (H - H_0)$ b or polynomials of the form $Q = c \times H^2 + d \times H + e$, are used to best approximate the water level versus discharge relation (where: Q is water discharge in m^3/s; H is gauge height in meters; H_0 is the gauge height at zero flow (datum correction) in meters; and a, b, c, d and e are coefficients).

As previously stated, the Bak Trakoun hydrological station was relocated in 2010. Therefore, two rating curves were developed at this station to compute discharges before and after 2010. All developed rating equations for Bak Trakoun are shown in Table 3-2.

Table 3-2: Rating curves for Bak Trakoun hydrological station (MOWRAM)

N_0	Period	Rating equation	R^2	Source
1	1994-2009	$Q = 27.5335\times (H - 0.05)^{1.930}$	0.9933	M16, 2013
2	2010-2014	$Q = 28.41\times H^2 + 0.978\times H + 5.260$ or: $Q = 23.2066\times H^2 + 20.3279\times H - 6.62$	0.9915 0.9946	MOWRAM
3	2010-2014	$Q = 35.709 \times (H - 0.06)^{1.876}$	0.9901	ACI team

Although both polynomial approximation rating curves “2” fit the data very well, the lower range of water levels results in a significant miss-estimation of the associated discharge. Polynomial approximation bears the problem that negative discharges may be calculated for the lowest range of water levels.

However, for practical purposes and accurate low flow studies, it might be useful to establish a segment of the rating curve specific to low flow only, and the conversion of water level into discharge shall be made by a rating table. Rating table are subject to review after a period of time depending on the station characteristics (stable, relatively stable etc.). The investigation of low flows is important for the setting of the environment flow of a river.

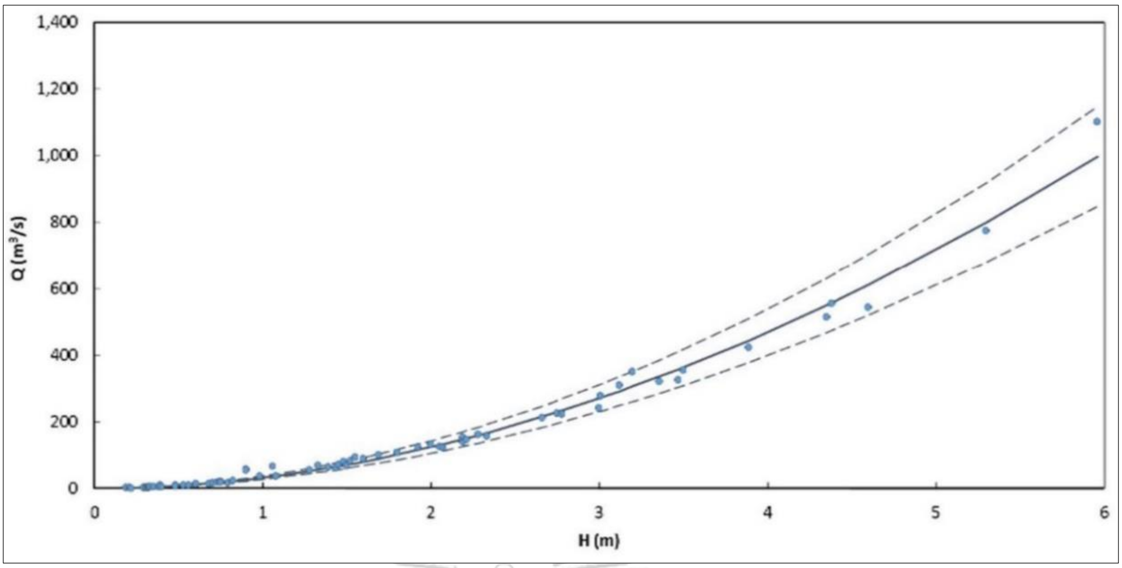

Figure 3.3: Rating Curve for the period 2010 to 2014 (MOWRAM)

To finally transform the water levels into discharges rating curve “1” was used for the period 1994 to 2009, and rating curve “3” was used for 2010 to 2014.

3.2.3 Discharge at Bak Trakoun Hydrological Station

Based on the observed water level for the period 1994 to 2014, the discharge of the Pursat River at Bak Trakoun varies between essentially no flow on some days during drought conditions to 1264 m^3/s during the during an extreme flood event. The time series of the flow hydrograph for this period is shown in Figure 3.4. The distinct seasonality can be observed with flows during the dry period (December to March) with flows sometimes less than 1 m3/s and during the wet season (May to November) where peaks of 500 to 600 m^3/s are not uncommon.

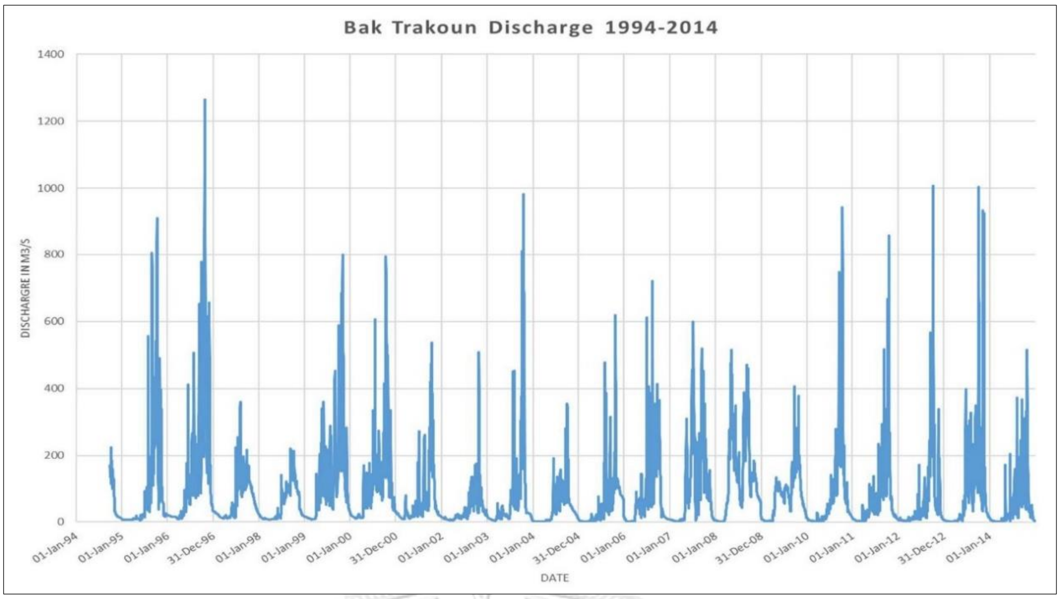

Figure 3.4: Discharge Hydrograph of Pursat River at Bak Trakoun (MOWRAM)

Table 3-3: Listing of annual maximum flood in m^3/s

Date	11/10 1995	27/10 1996	06/08 1997	15/09 1998	05/11 1999	14/10 2000	15/10 2001	28/10 2002	18/10 2003	06/10 2004
Flow (m3/s)	909	1264	360	221	801	795	537	509	982	355
Date	25/10 2005	17/08 2006	08/07 2007	07/05 2008	24/09 2009	15/10 2010	21/10 2011	08/10 2012	07/10 2013	28/10 2014
Flow (m3/s)	620	722	599	515	406	1001	911	1007	1004	515

Assuming a threshold of approximately 800 m^3/s, it can be observed from Figure 3.4 that the flow in the river has exceeded this threshold possibly five times since 1994. Therefore, an 800 m^3/s flow is estimated to currently occur on average 2.3 years.

3.2.4 Seasonality of Flows

Cambodia’s climate is determined by the monsoon and hence distinctly seasonal. In Figure 3.5 the seasonality of the flow in the Pursat river is addressed on a monthly time scale as it can be seen the average flow in the months January to March is in the range of only 6 to 11 m^3/s, whereas in August to October the average flows are in the range of 125 to 260 m^3/s. the dry season spans from December to May the following year and the wet season from June to November. The flow volume during the dry season is only about 18% of the total annual flow of approximately 2400 million m^3. The seasonality of the flows and the significant monthly variations will have an influence on secure water supply for the irrigation scheme, particularly during the dry season.

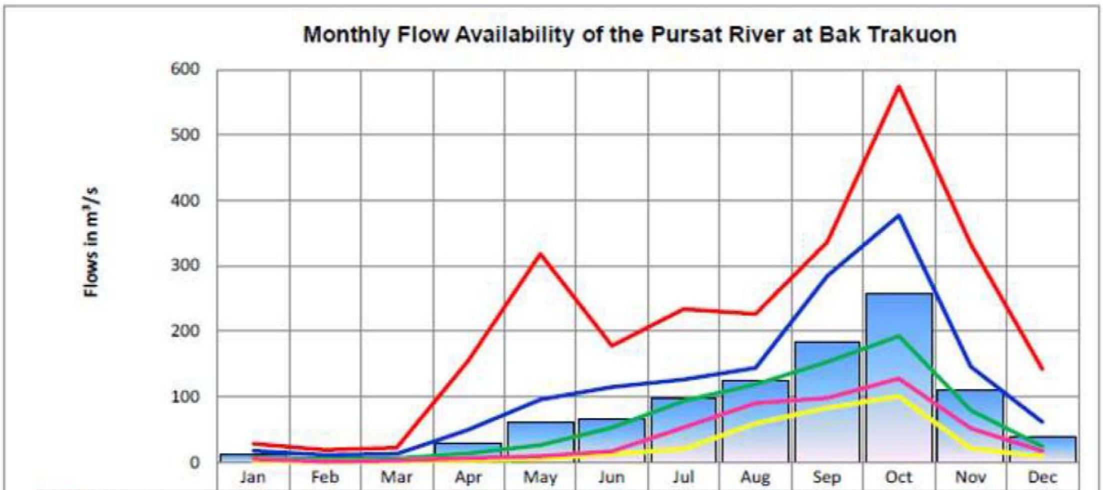

	Jan	Feb	Mar	Apr	May	Jun	Jul	Aug	Sep	Oct	Nov	Dec
Average	11.1	6.3	7.8	28.2	62.2	66.1	99.1	123.8	183.5	258.3	110.1	39.1
Maximum	28.4	19.0	22.3	156.1	318.4	177.9	234.1	226.7	336.7	574.3	333.3	141.8
Minuimum	1.7	0.5	0.5	2.7	5.0	12.5	20.5	59.6	83.4	100.7	21.3	8.8
20% Exceedence	17.8	11.1	12.8	50.0	95.9	115.2	126.7	144.4	285.1	377.1	146.4	61.1
50% Exceedence	7.6	5.2	6.0	13.7	26.6	53.3	94.0	119.3	153.5	193.1	79.7	24.2
80% Exceedence	5.2	1.1	2.6	6.3	9.4	17.1	53.5	90.5	98.2	128.0	52.2	17.2

Figure 3.5: Monthly discharge hydrograph from 1995 to 2011 (JICA 2013)

3.3 Bakan and Phnom Kravanh Districts (45 villages)

The survey was conducted in the central part of the Pursat River Basin, as shown in Figure 3.1 (Black points), including 45 villages in 5 communes, within 2 districts (Bakan and Phnom Kravanh districts) in Pursat Province with the total area of 41,638 hectares (416 km^2), covering approximately 55,000 people living in around 12,000 households. This location is very prone to climate hazards especially flood since it is located just downstream of the joints of three rivers. The survey was conducted in the selected study area to understand the real situation of the following aspects:

3.3.1 Geographical data

The geographical data provided the detail about the location and geographical characteristics of each village such as latitude, longitude, and percentage of lowland, upland and flat area, elevation and the border structures surrounding the village, area and land use. To make the proportions simple, the data was converted into the percentage as shown in and Figure 3.6, which illustrate that almost 80% of the land is for agricultural area. The percentage of residential, forest and water body area are 17.80%, 1.40% and 1.50%, respectively. The coordinates of the villages were also observed as shown in Figure 3.7, while the average, minimum and maximum in percentage are as: lowland as 20/0/60, upland as 31/0/90, flat area as 49/0/100.

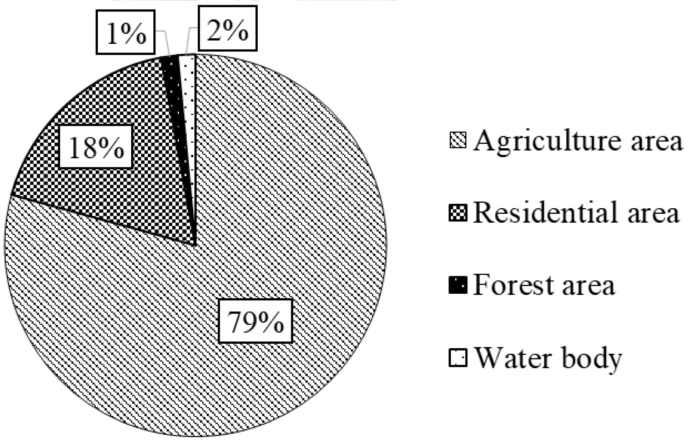

Figure 3.6: Types of land use in the study area (HVCA)

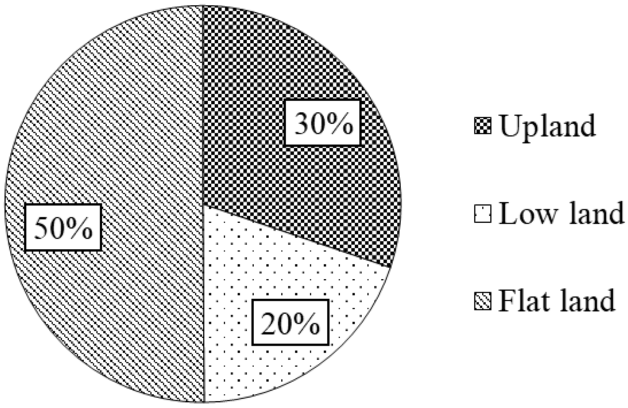

Figure 3.7: Land elevation in the study area (HVCA)

3.3.2 Population Data

The population data provides the basic information about the detailed statistics of the respondents living in the villages, which included following important sub-details in the order of average, minimum, and maximum of male and female population as 628/160/1,164, number of households as 264/66/481, number of children (0-15 years old) as 415/10/852, number of elderly persons (> 60 years old) as 79/13/249, number of orphan as 3/0/21, number of landless families as 11/0/47, number of people migrating per year (average last 5 years) on a seasonal basis as 44/0/153, number of people migrating per year (average last 5 years) on long-term basis as 22/0/212.

The total population in the 45 villages are 54,880 people in which 51.5 % are female with 11,870 of households meaning that there are around 4 or 5 people in a family on average. The main source of income of the people is agricultural activities where typical activities are growing rice, cassava, and other vegetables as well as livestock. People migrated out for work are about 9.6 % of the total population, in which 50.2% migrated within Cambodia and 49.8% did outside Cambodia. People migrated out for are adults who mostly finished their study in primary and secondary school.

Table 3-4: Population data in the study area (HVCA)

Population	**Number**	**Percentage**	**Remark**
Total population	54,880	100%	
Female	28,255	51.5%	
Number of households	11,870	100%	
Main source of income: Agriculture	All most	100%	Rice, cassava, other crops, Livestock
Migration out	5,285	9.6%	Exclude seasonal labors
Migration within Cambodia	2,655	50.2%	Adult
Migration outside Cambodia	2,630	49.8%	Adult

3.3.3 Socio-Economic Data

Figure 3.8 indicates the challenges of the socio-economic development in the villages. The most difficult issue of the people in the villages is lacking irrigation system. Because almost 100% of the main sources of the income of the people in the village is agriculture, lacking irrigation system makes their agricultural activities less intense. For example, people can grow rice only once per year depending on rainwater, which is very risky and vulnerable to the impact of climate hazards such as flood and drought. Moreover, according to Thomas, Ponlok et al. (2013), agriculture in Cambodia is more or less affected by climate change without climate change adaptation measure. Other challenges are lack of market and low prices for agricultural production, especially the price for the rice and cassava, lack of stable employment and no factories nearby the community resulted in migration out for work, lack of infrastructure such as road, water supply and sanitation. Other difficulties are the lack of technical support for agriculture, health problems and being in debt of micro-finance (50% of the households).

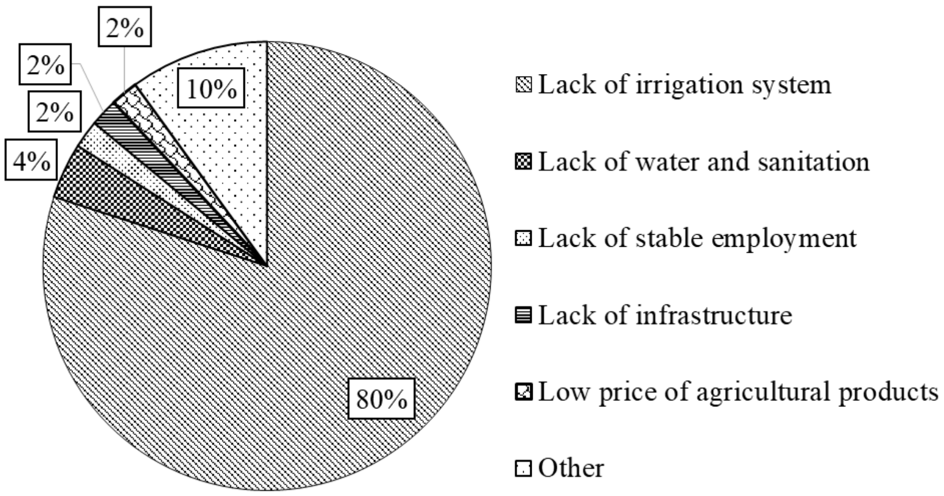

Figure 3.8: Socio-economic development challenges (HVCA)

CHAPTER 4
METHODOLOGY

The methodology used in this research consists of four main steps: 1) Data collection and analysis; 2) Flood damage assessment using GEE; 3) Flood damage analysis: 2000 to 2014; 4) Flood damage estimation and mitigation plan: 2030 and 2050 as indicated in Figure 1.1.

Data collection and analysis: primary and secondary data were collected from the real site survey and other Cambodian government agencies. Satellite data such as Monthly Water History, v1.0 (MWH), Night-time Light (NTL), Normalized Difference vegetation Index (NDVI) and Leaf Area Index (LAI) are extracted from GEE. The details of data collection and data visualization are indicated in Table 1-1 and Figure 4.1 respectively.

Flood damage assessment using Google Earth Engine (GEE): Monthly Water History, v1.0 in GEE and Earth Engine APIs allow users to detect monthly water extent in the area of interest from January 1984 to September 2015 (32 years). By using the records of extreme flood events and the threshold discharge at Bak Trakoun flow station (800 m^3/s), those extreme events are captured and considered as flood extents in a particular year. Moreover, the affected areas in each sector are obtained from the integration between flood maps and the land covers.

Flood damage analysis 2000 - 2014: the record of daily water levels in Bak Trakoun flow station from 1994 to 2018 is collected to convert into discharges by using rating equation in Table 3-2. The annual maximum discharges from 1994 to 2018 (25 years) were selected to do the frequency analysis under three extreme value distributions: Extreme value Type I (Gumbel) and Type II (Frechet), and Log-Pearson Type III. However, only the best fitted of extreme value distribution to the observed discharges will be selected to be the flood frequency curve and damage probability curve.

Flood damage estimation and mitigation plan in 2030 and 2050: socio-economic development in 2030 and 2050 are considered as the critical year of changes in the Cambodia due to the national strategic plan of the Royal Government of Cambodia. In the year of 2030 and 2050, the damage probability curve and average annual damage are estimated based on socio-economic development scenarios. Furthermore, the annual risk reduction by whatever mitigation measure in 2030 and 2050 is estimated and converted into Net Present Value (NPV) both risk reduction and residual risk. The summarized task performed of the methodology to meet the objective is shown in Table 4-1.

Table 4-1: Detail of study elements

No.	Objective	Task perform/Tools	Output
1	Flood damage assessment using Google Earth Engine	Flood detection (GEE); Geo-spatial analysis (GIS); Relationship between water extent and observed water levels; Land cover change analysis; Integration between water extent and land-cover types/ Infrastructure data (GIS); Time series of NTL, NDVI and LAI analysis (GEE and GIS); Observed physical damage and damage value analysis;	Annual flood damage between 2000 and 2014
2	Development of flood damage probability curve from 2000 to 2014	Discharge conversion by using rating equation; Flood frequency analysis (Gumbel, Frechet and Log-Pearson Type III); Flood damage curves in each sector; Flood damage probability curve;	Flood damage probability curve 2014;
3	Flood damage estimation and mitigation planning in 2030 and 2050	Future prediction of socio-economic development (Agriculture and Housing and Infrastructure); Flood damage curve; Flood damage probability curve; Average annual damage (AAD); Net present value (NPV) of risk reduction and residual risk;	Net present value of average annual damage with mitigation in 2030 and 2050;

4.1 Data Collection and Data Analysis

As shown in Table 3-1, rainfall data from eight rainfall stations and water level from three water level stations have been recorded in Pursat River Basin; however, only water level at Bak Trakoun station (ID: 580103) is used in this study to analyze the flood depth-damage curve since this station is located in the middle of Bakan and Phnom Kravanh districts as shown in Figure 3.1. Rainfall data from Dep Bat station (ID: 120304) is used to verify rainfall pattern with water level in the valid year in the basin. The summarized important data collection of this research including type of data, source of the data and data availability was illustrated in Table 1-1. Moreover, the visualization of some data related to water resources and socio-economic development are shown Figure 4.1 to understand the basic trend and relationship of those data.

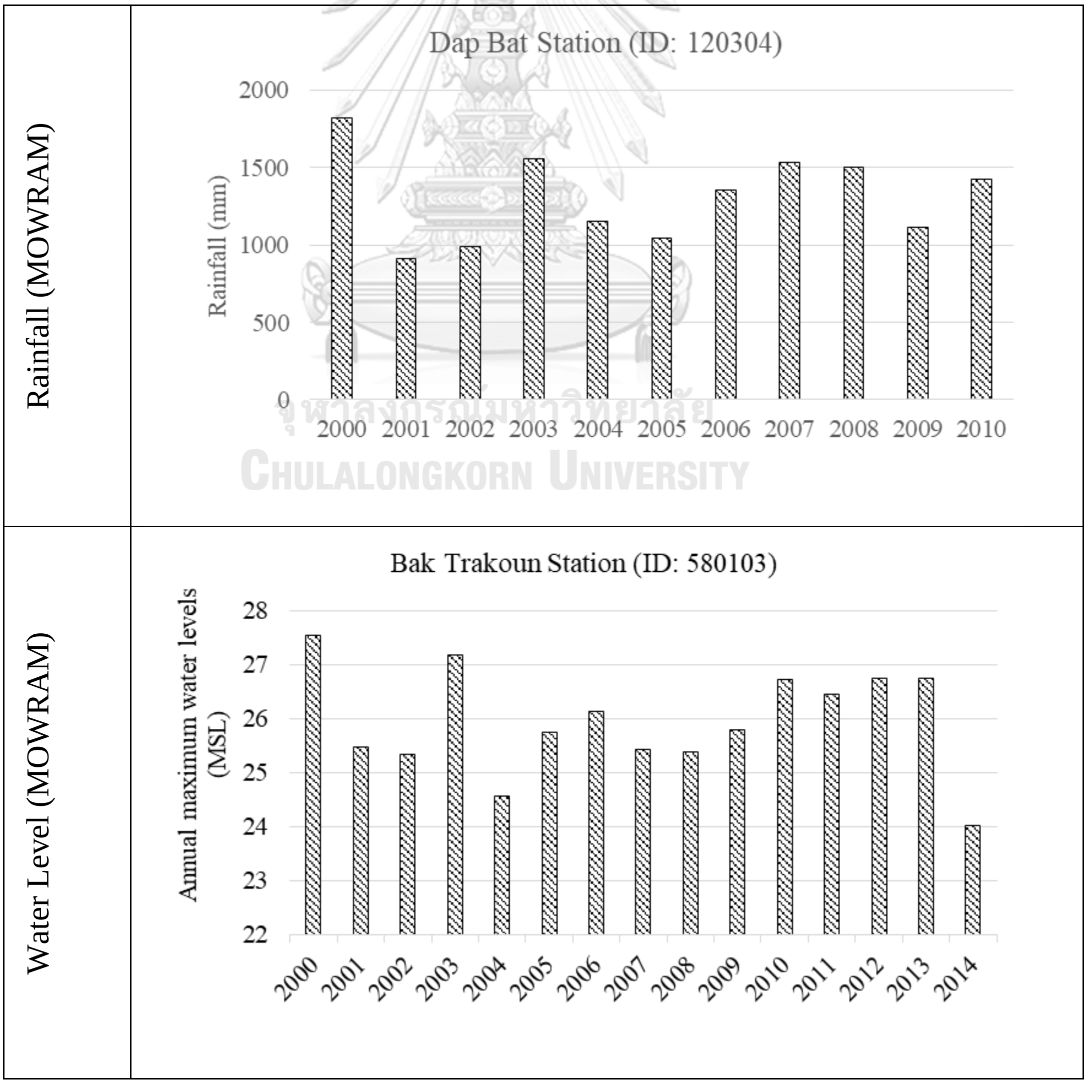

<table>
<tr>
<td>Growth Domestic Product (GDP) (World Bank)</td>
<td>
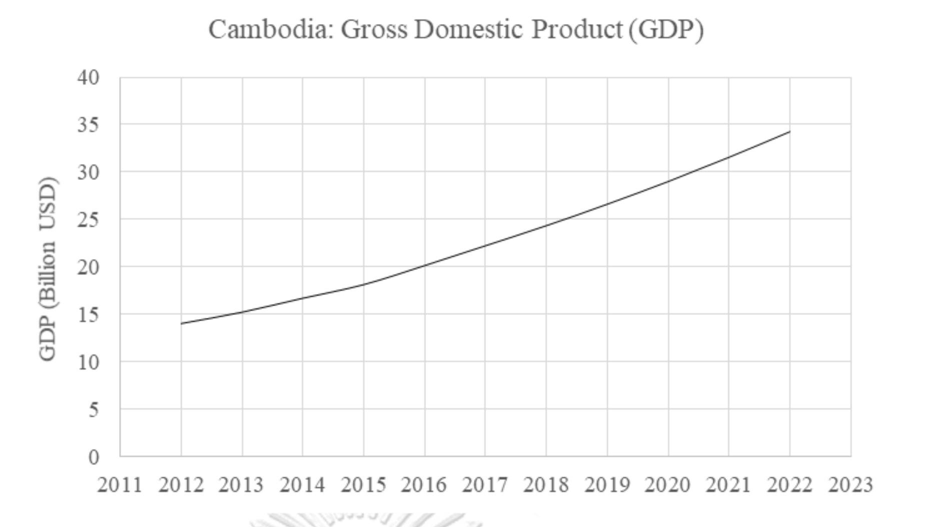

</td>
</tr>
<tr>
<td>GDP Shared by Sectors (World Bank)</td>
<td>
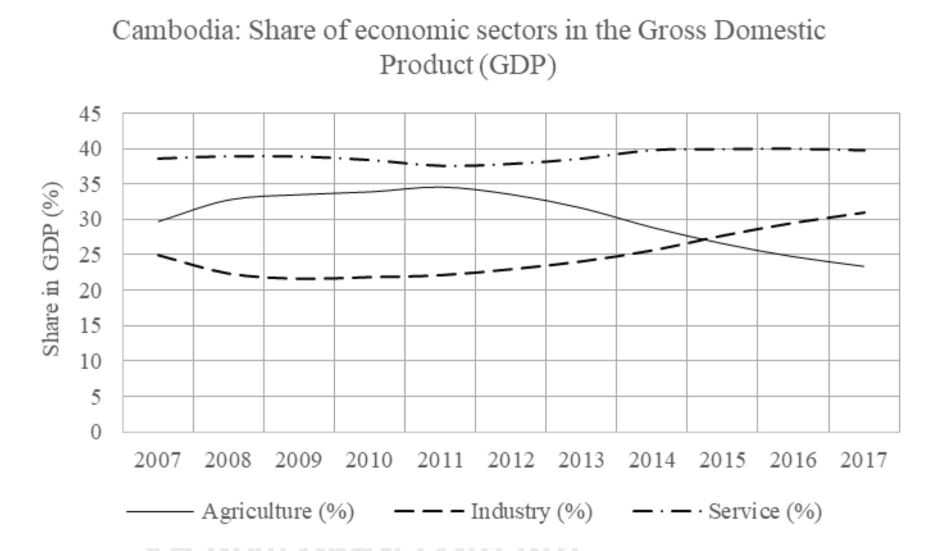

</td>
</tr>
<tr>
<td>Growth Domestic Product (GDP) per Capita (World Bank)</td>
<td>
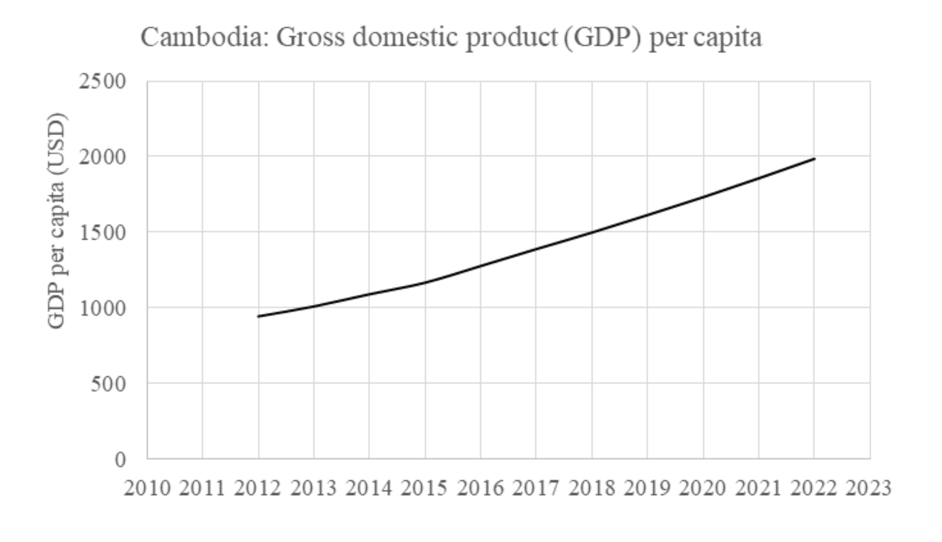

</td>
</tr>
</table>

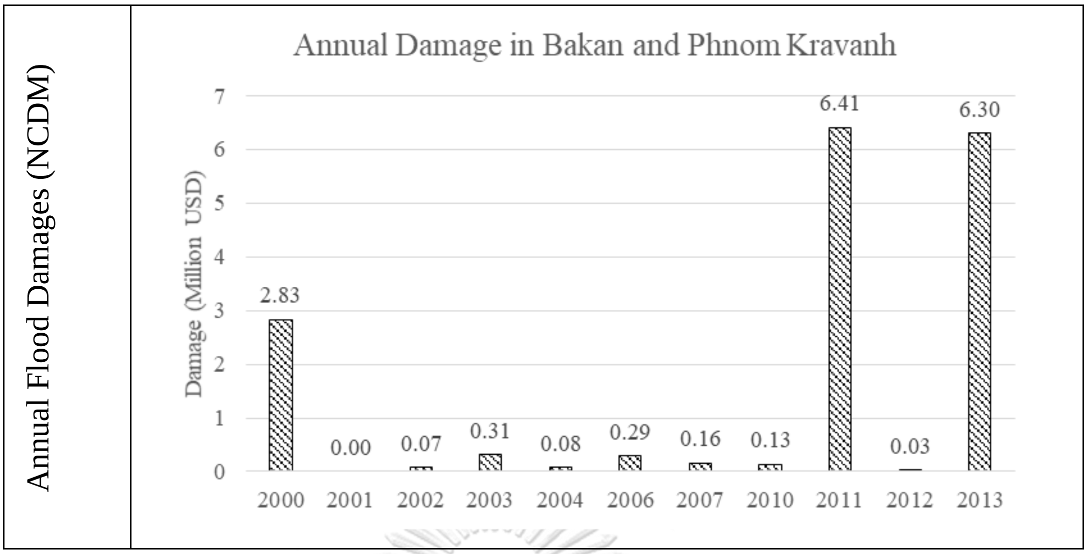

Figure 4.1: Data visualization

4.2 Flood Damage Assessment using Google Earth Engine (GEE)

Flood damage assessment by using Google Earth Engine is indicated in Figure 4.2. The process of determining the annual flood damage and damage value is already described in section 1.5 and Table 4-1. The most important tasks performed in the part are the development of Earth Engine APIs to extract the satellite data such as Monthly Water History, v1.0, NDVI, LAI, NLI and Land Cover, the geo-spatial analysis of satellite data using ArcGIS and statistical analysis, especially refers to regression analysis.

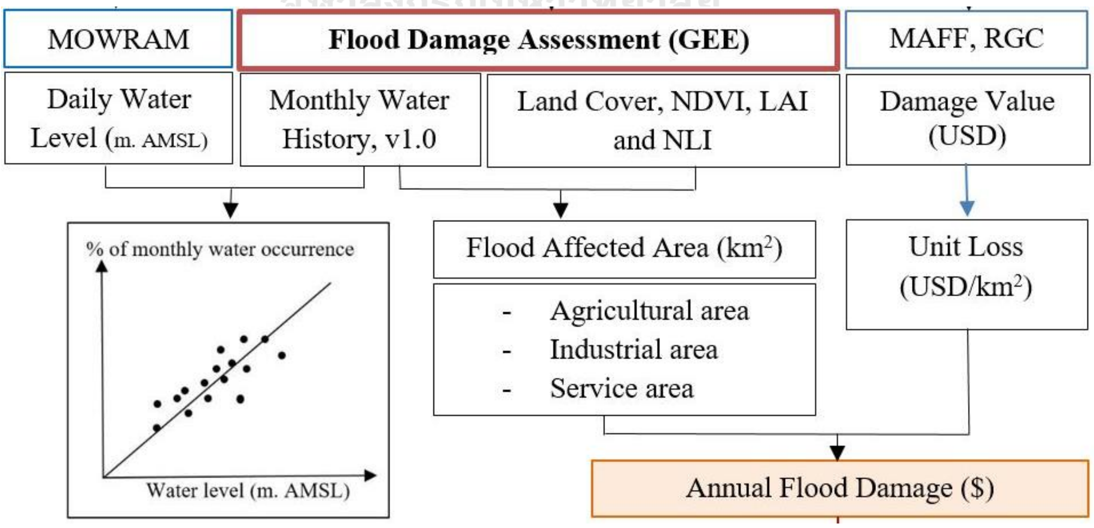

Figure 4.2: Methodological framework of flood damage assessment using GEE

4.2.1 Regression Analysis

Regression analysis is a procedure to fit an equation to a set of data by giving a set of observed data or measurements on two random variables, y and x. Regression is a good way to determine the value of coefficients, b_0 and b_1, for the straight line ($y = b_0 + b_1x$) that best fit the data. The mathematical model relates two random variables, called the dependent variable (y) and predictor variable (x), which sometimes called independent variable. The most frequently used linear model relates a dependent variable y to a single predictor variable x by the equation:

$$\hat{y} = b_0 + b_1 x \qquad \text{(Eq. 4.1)}$$

Where b_1 is the slope coefficient and b_0 is the intercept coefficient; b_1 and b_0 are often called regression coefficients because they are obtained from a regression analysis. $\hat{y}$ is the predicted value of y (dependent variable).

There is also a dependent variable (y) predicted by more than one predictor variables; this is called “Multiple Regression”. The linear multivariate model relates a dependent variable to two or more predictor variables by equation:

$$\hat{y} = b_0 + b_1 x_1 + b_2 x_2 + \ldots + b_n x_n \qquad \text{(Eq. 4.2)}$$

In which n is the number of predictor variables, x_i the i^{th} predictor variable, b_i the i^{th} slope coefficient, and b_0 the intercept coefficient, where i = 1, 2, 3,…,n.

To evaluate the reliability of the regression equation, the following criteria should be assessed: (1) the correlation coefficient, (2) the standard error of estimate, and (3) the rationality of the coefficients and the relative importance of the predictor variables, both of which can be assessed using the standardized partial regression coefficients.

Graphical analysis is the first step in evaluating the relation between variables. Data visualization by graphical analysis can provide the following information:

- Identify the degree of common variation, the degree to which the two variables are related.
- Identify the distribution and range of the sample data point.
- Identify the existence of extreme events.
- Identify the form of the relationship between the two variables.
- Identify the type of the relationship.

Correlation is the degree of association between the elements of two samples of data, that is, between the observations on two variables. There is always certain amount of variation of a set of observations on random variable y, which may be characterized by the variance of the sample. This variation can be separated into two parts; first is associated with a predictor variable x and the second is not. The total variation (TV) is the sum of these two variations, where the variation that is explained by the predictor variable called explained variation (EV) and variation that is not explained, that is, the unexplained variation (UV). Thus, we get

$$TV = EV + UV \qquad \text{(Eq. 4.3)}$$

This separation of variation concept is useful for quantifying the correlation coefficient developed by Karl Pearson. Specifically, dividing both sides of Equation () by the total variation (TV) gives

$$1 = \frac{EV}{TV} + \frac{UV}{TV} \qquad \text{(Eq.4.4)}$$

The ratio EV/TV represents the fraction of the total variation that is explained by the linear relationship between y and x; this is called the coefficient of determination:

$$R^2 = \frac{EV}{TV} = \frac{\sum_{i=1}^{n} (\hat{y}_i - \bar{y})^2}{\sum_{i=1}^{n} (y_i - \bar{y})^2} \qquad \text{(Eq.4.5)}$$

The square root of the ratio is the correlation coefficient, R. If the explained variation equals the total variation, the correlation coefficient will equal 1. Of the relationship is inverse and the explained variation equal the total variation in magnitude, R will equal -1. These represent the extremes but both values indicate a perfect association, with a sign only indicating the direction of the relationship. If explained variation equals 0, R equals 0. Thus, a correlation coefficient of 0, which is sometimes called the null correlation, indicates the lack of a linear association between the two variables x and y.

4.3 Flood Damage Analysis: 2000 to 2014

Flood damage analysis consists of three main steps: flood frequency curve, flood damage curve, and flood damage probability curve. Flood frequency curve mainly focuses on the extreme value distribution where the maximum observed discharges are fitted. Flood damage curve is the relationship between flood parameters and flood damages. Flood damage probability curve is the combination between flood frequency curve and flood damage curve.

4.3.1 Flood Frequency Curve

This part describes the method to develop flood frequency curve starting from the plotting position to the selection of extreme value distribution. The order of each flood needs to be calculated and classified according to its magnitude, from the largest to smallest. Number each of the floods in the order, starting with the biggest as number “1”. The order of flood is denoted by the letter “m”. For example, if 50 years of peak discharge data had been recorded, the flood order calculation would be for m = 1, m = 2, m = 3, …, m = 50. The recurrence interval or return period, an estimated likelihood of flood for a given magnitude occurs, can be determined using the following formula:

$$T = \frac{n+1}{m} \quad \text{(Eq. 4.6)}$$

Where

T : the recurrence interval or return period

n : the number of years in the record

m : the assigned number of the order of annual flood water level

Flood probability P(X ≥ x), the probability that flood in a given magnitude equaling or exceeding a specific magnitude is calculated by:

$$P(X \geq x) = \frac{1}{T} \quad \text{(Eq. 4.7)}$$

In this study, the daily observed water levels from Bak Trakoun flow station from 1994 to 2018 have been converted into discharges by rating equation in Table 3-2. The frequency analysis is implemented by fitting the annual maximum observed discharges with three extreme value distributions: Extreme Value Type I (Gumbel), Extreme Value Type II (Fréchet), and Log-Pearson Type III. In this case, the tests for goodness of fit (Chi-Square test) among the three distributions are performed in order to figure out which extreme value distribution is fitted well with the maximum observed discharges.

The Generalized Extreme Value (GEV) distribution was explained in (Chow, Maidment et al. 1988). The probability distribution function for the GEV is

$$F(x) = \exp\left[-\left\{1-\frac{k\ x-u}{\alpha}\right\}^{1/k}\right] \quad , \alpha > 0 \qquad \text{(Eq. 4.8)}$$

Where k, u, and α are parameters to be determined.

The three limiting cases are:

(1) For k = 0, the Extreme Value Type I distribution (Gumbel), for which the probability density function (PDF) is given in Table 11.5.1 in (Chow, Maidment et al. 1988).

(2) For k < 0, the Extreme Value Type II distribution (Frechet), for which Table 11.5.3 in (Chow, Maidment et al. 1988) applies for (u + α/k) ≤ x ≤ +∞, and

(3) For k > 0, the Extreme Value Type III distribution (Weibull), for which Table 11.5.3 in (Chow, Maidment et al. 1988) applies for -∞ ≤ x ≤ (u + α/k).

The parameters are estimated by:

$$\alpha = \frac{\sqrt{6}s}{\pi} \qquad \text{(Eq.4.9)}$$

$$u = \bar{x} - 0.5772\alpha \qquad \text{(Eq. 4.10)}$$

Where $\bar{x}$ and s are the average value and standard deviation of the annual maximum observed discharge respectively. For the Extreme Value distribution Type I, the theoretical discharge x_T is related to y_T by:

$$x_T = u + \alpha y_T \qquad \text{(Eq.4.11)}$$

And y_T is defined by:

$$y_T = -\ln\left[\ln\left(\frac{T}{T-1}\right)\right] \quad \text{(Eq. 4.12)}$$

However, the third condition of GEV (Weibull distribution) have not been selected for the frequency analysis. Instead, Log-Pearson Type III is used because the Log-Pearson Type III is a well-known extreme value distribution for the maximum value such as peak discharge of flood, while Weibull distribution is recommended for minimum value such as drought. The first step of Log-Pearson Type III is to take the logarithms of the hydrologic data (discharge), y = log x. The logarithm of theoretical discharge is defined by:

$$x_T = \bar{x} + K_T s \quad \text{(Eq. 4.13)}$$

Where $\bar{x}$ and s are the average value and standard deviation of logarithms of the annual maximum observed discharge respectively. K_T is the frequency factor, which can be expressed for Log-Pearson Type III as

$$K_T = z + (z^2-1)k + \frac{1}{3}(k^3-6z)k^2 - (z^2-1)k^3 + zk^4 + \frac{1}{3}k^5 \quad \text{(Eq. 4.14)}$$

Where k = C_s/6, and C_s is the coefficient of skewness. The value of z corresponding to an exceedance probability of p (p = 1/T) can be calculated by:

$$z = w - \frac{2.515517 + 0.802853w + 0.010328w^2}{1 + 1.432788w + 0.189269w^2 + 0.001308w^3} \quad \text{(Eq. 4.15)}$$

Where w is the value of intermediate variable, which can be calculated by

$$w = \left[\ln\left(\frac{1}{p^2}\right)\right]^{1/2} \quad \text{(Eq. 4.16)}$$

After analyzing each extreme value distribution, the test for goodness of fit (Chi-Square test) is implemented among those results. Chi-Square goodness of fit is a non-parametric test that is used to find out how the observed value of a given phenomenon is significantly different from the expected value. To compute the value of Chi-Square goodness of fit test, the following formula is applied for n observations in a frequency histogram, having k bins or class intervals:

$$\chi_0^2 = \sum_{i=1}^{k} \frac{(O_i - E_i)^2}{E_i} \quad \text{(Eq. 4.17)}$$

Where O_i : the observed frequency in the i^{th} class interval

E_i : the expected frequency in the i^{th} class interval

A goodness-of-fit statistic tests the following hypothesis:

- H_0 : the observed discharges fit with the model M_0
- H_1 : the observed discharges does not fit with model M_0

M_0 is the example of each extreme value distribution. To reject the hypothesis that the distribution of the population is the hypothesized distribution if:

$$\chi_0^2 > \chi_{k-p-1,\alpha}^2 \qquad \text{(Eq. 4.18)}$$

Where k: the number of bins in the frequency histogram

p: the number of parameters of the hypothesized distribution estimated by sample statistics

α: the significant level

4.3.2 Flood Damage Curve

Flood damage curve is the relationship between expected damage and varying depth of flood water as shown in Figure 4.4. Beside flood depth, flood discharge, flood duration and flood velocity can be used as a function with corresponding damages to create the flood damage curve. There are two methods used to assess stage-damage curve; first method is the utilization of actual damages recorded in the past and the second method relies on synthetic stage-damage function curve as shown in Figure 4.3. In this study, flood damage curve or stage-damage curve is developed using the damage in Agriculture and Affected people assessed by Google Earth Engine (GEE) and the record of annual maximum water level.

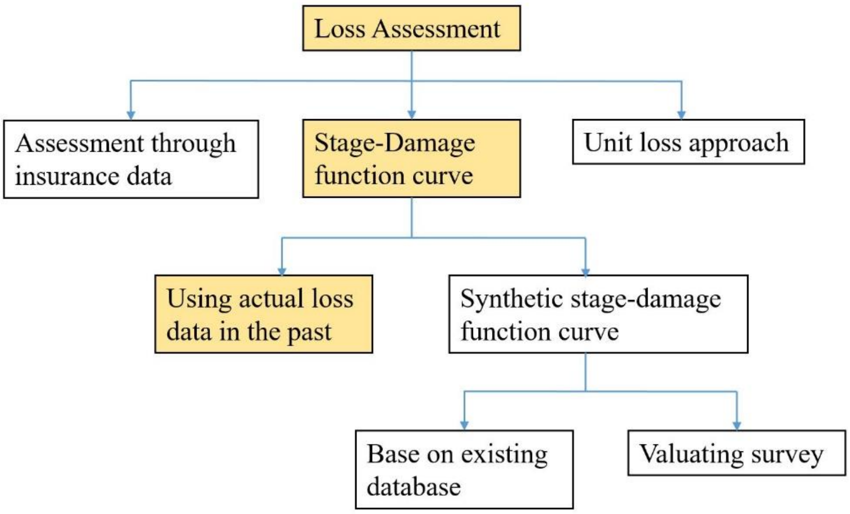

Figure 4.3: Method for the development of stage-damage function curve

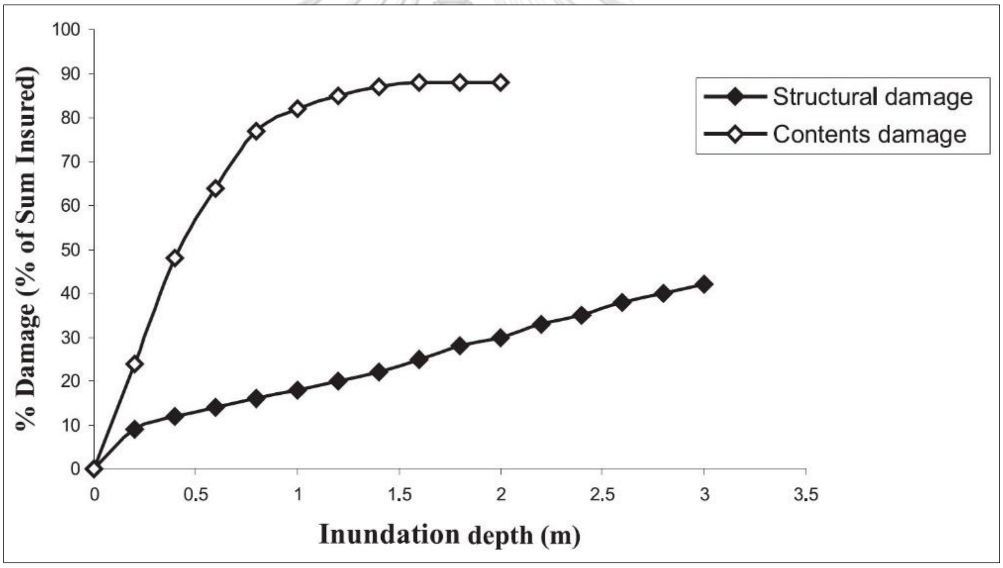

Figure 4.4: Example of flood damage curve or stage-damage curve (Australia 2002)

4.3.3 Flood damage Probability Curve and Average Annual Damages (AAD)

Damage probability curve is the graph representing the probability of an event versus extent of losses due to that event. The average annual damage (AAD) is the area under the damage probability curve, representing the average damages or losses due to annual exceedance probability of that event.

To calculate AAD, we need loss assessment for a range of possible events with its annual occurrence probability. These losses are plotted against their event occurrence probability as shown in Figure 4.5. At least three distinctly different events should be plotted to give some confidence in the resulting graph. The average annual damages are equal to the area under the curve, which can be obtained mathematically by integration. Thus, the high damage resulting from an extreme event would be multiplied by a very low probability, so that its average annual contribution would be small although the event loss would be very large. The degree of confidence in these occurrence probabilities varies widely depending on the type of hazard and the length and quality of the local record. Confidence is much lower for low probability events.

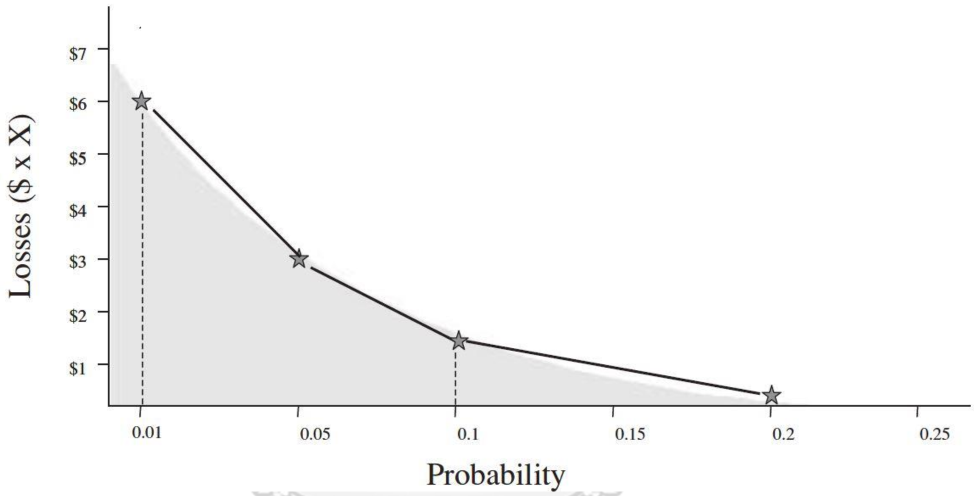

Figure 4.5: Example of average annual damages (Australia 2002)

4.4 Flood Damage Estimation and Analysis: 2030 and 2050

The detail of the data of Cambodia Economic Development in Agriculture, Industry, and Service have been released once in every five years by The Royal Government of Cambodia (RGC). The final National Strategic Development Plan of the RGC is from 2014 to 2018; however, some estimation and assumption in the future economic development have been made based on the long-term version of the RGC; for instance, Cambodia now is a lower-middle income country; therefore, the RGC plans to develop Cambodia to be an upper-middle-income country in 2030 and to be a high-income country in 2050.

Since the future socio-economic development has been estimated and assumed in the particular sector, the damages in the future caused by flood are also increased.

Vu and Ranzi (2017) stated that the improvement of living standards and an increase in property value as well as less awareness and preparedness of people to flood results a huge vulnerability of the society to flood hazard. In this analysis, 2030 and 2050 are considered as the event in the future for flood damage analysis. Future flood damages are also divided into two sectors as mentioned in the previous section: Agriculture and Affected people (People). The indicators of each sector to be estimated is shown in Figure 4.6.

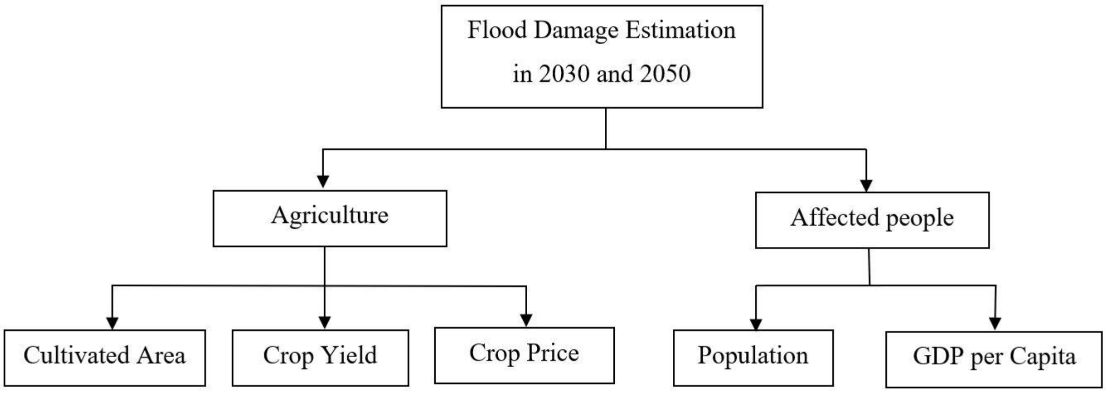

Figure 4.6: Flood damage estimation in 2030 and 2050

4.4.1 Damage in Agriculture

In this analysis, year 2030 and 2050 are considered as events in the future. Year 2030 is considered as an example of the calculation. The Agricultural Damage Probability Curve in 2030 (ADPC2030) is generated using the Agricultural Damage Curve in 2014 (ADC2014) and Flood Frequency Curve in 2030 (FFC2030). Based on the scope of this study, it is assumed that there is no change in discharge in 2030. Therefore, the Flood Frequency Curves in 2030 (FFC2030) are equal to the Flood Frequency Curve in 2014 (FFC2014). Hence, the ADPC2030 recommended by the Mekong River Commission (MRC) for the developing countries is estimated by:

$$V_{2030} = Sum(A_C \times Y_C) \quad \text{(Eq. 4.19)}$$

$$V_{2014} = Sum(A_C \times Y_C) \quad \text{(Eq. 4.20)}$$

$$AF1 = V_{2030}/V_{2014} \quad \text{(Eq. 4.21)}$$

$$ADPC2030 = AF1 \times ADPC2014 \quad \text{(Eq. 4.22)}$$

Where

- V is value of each crop type in each area

- A is area
- Y is unit price per area
- C is crop type
- AF1 is ratio of value of each crop type in each area between 2030 and 2014
- ADPC is Agricultural Damage Probability Curve
- NPV2030: assume discount rate of X% for the opportunity cost of capital of the project in the future

For a given crop at 2014 and 2030, the farm-gate value of a crop can be represented by:

$$FGV_C = A_C \times Y_C \times FGP_C \qquad \text{(Eq. 4.23)}$$

Where

- FGV_C : the farm-gate value (USD) of crop C
- A_C : the cultivated area of crop C (ha)
- P_C : the productivity of crop C (kg/ha), and
- FGP_C : the farm-gate price of crop C (USD/kg)

4.4.2 Affected people

The same condition as agriculture sector, year 2030 and 2050 are considered as the event in the future. For example, in the case of year 2030, Housing Damage Probability Curve (HDPC2014/2030) is generated using the 2014 Damage Curve (HDC2014) and the 2030 Flood Frequency Curve (FFC2030). This curve is generated by using the following formula:

$$HF1 = \frac{Pop\ 2030}{Pop\ 2014} \qquad \text{(Eq. 4.24)}$$

$$HF2 = \frac{GDPC2030}{GDPC2014} \qquad \text{(Eq. 4.25)}$$

$$HDPC2030 = HF1 \times HF2 \times HDPC2014 \qquad \text{(Eq. 4.26)}$$

Where

- HF1 : ratio of number of populations between 2030 and 2014
- Pop : number of populations
- HF2 : ratio of GDP per capita between 2030 and 2014

- GDPC : GDP per capita
- NPV2030 assume discount rate of X% for the opportunity cost of capital of the project in the future

4.4.3 Annual Risk Reduction and Residual Risk: 2030 and 2050

Annual risk reduction refers to a part of risk which has been cut out by any mitigation measures. Once Average Annual Damage (AAD) of flood is estimated, the measures to reduce the damages will be defined based on the condition of the flood prone areas. It implies that risk can only be minimized or reduced; it cannot be deleted. Therefore, after some parts of risk have been reduced, there are some risks left called “Residual Risk” as shown in Figure 4.7.

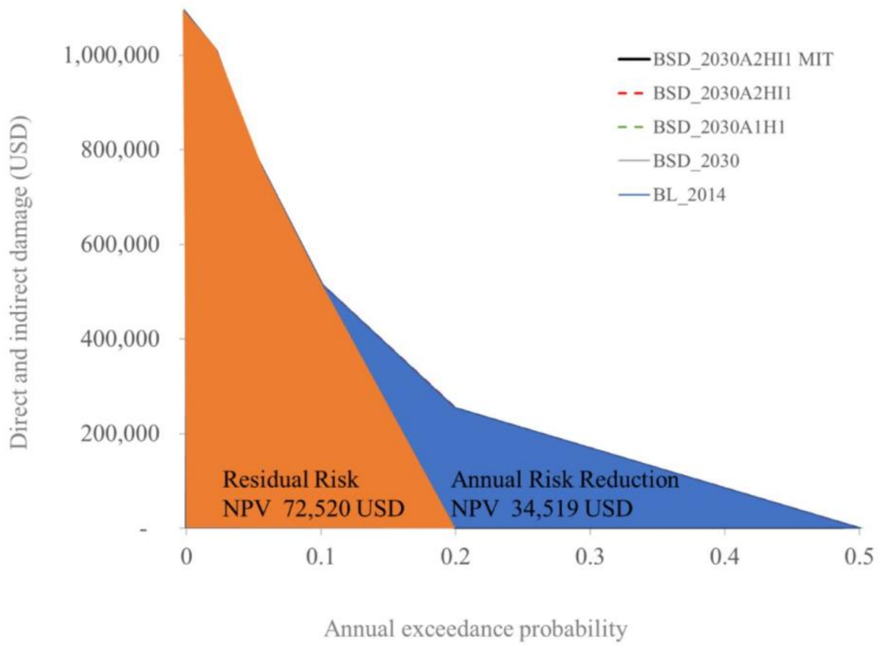

Figure 4.7: Annual risk reduction and residual risk (Suttinon 2017)

CHAPTER 5
RESULTS AND DISCUSSIONS

5.1 Flood Detection (Google Earth Engine)

Monthly Water History, v1.0 records global monthly water extent from 1984 to September 2015 (31 years). It is developed from Landsat 5 Thematic Mapper (TM), Landsat 7 Thematic Mapper-plus (ETM+), and Landsat 8 Operational Land Imager (OLI). Monthly Water History produces one map of water extent per month globally. Landsat is repeatedly covering the earth's surface every 16 days and two satellites operate concurrently with an 8-day cycle. It means that one satellite of Landsat can produce one image in every 16 days and with two satellites operating concurrently with an 8-days cycle, water can be detected in every 8 days. In this aspect, it is possible that a peak flood extent of a particular flood event can be detected if flood occurs more than 8 days or if the peak discharge of the flood event coincidently occurs with the same day of satellite record.

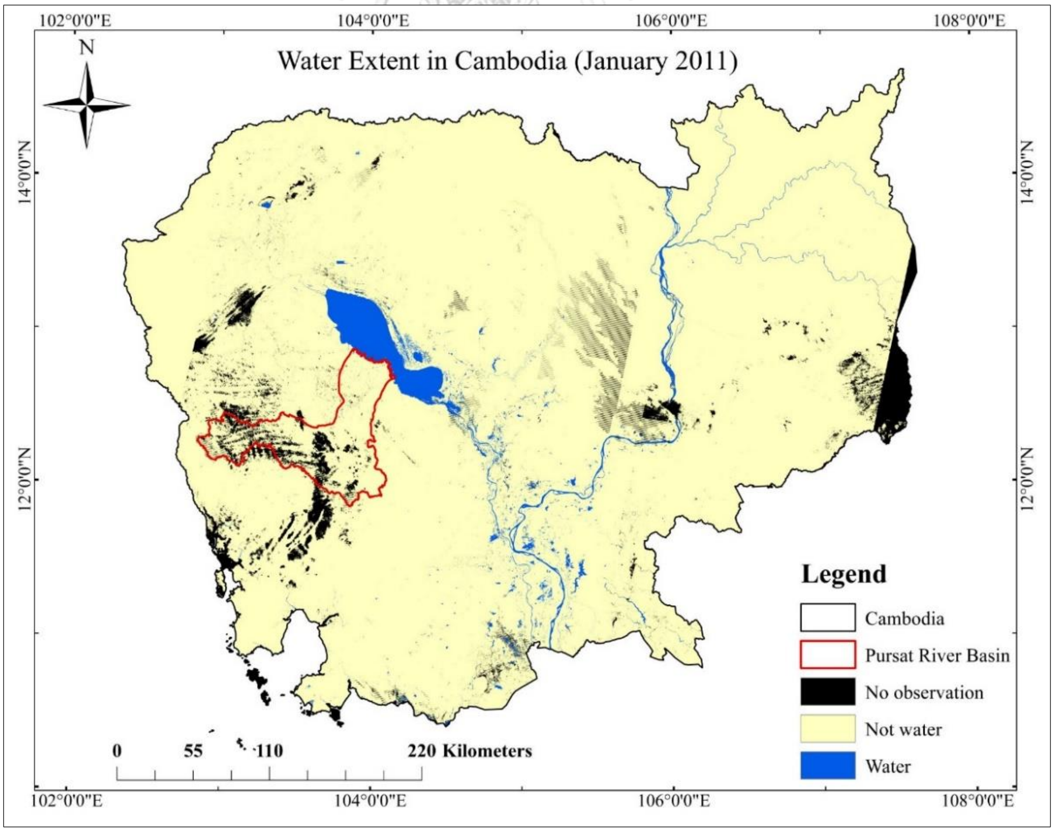

Figure 5.1: Water Extent in Cambodia in January 2011 (dry season)

The data was confirmed to be a very high accuracy in term of applying the suitable method to discriminate water pixels from other elements on the global scale over multiple decades with overall error of omission less than 5% and error of commission less than 1% (Pekel, Cottam et al. 2016). Available at monthly level with 30-meter resolution, the Monthly Water History, v1.0 is considered as a high-resolution mapping, which can be used to assess both seasonal and long-term change of global surface water. The data is available in Google Earth Engine Datasets. In order to access and extract the data, Earth Engine APIs (JavaScript or Python) is needed (APPENDIX A: Earth Engine Codes). There is only an important band for this dataset, which is "Water", but the value in this band was classified into three types, which are 0 (No observation), 1 (Not water) and 2 (Water) as indicated in Figure 5.1, Figure 5.2 and Figure 5.3. The "No observation" means the data cannot be detected due to technical error of operating system of the scan line corrector (SLC), and dynamic cloud shadow.

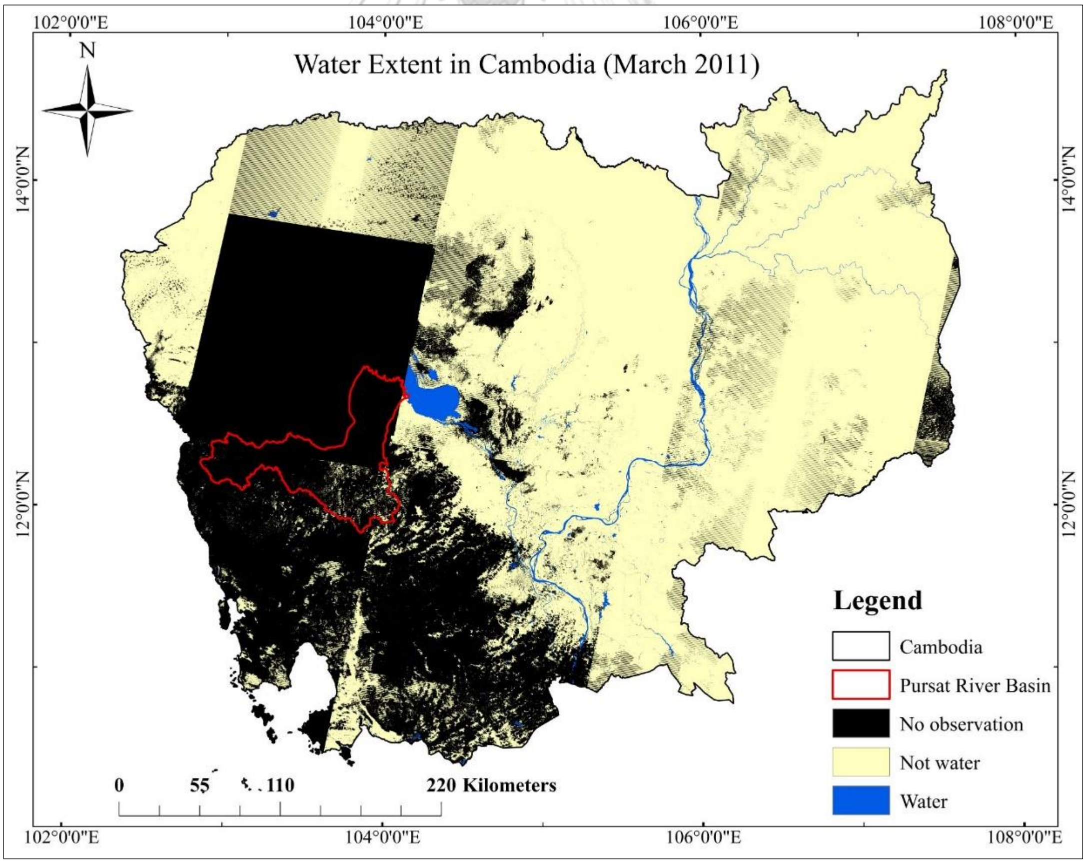

Figure 5.2: Water Extent in Cambodia in March 2011 (dry season)

Figure 5.1, Figure 5.2 and Figure 5.3 illustrate water extent in Cambodia in 2011 in January, March and October respectively. Figure 5.2 gives an example of March 2011, where the limitation of the data occurs making the map cannot be used to identify water extent due to no observation pixel covering the whole study area. Figure 5.2 and Figure 5.3 give an example of the difference of water extent between dry and rainy season in 2011 respectively. As can be seen in Figure 5.1, there is only water in the main rivers, reservoirs and lakes especially in Tonle Sap Lake in January (dry season), while Figure 5.3 indicates the large area of flood extent on other land covers around the rivers and lakes in October 2011, a month where flood occurred in the record. The dissimilarity of flood extent between dry and wet month can be clearly observed even though being annoyed by no observation pixels.

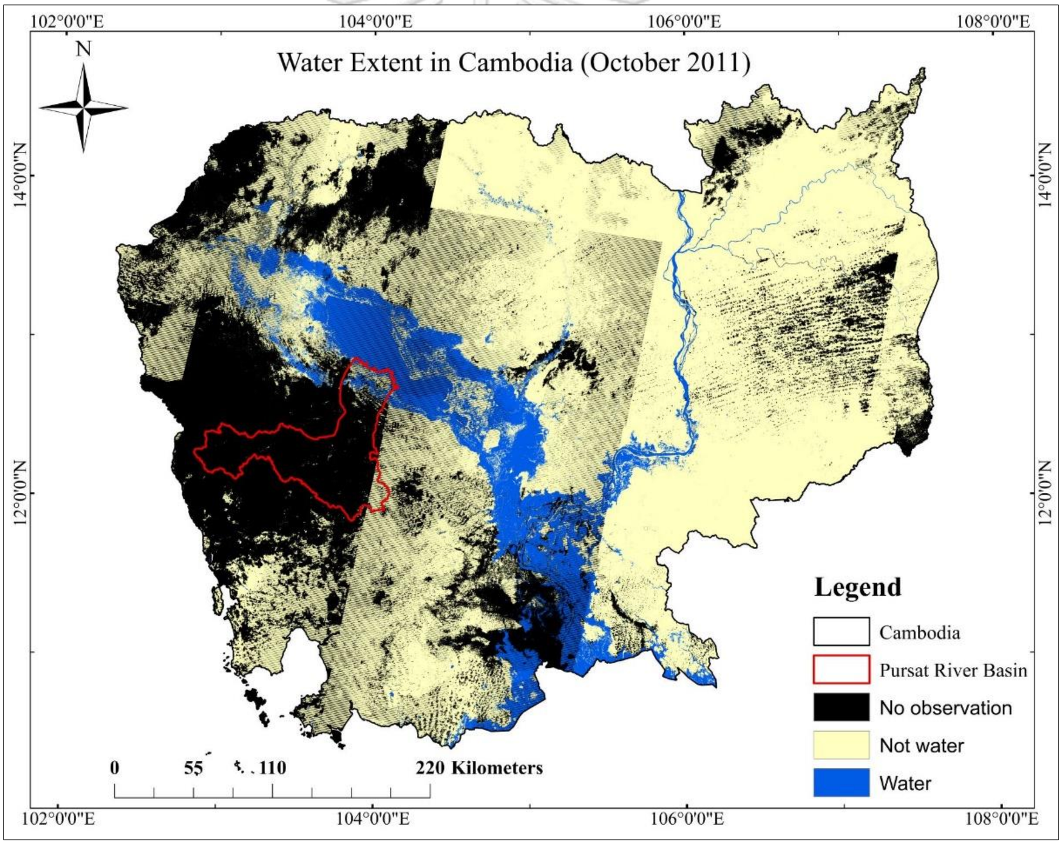

Figure 5.3: Water Extent in Cambodia in October 2011 (Rainy Season)

The seasonal pattern of monthly water extent keeps following the same trend, where the small area of water extent exists in the dry season and the large area of water extent presents in rainy season. The time-series mapping of monthly water extent in each year also provides a better understanding about the characteristic of wet year (flood year), normal year and dry year (drought year) of a particular year. The example of time-series monthly water extent area for the whole year (12 months) in 2013 are shown in APPENDIX B: Monthly Water Extent Map in 2013.

Since Monthly Water History, v1.0 can provide a better monthly detection of surface water, we would like to figure out the relationship between monthly water level from Tak Trakoun flow station and monthly water extent from Google Earth Engine. The peak value of water level or discharge is taken into account because the objective of this research is about the flood. In this regard, the maximum monthly water level and maximum monthly water extent are used to find the correlation. Two sets of monthly water extent images are analyzed, which are monthly water extent in Pursat River Basin and monthly water extent in Bakan and Phnom Kravanh districts. Water level from only Bak Trakoun flow station is used since Bakan and Phnom kravanh distrits are a part of Pursat River Basin.

5.1.1 Pursat River Basin

Table 5-1 shows the available maps of monthly water extent in Pursat River Basin from 2000 to 2014 excluding 2004, where there is no record of water level. In this case, number 0 (zero) means the map is not available or cannot be used in that month due to the disturbance of no observation pixels as shown in Figure 5.2 and number 1 (one) means the map is available and the quality of the map is acceptable without the disturbance of no observation pixels. The total maps should be used within these 14 years are 168 maps, yet only 75 maps are usable. The analysis of water extent area is made using the geospatial analysis tools in ArcGIS and the areas of water extent in each month are indicated in APPENDIX C: Water Extent Area.

Figure 5.4 indicates the relationship between maximum monthly water level (m.AMSL) and maximum monthly water extent (km^2) using the graphical analysis to examine the reliability of the regression analysis. Using water level as the predictor variable and water extent as the dependent variable, the coefficient of determination (R^2) is equal to 0.53 and correlation coefficient (R) is equal to 0.73. Using 95% confidence level, the significant level (α) is equal to 8.71×10^{-13} much smaller than 0.05, which mean the regression analysis is acceptable. Both variables have a positive correlation with each other, which means water extent area get larger when water level is higher; it can be also said that water extent in the Pursat River Basin can be only 53.5% explained by the water level at Bak Trakoun flow station, while the other 46.5% is unexplainable or affected by other sources.

Table 5-1: Monthly Water History, v1.0 in Pursat River Basin

Month	Image Cambodia (75 images)															
	2000	2001	2002	2003	2004	2005	2006	2007	2008	2009	2010	2011	2012	2013	2014	2015
January	0	0	1	1	0	0	1	1	1	1	1	1	1	1	1	0
February	0	0	0	1	0	0	1	1	1	1	1	1	0	0	0	0
March	1	0	1	1	0	0	0	1	1	1	1	1	0	0	1	0
April	0	0	1	1	0	1	1	1	0	0	1	0	0	0	1	0
May	0	0	0	0	0	1	0	1	0	0	1	0	0	0	0	0
June	0	0	0	0	0	1	1	0	0	0	0	0	0	1	0	0
July	0	0	0	0	0	0	0	0	0	0	1	0	1	1	0	0
August	1	0	0	0	0	1	0	0	1	0	0	1	0	0	0	0
September	0	0	1	0	0	1	1	0	0	0	0	0	0	1	0	0
October	0	0	0	0	0	0	1	0	0	0	0	1	1	1	1	0
November	1	0	1	1	0	1	1	1	0	0	0	0	1	0	0	0
December	1	0	1	1	0	1	1	1	1	1	1	0	0	1	1	0

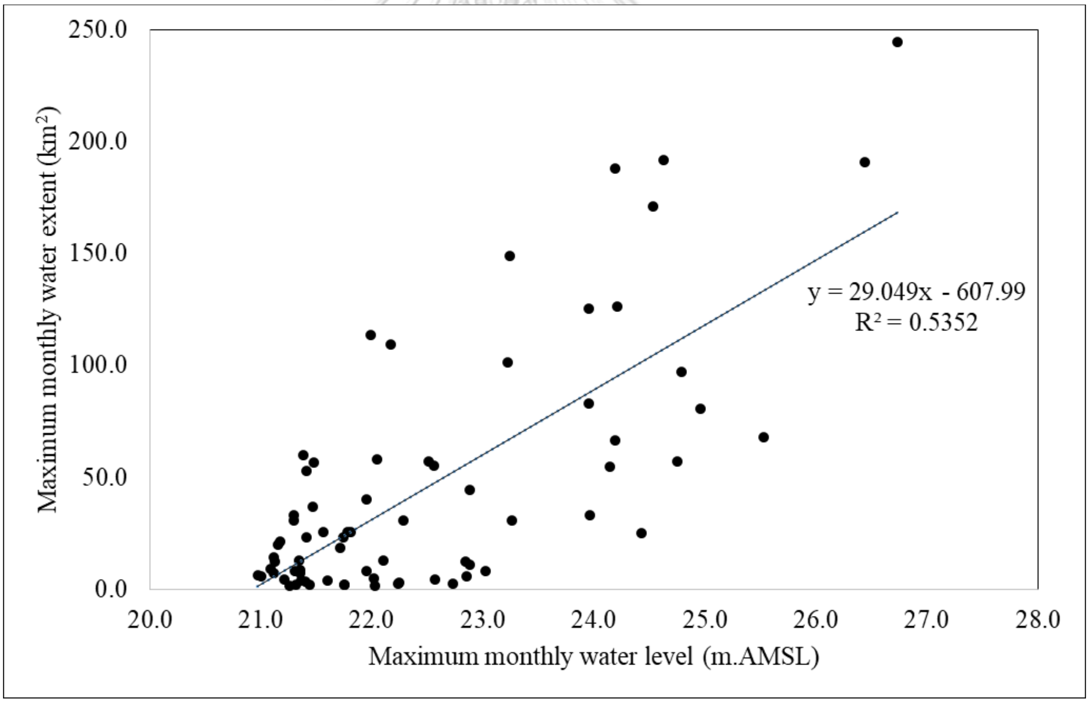

Figure 5.4: Relationship between maximum monthly water level and maximum monthly water extent in Pursat River Basin

Beside the discharge from the upstream represented by water level at Bak Trakoun flow station, there are factors possibly affecting the changes of water extent in the Pursat River Basin. For example, the downstream part of Pursat River Basin is located close to the Tonle Sap Lake; it is possible that water extent in the basin near

Tonle Sap Lake is highly impacted by water extent from Tonle Sap Lake in the rainy season, especially in the flooded forest areas around the Lake. Another possible and important reason is that, the no observation pixels on the image can also cause the underestimation of water extent in the basin especially when the peak discharge occurs meaning that those water extents are not well-represented the peak discharge. This issue will cause a very low correlation if those data is taken into account for the regression analysis.

5.1.2 Bakan and Phnom Kravanh Districts

Bakan and Phnom Krvanh districts, the two districts of Pursat province, are a part of Pursat River Basin as shown Figure 3.1. These two districts are located in the middle and the downstream parts of Pursat River Basin. Since the economic analysis is made based on the administrative map, the correlation between maximum monthly water level and maximum monthly water extent in these two districts needs to be examined so that the further economic analysis in these two districts can be confirmed to be reliable and acceptable based on the background of hydrological analysis.

Table 5-2: Monthly Water History, v1.0 in Bakan and Phnom Kravanh districts

Month	**Image Cambodia (80 images)**															
	2000	**2001**	**2002**	**2003**	**2004**	**2005**	**2006**	**2007**	**2008**	**2009**	**2010**	**2011**	**2012**	**2013**	**2014**	**2015**
January	0	0	1	1	0	0	1	1	1	1	1	1	0	1	0	1
February	0	0	0	1	0	0	0	1	1	1	1	1	1	1	1	1
March	1	0	1	0	0	0	1	1	1	1	1	0	0	0	1	1
April	0	0	1	1	0	1	0	1	0	0	1	0	1	0	1	1
May	0	0	0	0	0	0	0	1	0	1	1	0	0	1	1	1
June	0	0	0	0	0	1	1	0	0	0	1	1	0	1	0	0
July	0	0	0	0	0	0	0	0	1	0	0	1	1	0	0	1
August	1	0	0	0	0	1	0	0	1	0	0	1	1	0	0	1
September	0	0	0	0	0	0	1	0	0	0	1	0	0	1	0	0
October	0	0	0	1	0	0	1	0	0	0	1	1	1	1	1	0
November	1	0	1	1	0	1	0	1	0	0	0	1	1	0	0	0
December	1	0	0	1	0	1	0	1	1	0	1	0	0	0	1	0

Table 5-2 indicates the available maps of monthly water extent in Bakan and Phnom Kravanh districts from 2000 to 2015. The same condition is made (0: No map and 1: Map). The total maps can be used are 80 maps out of 180 maps. The same statistical analysis is applied in Bakan and Phnom Kravanh districts. The result shows the better correlation between maximum monthly water level and maximum monthly water extent in Bakan and Phnom Kravanh distiricts. Correlation of determination

(R^2) is equal to 0.57, higher than that of Pursat River Basin. The result indicates that around 58% of maximum monthly water extent in Bakan and Phnom Kravanh districts can be explained by maximum monthly water level or discharge at Bak Trakoun flow station. The correlation between maximum monthly water level and water extent in Bakan and Phnom Kravanh districts is a little bit better than that of Pursat River Basin; this is because Bakan and Phnom Kravanh districts are located in the middle part of the basin closed to Bak Trakoun flow station, while the whole basin is too large to use one flow station to represent the area of water extent. Moreover, it is observed that maximum water extent in Bakan and Phnom Kravanh districts is normally smaller than that of Pursat River Basin because the two districts cover only some parts of the flat land at the middle and downstream area while the whole basin should be greater.

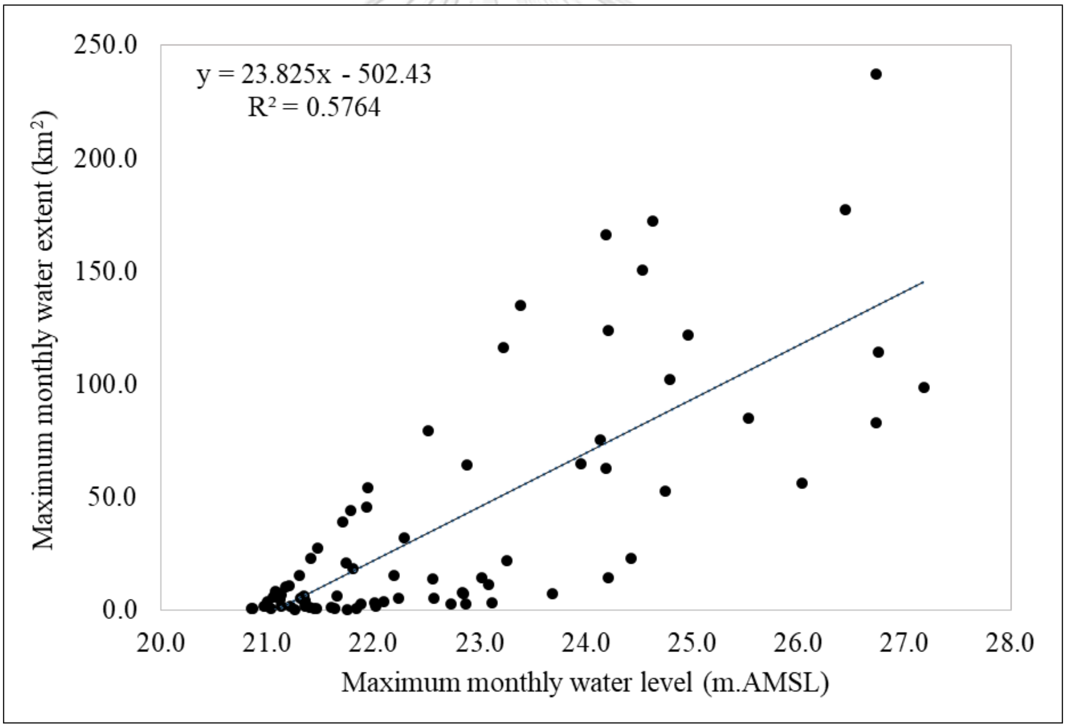

Figure 5.5: Relationship between maximum monthly water level and maximum monthly water extent in Bakan and Phnom Kravanh districts

Since one of the purposes of applying regression analysis is to find the form of the relationship between the two variables, it is important to identify the better fitted line of the relationship. In this case, there are some techniques applied to the raw data of both variables before conducting the statistical test to get a better fitted linear regression line. As shown in Figure 5.6, the deviation from annual average provides a better correlation with R^2 equal to 0.59 and better predicted value of water extent from the fitted line.

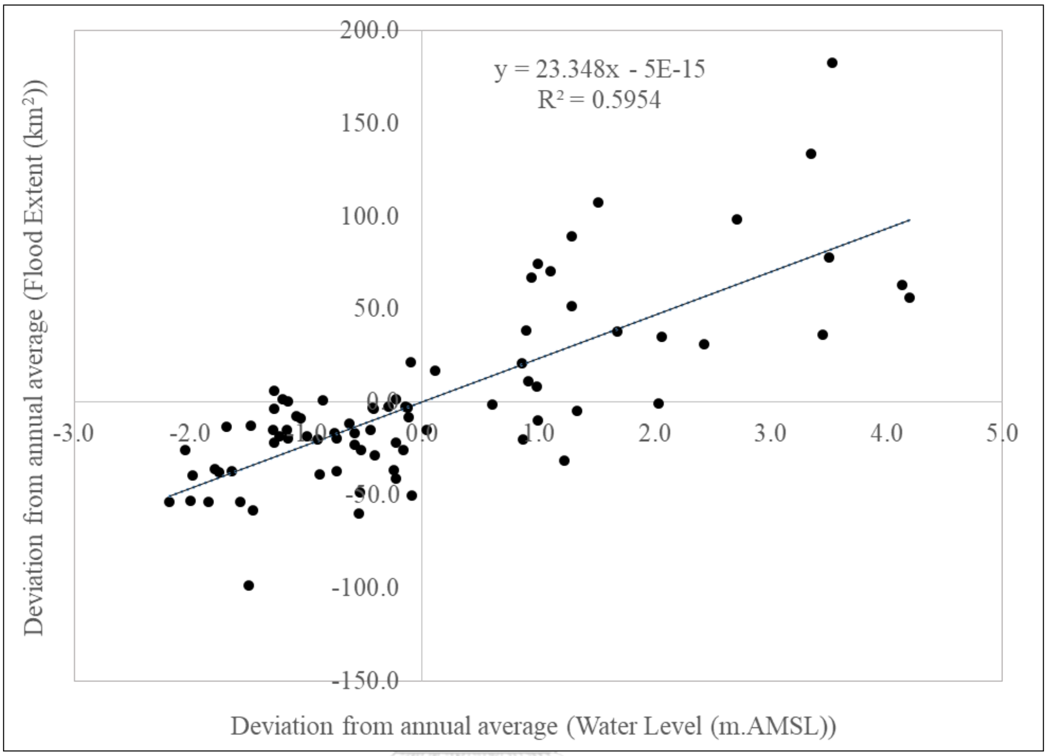

Figure 5.6: Relationship between maximum monthly water level and maximum monthly water extent in Bakan and Phnom Kravanh districts

Based on this analysis, it is possible to select one option between Pursat River Basin and Bakan and Phnom Kravanh districts to further analyze the economic losses due to flood impact. However, it is recommended that the administrative area should be selected to do the economic analysis so that the policy makers can have a better understanding whether which part of the districts will be potentially damaged and how much money that is estimated to be lost if flood will occur in these districts. Moreover, the correlation between maximum monthly water level and maximum monthly water extent in Bakan and Phnom Kravanh districts is also better making it even more reasonable to select Bakan and Phnom Kravanh for flood damage analysis.

5.1.3 Flood Extent in Bakan and Phnom Kravanh Districts

According to MOWRAM, the threshold discharge at Bak Trakoun flow station to be warned for flood preparation and mitigation is at 800 m^3/s or 26.06 m.AMSL.

Based on this declaration, the year considered to be the flood year must have the discharge more than or equal to 800 m^3/s or water level higher than or equal to 26.06 m.AMSL. Figure 5.7 indicates the record of annual maximum water level from 1994 to 2018 comparing with the threshold water level.

Because the analysis of flood damage is taken into account only 15 years between 2000 and 2014, floods within this period are taken place in 2000, 2003, 2006, 2010, 2011, 2012 and 2013. Based on the historical flood record from NCDM, Cambodia experienced major floods in 2000, 2011 and 2013 within the last two decades, however, there were also minor floods in a particular area of the country producing minor damages, which were not included in the historical flood record.

As mentioned by MOWRAM, the rainy season in Cambodia starts from May to October, while the dry season takes place between November and April. The average monthly water level in Figure 5.8 shows that September and October, the last two months of the rainy season, have a high probability of flood occurrence since the annual maximum water level mostly exists between these two months. In this aspect, the cumulative of maximum monthly water extent between September and October are extracted from Google Earth Engine to utilize as the flood extent map for the corresponding flood year based on the annual maximum discharge or water level.

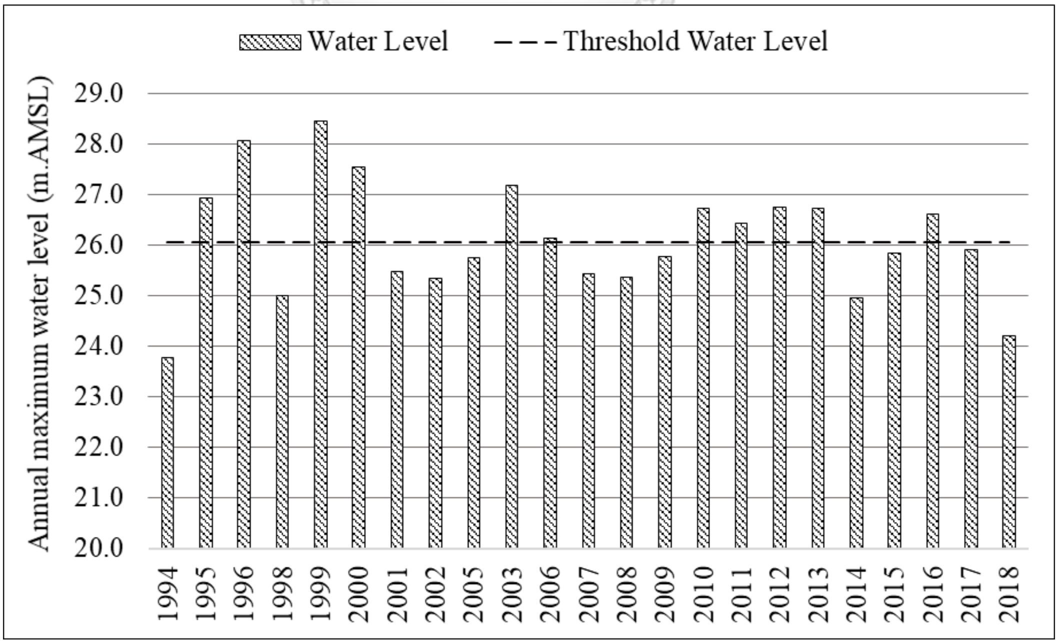

Figure 5.7: Annual maximum water level at Bak Trakoun flow station

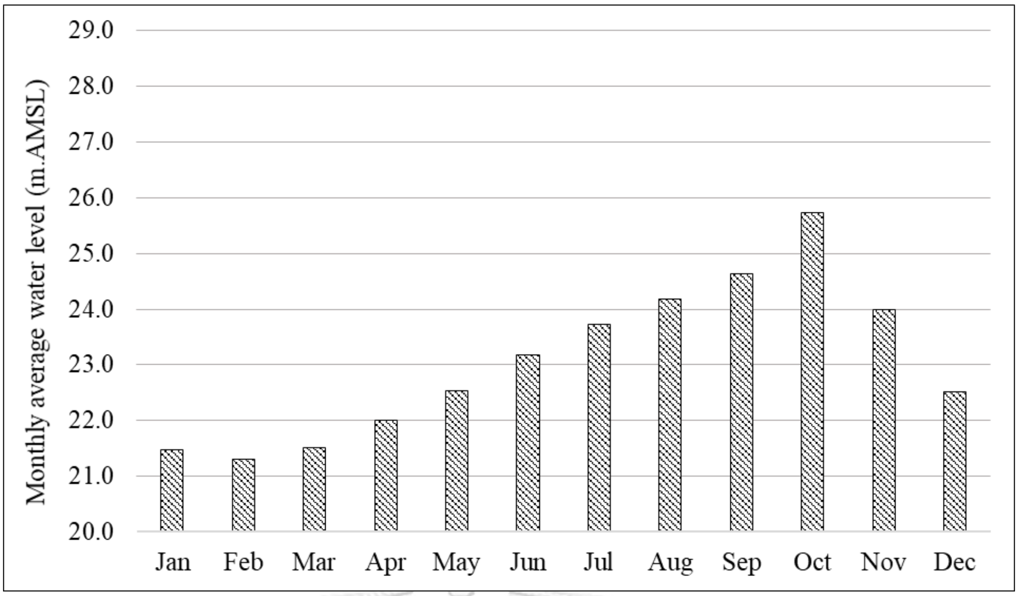

Figure 5.8: Monthly average water level from 1994 to 2018

The benefit of the two-month combination of image is to significantly reduce the no observation pixels from the maps because some pixels of no observation overlap with water pixels, which automatically decrease the actual water extent area. This situation will cause the underestimation of flood extent area during performing the spatial analysis in ArcGIS. However, this method still cannot improve the flood maps in case that the no observation pixels exist on the monthly images of both September and October.

Flood map in 2000, 2003, 2006, 2010, 2011, 2012 and 2013 in Cambodia as well as in Bakan and Phnom Kravanh districts are shown in Figure 5.9. As can be seen in Figure 5.9, the cumulative flood extent between September and October in each flood year provides a better result with the reduction of no observation pixels on the images. The fact about this flood map is that flood extent in the map can be as big as the real flood extent if the detection time is coincident with the peak flood period or it can be smaller than that of the real flood extent if the detection time is before or after the peak flood extent. There is no way that flood extent area in the map is bigger than that of the real flood extent. Hence, the concept of reducing the no observation pixels from the image is to enlarge the area of flood extent on the maps as much as possible to be similar to the original flood detection from satellite (smaller or equal to the real flood extent) without disturbance from dynamic cloud shadows.

2000	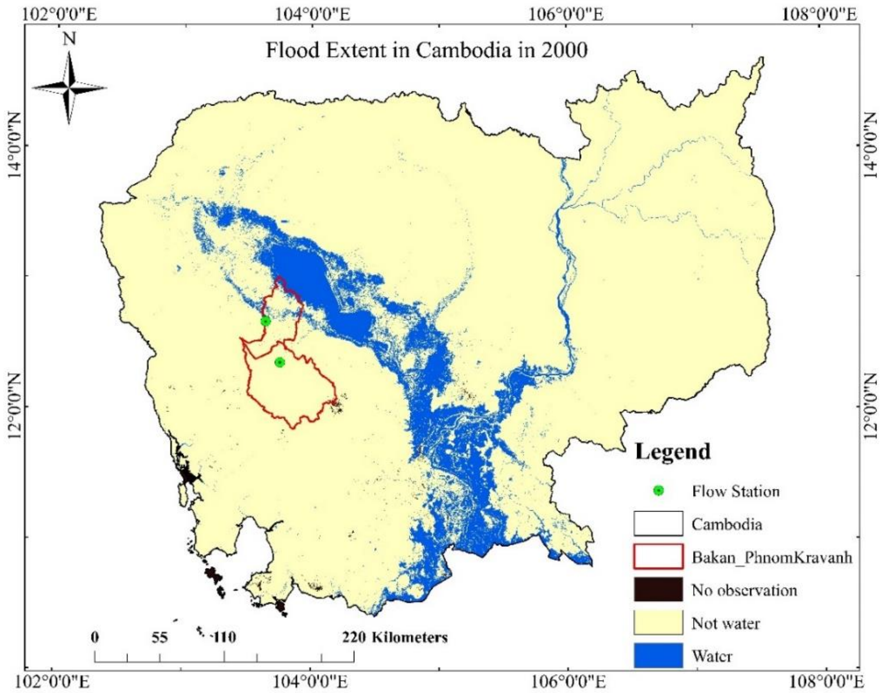
2003	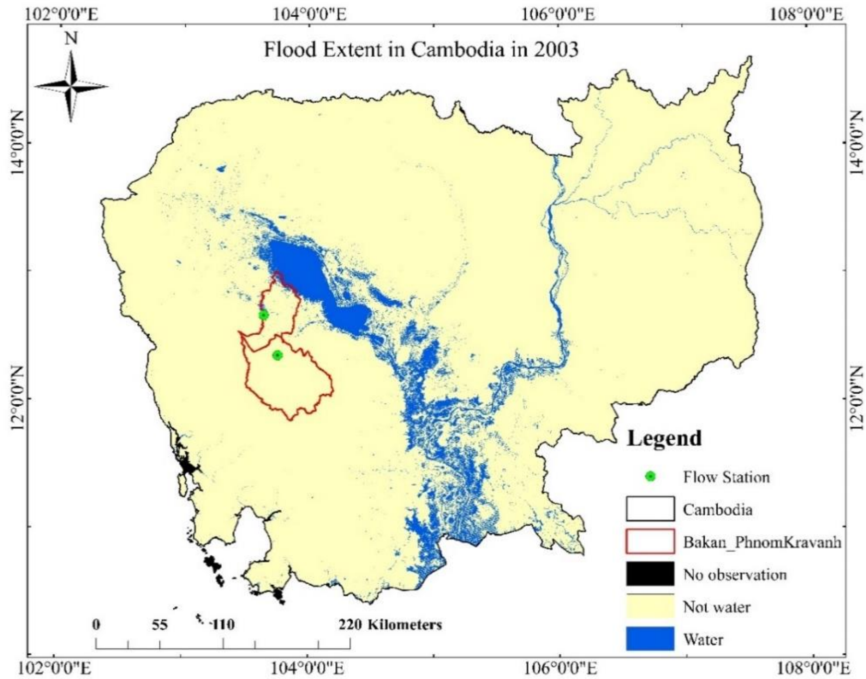

Flood Extent in Cambodia in 2000
102°0'0"E
104°0'0"E
106°0'0"E
108°0'0"E
14°0'0"N
12°0'0"N
N
Legend
Flow Station
Cambodia
Bakan_PhnomKravanh
No observation
Not water
Water
0
55
110
220 Kilometers

Flood Extent in Cambodia in 2003
102°0'0"E
104°0'0"E
106°0'0"E
108°0'0"E
14°0'0"N
12°0'0"N
N
Legend
Flow Station
Cambodia
Bakan_PhnomKravanh
No observation
Not water
Water
0
55
110
220 Kilometers

2006	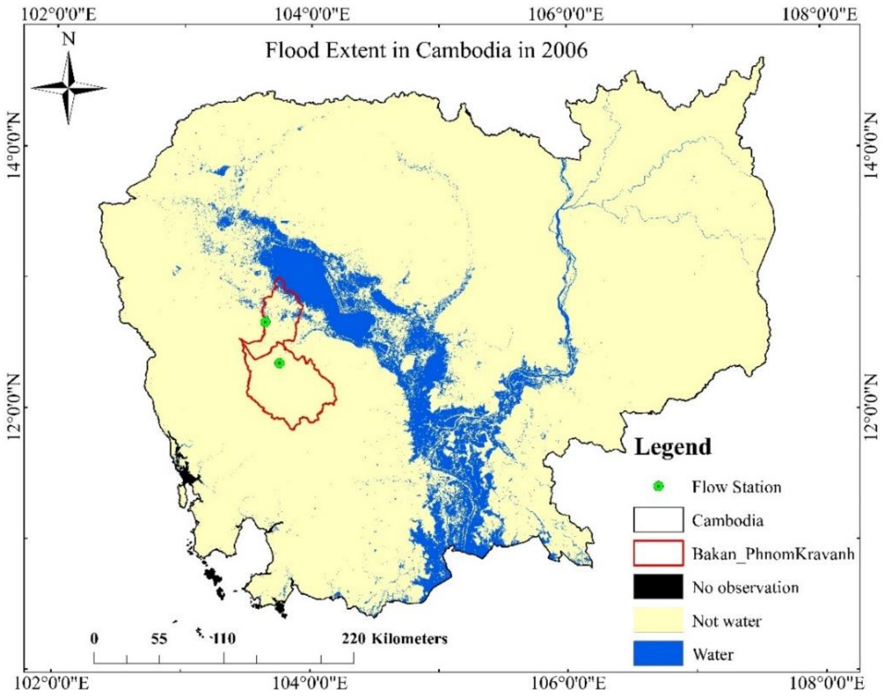
2010	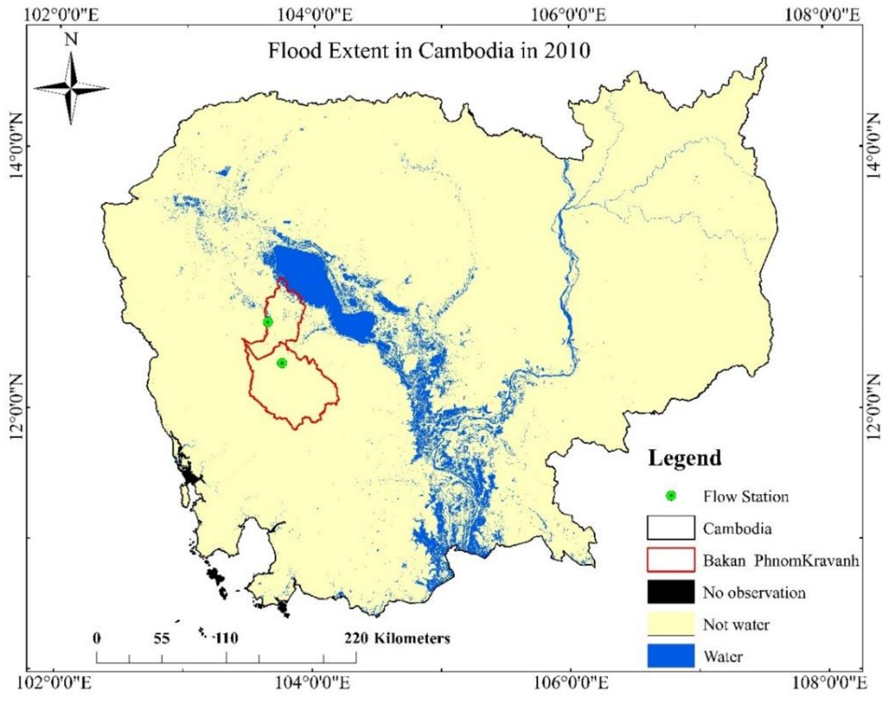

Flood Extent in Cambodia in 2006
102°0'0"E
104°0'0"E
106°0'0"E
108°0'0"E
14°0'0"N
12°0'0"N
N
Legend
Flow Station
Cambodia
Bakan_PhnomKravanh
No observation
Not water
Water
0 55 110 220 Kilometers

Flood Extent in Cambodia in 2010
102°0'0"E
104°0'0"E
106°0'0"E
108°0'0"E
14°0'0"N
12°0'0"N
N
Legend
Flow Station
Cambodia
Bakan_PhnomKravanh
No observation
Not water
Water
0 55 110 220 Kilometers

2011	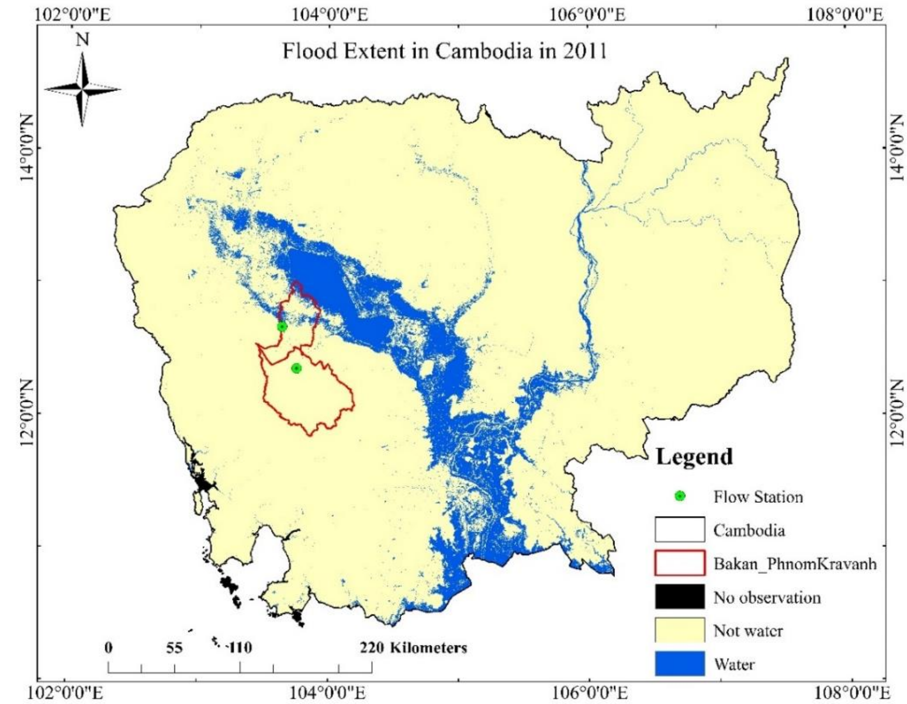Flood Extent in Cambodia in 2011 N 102°0'0"E 104°0'0"E 106°0'0"E 108°0'0"E 14°0'0"N 12°0'0"N 0 55 110 220 Kilometers Legend Flow Station Cambodia Bakan_PhnomKravanh No observation Not water Water
2012	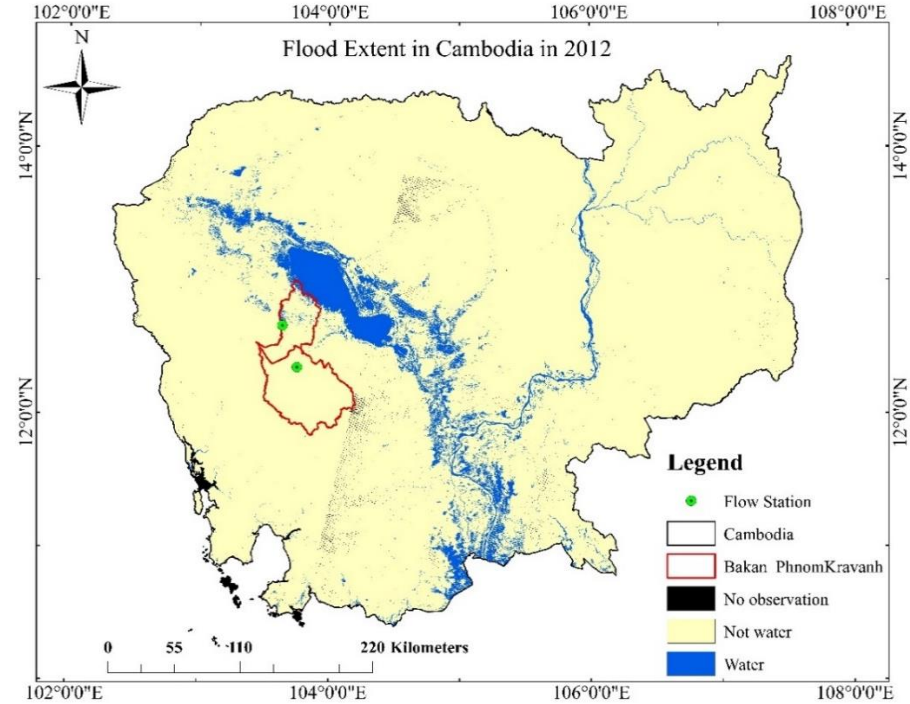Flood Extent in Cambodia in 2012 N 102°0'0"E 104°0'0"E 106°0'0"E 108°0'0"E 14°0'0"N 12°0'0"N 0 55 110 220 Kilometers Legend Flow Station Cambodia Bakan_PhnomKravanh No observation Not water Water

2013	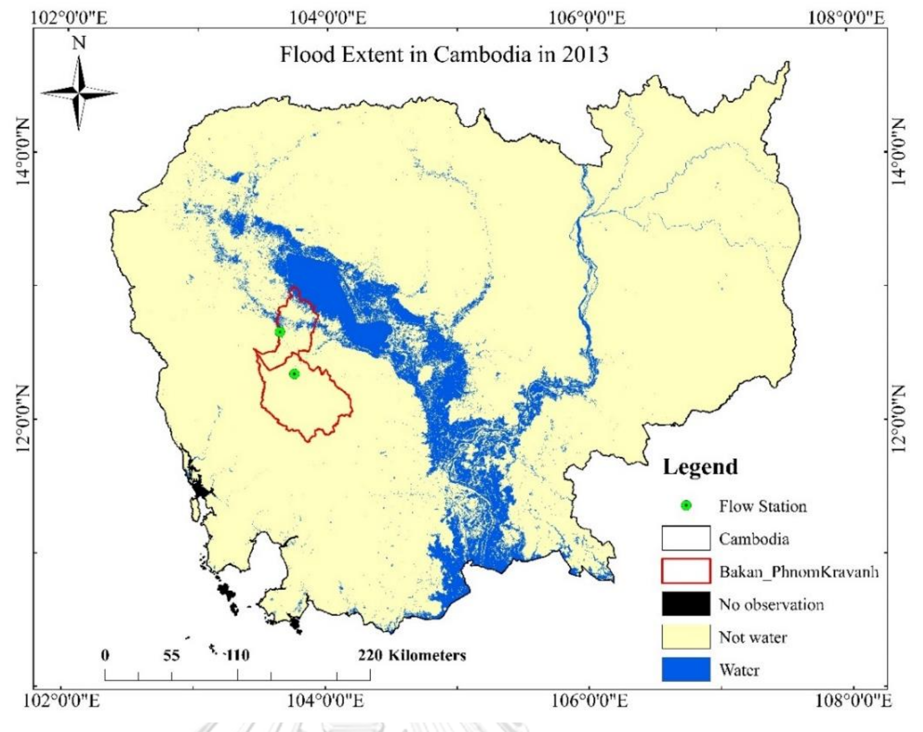

Figure 5.9: Cambodia Flood Extent: Bakan and Phnom Kravanh districts

The correlation coefficient (R) between the annual maximum flood extent and corresponding annual maximum water level is 0.38 as shown in Figure 5.10 with the significant level $\alpha = 0.03$ (smaller than 0.05). It is acceptable that annual maximum flood extent can be explained by the annual maximum water level (38%), but in a low and limited relationship since the unexplained variable is greater. The reason why the percentage of unexplained variation is higher than that of explained variation is because the sources of flood in Pursat River Basin as well as Bakan and Phnom Kravanh districts are the flow from the upstream, the rainfall in the River Basin and the backwater effect from the Tonle Sap Lake in rainy season at the downstream of the River Basin. In this case, only the upstream flow represented by water level at Bak Trakoun flow station is used as the predictor variable in the regression analysis, which is not well-represented the reality of the sources creating the floods in Pursat River Basin and well as Bakan and Phnom Kravanh districts. However, still these flood maps will be used as the corresponding flood extent maps in each flood year to overlay with time-series land covers and Nighttime Light Index maps to find the affected area in Agriculture and the Affected people in Bakan and Phnom Kravanh districts.

Normal	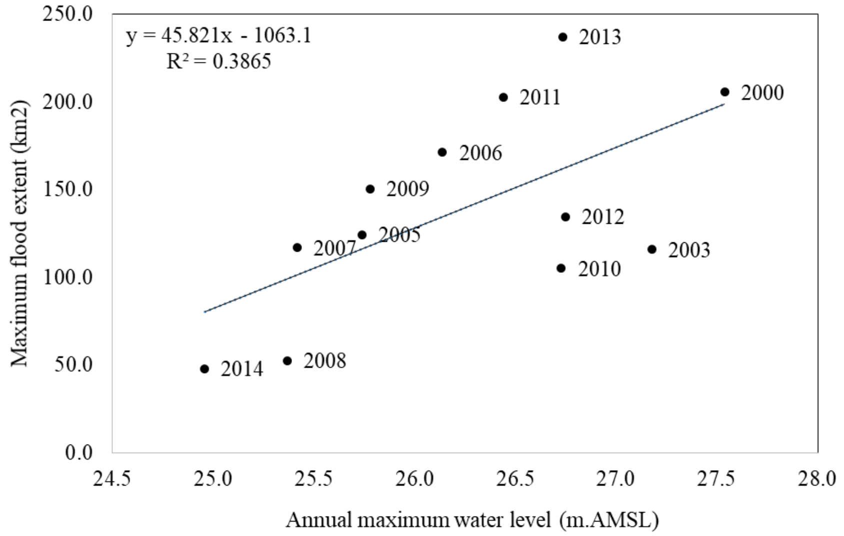
Logarithm	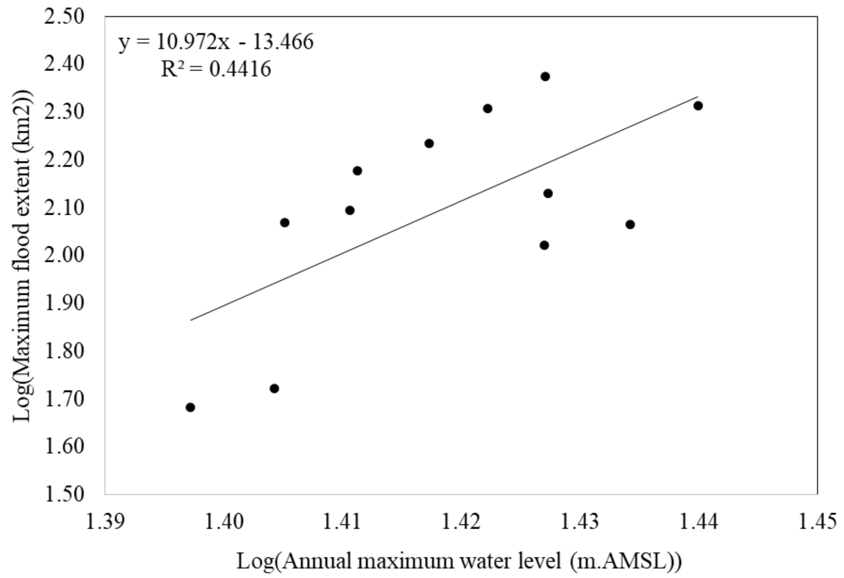

Figure 5.10: Relationship between annual maximum water level and annual maximum flood extent in Bakan and Phnom Kravanh districts

5.2 Flood Damage Estimation: 2000 - 2014

This part describes the estimation of physical flood damage and flood damage in monetary terms in Bakan and Phnom Kravanh districts from 2000 to 2014. Flood damage refers to the areas affected and destroyed by flood extent, which can be evaluated by the integration between flood extent and land cover. Since Pursat is one of the typical agricultural provinces in Cambodia, the common damages caused by flood are agriculture and people and infrastructure.

5.2.1 Agriculture

According to the Land Cover Portal of MEKONG SERVIR, Land cover is classified into 18 cover types in the Lower Mekong Countries as shown in Table 5-3. The annual land cover from 2000 to 2014 are extracted from Land Cover Portal, which originated in Google Earth Engine.

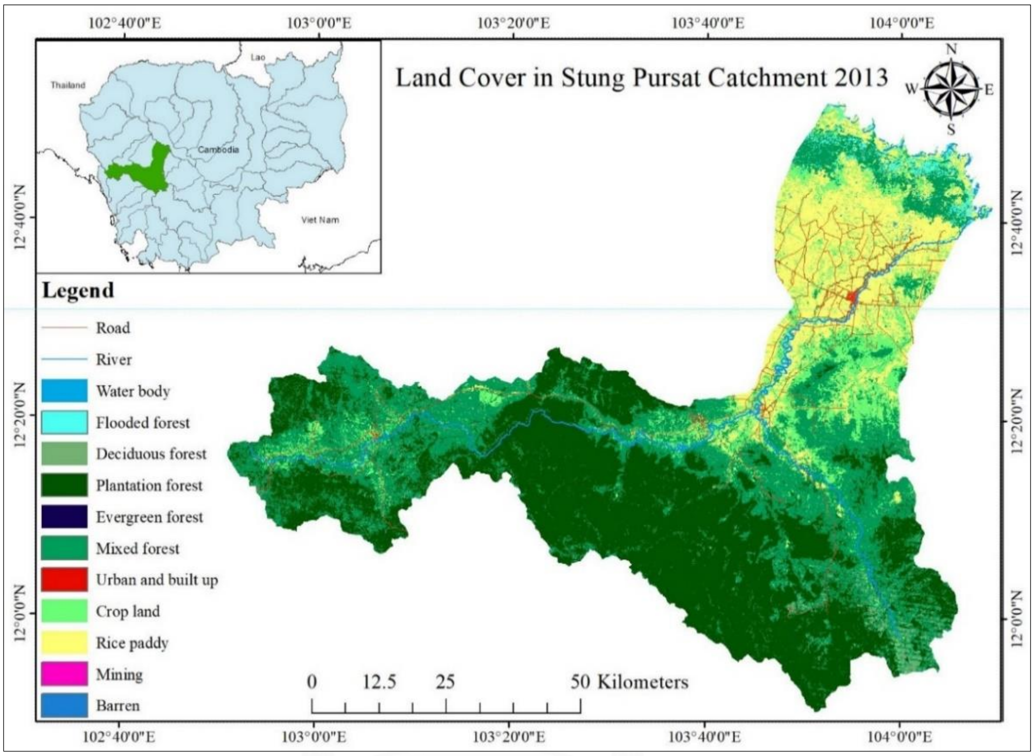

Figure 5.11: Land Cover in Pursat River Basin in 2013

Table 5-3: Land cover typology (https://rlcms-servir.adpc.net/en/landcover/)

Land Cover Typology	Pixel Value	Band Code in GEE
Unknown	0	6f6f6f
Surface Water	1	aec3d4
Snow and Ice	2	b1f9ff
Mangroves	3	111149
Flooded Forest	4	287463
Forest	5	152106
Orchard or Plantation Forest	6	c3aa69
Evergreen Broadleaf	7	7db087
Mixed Forest	8	387242
Urban and Built Up	9	cc0013
Cropland	10	8dc33b

Rice	11	ffff00
Mining	12	cec2a5
Barren	13	674c06
Wetlands	14	3bc3b2
Grassland	15	f4a460
Shrubland	16	800080
Aquaculture	17	51768e

Figure 5.11 indicates the cover types in Pursat River Basin in 2013, which is the same as that of Bakan and Phnom Kravanh districts. Based on the similar characteristic, these cover types are reclassified into 5 important types: Water body, Forest, Urban and Built up, Agriculture and others. Forest is the combination of Flooded, Deciduous, Plantation, Evergreen, and Mixed forest; Agriculture is the combination of Cropland and Rice paddy; and others is the combination of Mining and Barren.

The integration between annual maximum flood extent and annual land covers is resulted in the affected land cover types in Bakan and Phnom Kravanh districts as shown in Figure 5.12, particularly Agriculture, which are Cropland and Rice in Figure 5.13. As can be seen in Figure 5.12, flood extent in the last 15 years did not affect Urban and Built up area, and others (Mining and Barren). This is because the Urban and Built up area includes only the city or small town in the province, while the small villages in the rural areas, which are prone to flood are excluded. In term of Mining and Barren, these areas are minor and located on the high land so that there is no effect from flood. The Forest under flood extent is mostly flooded and plantation forest near Tonle Sap Lake; however, no significant damages in Forest is taken into account according to the record from National Committee for disaster management (NCDM). Likewise, Water body under flood extent means nothing especially for the natural water bodies such as rivers and lakes.

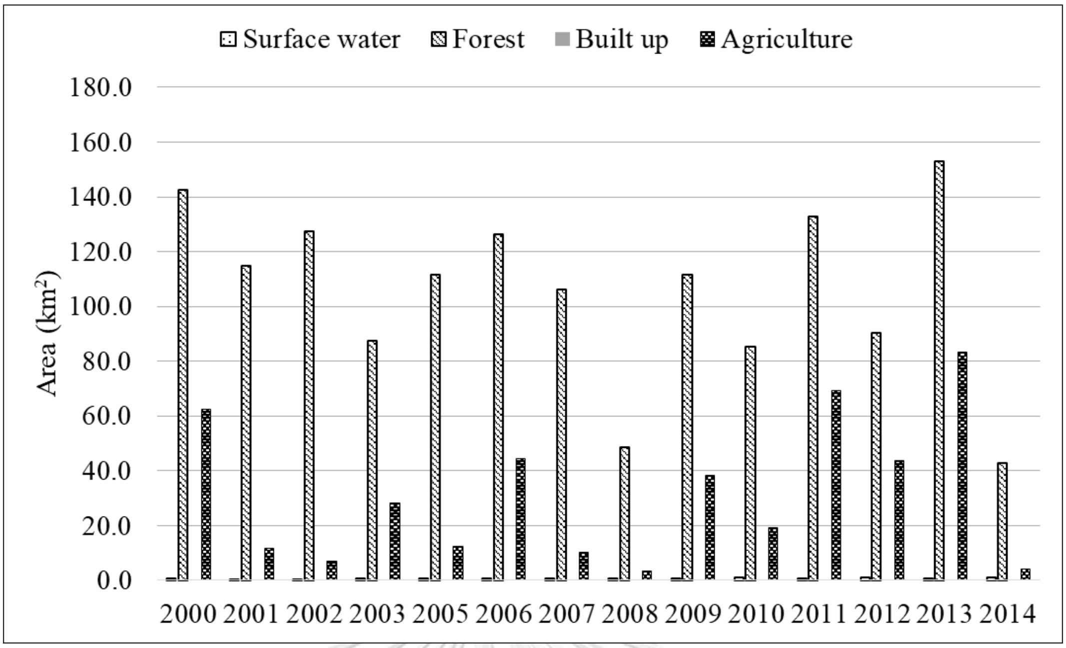

Figure 5.12: Land cover types affected by flood

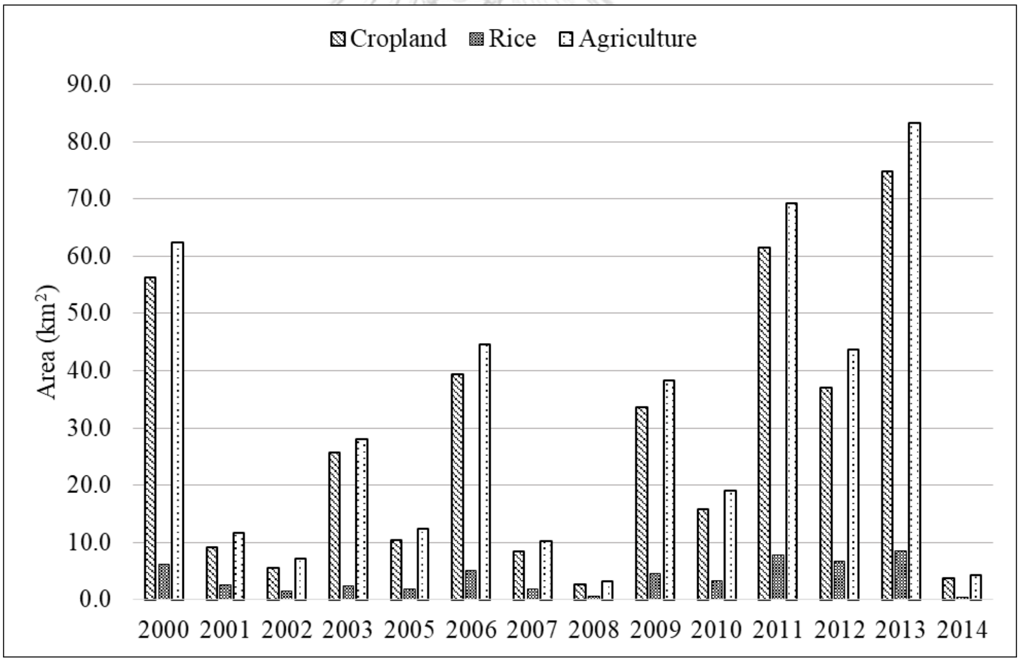

Figure 5.13: Annual flood affected area in Agriculture

The objective in this special analysis is Agriculture, which are Cropland and Rice as indicated in Figure 5.13. Overall, the affected area of Cropland is higher than that of Rice paddy. The highest affected areas in Agriculture within the 15 year of analysis is in 2011 (around 10543 Ha.) followed by 2013 (around 8328 Ha.) and 2000 (6248 Ha.), which is similar to the historical flood record in Cambodia that the biggest flood within the last two decades was in 2000 2011 and 2013. Besides, there are also the significant affected area especially in Cropland in 2003, 2006 and 2012.

The analysis is also conducted in those years under threshold such as in 2001, 2002, 2005, 2007, 2008, 2009, and 2014 in the reason that there were slightly damage records in those years by the National Committee for Disaster Management (NCDM). In this case, the analysis proves that it is possible to have slightly affected areas even though the water discharge is smaller than that of threshold.

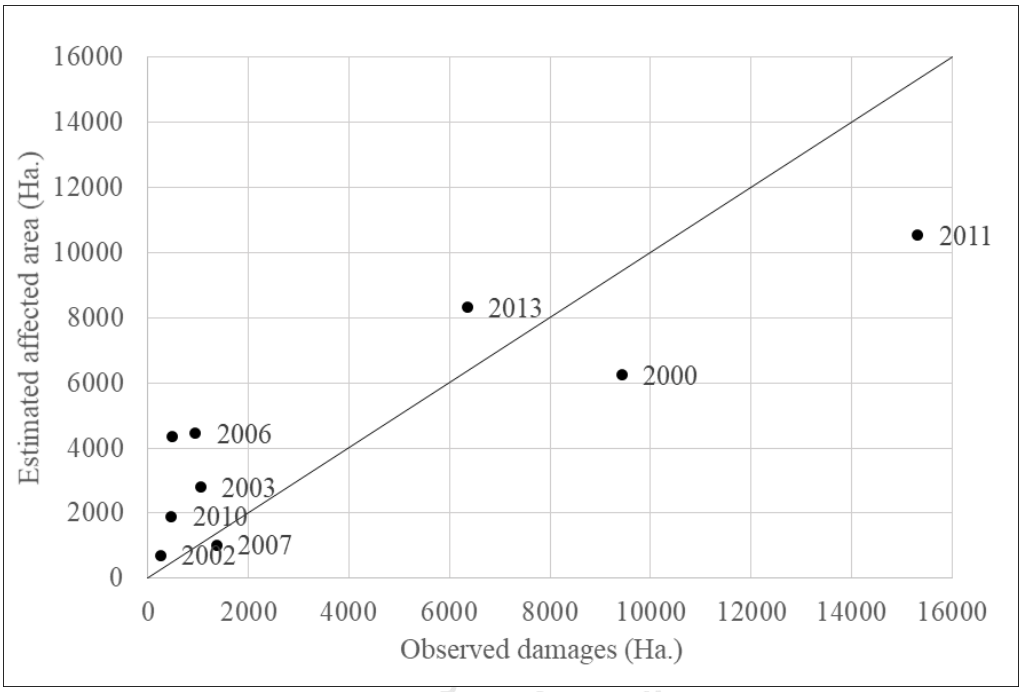

Figure 5.14: Comparison between observed damages and estimated affected area in Agriculture (Ha.) in Bakan and Phnom Kravanh districts

Even if the result of the estimated affected area of Agriculture shows the positive agreement with the flood records, still those affected areas cannot be confirmed to be damaged or destroyed by flood. In this case, the comparison between the observed damage in Agriculture by the NCDM and the estimated affected area of the integration between Monthly Water History, v1.0 and land cover have been made as shown in Figure 5.14. The observed damage tends to be around 30% larger than the estimated affected area in 2000 and 2011, while it is 200% smaller than the estimated affected area in the normal flood years. The observed data tends to provide the extreme damage record. For example, flood damage in Agriculture was recorded to be 492 Ha in 2012 much smaller than that of recorded damage in 2011 (15309 Ha), while the observed discharge in 2012 is 1025 m^3/s greater than that in 2011 (802 m^3/s). This will cause a low correlation when the observed damage is used for further prediction and analyses. Instead, the estimated affected area narrows down the value of maximum and minimum records. It provides better correlation between the estimated affected area in Agriculture and the observed discharges. The correlation between observed damage and estimated affected area in Agriculture is examined; the Coefficient of Determination (R^2) is equal to 0.76 and Root Mean Square Error (RMSE) is 1541 Ha.

We would like to use the estimated affected area as the damage in Agriculture. It is possible to consider the estimated affected area in 2000 and 2011 as the damage area in Agriculture since the observed damage in these two years is greater than the finding of estimated affected area. However, there is no proves that the overestimation of the affected area in other years is damaged by flood. Hence, the objective of the next analysis is to confirm of damages of those affected areas in Agriculture using the Normalized Difference Vegetation Index (NDVI) and Leaf Area Index (LAI).

Normalized Difference Vegetation Index (NDVI)

Normalized Difference Vegetation Index (NDVI) quantifies vegetation by measuring the difference between near-infrared, which vegetation strongly reflects and red light, which vegetation adsorbs. NDVI always ranges from -1 to +1, but there is not a fixed boundary value of NDVI for each type of land cover. If NDVI value closest to +1, there is a high possibility that it is the dense green leaves. Conversely, if NDVI value is negative, it is highly likely that it is water. But when NDVI is close to zero, there is no green leaves or water, it could be a terrain or urbanized area.

Figure 5.15 indicates the value of NDVI in each growing stage of the Rice paddy. As can be seen, the seeding and harvest stage have almost the same value of NDVI (around 0.4), while this value increases to the maximum (around 0.77) for the maturity stage of Rice paddy.

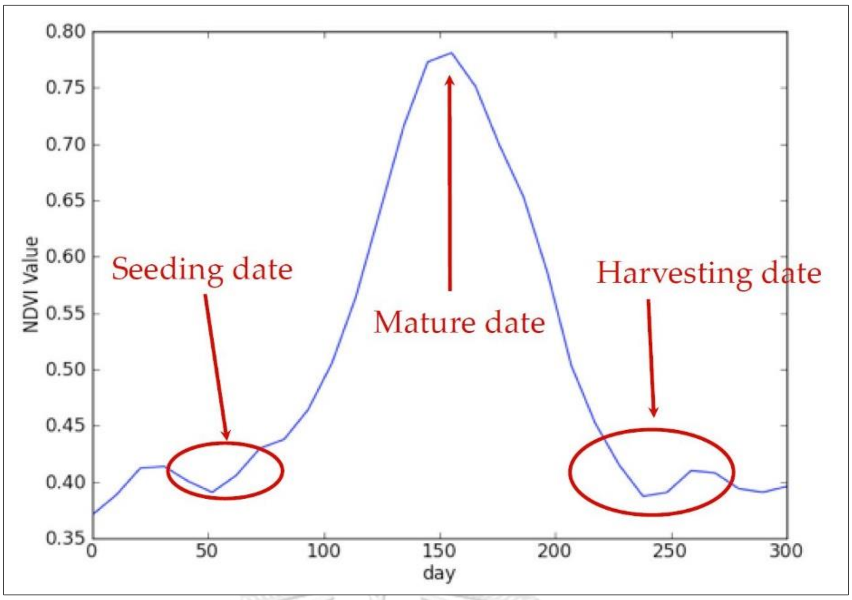

Figure 5.15: NDVI value of different growing stage of Rice paddy (Puttanapong, Chantarat et al. 2014)

Table 5-4 indicates the major crop calendar in Cambodia by Food Agriculture Organization (FAO). The gray color represents the sowing or seeding stage; the green color represents the growing; and the orange color represents the harvesting stage. There are three types of major food crop, which are Maize, Rice (dry season) and Rice paddy (main wet season). In this case, Rice paddy in wet season from July to January (around 7 months) is considered to identify the value of NDVI since the majority of the Cambodian farmers grow Rice paddy. Based on the crop calendar of Rice paddy, the high value of NDVI takes place between September and November because it is the growing stage, while the low NDVI is in July and August (seeding stage), and December and January (harvesting stage).

Table 5-4: Cambodian crop calendar (FAO/GIEWS)

Cambodia Crop Calendar (Major Foodcrop)												
Crop	**Jan**	**Feb**	**Mar**	**Apr**	**May**	**Jun**	**Jul**	**Aug**	**Sep**	**Oct**	**Nov**	**Dec**
Maize												
Rice (Dry Season)												
Rice (Main Wet Season)												

Time-series MODIS NDVI 250-meter resolution (8-day average record) and monthly image of MODIS NDVI are extracted from Google Earth Engine. Figure 5.16 and Figure 5.17 visualize the example of the difference of NDVI between flood year (October 2011) and normal year (October 2015). As can be seen in Figure 5.17, without flood the value of NDVI in the area around the Tonle Sap Lake as well as in Bakan and Phnom Kravanh districts is higher than 0 (no yellow pixel), which means those areas are covered by forest or crop fields due to the growing stage of Rice paddy as mentioned in Table 5-4. Conversely, when flood occurs as shown in Figure 5.16, the value of NDVI in the same areas is lower than zero (yellow pixel), which means some parts of the area are covered by water. The visualization of NDVI between normal and flood year gives us the idea that flood will reduce the value of NDVI or it can be said that flood actually causes the damage to vegetation especially crop area that is affected by flood.

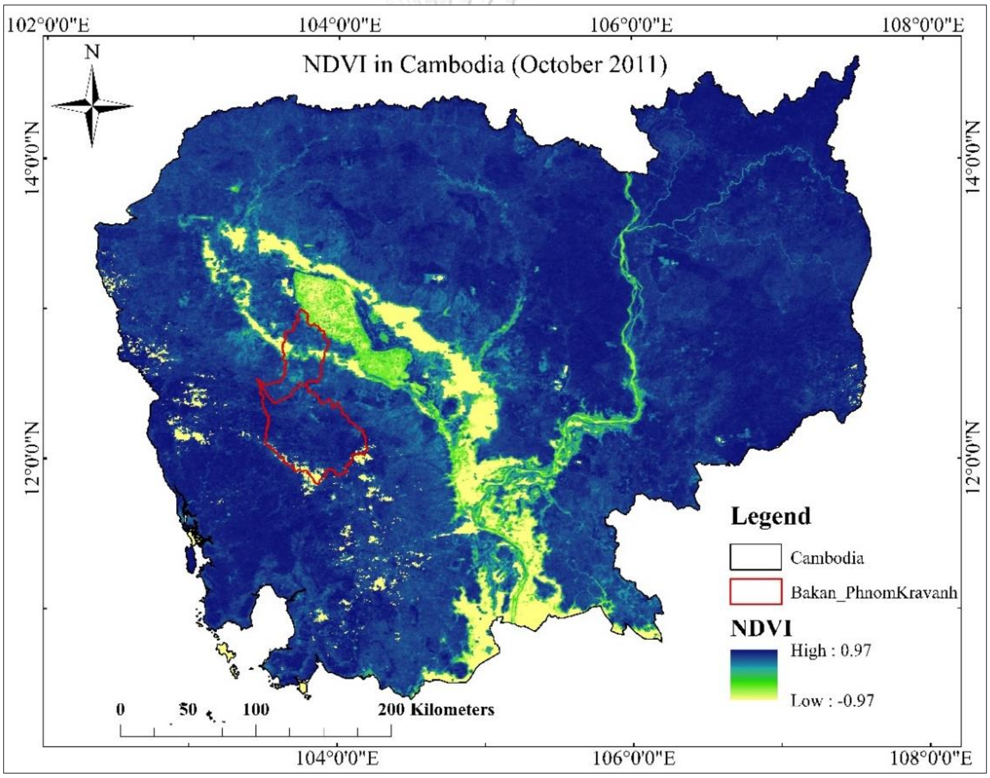

Figure 5.16: Cambodia NDVI in October 2011

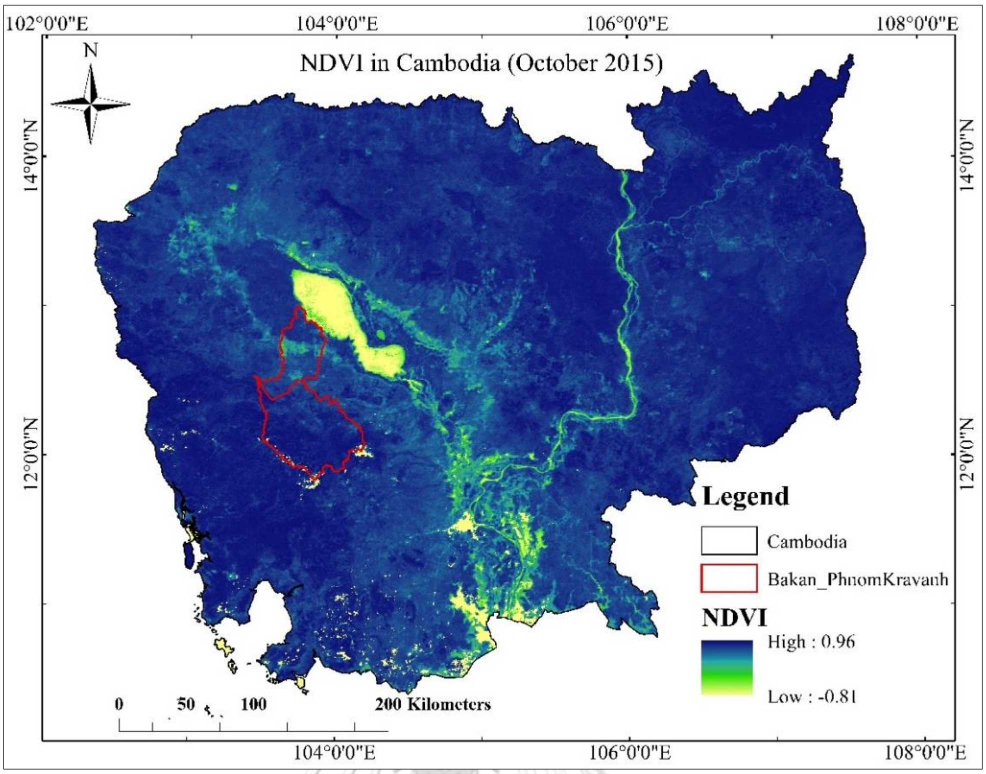

Figure 5.17: Cambodia NDVI in October 2015

The annual time-series of NDVI (8-day average record) under flood pixels in Bakan and Phnom Kravanh districts in 2000, 2003, 2010, 2011, 2012 and 2013 are extracted from Google Earth Engine to observe time-series changes of NDVI. The result is indicated in Figure 5.18. The value of NDVI in those flood years decreases in the growing stage of Rice paddy especially in 2000, 2011 and 2013 is almost 0, while it should be around 0.77. It indicates the damage or partial damage of those vegetation under flood. However, the graph also illustrates the high NDVI after flood period (0.5 or 0.6). There are two possible reasons supporting the increases of NDVI after flood. First, it is possible that crops partially destroyed by flood are recovered. Second, since the value of NDVI between forest, cropland and Rice paddy under flood cannot be differentiated, it is possible that Rice paddy or other crops are totally destroyed, but the forest especially flooded forest (the largest area affected by flood) remains the same when flood gone so that the NDVI is rapidly increased from almost 0 to 0.5 or 0.6, which is possible to be the average value of NDVI between the damaged crop fields and recovered flooded forest after flooding.

The second reason is likely to be occurred. It is noticed that the decrease of NDVI in the growing stage of Rice paddy normally lasts for more than two weeks (Figure 5.18), which is possible to destroy the crop underwater especially paddy rice. Figure 5.19 indicates the relative damage curve of rice paddy caused by flood depth and duration developed by MRC. In this case, the depth of flood is unknown due to the limitation of satellite data, yet the significant drop of NDVI value from around 0.75 to 0.1 or 0.2 indicates the immediate replacement of vegetation by water pixels meaning that water is high enough to cover the majority of crops in the affected area.

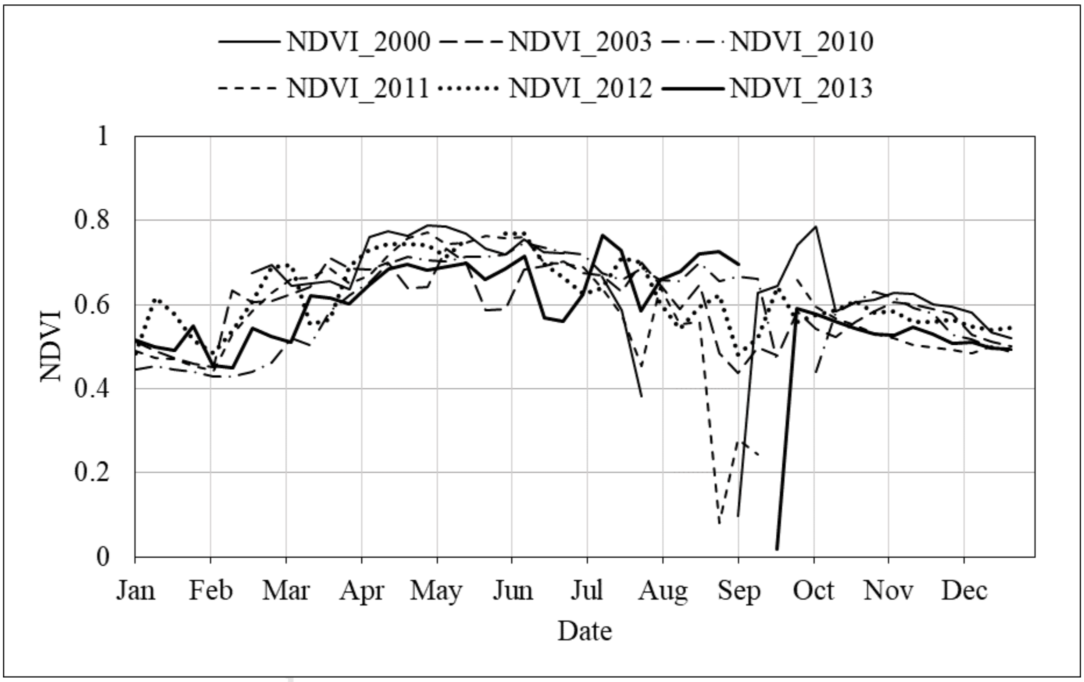

Figure 5.18: NDVI in flood years

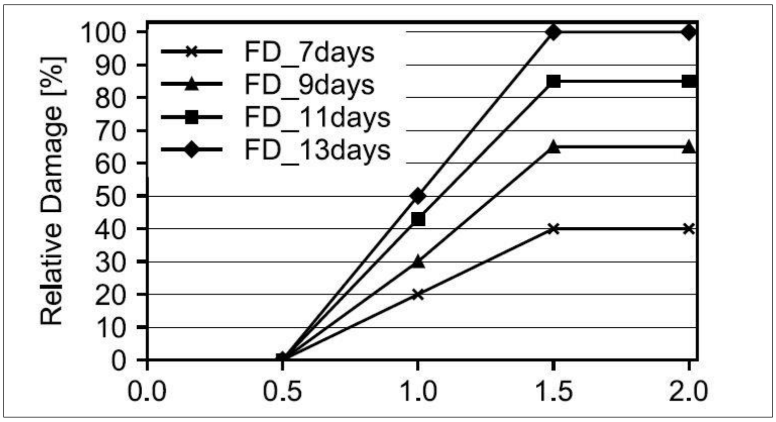

Figure 5.19: Relative damage for Rice paddy (MRC 2009)

To confirm the damage, the correlation between cumulative Z-Score of NDVI from June to December (crop season) and the affected area in Agriculture is determined and illustrated in Figure 5.20. The result shows the negative correlation between the two variables with R^2 = 0.41. The cumulative Z-Score of NDVI decreases when the affected area in Agriculture increases implying that the reduction of NDVI is the result of crops that are entirely or partially destroyed by flood.

In case of 2000 and 2011, the affected agricultural area is almost the same, but the value of cumulative Z-score is different. Since the cumulative Z-score of NDVI is made between June and December, it is possible that the value of NDVI in some months is higher than the mean value of NDVI meaning that there is no effect from flood, while some months, the value of NDVI is lower than the mean value of NDVI meaning that the vegetation is affected by flood. It does reflect that in 2011, after flood there is no vegetation left in the affected area meaning that those crops under flood was 100% destroyed. On the other hand, there is vegetation left after the flood in 2000 meaning that the crops under flood in 2000 was not 100% destroyed. There is not further method to assess the percentage of the flood damage on crop based on the value of NDVI in this research. Hence, based on the scope of the research the affected of NDVI by flood in Agriculture is considered as 100% destroyed area in Agriculture.

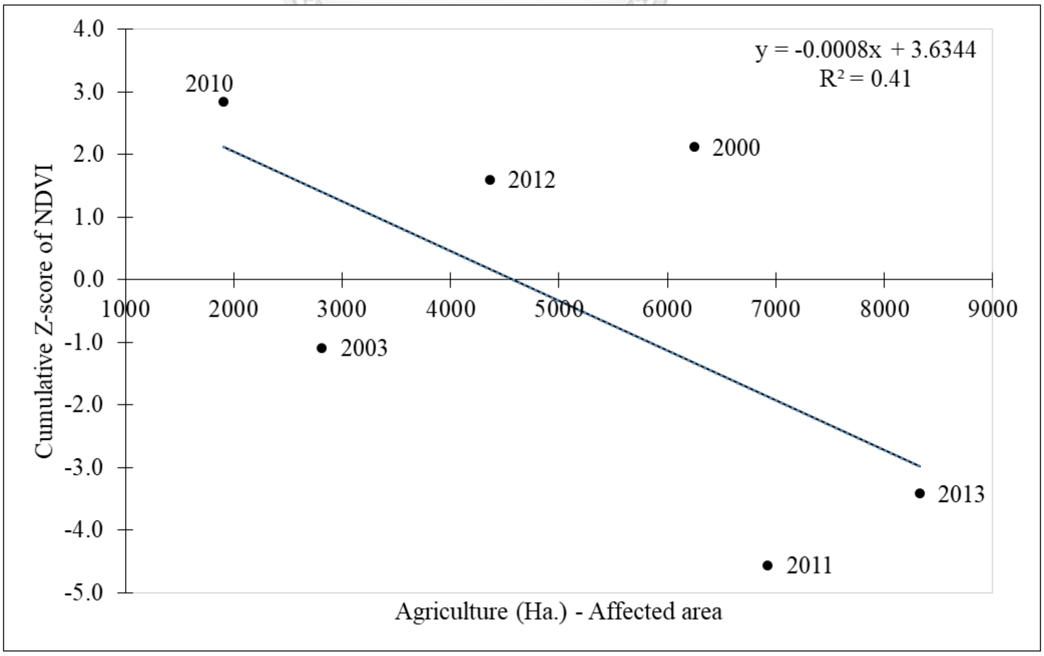

Figure 5.20: Correlation between Agriculture Damage (Ha.) and Cumulative Z-Score of NDVI in crop season

Even though the cumulative Z-score of NDVI is between June and December, which is mostly in the rainy season, still the value of NDVI can be affected by drought since drought can occur within the short period of time between two months of rainy season. However, since the selected years to be considered is the flood year, there is a high probability that changes value of NDVI does represent the affect from flood.

Leaf Area Index (LAI)

Leaf Area Index (LAI) of a plant canopy is defined as its leaf area per unit of ground area. In other words, it tells us how many layers of leaves would be on the ground if they would all fall down and be arranged exactly side by side as shown in Figure 5.21. The highest value of LAI can be found in the dense forest, where many layers of the leaves overlaid, while the lowest value of LAI ($0 \leq LAI < 1$) refers to desert, water and urban area, where the area of vegetation is very small compared to that of the ground. In Google Earth Engine, LAI is ranged from 0 to 100.

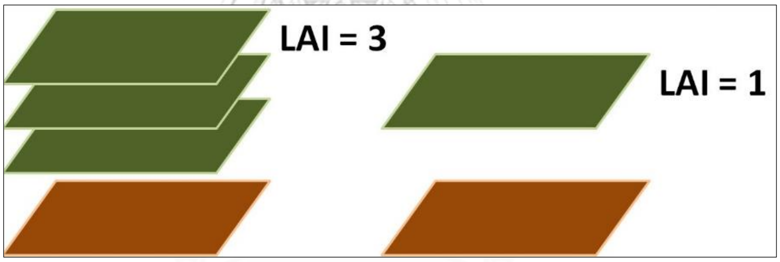

Figure 5.21: Concept of Leaf Area Index (LAI)

Similar to NDVI, LAI can also provide the information about the changes in canopy of vegetation. Figure 5.22 indicates the value of LAI in Cambodia as well as in Bakan and Phnom Kravanh districts in October 2011 (flood period), while Figure 5.23 indicates the same LAI, but in October 2015 (normal year). The highest value of LAI in Cambodia is 70 (the dark blue area) and the lowest value is 0 (the yellow area). The yellow area or the zero value of LAI remarkably exists around the Tonle Sap Lake and in other parts of the low land area in Cambodia during flooding in October 2011, while the same month in 2015 (no flood), the yellow area decreases, which means the value of LAI increases. This represents the change of LAI affected by flood or in other words, vegetation in the affected area are replaced by water during flooding.

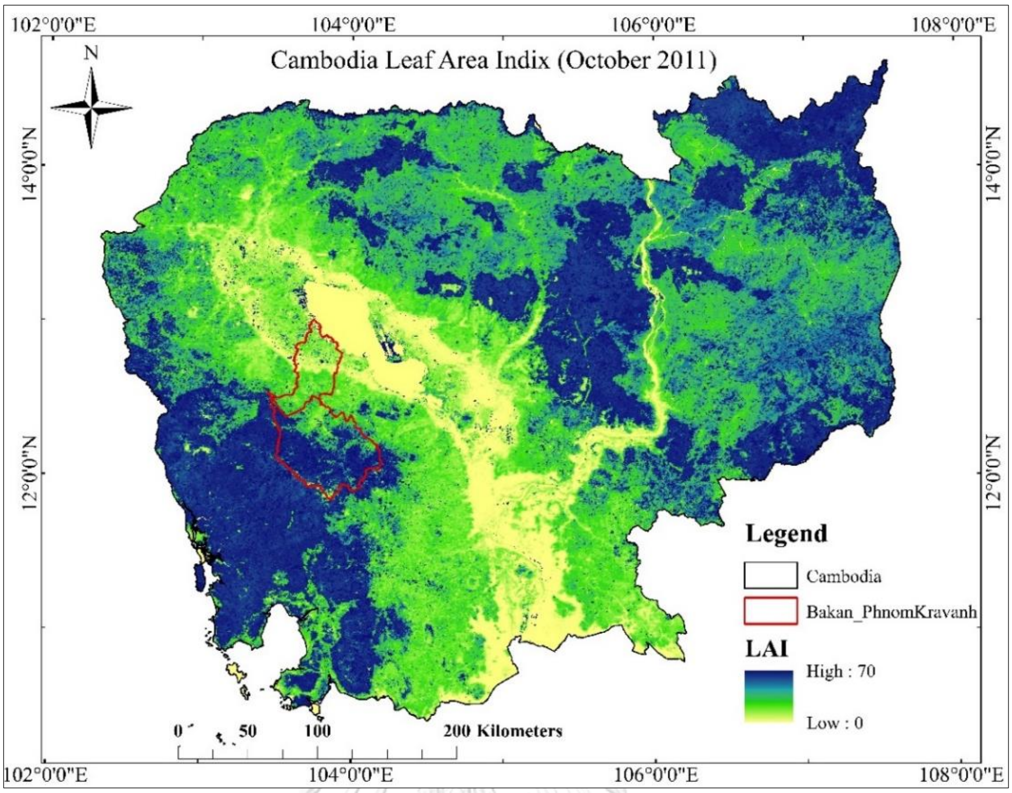

Figure 5.22: Cambodia Leaf Area Index in October 2011

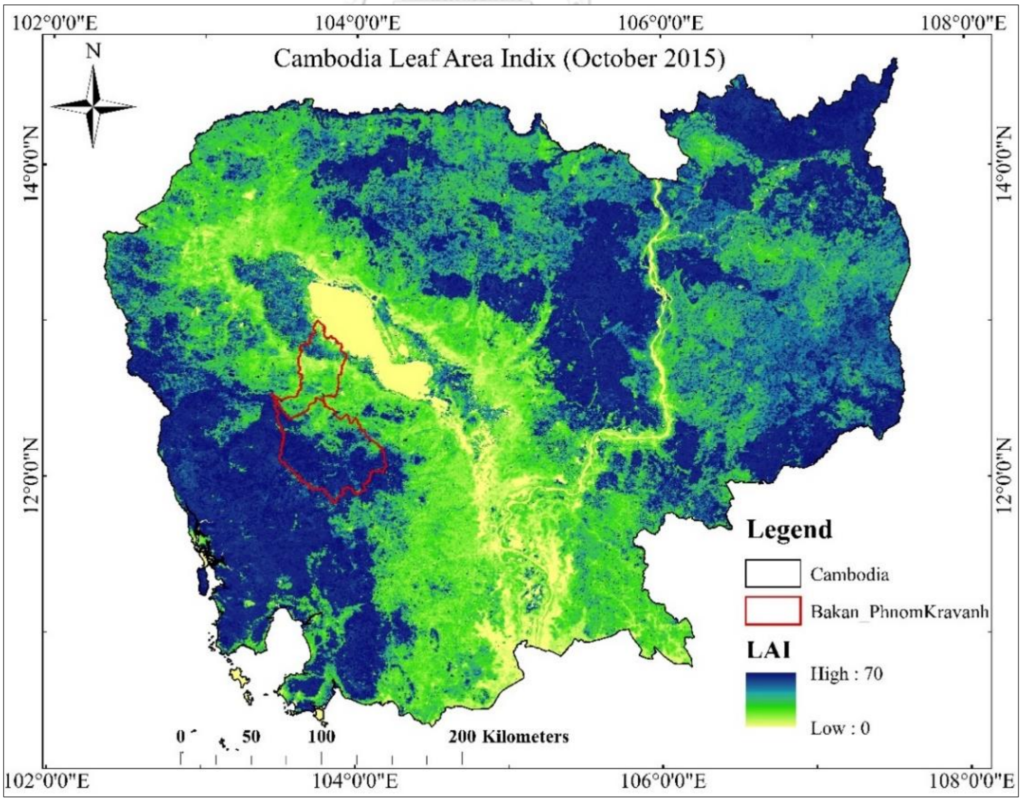

Figure 5.23: Cambodia Leaf Area Index in October 2015

To identify the changes value of LAI affected by flood, the annual LAI (4-day average record) in the area under flood pixels are extracted to find two correlations: the correction between NDVI and LAI as shown in Figure 5.24 and the correlation between affected agricultural area and cumulative Z-Score of LAI as shown in Figure 5.25.

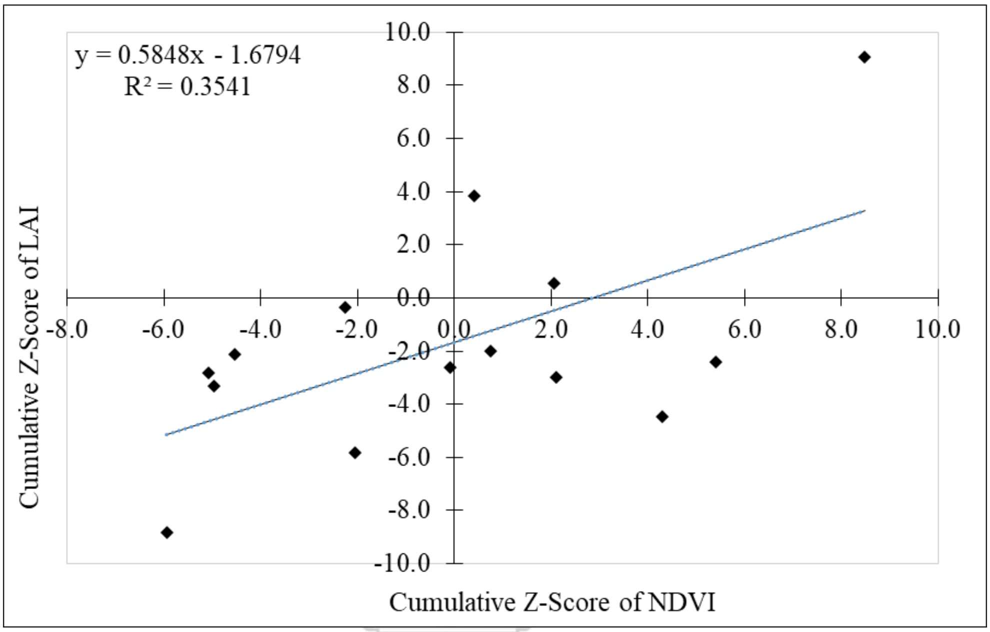

Figure 5.24: Cumulative Z-Score of LAI and Cumulative Z-Score of NDVI (12 months)

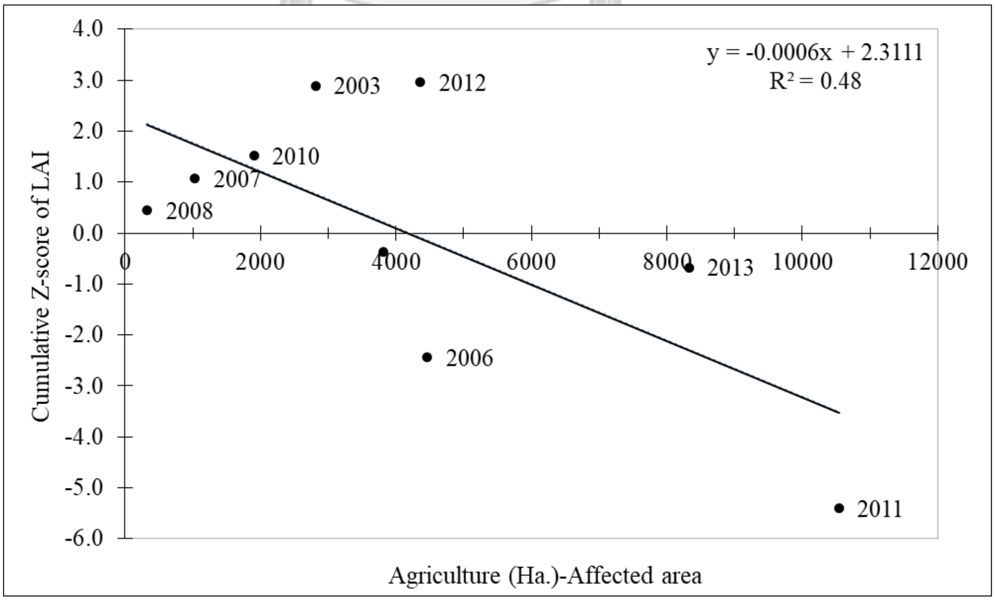

Figure 5.25: Correlation between Agriculture Damage (Ha.) and Cumulative Z-Score of LAI

Even though NDVI and LAI are measured with different scales, the value can be standardized by using the Z-Score to find the relationship as shown in Figure 5.24. The result indicates the positive correlation between NDVI and LAI. This is a basic correlation between NDVI and LAI that would be expected since both indices represents the greenness density of vegetation.

Figure 5.25 indicates the relationship between the affected area in Agriculture in Bakan and Phnom Kravanh districts and the cumulative Z-Score of LAI under flood during crop season. The negative correlation between both variables with R^2 = 0.48 provides the common truth that the crops in the affected area in Agriculture represented by LAI are destroyed or partially destroyed or replaced by flood, which makes the LAI decreases when affected area in Agriculture increases.

Based on the result of NDVI and LAI analyses, it can be concluded that flood does produce the damages in the affected area in Agriculture. Hence, those affected areas will be used as the damage area in Agriculture in the next analysis.

5.2.2 Affected people

The damage in this sector is considered as the interruption of economic activities from which people in the affected area produce income. It is called Indirect Tangible Damage. As mentioned in section 5.2.1, Urban and Built up area in land covers includes only the cities and small towns in each district, which do not really represent the people living in common villages in rural area in Bakan and Phnom Kravanh districts. That is why the integration between flood maps and land covers could not identify the effect of flood in Urban and Built up area even though some records show that many people were affected by floods in the previous years. Because of this limitation, Nighttime Light Index (NLI) will be used to support the method in this research to identify the number of people affected by flood.

Nighttime Lights Index (NLI)

Nighttime Light, a satellite data developed from visible and near-infrared (VNIR) emission sources at night, is detected by The Defense Meteorological Program (DMSP) Operational Line-Scan System (OLS). In Google Earth Engine as well as other sources of NLI, the value of NLI is ranged from 0 to 63, which is called

Digital Number (DN). DN0 means no light, while DN63 represents the stable light in the urban. This data is mostly used to observe the expansion of the urbanization; however, there are some studies such as Chaiwat (2016) used NLI to estimate the growth dispersion of ASEAN Countries, Elvidge, Baugh et al. (2012) used NLI to study about the spatially explicit measure of human development including population density, and (Keola, Andersson et al. 2015) used NLI with land cover to measure the economic growth in the developing countries. The result of these studies indicates in overall that NLI is one of the satellite data that can be used to represent the growth of the country economy such as urbanization, GDP, population density and even electricity consumption. However, some objectives do need the combination between NLI with other data in order to get better results.

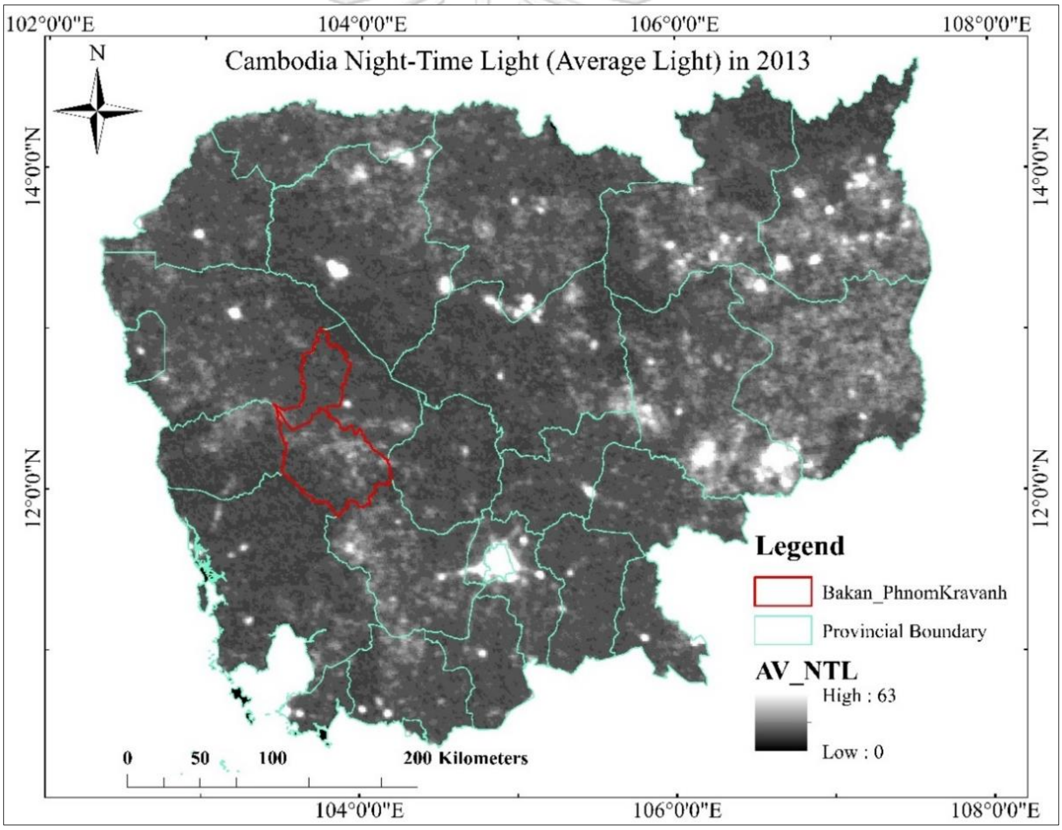

Figure 5.26: Cambodia Nighttime Light in 2013 (Average Light)

In this case, the annual NLI at 30 arc seconds resolution (around 1000m) from 1992 to 2014 are extracted from Google Earth Engine. There are several bands of NLI; however, only two bands that are considered, which are Average Light and Stable Light as in shown in Figure 5.26 and Figure 5.27 respectively. Average Light is the average of the visible band digital number values with no further filtering (Raw data of NTL), while Stable Light is the cleaned up Average Light contains the lights from cities, towns, and other sites with persistent lighting, including gas flares. Ephemeral events, such as fires, have been discarded. The background noise was identified and replaced with values of zero.

As can be seen in Figure 5.27, Stable Light is really well-represented the urbanization in the city, which cannot be used to represent the various density of the population in the country. Hence, Average Light will be used for the analysis since it is the original data that contains the average visible from all sites even the low digital number of lights produced by people activities in the rural area. However, both NLI still have uncertainty regarding some unknown activities in the forest, especially in the eastern part of Cambodia that produce a high digital number of lights. Those provinces are mostly covered by dense forest with a very low population density (around 15 people/km^2) and those lights do not represent the density of population at all.

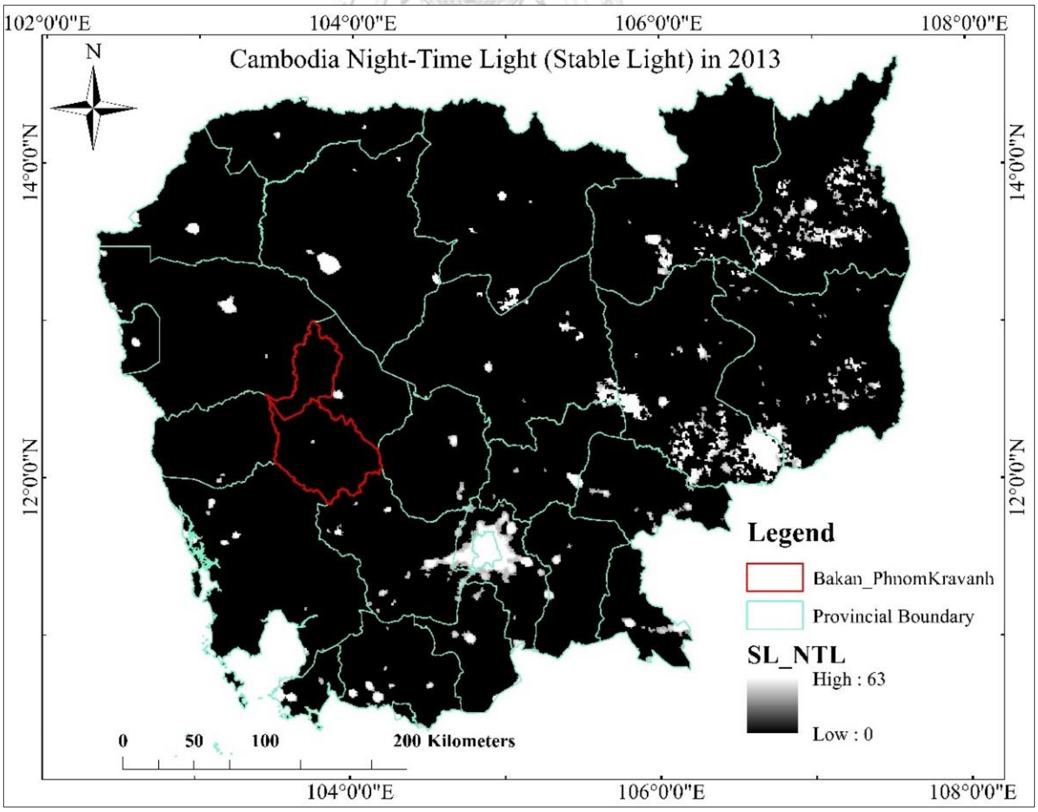

Figure 5.27: Cambodia Nighttime Light in 2013 (Stable Light)

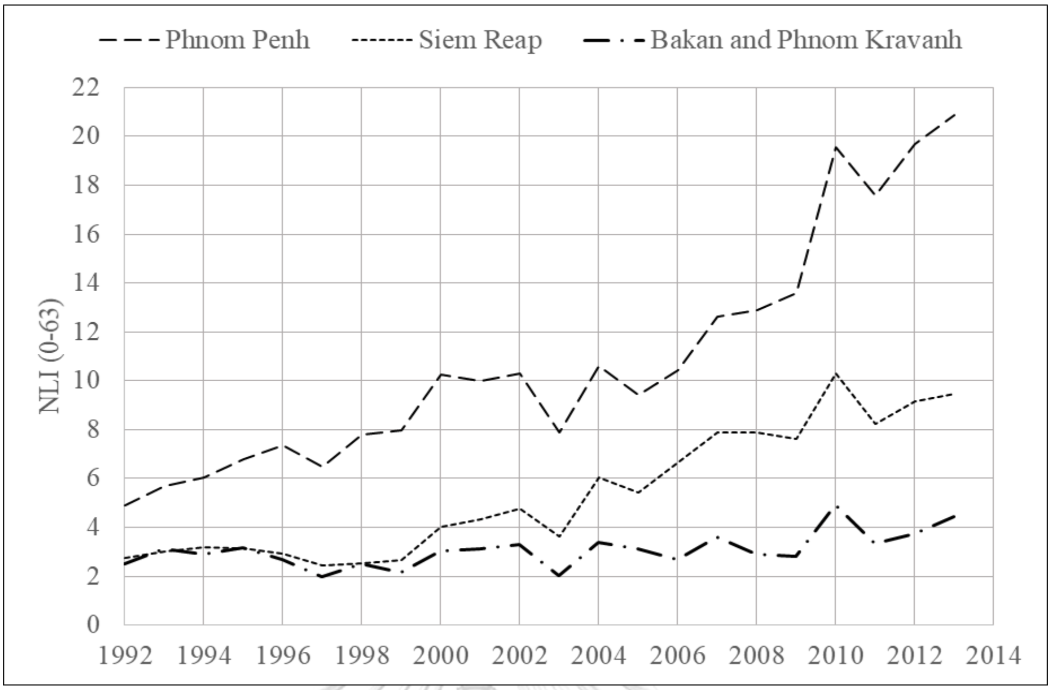

Figure 5.28: Annual Average Light of NLI in Phnom Penh, Siem Reap City and Bakan and Phnom Kravanh (1992-2013)

Figure 5.28 indicates time-series Average Light of NLI in three locations: Phnom Penh (the capital city), Siem Reap City and the study area (Bakan and Phnom Kravanh districts) from 1992 to 2013. Overall, the Average Light of NLI shows the urbanization between these three locations, which started at almost the same DN in 1992 and experienced different development within the last 20 years. The low DN of NLI indicates the slow development, while the high indicates the fast-growing city. In this case, the DN of NLI in Bakan and Phnom Krvanh districts is low compared with that in Siem Reap and Phnom Penh. It means that there is no much urbanization activities in these two districts; it does reflect the reality that the districts have high potential in agricultural development, yet no much urbanization.

Table 5-5: Average provincial NLI in Cambodia in 2013

FID	Province	Pop Density	Average NLI	Average DN
0	Banteay Mean Chey	116	4.44	6.62
1	Battambang	100	4.38	6.08
2	Kompot	127	4.46	6.01
3	Kampong Cham	218	4.29	6.29
4	Kampong Chhnang	96	3.92	4.17
5	Kampong Speu	112	4.97	6.07
6	Kampong Thom	49	4.20	5.67
7	Kandal	404	6.28	11.88
8	Koh Kong	13	3.86	4.84
9	Kep	127	4.46	6.69
10	Kratie	33	6.00	8.98
11	Krong Pailin	121	4.38	6.21
12	Krong Preah Sihanouk	300	5.07	11.31
13	Mondol Kiri	5	5.66	6.57
14	Oddar Mean Chey	38	4.79	5.80
15	Phnom Penh	2513	36.34	31.05
16	Pursat	34	4.20	4.99
17	Preah Vihear	14	4.58	6.13
18	Prey Veng	201	4.10	4.64
19	Ratanakiri	16	5.53	7.68
20	Siem Reap	102	4.80	8.76
21	Steung Treng	12	4.66	6.04
22	Svay Rieng	169	4.70	7.60
23	Takeo	247	4.28	5.83
24	Tbong Khmum	153	4.38	5.07

Beside the recognition of urban expansion, the main goal in this part is to use the Average Light of NLI to represent provincial population density in Cambodia. In this aspect, the relationship between provincial Average Light of NLI and provincial population density is developed. Only Average Light of NLI in 2013 is used since the available provincial population data is also in 2013. Table 5-5 and Figure 5.29 indicate the average NLI and provincial population density and its correlation respectively. The average NLI can be calculated by:

$$\text{Average NLI} = \frac{\Sigma \ \text{Area of NLI} \times \text{DN}}{\Sigma(\text{Area of NLI})} \qquad \text{(Eq. 5.1)}$$

It can be seen that Phnom Penh, the capital of Cambodia, has a very high Average Light of NLI corresponding to its high population density. The correlation between the two variables is good with R^2 = 0.97; this high correlation is dominated by the extreme point of Phnom Penh City, which has higher value of NLI comparing with the mean value of NLI of cluster point of other provinces. In this case, the cluster of point of NLI of other provinces acts like a single observation. The predicted linear regression equation from this analysis (y = 0.013x + 2.7768) will be used to identify the number of people affected by flood in Bakan and Phnom Kravanh districts.

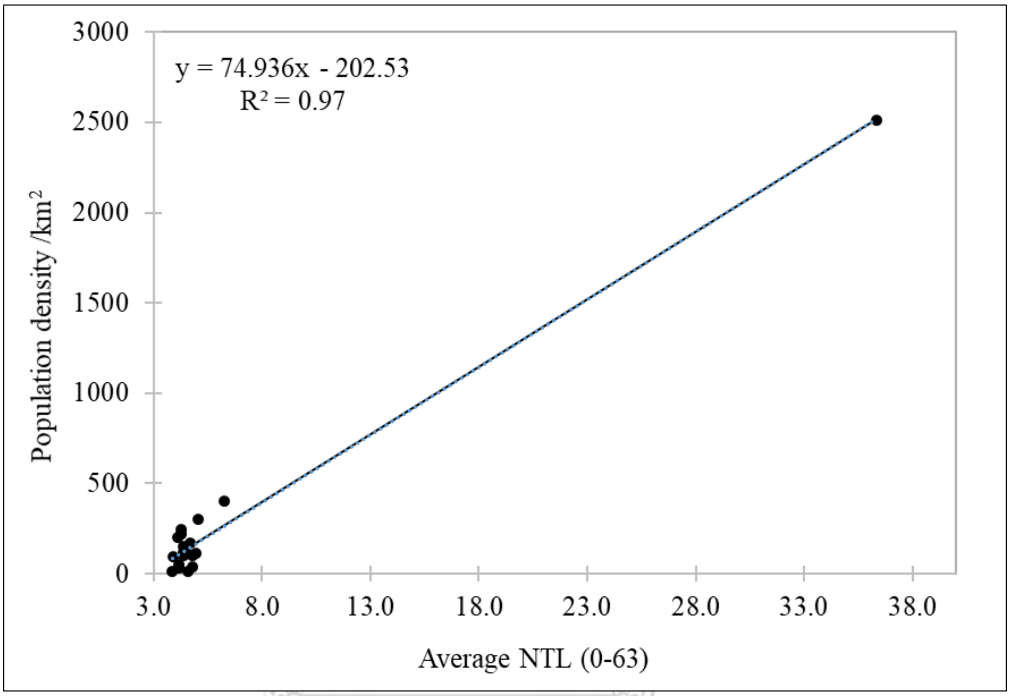

Figure 5.29: Correlation between average NLI and population density (2013)

On the other hand, when excluding the data point of Phnom Penh City, the correlation between average NLI and provincial population density is lower with R^2 = 0.39 as shown in Figure 5.30. The data point of Phnom Penh City is called "outlier", which does not represent the realities of the population density in Bakan and Phnom Kravanh districts in the present time. However, it is not false to include Phnom Penh City as a data point in this study since it does happen in Cambodia that there is a city with a high population density as well as a high number of average NLI. Moreover, this study also considers about the degree of expansion in each sector such as the population growth in the future; hence, it is reasonable that Phnom Penh should be included with other provinces to generate the regression coefficient since Phnom Penh can be used as the model of the future population density of other provinces as well as Bakan and Phnom Kravanh districts.

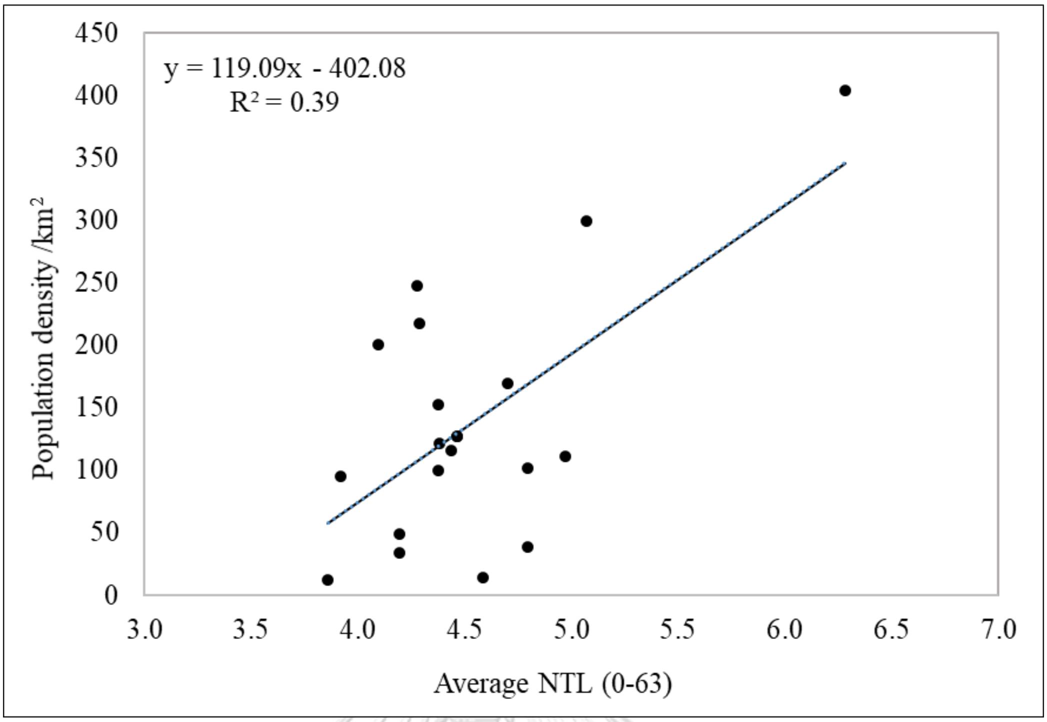

Figure 5.30: Correlation between average NLI and population density without Phnom Penh City (2013)

The average Light of NLI under flood in Bakan and Phnom Kravanh districts are extracted to do spatial analysis in GIS. The area of NLI affected by flood in each year is shown in Table 5-6 and the result of people affected by flood calculated by using the relationship from Figure 5.29 are shown in Figure 5.31. As can be seen, the largest area of NLI affected by flood is in 2013 followed by 2000 and 2011, where the biggest flood occurred as in historical flood record. Even though the area of NLI affected by floods in 2000 is larger than that of 2010, 2011 and 2012, the number of people affected by floods in 2000 is lower because the average NLI in 2010, 2011 and 2012 is higher than that of 2000. There are two possible reasons to support this finding. First, flood have affected the same location where the population density and the household have increased, and second is that flood have switched the location from the area of low population density to the higher one. Both assumptions are possible, but the first one is likely to happen since the Average Light of NLI in Bakan and Phnom Kravanh districts have slowly increased from 1992 to 2013 as shown in Figure 5.28. If the average NLI really represents the population density, it means that those increases in NLI is the result of the growth of population and the improvement of their living standard. It is corresponding to what we have found in this case that the same flood could possibly produce more damages at the same place in the future if the elements at risk is improved both quantity and quality, but low coping capacity.

Table 5-6: Flood affected people

Year	Affected NLI (km^2)	Average NLI	Population Density	Population
2000	205.53	2.98	15.71	3229
2003	116.01	3.01	17.94	2081
2006	45.77	3.00	17.17	786
2010	104.91	3.95	90.03	9445
2011	202.87	3.14	27.62	5604
2012	134.13	3.31	41.16	5520
2013	236.64	3.78	76.89	18194

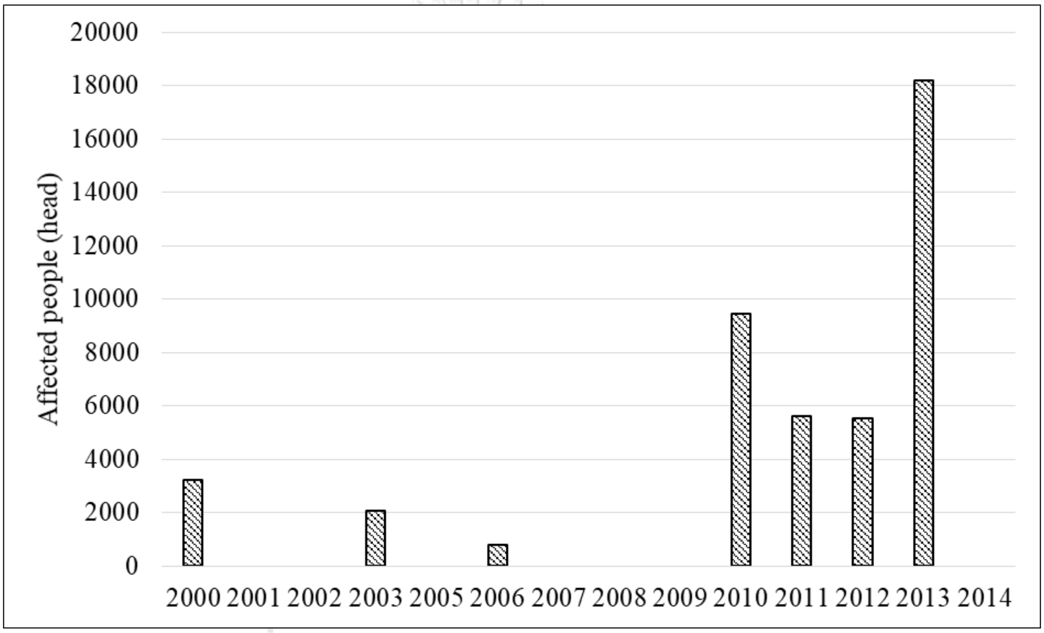

Figure 5.31: Number of people affected by flood in Bakan and Phnom Kravanh districts (2000-2014)

5.2.3 Flood Damage Value (USD)

Flood damage value is needed for flood damage analysis. The physical flood damages from section 5.2.1 and section 5.2.2 are converted into monetary terms using the price recorded by the Ministry of Agriculture, Forestry, and Fisheries (MAFF).

Agriculture

As mentioned in section 5.2.1, the damage in Agriculture is the combination between Cropland and paddy rice. Paddy rice is easy to classify, while Cropland consists many types of crop.

Cropland

The information was reported by a local newspaper called "thmeythmey" in August 16, 2017. They made the interview with Pursat Provincial Governor, His Excellency Mao Thonin. The theme was about "Good Opportunity to Invest in Agro-Industry Crops in Pursat Province" and the content of the interview was written in Khmer language. According to the interview, the potential crops in the province are Rice paddy and Cassava; while the secondary crops are Red corn, Black pepper, and Sugarcane. Fruit trees and vegetables are minor. Below is the average yield per year of those crops in the province. This data was recorded at the farm gate production.

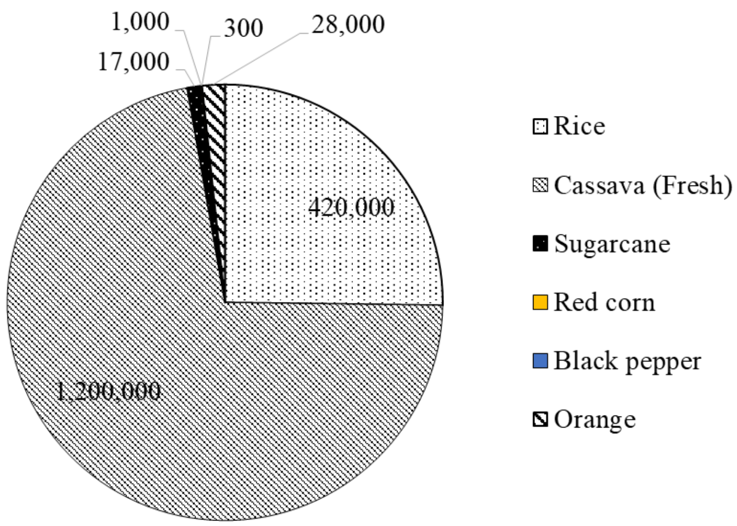

Figure 5.32: Annual average crop yield in Pursat province (tons)
(https://thmeythmey.com/?page=detail&id=55541)

In this case, Rice paddy of the land cover is Rice and the other crops such as Cassava, Sugarcane, Red corn and Black pepper, and orange belong to Cropland. As can be seen in Figure 5.32, Cassava is the main crop with the large amount of annual yield compared with that of other crops. Hence, Cassava will be represented in Cropland. According to the report from the Ministry of Agriculture, Forestry and Fisheries (MAFF), the average yield of Fresh Cassava from 1980 to 2001 is 7.07 t/Ha as shown in Figure 5.33 and the average price of Fresh Cassava from January 2016 to May 2019 is around 300 KHR/kg (1 USD = 4000 KHR) as shown in Figure 5.34.

The annual average damage of Cassava in Cropland is around 530.3 USD/Ha calculated by:

$$\frac{7.07(tons / Ha) \times 1000(kg / ton) \times 300(KHR / kg)}{4000(KHR / USD)}$$

This value will be used as the unit loss per hectare in Cropland from 2000 to 2014 and the total damage in Cropland is indicated in Figure 5.37.

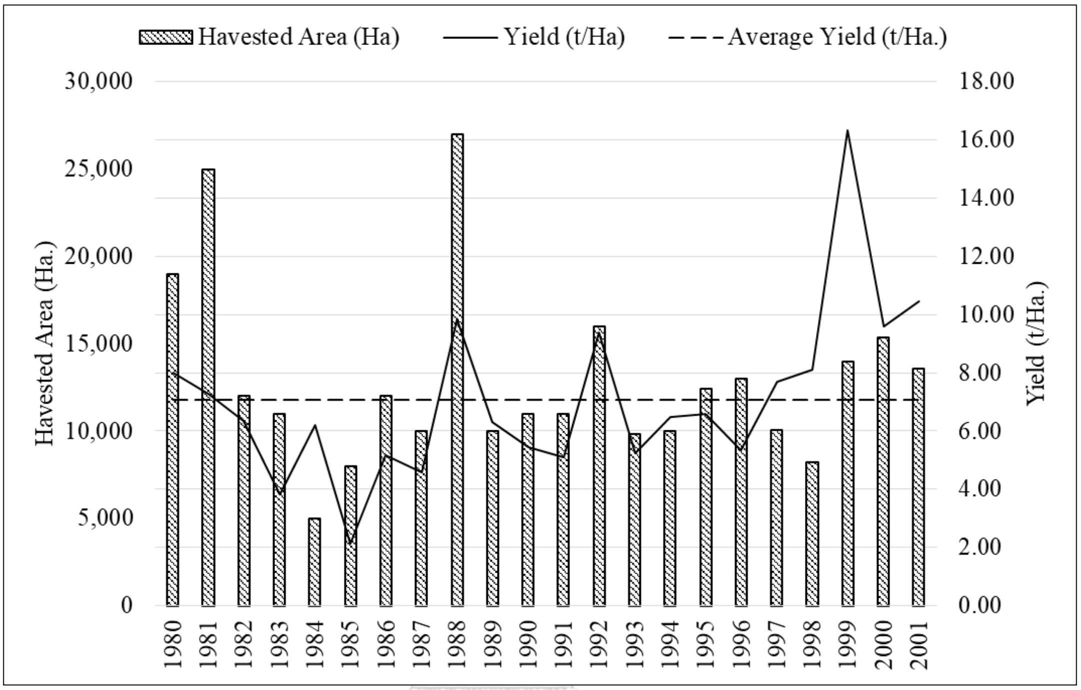

Figure 5.33: Cassava harvested area and yield in Cambodia (MAFF)

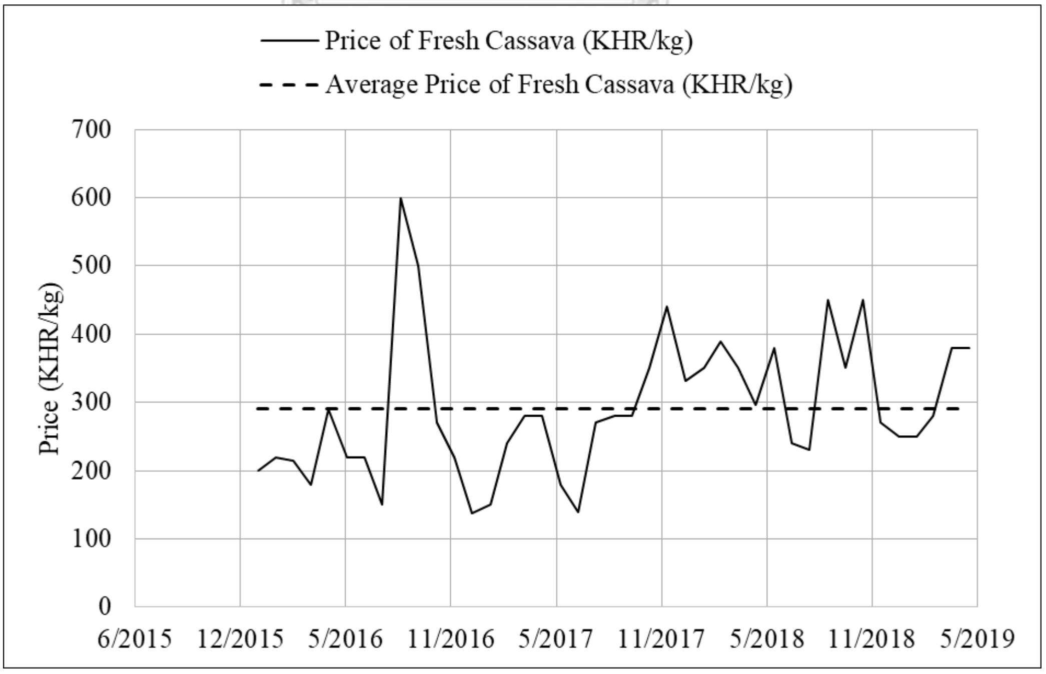

Figure 5.34: Price of fresh cassava in Cambodia (MAFF)

Rice paddy

Rice yield in Cambodia recorded from Ricepedia.com and Rice price recorded from MAFF are indicated in Figure 5.35 and Figure 5.36 respectively. The annual average rice yield has increased from around 2.0 t/Ha in 2000 to 3.0 t/Ha in 2014; the net increase is around 1.0 ton within 15 years. The average yield is around 2.56 t/Ha and the average price of normal rice (Farm Gate Price) within the last 4 years is around 1,077 KHR/kg. In this case, the annual average rice yield from 2000 to 2014 and the average price is used to calculate the average damage per hectare in Paddy rice. Hence, an example of the average damage in 2000 is around 570.8 USD/Ha calculated by:

$$\frac{2.12(ton/Ha)\times 1000(kg/ton)\times 1077(KHR/kg)}{4000(KHR/USD)}$$

The unit loss per hectare and the total damage in Rice paddy from 2000 to 2014 are indicated in Table 5-7 and Figure 5.37respectively.

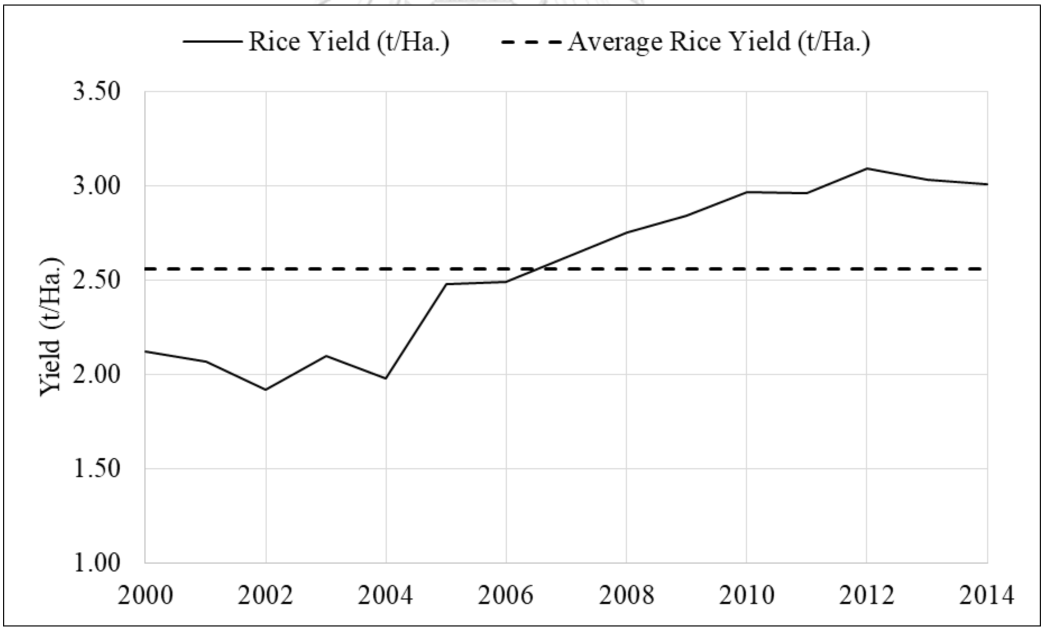

Figure 5.35: Rice yield in Cambodia from (http://ricepedia.org/)

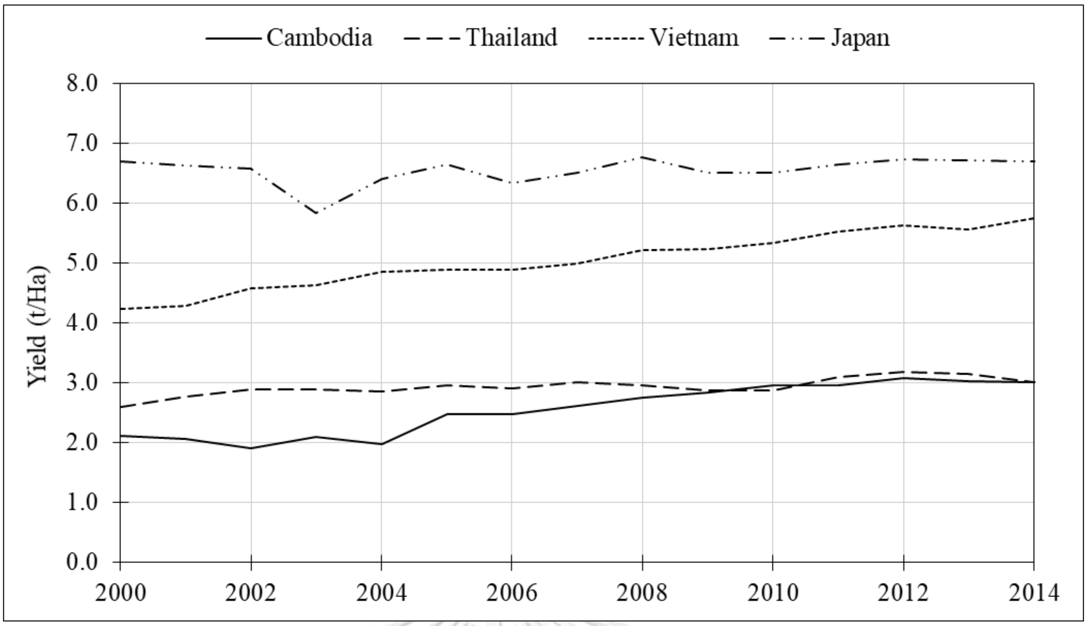

Figure 5.36: Rice price in Cambodia from 2016 to May 2019 (MAFF)

Table 5-7: Annual average damage of Rice paddy (USD/Ha)

Year	Yield (t)	Price (KHR/kg)	Unit loss (USD/Ha)
2000	2.12	1,077.0	570.8
2001	2.07	1,077.0	557.3
2002	1.92	1,077.0	517.0
2003	2.10	1,077.0	565.4
2005	2.48	1,077.0	667.7
2006	2.49	1,077.0	670.4
2007	2.62	1,077.0	705.4
2008	2.75	1,077.0	740.4
2009	2.84	1,077.0	764.7
2010	2.97	1,077.0	799.7
2011	2.96	1,077.0	797.0
2012	3.09	1,077.0	832.0
2013	3.03	1,077.0	815.8
2014	3.01	1,077.0	810.4

Note: 1USD = 4000KHR

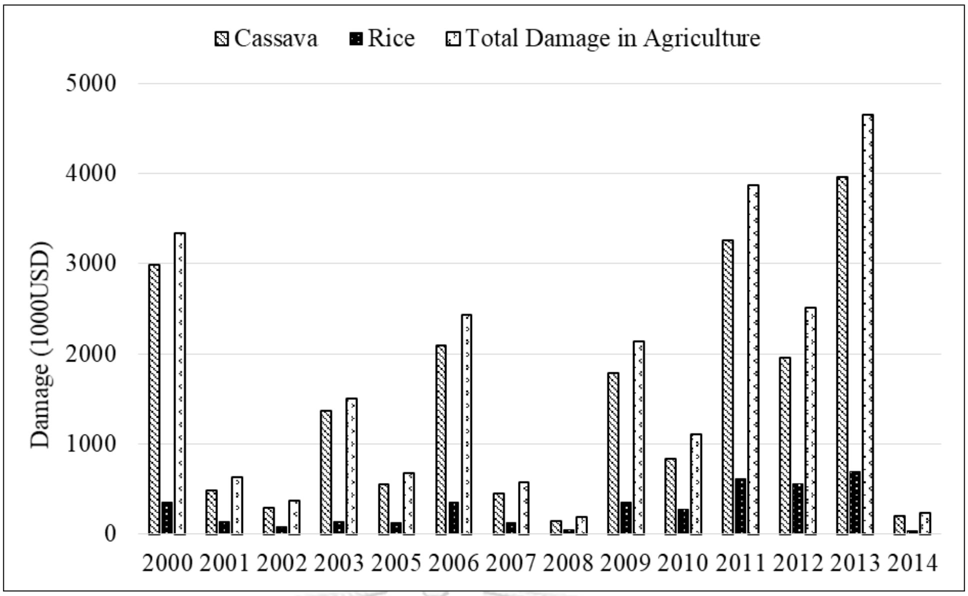

Figure 5.37: Damage in Agriculture

Affected people

In case of affected people, the GDP per capita is used to identify the amount of damage caused by flood to the people in the residential area. As can be seen in Figure 5.38, the GDP per capita of the Cambodian people have significantly increased from 300 USD in 2000 to 1139 USD in 2014, almost 4 times within the last 15 years. The national GDP per capita will be applied to the local GDP per capita in Bakan and Phnom Kravanh districts due to the unavailability of the Provincial GDP per capita.

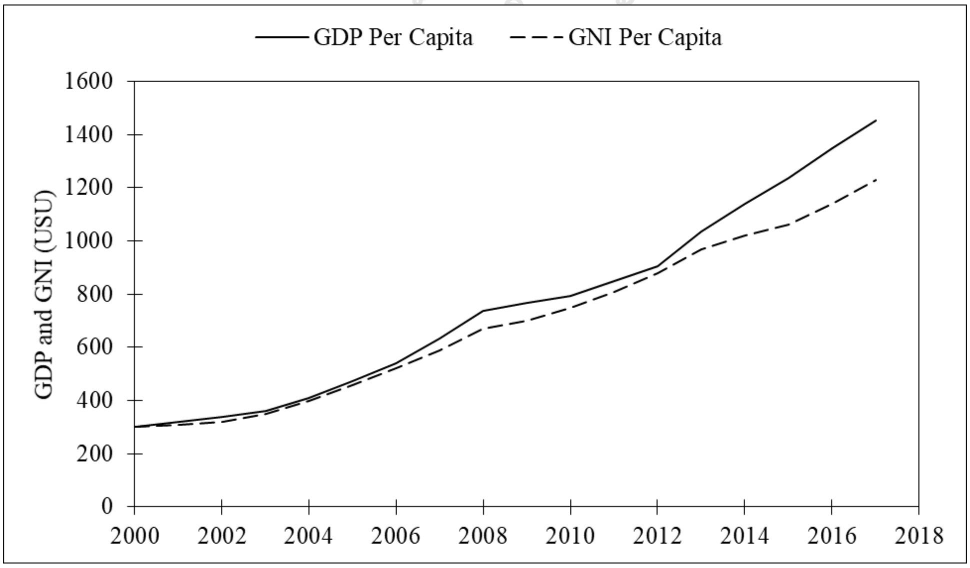

Figure 5.38: Cambodia: GDP per capita

Table 5-8: Annual average damage in Affected people (USD)

Year	Affected people (person)	GDP per capita (USD)	Unit loss (USD/person)	Total damage (USD)
2000	3,229	300.0	14.0	45,212.9
2001	-	321.0	15.0	-
2002	-	339.0	15.8	-
2003	2,081	362.0	16.9	35,157.0
2005	-	474.0	22.1	-
2006	786	540.0	25.2	19,806.4
2007	-	632.0	29.5	-
2008	-	739.0	34.5	-
2009	-	769.0	35.9	-
2010	9,445	795.0	37.1	350,399.3
2011	5,604	849.0	39.6	222,027.6
2012	5,520	906.0	42.3	233,389.7
2013	18,194	1,036.0	48.3	879,637.4
2014	-	1,139.0	53.2	-

It is assumed that flood have affected people for the whole month of October based on the experiences of flood in 2011 and 2013; therefore, people affected by flood are not able to work as usual in October. With 56% of working people in Pursat province (44% of the people are children under 15 years old and older people above 65 years old) as indicated in CHAPTER 3, the unit loss and annual average damage in Affected people sector caused by flood from 2000 to 2014 are shown in Table 5-8.

5.2.4 Summary

The first objective of the research is to assess flood damage in Agriculture and Affected people from 2000 to 2014 by using Google Earth Engine.

Flood extent is derived from Monthly Water History, v1.0. The damage in Agriculture is the result from the integration between flood extent and land cover. The affected area in Agriculture between 2000 and 2014 is confirmed to be damaged by flood by using the Normalized Difference Vegetation Index (NDVI) and Leaf Area Index (LAI), while the affected people by flood is the result from the integration between flood map and Nighttime Light Index. The physical damages in both sectors is converted into monetary terms using the unit loss approach.

The result shows that:

1) The Coefficient of Determination (R^2) between maximum monthly water level and maximum monthly water extent from 2000 to 2013 is equal to 0.57, while the Coefficient of Determination (R^2) between annual maximum water level and annual maximum flood extent is only 0.38.
2) The total damage area in Agriculture from 2000 to 2013 is around 43,745 Ha including Rice paddy (5,327 Ha) and Cropland (38,418 Ha). The highest damage in Agriculture is found to be 8,328 Ha in 2013, while the lowest damage is around 328 Ha in 2008.
3) The total number of affected people in Bakan and Phnom Kravanh districts from 2000 to 2014 is around 44,860 persons. The highest number of people affected by flood is 18,194 persons in 2013 and the lowest number of people affected by flood is 786 people in 2006. There are no affected people by flood in 2001, 2002, 2005, 2007, 2008, and 2009.

5.3 Flood Damage Analysis: 2000 – 2014

Flood damage analysis consists of flood frequency analysis, flood damage curve and flood damage probability curve. The result of flood damage analysis reposes to the second objective of the research, which is about the actual flood damage probability curve from 2000 to 2014. Moreover, the result from this part is considered as an important input for flood damage estimation and analysis in 2030 and 2050.

5.3.1 Frequency Analysis

This part discusses in detail about the frequency analysis and the selection of the best fitted distribution to the observed discharges. The frequency analysis of extreme value is very important in many hydrological engineering planning, design and management. In this case, daily water levels from Bak Trakoun flow station from 1994 to 2018 are converted into discharges using the rating equations developed by MOWRAM as shown in Table 3-2. The annual peak discharges of the 24-year records shows that the highest peak discharge is 1394 m^3/s in 1999 and the lowest peak discharge is 224 m^3/s in 1994.

Basically, the Extreme Value Type I (Gumbel distribution) is suggested for flood frequency analysis (Yue, Ouarda et al. 1999). However, in this analysis three extreme value distributions are selected to perform the analysis, which are Extreme Value Type I (Gumbel), Extreme Value Type II (Fréchet) and Log-Pearson Type III. The results of the analysis of each distribution are shown in Figure 5.39.

The computed value of peak discharges of Gumbel and Log-Pearson Type III distributions are quite similar compared with the observed peak discharges even though Gumbel distribution has only to parameters. The highest computed peak discharges of Gumbel and Log-Pearson Type III distributions are 1365 m^3/s and 1356 m^3/s respectively, which are only 29 m^3/s and 38 m^3/s lower than that of observed peak discharge. Nonetheless, Fréchet distribution tends to underestimate the low observed peak discharges and overestimate the high observed peak discharge. The computed highest peak discharge of the Fréchet distribution is 1696 m^3/s, which is 302 m^3/s higher than of the observed peak discharge. Moreover, the fitted line of

Fréchet distribution will overestimate the magnitude of peak discharge when the return period of the peak increased.

Extreme Value Type I: Gumbel Distribution

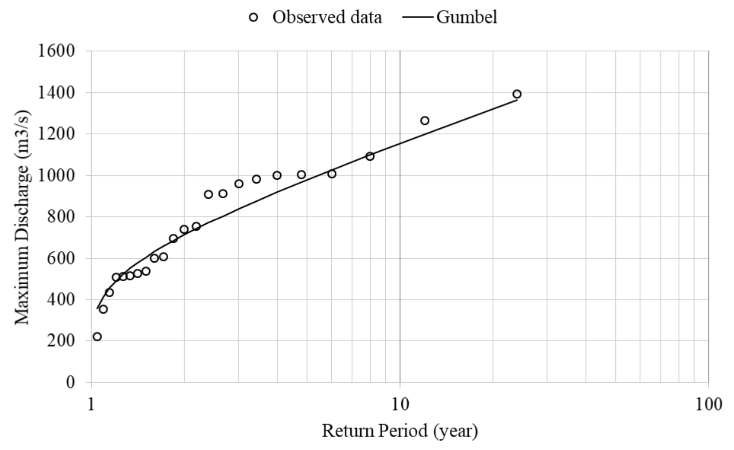

Extreme Value Type II: Fréchet distribution

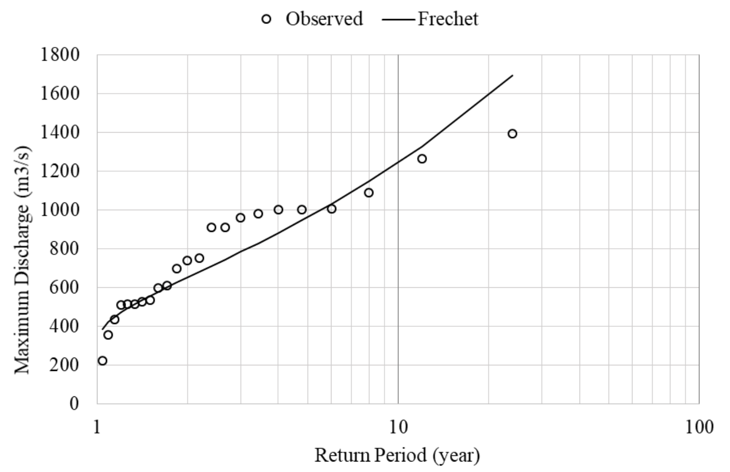

Log-Pearson Type III Distribution

Figure 5.39: Extreme value distributions

Anyways, the decision cannot be made based on this visualization. The test goodness of fit or the Chi-Square test is needed to perform in order to select the best fitted distribution to the observed peak discharges by using the hypothesis testing.

Test Goodness of Fit (Chi-Square Test)

The three distributions are tested the goodness of fit individually under the hypothesis that the distribution is rejected if X_0^2 of each extreme value distribution from Table 5-9 is smaller than $X^2_{k\text{-}p\text{-}1,\alpha}$ from Chi-Square table.

Table 5-9: Expected frequency of the distributions

Observed		**X_0^2(Gumbel)**		**X_0^2(Frechet)**		**X_0^2(Log Pearson III)**	
Dicharge Bin	**Frequency**	**Frequency**	**(Oi-Ei)^2/Ei**	**Frequency**	**(Oi-Ei)^2/Ei**	**Frequency**	**(Oi-Ei)^2/Ei**
400	2	1	1.00	1	1.00	2	0.00
600	7	6	0.17	8	0.13	5	0.80
800	4	7	1.29	7	1.29	6	0.67
1000	4	5	0.20	3	0.33	5	0.20
1200	4	3	0.33	2	2.00	3	0.33
1400	2	1	1.00	1	1.00	2	0.00
1600	0	0	0.00	0	0.00	0	0.00
1800	0	0	0.00	1	1.00	0	0.00
Total	23	23	3.99	23	6.74	23	2.00

Table 5-10: Chi-Square test of the distributions

Distribution	**Chi-square X_0^2**	**De. of Freedom**	**Chi-square $X^2_{k\text{-}p\text{-}1,\alpha}$**	**ΔX**
Gumbel	3.99	5.00	11.07	7.08
Frechet	6.74	4.00	9.48	2.74
Log-Pearson type III	2.00	4.00	9.48	7.48

Taking into account the 95% of confidence interval of the test, the significant level α is 0.05. The result from Table 5-10 shows that all distributions are fitted with the observed peak discharges based on the above hypothesis. The value of X_0^2 of each extreme value distribution from Table 5-9 is smaller than that of $X^2_{k\text{-}p\text{-}1,\alpha}$ from Chi-Square table (Critical Chi-square value); however, the level that these distributions are fitted with the observed peak discharges is not similar. The level of difference of Chi-Square value from Table 5-10 indicates the best fitted distribution since the greater the level of difference, the better fitted distribution to the observed peak discharges. In this case, the level of difference of Chi-Square value of Gumbel, Fréchet and Log-Pearson Type III are 7.08, 2.74 and 7.48 respectively meaning that Log-Pearson Type III is the best fitted distribution to the observed peak discharges.

Log-Pearson Type III fits well with the observed peak discharges because this distribution has three parameters (λ, β, and ε), which is more accurate to generate the computed peak discharges comparing with Gumbel distribution, which only has two parameters (α and u). Unlike Log-Pearson Type III, Fréchet distribution with three parameters (α, u and k), estimates a very high computed peak discharges compared with the observed peak discharge. It might be good in the sense of safety in flood mitigation project, yet this will cost more money in terms of the mitigation measure due to the overestimation of the peak discharges.

From this analysis, the magnitude of the flow within different return periods: 2, 5, 10, 15, 20, 25, 30, 50 and 100 years, are developed by using Log-Pearson Type III distribution. Finally, flood frequency curve at Bak Trakoun flow station is developed as shown in Figure 5.40.

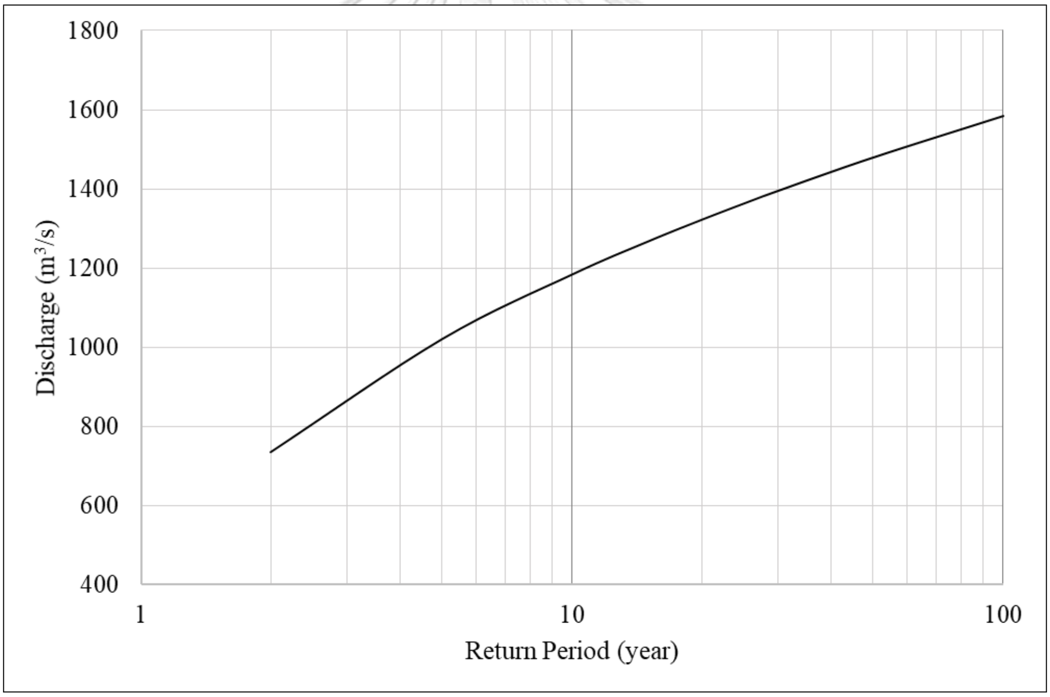

Figure 5.40: Flood Frequency Curve: Bak Trakoun Flow Station

5.3.2 Flood Damage Curve

Flood Damage Curve is a relationship or a function between flood damages and flood parameters. Basically, a flood parameter selected to be a function with flood damage is flood depth, which is called “Stage-Damage Curve”. It is possible to develop flood damage curve by using other flood parameters such as flood velocity, flood duration, flood discharge and flood extent, or even the combination between two or more flood parameters. There are straights and weaknesses at the same time when a flood parameter is used as a function with flood damage because the degree of damages and losses can be caused by more than one flood parameter. However, using one flood parameter, for example using flood depth as a predictor variable, can only identify the degree of the damage caused by flood depth (explained variation).

In this case, two types of flood damage curve: Stage-Damage Curve and Discharge-Damage Curve, are developed by using simple linear regression analysis. Since discharge is developed from water level, the two types of flood damage curves are similar. Yet, we still develop these flood damage curves because:

- **Stage-Damage Curve**: it is a very common flood damage curve since water depth in the river is easily recognized by local people and the explanation of flood damage as a function of water depth is very well-understood.
- **Discharge-Damage Curve**: it is not common that this type of flood damage is developed since it is quite similar to the stage-damage curve. However, in this case, the regression coefficients from this relationship is very important and needed to further develop the damage probability curve.

Stage-Damage Curve

As previously mentioned, stage-damage curve is a function between flood damage and flood depth. In this case, stage-damage curve is divided into three parts based on the damage sectors, which are agriculture, affected people and total damage. By using simple linear regression, the curves are transformed into logarithm scale to improve the correlation coefficient (R).

Overall, as shown in Figure 5.41, Figure 5.42 and Figure 5.43 the coefficient of determination (R^2) of the simple linear regressions between annual maximum water level and flood damage in agriculture, affected people and total damage are 0.48, 0.17, and 0.47 respectively. These values have been improved to 0.62, 0.66, and 0.64 respectively once the value of both variables is transformed into logarithm scale.

Normal

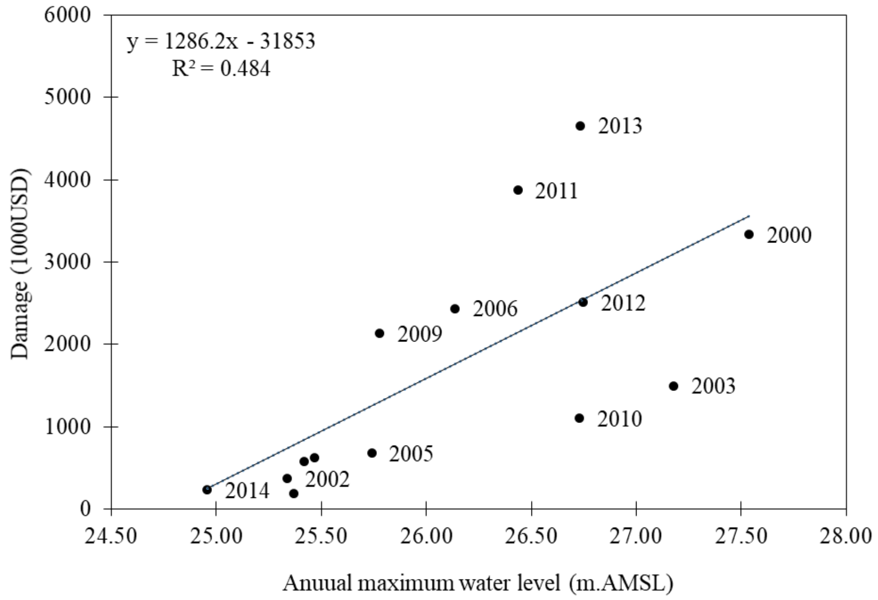

Logarithm

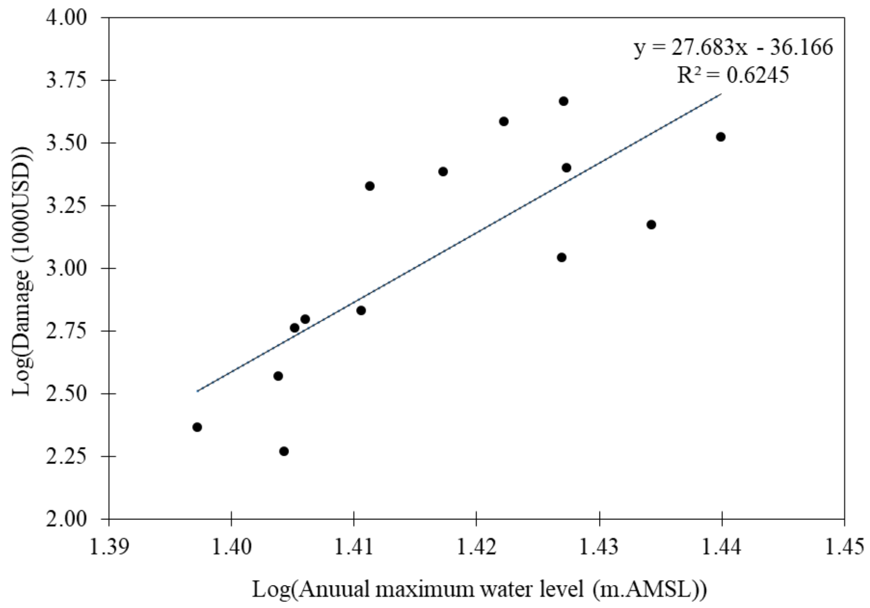

Figure 5.41: Stage-Damage Curve: Agriculture damage for Bakan and Phnom Kravanh districts (2014 price)

Normal	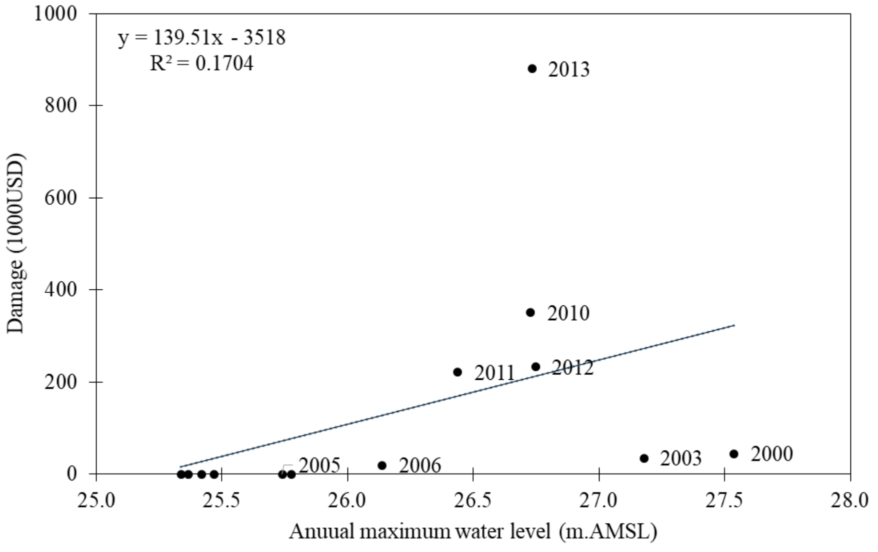
Logarithm	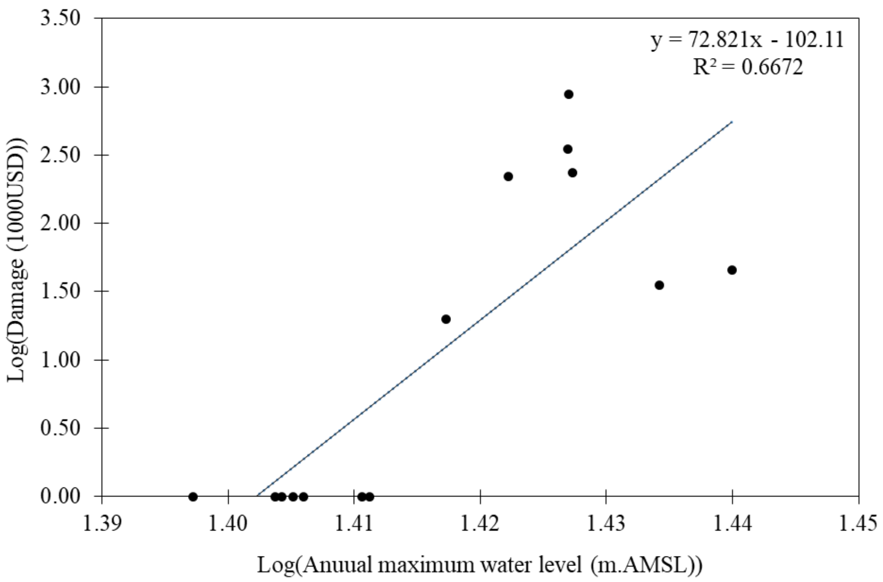

Figure 5.42: Stage-Damage Curve: Affected people for Bakan and Phnom Kravanh districts (2014 price)

Normal

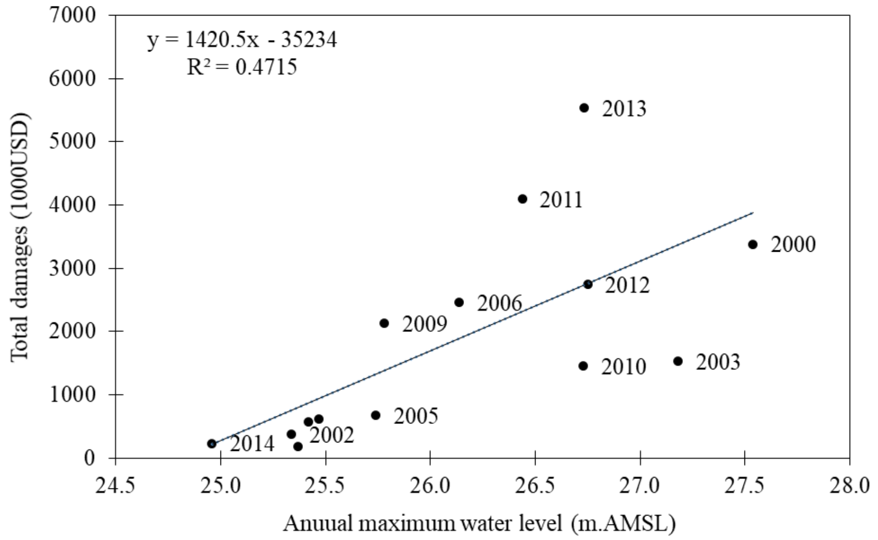

Logarithm

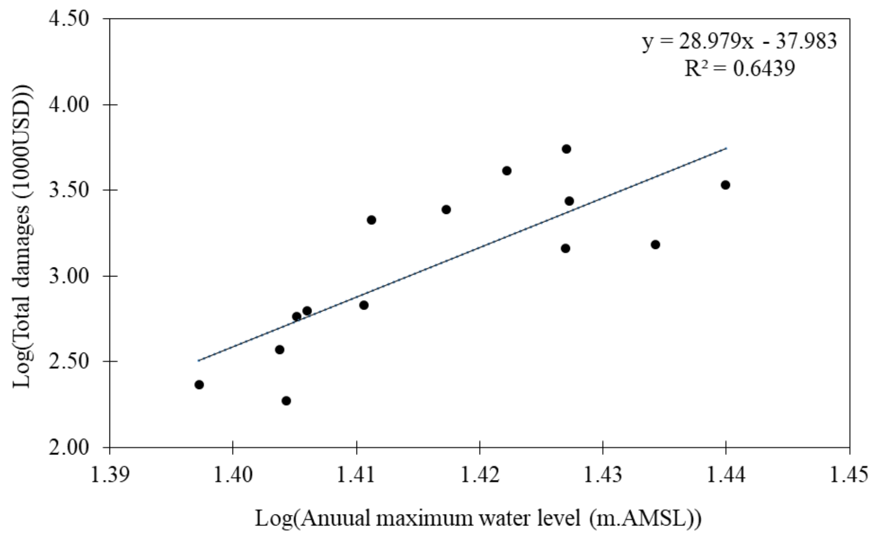

Figure 5.43: Stage-Damage Curve: Total damage for Bakan and Phnom Kravanh districts (2014 price)

Discharge-Damage Curve

Using the transformed logarithm on both variables, the discharge-damage curve is developed for five different curves based on the different characteristics of the damage types caused by flood such as damage in cropland, damage in paddy field, damage in agriculture (cropland and paddy field), affected people, and the total damage in all sectors as shown in Figure 5.44. The result of the regression analysis of each discharge-damage curve is summarized in Table 5-11. The regression analysis consists of coefficient of determination (R^2), significant level (α) and regression coefficient (b_0 and b_1). The significant level indicates whether the result of analysis is reliable and statistical significance. By using 95% confidence level, the significant level should be smaller than 0.05 so that the result of analysis is accepted.

The result shows that the significant levels of the analysis of discharge-damage curves are smaller than 0.05, implying that it is possible to use discharge as the predictor variable and flood damage, which is considered as the dependent variable that can be explained by the discharge from the fitted regression equation. The regression coefficients from the analysis will be used to develop the damage probability curve in 2014.

Cassava	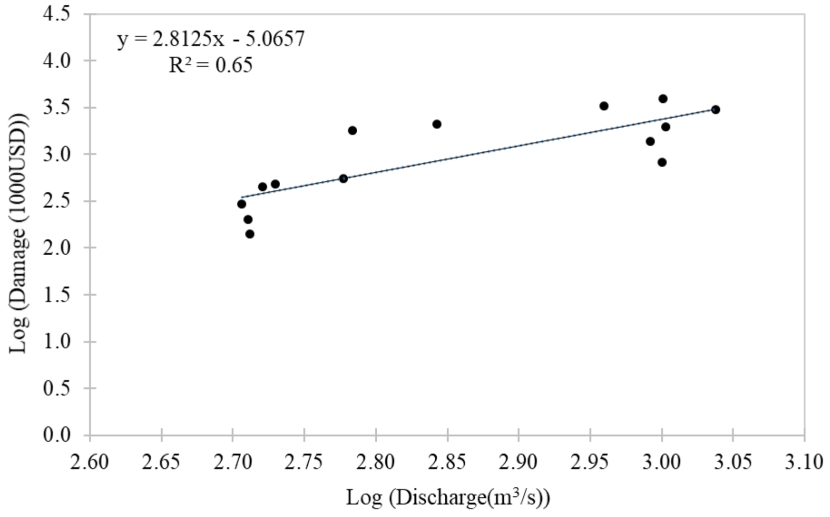
Rice paddy	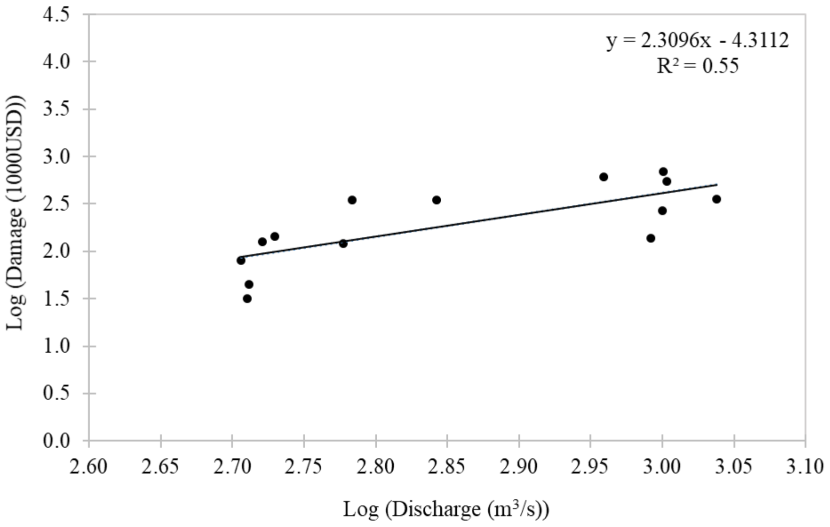

Agriculture	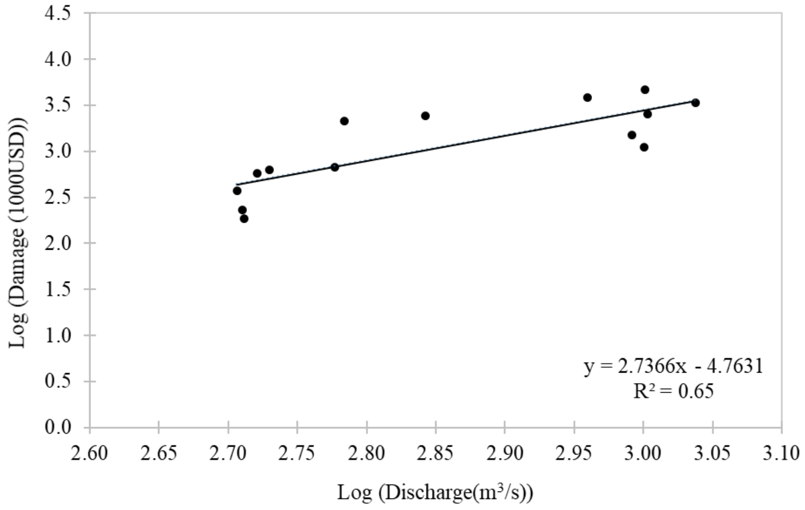
Affected people	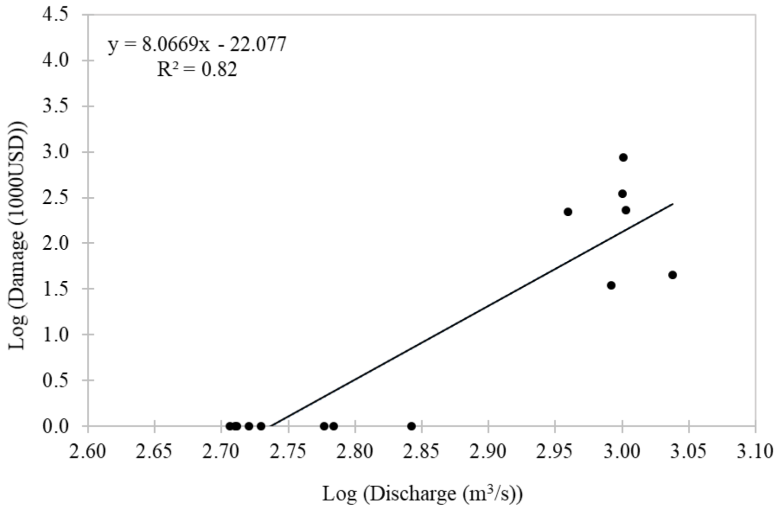
Total damage	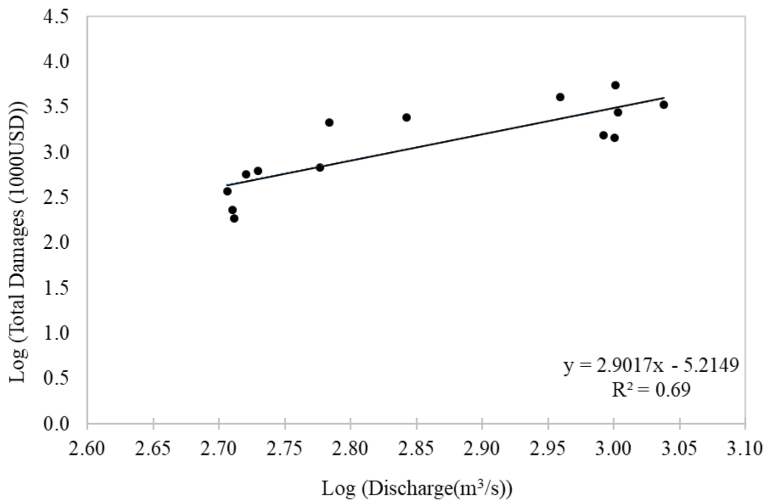

Figure 5.44: Discharge-Damage Curve in logarithm scale in each damage sector for Bakan and Phnom Kravanh districts (2014 price)

Table 5-11: Regression analysis for Discharge-Damage Curve in logarithm scale in all sectors (2014 price)

Logarithm	R Square	Significance level	Regression Coefficient	
		< 0.05 (ok)	a: Slope	b: Intercept
Cassava	0.65	0.000510	2.81	-5.07
Rice	0.56	0.002186	2.31	-4.31
Agriculture	0.65	0.000503	2.73	-4.76
Affected people	0.83	0.000006	7.97	-21.83
Total damage	0.69	0.000246	2.90	-5.21

5.3.3 Damage Probability Curve: 2014

Damage Probability Curve (DPC) is the result of the multiplication between flood frequency curves in 2014 from Figure 5.40 and the regression coefficients of the discharge-damage curves in the sector of interest as shown in Table 5-11. It provides the information about the expected annual damage in a given annual exceedance probability, the probability that the specified capacity or target water level will be exceeded in any given year. Damage probability curve allows the estimation of the average annual damage (AAD) in a particular year of flood event by doing the integration of the area under the curve.

Agriculture	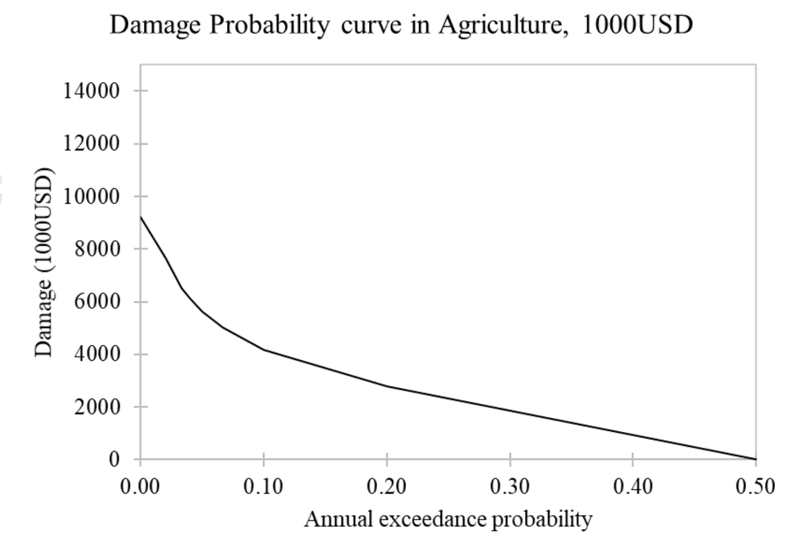

<table>
<tr><td>Affected people</td><td>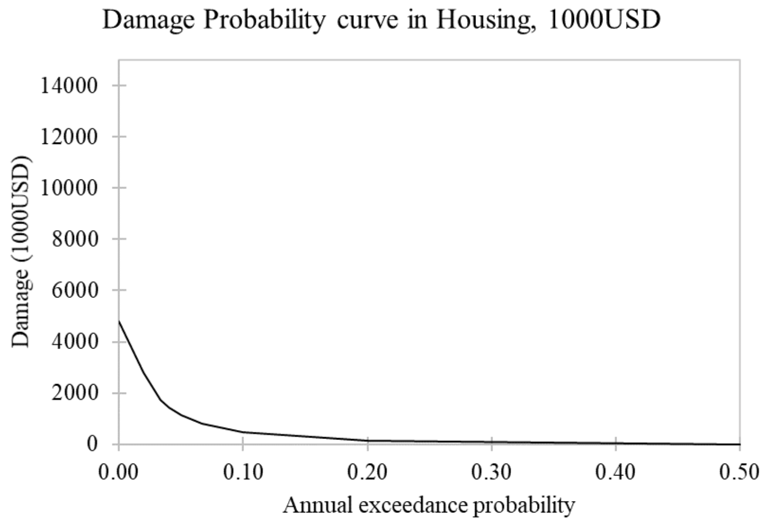
</td></tr>
<tr><td>Total damage</td><td>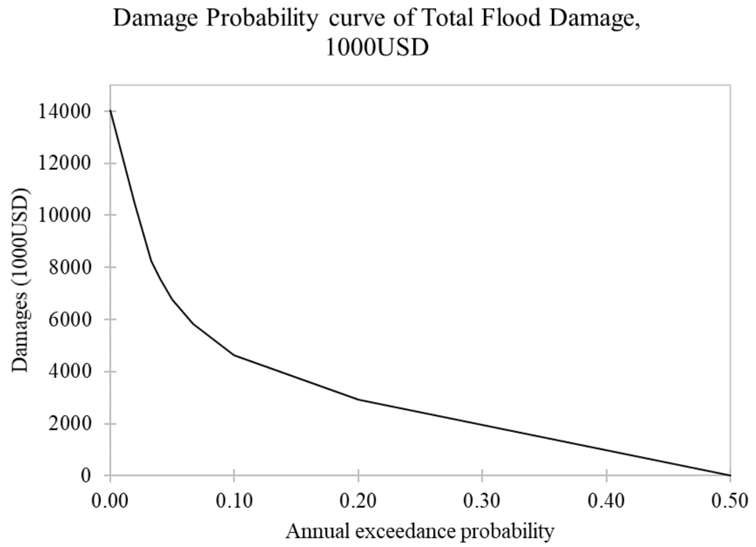
</td></tr>
</table>

Figure 5.45: Damage Probability Curve 2014: for Bakan and Phnom Kravanh districts

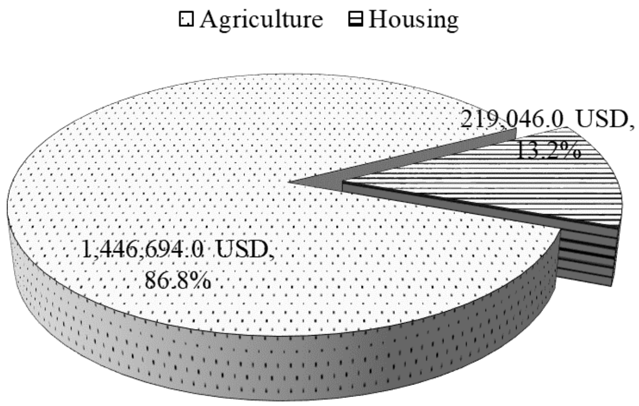

Figure 5.46: Annual average damages in each sector in Bakan and Phnom Kravanh districts for the reference case (2014)

The damage probability curves in agriculture and affected people and all sectors in Bakan and Phnom Kravanh districts are shown in Figure 5.45. To make the explanation simple, a flood of 100-year return period (1585 m^3/s at Bak Trakoun flow station) will be selected to be an example event in 2014 even the fact that there was no such a big flood in 2014. The result shows that if a flood of 100-year return period had occurred in 2014, it would have caused damages around 9.22 million USD in agriculture and 4.80 million USD from the affected people. The total damages are the combination between damage in agriculture and affected people. In this case, the expected total damage in 2014 caused by flood of 100-year return period is estimated to be 14.03 million USD.

Figure 5.45 also indicates the dissimilarity of the damage between agriculture and affected people. Agriculture starts having slightly damages when the flood of 2-year return period (around 734 m^3/s) occurs, while people in Bakan and Phnom Kravanh districts start having affected by flood and having the slightly damages at 5-year return period of flood (around 1020 m^3/s). Hence, it is concluded that when people are alerted about flood warning based on the threshold discharge mentioned by MOWRAM (800 m^3/s at Bak Trakoun flow station), floods have already caused slightly damages in Agriculture, while no significant damages to the people.

However, flood magnitude that would occur in each event depends mainly on the annual exceedance probability. The area under the damage probability curve is the possible annual flood damage that can exist corresponding to the annual exceedance probability. For example, there is a 10% chance that flood with the peak discharge of 1184 m^3/s occurs in 2014, which would have produced the expected flood damages of around 4.16 million USD in agriculture. As can be seen in Figure 5.46, the annual average damage in agriculture is around 1.45 million USD, almost 90% of the total damage, while AAD of affected people is around 0.22 million USD or 10% of the total damage. This result indicates that the affected area in Bakan and Phnom Kravanh districts is the rural area, where agriculture is the main sector in that area.

5.3.4 Summary

The second objective of the research is to develop damage probability curve in 2014 in Bakan and Phnom Kravanh districts.

Flood frequency curve is developed using the annual maximum discharge from Bak Trakoun flow station between 1994 and 2018. Three extreme value distributions (Gumbel, Fréchet and Log-Pearson Type II) are selected to do the frequency analysis, but only the best fitted extreme value distribution is selected based on the test of goodness of fit. The regression coefficients in logarithm scale between the annual maximum discharge and annual damage in each sector is used to develop the damage probability curve in 2014. The average annual damage in 2014 is the integration of the area under the damage probability curve in each sector.

The result shows that:

1) Log-Pearson Type III is the best fitted distribution to the maximum observed discharges at Bak Trakoun flow station. The highest return period to be considered in this study is 100-year return period, where the corresponding predicted discharge by Log-Pearson Type III is estimated to be 1485 m^3/s.
2) The coefficient of determination (R^2) in logarithm scale of the discharge-damage curve for Agriculture (Cassava and Rice) and Affected people is found to be 0.65 and 0.83 respectively, while the significant level (α) considering the 95% confidence level is 0.000503 in Agriculture and 0.000006 in Affected people. These significant levels are smaller than 0.05 meaning that the regression analysis is acceptable, or those variables are correlated.
3) The total annual average damage (AAD) in 2014 is estimated to be 1.66 million USD in which almost 90% of the damage is in agriculture, and 10% of the damage is in the residential area (people).

5.4 Flood Damage Estimation and Mitigation: 2030 and 2050

Flood damage estimation and analysis in 2030 and 2050 consists of the degree of expansion of socio-economic development, flood damage probability curve for the first and the second scenario and flood mitigation plans. The result of this part responses to the third objective, which is about the analysis of flood damage in 2030 and 2050 corresponding to socio-economic development including mitigation plan.

5.4.1 Degree of Expansion

The degree of expansion refers to the ratio of socio-economic development in 2030 and 2050 comparing with that of 2014 (baseline scenario) calculated by using the Equation 4.21 for agriculture and Equation 4.23 and 4.24 for the affected people. The degree of expansion is considered as an important indicator to identify the changes in both the quantity and quality of elements at risk in the future. In this case, the possible socio-economic development scenarios are assumed based on the exact information obtained from the Royal Government of Cambodia (RGC), local expert perception (the experiences of local experts in Pursat province) and the trend of the development information recorded from the previous year in the local and national level. However, some assumptions are followed the prediction made by international organizations in case the data needed is not available in local and national level. The sector to be estimated of socio-economic development is relatively relevant to those in section 5.3, which are cultivated area, crop yield and crop price for agriculture and population and GDP per capita for the affected people in the future.

Agriculture

To estimate the degree of expansion in agriculture, each component causing changes in this sector as shown in Figure 4.6 is needed to be examined such as cultivated area, crop yield and crop price.

Cultivated Area

Cultivated area can be estimated using a combination of Cropland and Rice in land covers from 2000 to 2015 in Bakan and Phnom Kravanh districts. Paddy rice and cassava are selected to represent Rice and Cropland in the cultivated area based on the information given by the Pursat provincial governor as indicated in section 5.2.3.

Figure 5.47 indicates that the cultivated area of paddy rice is decreased from 26.8 km^2 in 2000 to 18.4 km^2 in 2007 but keep slightly increasing every year from 2007 to 20.2 km^2 in 2015. In this case, it is assumed that the ratio of the cultivated area of Paddy rice in 2030 and 2050 comparing with that in 2014 is **1.00** and **1.00** respectively meaning that there is no much change for cultivated area of paddy rice.

Conversely, Cropland is expanded from 1507.5 km^2 in 2000 to 1603.1 km^2 in 2015, 6% increases within the last 15 years. In this case, the ratios of Cropland in 2030 and 2050 comparing with that in 2014 is **1.06** and **1.06** respectively meaning that the cultivated area of Cassava is expected to increase 6% from 2014 to 2030 and no change from 2030 to 2050. This assumption is made based on the trend in the past and the availability of the potential arable land that can be developed to be permanent agricultural land in the future. Based on the interview with Pursat provincial governor, one-third of the potential arable land in Pursat province have not been developed to be a permanent agricultural land yet.

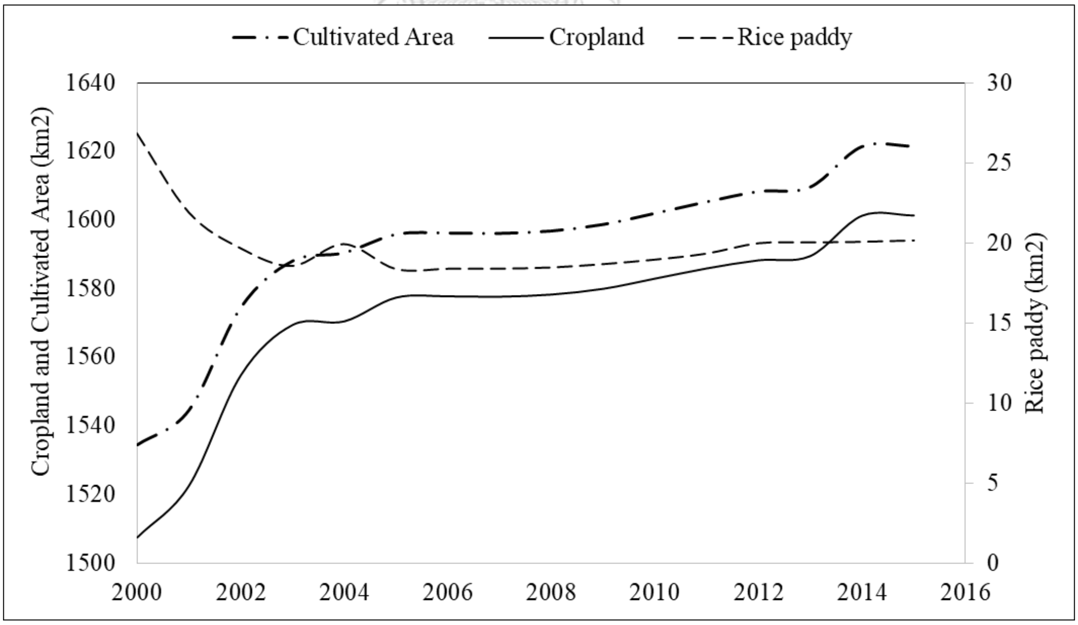

Figure 5.47: Cultivated Area in Bakan and Phnom Kravanh districts (land cover)

Crop Yield

As indicated in Figure 5.35, Rice yield in Cambodia had been increased around 1.0 t/Ha in the last 15 years, from 2.12 t/Ha in 2000 to 3.01 t/Ha in 2014. This yield is not quite high comparing with that of other countries such as Vietnam, China or Japan (around 6 to 7 t/Ha) as shown in Figure 5.48. In this case, it is assumed that the yield of rice in Cambodia as well as Pursat province is increasing 1.0 t/Ha in the next 16 years (4.0 t/Ha in 2030) and 2.0 t/Ha in the next 36 years (5.0 tons/ha in 2050). Hence, the multipliers of rice yield in 2030 and 2050 comparing with that in 2014 are **1.33** and **1.67** respectively.

Based on the record from the Ministry of Agriculture, Forestry and Fisheries (MAFF) in Figure 5.33, the yield of Cassava is fluctuated within the last 22 years between 1980 to 2001 and the average yield is around 7.07 t/Ha. 10.47 t/Ha is the last record of the yield of Cassava in 2001. The yield of Cassava between 2000 and 2014 is assumed to be 7.07 t/Ha and it is assumed that the ratio of the yield of Cassava in 2030 and 2050 comparing with that of 2014 is **1.00** and **1.00** respectively. It implies that the yield of Cassava is expected to be fluctuated around the average yield in the future.

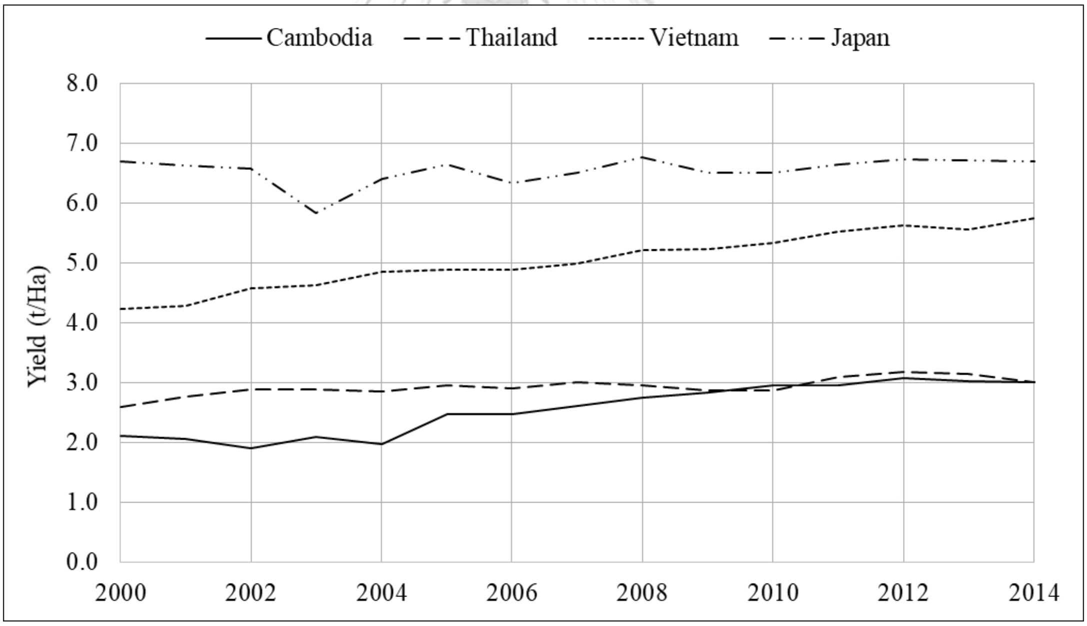

Figure 5.48: Rice yield in Cambodia, Japan, Thailand and Vietnam

Crop Price

Crop price is the most critical indicator to estimate. It can be varied by time based on the global market of agricultural products, private sector and government and NGOs intervention (subsidy) in agriculture in the country. Based on the record of MAFF, the price of agricultural products is different from year to year or even month to month; however, the average farm gate value of mixed rice (average-quality rice) is about 1077 KHR/kg and cassava is about 300 KHR/kg. It is assumed that the price of rice and cassava in 2030 and 2050 will be increased based on the importance of food security and high-quality organic products. In this case, two scenarios of rice price are made:

- **First Scenario (A1)**: the price of rice and cassava in 2030 and 2050 compared with that of 2014 are **1.3** and $(1.3)^2$ or **1.69** respectively (Normal rice).
- **Second Scenario (A2)**: the price of cassava in the second scenario is the same as in the first scenario, yet the price of rice is different. It is assumed that people produce the high-quality-organic rice in 2030 and 2050 in Bakan and Phnom Kravanh districts to increase the value added of rice. We assume that the price of high-quality-organic rice is triple higher than that of normal rice based on the experience of selling the organic vegetables in Cambodia. Hence, the price of rice in 2030 and 2050 for high-quality-organic rice comparing that of 2014 are **3.0** and $(3.0)^2$ or **9.0** respectively.

Affected people

Affected people sector is mainly focused on the people affected by flood in each flood year. The number of people affected by flood is the result of the integration between flood map and Nighttime Light Index (NLI) from GEE. We want to estimate the damage in the village, the affected people in the area in 2030 and 2050 based on the exceedance probability of flood magnitude. The changes of affected people to be estimated in this case are the population and GDP per capita in 2030 and 2050.

Population

Based on the record and the prediction of the Cambodian population by The United Nation from 1950 to 2099, the population in the country keep increasing from 1982 (after Pol Pot regime) until 2075 with a total population of around 23,458,459 before starting to decrease. The Cambodian population in 2014 is 15,022,692 and the predicted population in 2030 and 2050 is 18,606,102 and 21,899,525 respectively. The ratio of the population in 2030 and 2050 comparing with that in 2014 is **1.23** and **1.44** respectively. This ratio will be used for the prediction of the population in Bakan and Phnom Kravanh in 2030 and 2050.

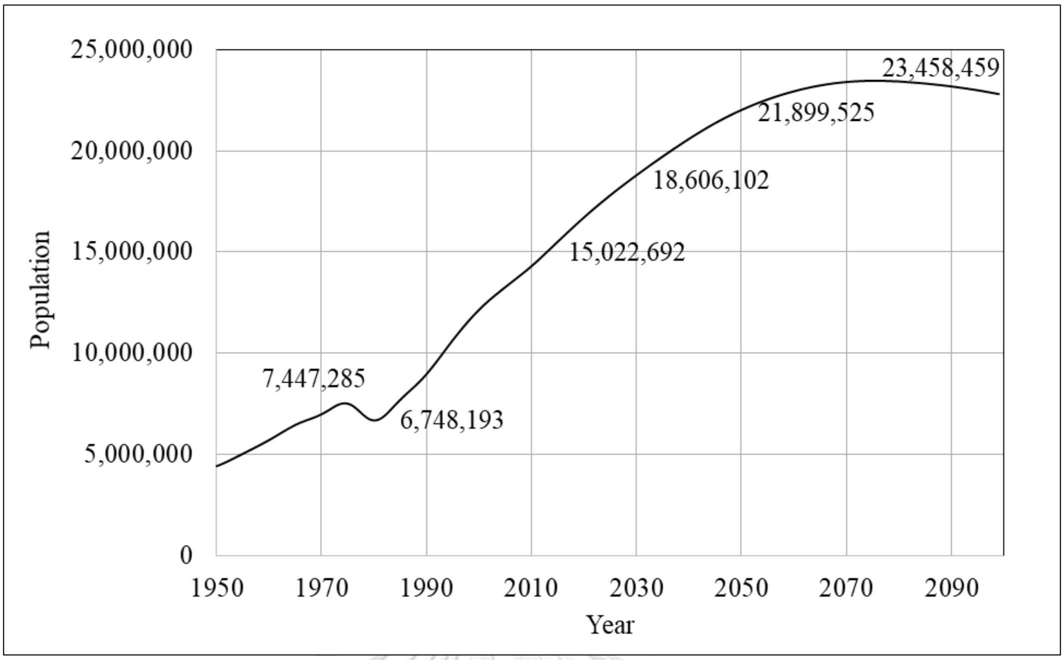

Figure 5.49: Cambodia population data (UN)

GDP per Capita

The Gross National Income (GNI) is the combination between the Gross Domestic Product (GDP) and Net External Income (the income of the people living and working abroad and send the money back to the country origin). In case of Cambodia, the GNI per capita is lower than the GDP per capita meaning that there are investments of foreign companies in Cambodia and the profit that those companies make goes back to their country origin. As can be seen in Figure 5.50, the GDP per capita of the Cambodian people in 2014 is 1139 USD, while the GNI per capita is only 1020 USD. There is no prediction of the GDP per capita of the Cambodian people in 2030 and 2050 by the government or any organizations. The hint of the assumption follows the policy of The Royal Government of Cambodia; they would like to develop Cambodia to be the Upper-middle income country in 2030 and High-income country in 2050. Based on the World Bank report, country can be classified by the Gross National Income (GNI) in order to identify whether a country is a Low-income country, Lower or Upper-middle income country, or High-income country.

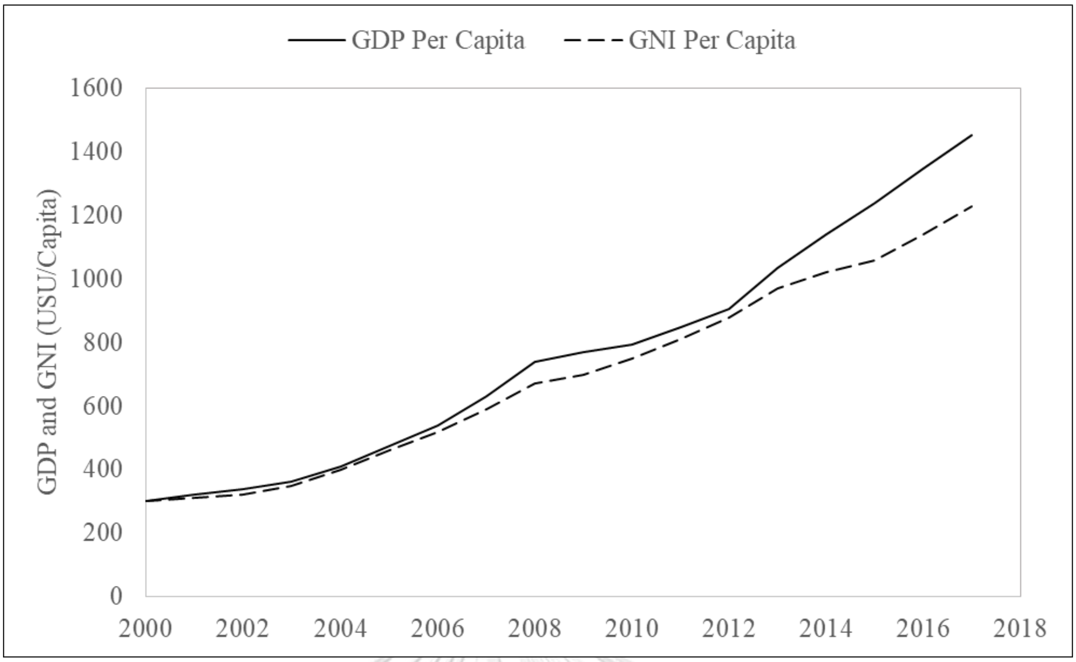

Figure 5.50: Cambodia GDP and GNI (RGC 2018)

Table 5-12 indicates that the Low-income country has the GNI per capita less than 996 USD; the Lower-middle income country has the GNI per capita between 996 USD to 3,895 USD; the Upper-middle income country should have the GNI per capita from 3,895 USD to 12,055 USD; and the GNI per capita of the High-income country is more than 12,055 USD. It is noted that the GNI per capita of the Cambodian people in 2014 is 1020 USD indicated that Cambodia is a Lower-middle income country at time. In this case, it is assumed that the GNI per Capita of the Cambodian people is 3,896 USD in 2030 and 12,056 USD in 2050. Hence, the GNI per Capita in 2030 and 2050 compared with that of 2014 are **3.82** and **11.82** respectively.

Table 5-12: Country classification by the Gross National Income (GNI)

Threshold	**GNI/Capita (current USD)**
Low-income	< 996
Lower-middle income	996 - 3,895
Upper-middle income	3,896 - 12,055
High-income	> 12,055

The degree of expansion in agriculture and affected people is summarized in Table 5-13 and Table 5-14 respectively. The ratio of changes in each indicator for both sectors does follow the trend in the past, which is likely to occur in the future if there are no significant political and economic crises in Cambodia. Some assumptions such as rice price in scenario A2 and the ratio of GNI per capita in 2030 and 2050 are most affected indicator to increase in value of elements at risk. However, these assumptions are possible to become the reality. It is noticed that the first policy of the RGC in the last 15 years (2000-2015) was to develop Cambodia from Low-income country (300USD/capita in 2000) to be the Lower-middle income country in 2015. In 2014, the World Bank announced that Cambodia had moved to the Lower-middle income country by 2014 with the GDP per capita 1139 USD, 3.79 times higher than that of the year 2000.

Table 5-13: Degree of expansion of each indicator in Agriculture

Indicator	**Crop type**	**Degree of Expansion**		
		2014	**2030**	**2050**
Cultivated Area	Cassava	1.00	1.06	1.06
Cultivated Area	Rice	1.00	1.00	1.00
Yield	Cassava	1.00	1.00	1.00
Yield	Rice	1.00	1.33	1.67
Price: A1	Cassava	1.00	1.30	1.69
Price: A1	Rice (Normal)	1.00	1.30	1.69
Price: A2	Cassava	1.00	1.30	1.69
Price: A2	Rice (Organic)	1.00	3.00	9.00

Table 5-14: Degree of expansion of each indicator in Affected people

Indicator	**Degree of Expansion**		
	2014	**2030**	**2050**
Population	1.00	1.23	1.44
GNI per capita	1.00	3.82	11.82

5.4.2 Damage Probability Curve: 2030 and 2050

Agriculture

The degree of expansion in each scenario is the result of multiplication of the degree of expansion of each indicator (cultivated area, crop yield and crop price) in

Agriculture. As mentioned in section 5.4.2, agricultural production and pricing is considered under 2 scenarios (in case 2030):

- Scenario 1 named "BSD-2030-A1H1" means the integration of (a) socio-economic scenario in agriculture "A1", farmer uses technology and innovation for rice production and (b) socio-economic scenario in affected people "H1" under population and GDP per capita in the future.
- Scenario 2 named "BSD-2030-A2H1" is the same structure as scenario 1 but socio-economic scenario in agriculture "A2" means farmer uses technology and innovation for rice production concentrated in organics way to increase the value added of rice.

The same scenario is taken into account for the case of 2050. The ratio of expansion in Cassava and Rice in both scenarios is shown in Table 5-15

Table 5-15: Degree of expansion of each scenario in Agriculture

Scenario	**Crop type**	**Degree of Expansion**		
		2014	**2030**	**2050**
Scenario 1: A1	Cassava	1.00	1.38	1.80
	Rice	1.00	1.73	2.82
Scenario 2: A2	Cassava	1.00	1.38	1.80
	Rice	1.00	4.00	15.00

From the previous information, the Damage Probability Curve in Agriculture (ADPC) in each scenario and each year is indicated in the abbreviation below:

- BL-2014: Baseline scenario in 2014 (ADPC2014)
- BSD-2030-A1H1: ADPC2030 Based Development Scenario 1 in 2030
- BSD-2030-A2H1: ADPC2030 Based Development Scenario 2 in 2030
- BSD-2050-A1H1: ADPC2050 Based Development Scenario 1 in 2050
- BSD-2050-A2H1: ADPC2050 Based Development Scenario 2 in 2050

2030

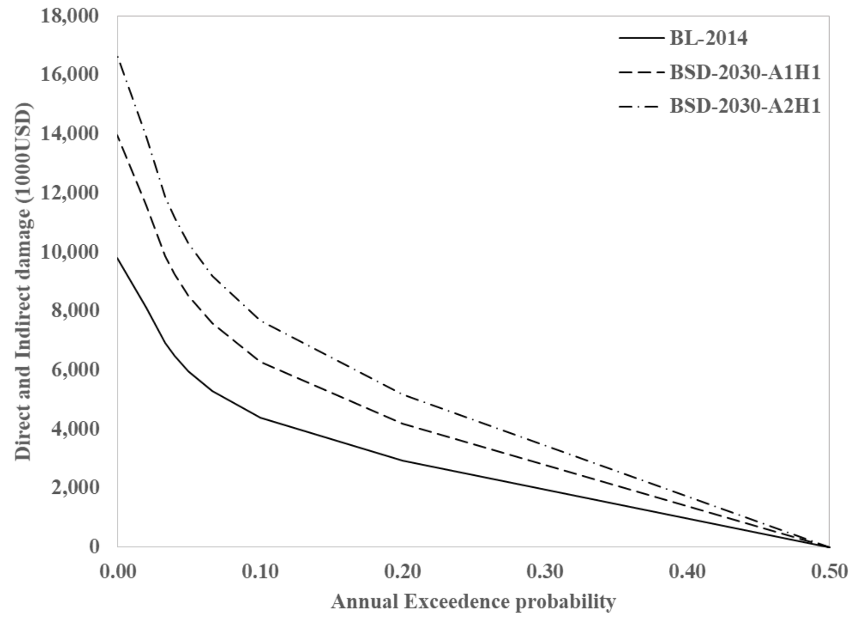

2050

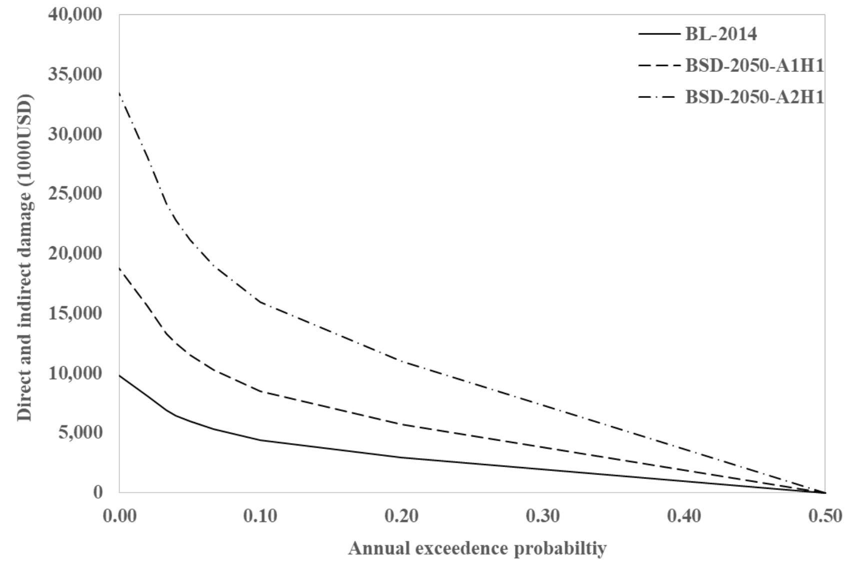

Figure 5.51: Damage Probability Curve: Agricultural damage for Bakan and Phnom Kravanh districts

Figure 5.51 indicates the damage probability curve in agriculture in 2030 and 2050. ADPC2030 and ADPC2050 is the result of the multiplication of ADPC2014 with the degree of expansion in each socio-economic development scenario with the assumption that there is no change in discharge caused by climate change in 2030 and 2050. The formula used in this section is already explained in Equation 4.22.

The expected damage depends mainly on the annual exceedance probability that a flood event would possibly occurs in the year of interest. To make the explanation simple, a flood of 100-year return period (1585 m^3/s at Bak Trakoun flow station) will be selected to be an example event in 2030 and 2050 even the fact that this flood has a very small probability to occur. The result shows that if a 100-year return period flood would happen in 2030, the expected damage in agriculture will be around 13.9 million USD in the first scenario (A1H1) and 16.8 million USD in the second scenario (A2H1), while the same flood would cause more damages in agriculture in 2050; for instance, 18.8 million USD in the first scenario (A1H1) and 33.4 million USD in the second scenario (A2H1).

As indicated in section 5.2, for example, flood extent in 2000 (205 km^2) is almost the same as that of 2011 (202 km^2); however, it is found that the damage area in agriculture by flood in 2000 (6,248 Ha) is less than that of 2011 (6,923 Ha) due to the increase in overall of the cultivated area as shown in Figure 5.47. Moreover, if the loss in monetary term (yield and price) is considered between 2000 in 2011, the loss in agriculture in 2000 (570.8 USD/Ha) is even less than that in 2011 (797.0 USD/Ha). Based on this scenario in the past, the economic development really changes the value of elements at risk. The same context is applied here. The value of flood damages in the future is different based on the temporal changes of socio-economic development scenarios. For example, the price of high-quality organic rice in the second scenario in 2050 is increased to be 9 times higher than that of the baseline scenario in 2014; therefore, the damage is higher following the development.

Each flood magnitude that would possibly occur in 2030 and 2050 has their own annual exceedance probability to produce the corresponding expected annual damages in Agriculture. Hence, it is possible to calculate the Average Annual Damage (AAD) by the integration of the area under the damage probability curve based on the corresponding annual exceedance probability as shown in Figure 5.52. The result of expected average annual damages in Agriculture in each scenario is indicated in Table 5-16.

Average Annual Damage (AAD) in 2030 and 2050 in Agriculture

The average annual damage (AAD) of flood damage in agriculture in each scenario and each year:

- BL-2014
- 2030: BSD-2030-A1H1, BSD-2030-A2H1
- 2050: BSD-2050-A1H1, BSD-2050-A2H1

<table>
<tr><td>BSD-2030-A2H1</td><td>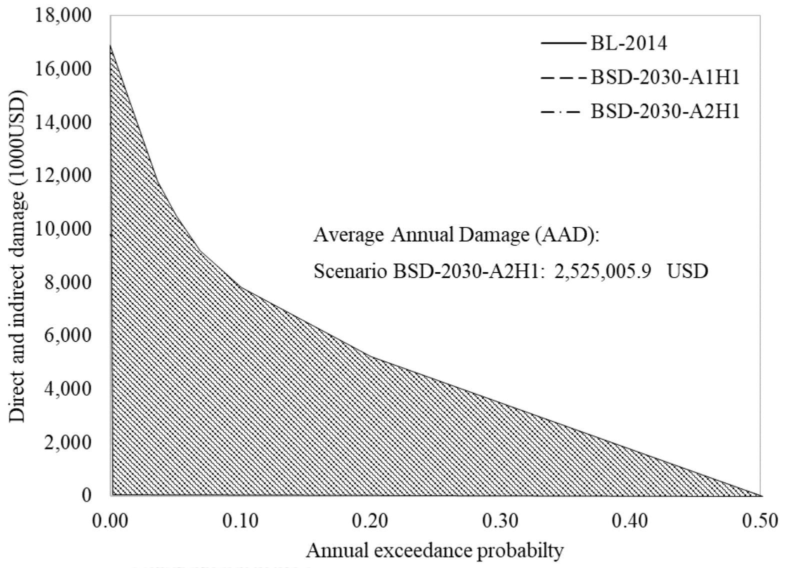
</td></tr>
<tr><td>BSD-2050-A2H1</td><td>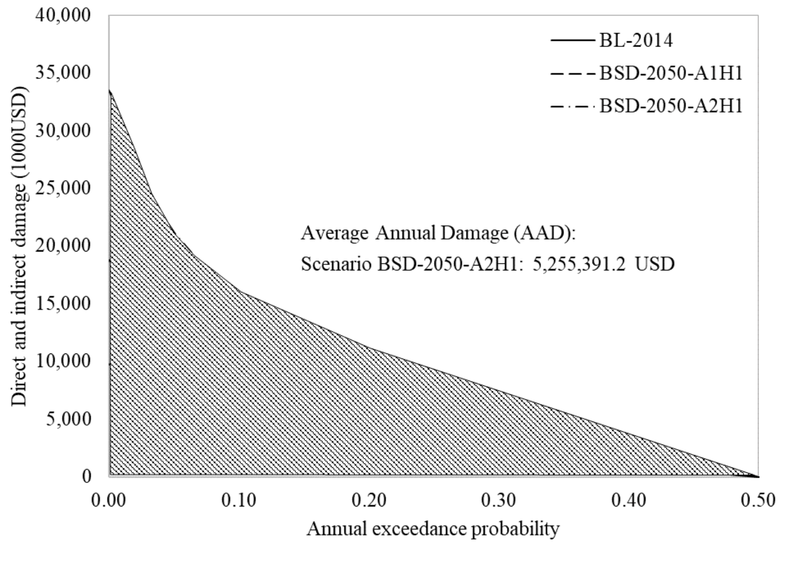
</td></tr>
</table>

Figure 5.52: Average Annual Damage (ADD): Agricultural damage in Bakan and Phnom Kravanh districts

Figure 5.52 visualizes an example of average annual damage of the second scenario (A2H1) in 2030 and 2050. The estimated average annual damage in 2030 is around 2.52 million USD, while the estimated average annual damage in 2050 is 5.25 million USD. The average annual damage in other scenarios is shown in Table 5-16.

Table 5-16: AAD in each development scenario in Agriculture

	BL-2014	**BSD-2030-A1H1**	**BSD-2030-A2H1**
Market price	1,446,693.9	2,068,692.7	2,525,005.9
	BL-2014	**BSD-2050-A1H1**	**BSD-2050-A2H1**
Market price	1,446,693.9	2,802,707.8	5,255,391.2

Moreover, since the damage in Agriculture is different based on the price between normal and organic rice, the sub-scenarios in agriculture between these two price classes are considered in the year 2030 and 2050. The assumption is made based on the possibility that there will be a combination between normal and organic rice in Bakan and Phnom Kravanh districts because the first scenario (A1: 100% normal rice) and the second scenario (A2: 100% organic rice) are the extreme cases between the lowest and the highest agricultural development scenarios. Moreover, based on the survey, some farmers have already cultivated the organic rice and vegetables in some part of these two districts. Hence, the sub-scenarios assumed below could possibly match the real situation.

The degree of expansion of rice price between normal and organic rice is indicated in Table 5-17. The meaning of the abbreviation is explained as below:

- A1 : 100% of normal rice
- 0.25A2 : 75% of normal rice and 25% of organic rice
- 0.50A2 : 50% of normal rice and 50% of organic rice
- 0.75A2 : 25% of normal rice and 75% of organic rice
- A2 : 100% of organic rice

Table 5-17: Degree of expansion of rice price

Year	**Sub-scenarios (Rice price)**				
	A1	**0.25A2**	**0.50A2**	**0.75A2**	**A2**
2030	1.30	1.73	2.15	2.58	3.00
2050	1.69	3.52	5.35	7.17	9.00

2030

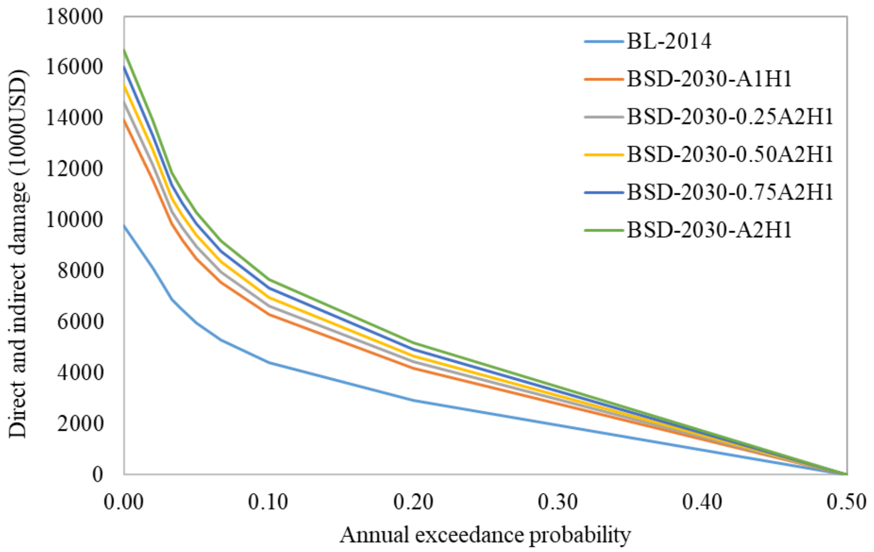

2050

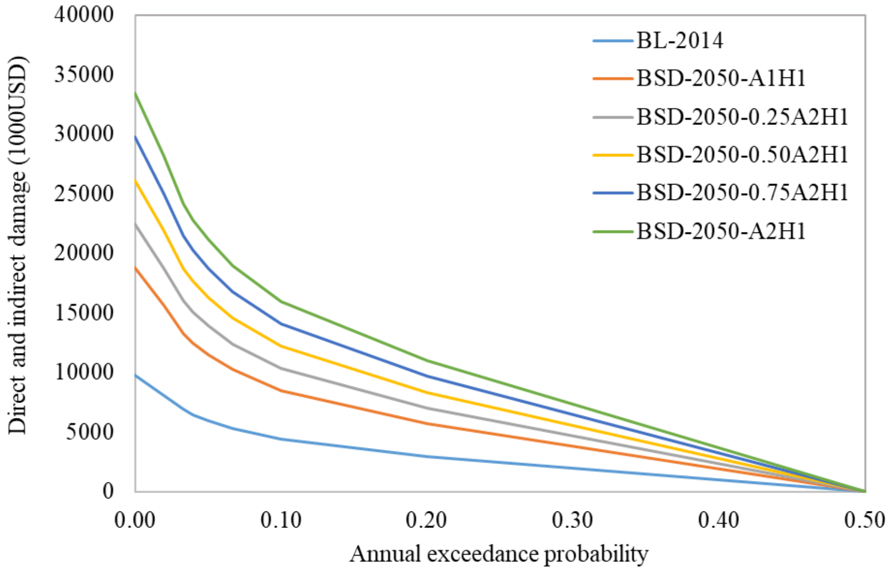

Figure 5.53: Damage Probability Curve: Agricultural damage, the scenarios in between normal and organic rice

If one of these scenarios can be existed in 2030 and 2050, the damage probability curve and the average annual damage (AAD) of each scenario is also different. The difference of the damage probability curve and average annual damage in agriculture based on the sub-scenarios of rice price between normal and organic rice is indicated in Figure 5.53 and Table 5-18 respectively. It can be seen from Table 5-17 that the average annual damage in agriculture increases in both 2030 and 2050 when the percentage of organic rice increases. This is because the value added of organic rice is higher than that of normal rice.

Table 5-18: AAD in Agriculture based on the changes of normal and organic rice

Scenario	Market price of AAD (1,000USD)	
	2030	2050
BSD-A1H1	2,068.7	2,802.7
BSD-0.25A2H1	2,182.8	3,415.9
BSD-0.50A2H1	2,296.8	4,029.0
BSD-0.75A2H1	2,410.9	4,642.2
BSD-A2H1	2,525.0	5,255.4

Affected people

Figure 5.54 indicates the damage probability curve of the affected people in 2030 and 2050. Similar to agriculture, HDPC2030 and HDPC2050 is the result of the multiplication of ADPC2014 with the degree of expansion in each socio-economic development scenario with the assumption that there is no change in discharge caused by climate change in 2030 and 2050. The formula used in this section is already explained in Equation 4.25.

Based on the degree of expansion in Table 5-14, there is only one socio-economic development scenario of the affected people meaning that the same scenario is applied for (A1H1) and (A2H1) in both 2030 and 2050. The Damage Probability Curve of the affected people (HDPC) in each scenario and each year is indicated in the abbreviation below:

- BL-2014: Baseline scenario in 2014 (HDPC2014)
- BSD-2030-A1H1 and BSD-2030-A2H1: HDPC2030 Based Development Scenario in 2030
- BSD-2050-A1H1 and BSD-2050-A2H1: HDPC2050 Based Development Scenario in 2050

Similar to agriculture, a flood of 100-year return period (1585 m^3/s at Bak Trakoun flow station) will be selected to be an example event in 2030 and 2050 even the fact that this flood has a very small probability to occur. The result shows that if a 100-year return period flood would happen in 2030, the expected damage of the affected people will be around 22.5 million USD, while the same flood would cause more damages in affected people around 81.8 million USD in 2050.

2030	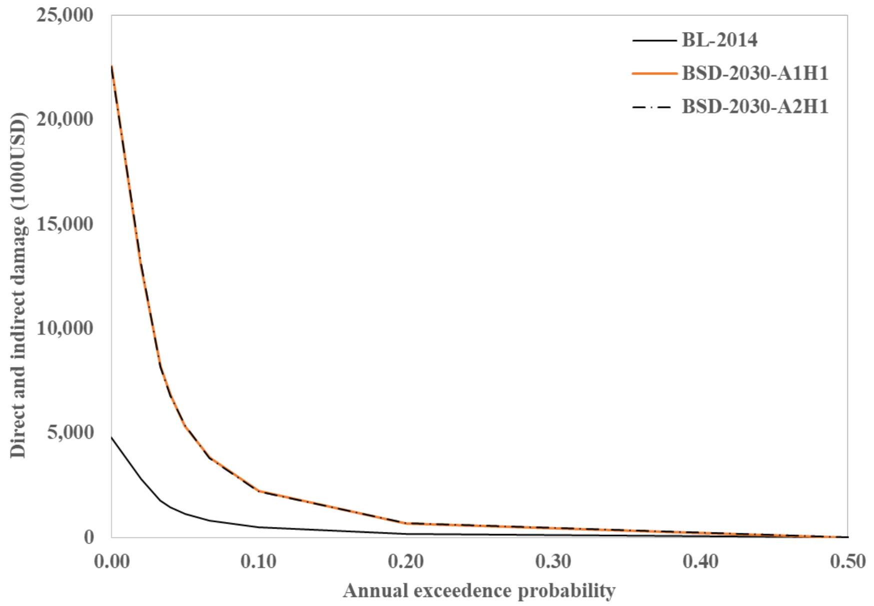
2050	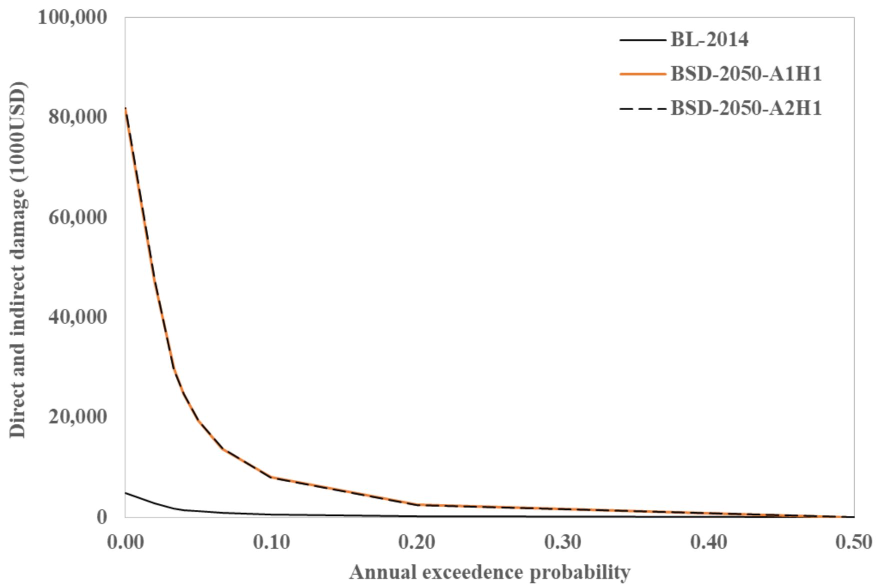

Figure 5.54: Damage Probability Curve: Damage of the affected people for Bakan and Phnom Kravanh districts

However, it is remarked that the HDPC2030 and HDPC2050 in Figure 5.54 starts having slightly damages only when a flood of 5-year return period occurs, while the ADPC2030 and ADPC2050 in Figure 5.51 starts having slightly damages when a flood of 2-year return period occurs indicating that agriculture is more exposed and vulnerable to flood than the people in the villages.

As indicated in section 5.2 for example, flood extent in 2000 (205 km^2) is almost the same as that of 2011 (202 km^2); however, it is found that the number of people affected by floods in 2000 (3,229 persons) is less than that of 2011 (5,604 persons) due to the improvement of Digital Number (DN) of Nighttime Light Index (NLI). Moreover, if the loss in monetary terms (GDP per capita) is considered between the affected people in 2000 and the affected people in 2011, the loss of the affected people in 2000 (14.0 USD/person) is even less than that in 2011 (39.6 USD /person). Based on the scenario in the past, the economic development really changes the value of elements at risk in the future if the coping capacity of the elements at risk is the same.

The same result is illustrated Figure 5.54. The potential damage of the affected people in 2050 is much more than that of 2030, while the potential damage in 2030 is more than that in 2014. It is because of the improvement of the socio-economic development in both the number of population and GDP per capita in 2030 and 3050.

Each flood magnitude that would possibly occur in 2030 and 2050 has their own annual exceedance probability to produce the corresponding expected annual damages of the affected people. The high annual exceedance probability of flood occurrence is expected to cause the low damages; conversely, the low annual exceedance probability of flood occurrence is expected to produce the high damages. Hence, the Average Annual Damage (AAD) is needed to determine. The result of expected average annual damages in Affected people in 2030 and 2050 is shown in Table 5-19.

Average Annual Damage (AAD) in 2030 and 2050 of the Affected people

The average annual damage (AAD) of flood damage of the affected people in each scenario and each year:

- BL-2014
- 2030: BSD-2030-A1H1= BSD-2030-A2H1
- 2050: BSD-2050-A1H1= BSD-2050-A2H1

BSD-2030-A2H1	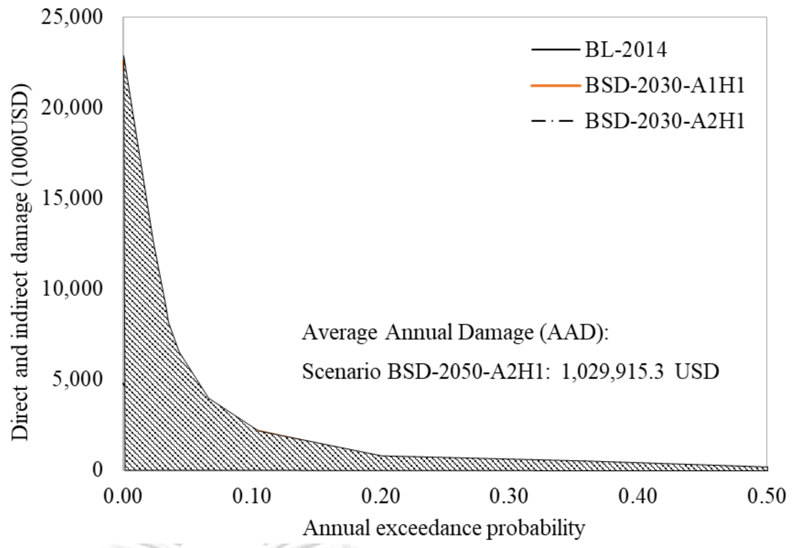
BSD-2050-A2H1	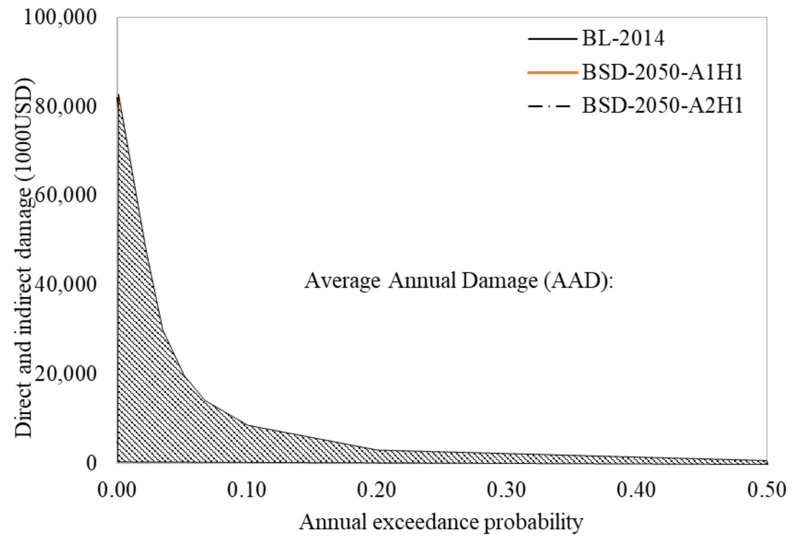

Figure 5.55: Average Annual Damage (ADD): Affected people damage in Bakan and Phnom Kravanh districts

Figure 5.55 visualizes an example of the average annual damage of the affected people in 2030 and 2050. The average annual damage in 2030 is around 1.03 million USD, while the estimated average annual damage in 2050 is 3.73 million USD. The average annual damage in other scenarios is demonstrated in Table 5-19.

Table 5-19: AAD in each development scenario in Affected people

	BL-2014	**BSD-2030-A1H1**	**BSD-2030-A2H1**
Market price	219,046.1	1,029,915.3	1,029,915.3
	BL-2014	**BSD-2050-A1H1**	**BSD-2050-A2H1**
Market price	219,046.1	3,732,837.7	3,732,837.7

All Sectors

The Total Damage Probability Curve (TDPC) in all sectors is the combination of ADPC and HDPC. The similar scenarios of agriculture and affected people are applied in this case as shown in the abbreviation below:

- BL-2014: Baseline scenario in 2014 (ADPC2014)
- BSD-2030-A1H1: ADPC2030 Based Development Scenario 1 in 2030
- BSD-2030-A2H1: ADPC2030 Based Development Scenario 2 in 2030
- BSD-2050-A1H1: ADPC2050 Based Development Scenario 1 in 2050
- BSD-2050-A2H1: ADPC2050 Based Development Scenario 2 in 2050

Figure 5.56 indicates the total damage probability curve of Agriculture and Affected people sector. Since the degree of expansion in affected people is the same between the first scenario (A1H1) and the second scenario (A2H1), the difference in TDPC is resulted from the development scenario in Agriculture.

To make the explanation simple, a flood of 100-year return period (1585 m^3/s at Bak Trakoun flow station) will be selected to be an example event in 2030 and 2050 even the fact that this flood has a very small probability to occur. The result shows that if a 100-year return period flood would happen in 2030, the expected damage in all sectors will be around 36.53 million USD in the first scenario (A1H1) and 39.26 million USD in the second scenario (A2H1), while the same flood would cause more damages in all sectors in 2050; for instance, 100.60 million USD in the first scenario (A1H1) and 115.29 million USD in the second scenario (A2H1). The difference of the expected damages is because of the degree of expansion of the price of the high-quality organic rice in the second scenario (A2H1).

2030

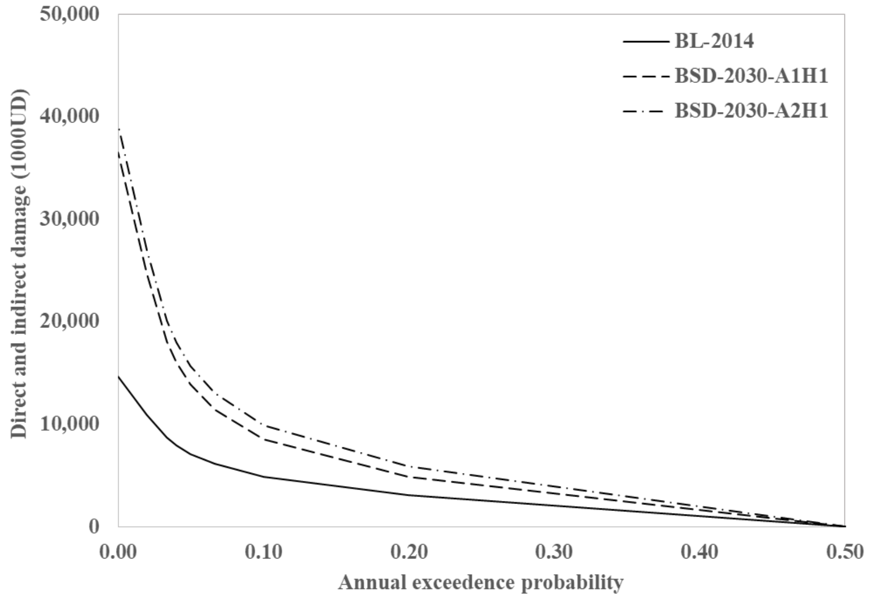

2050

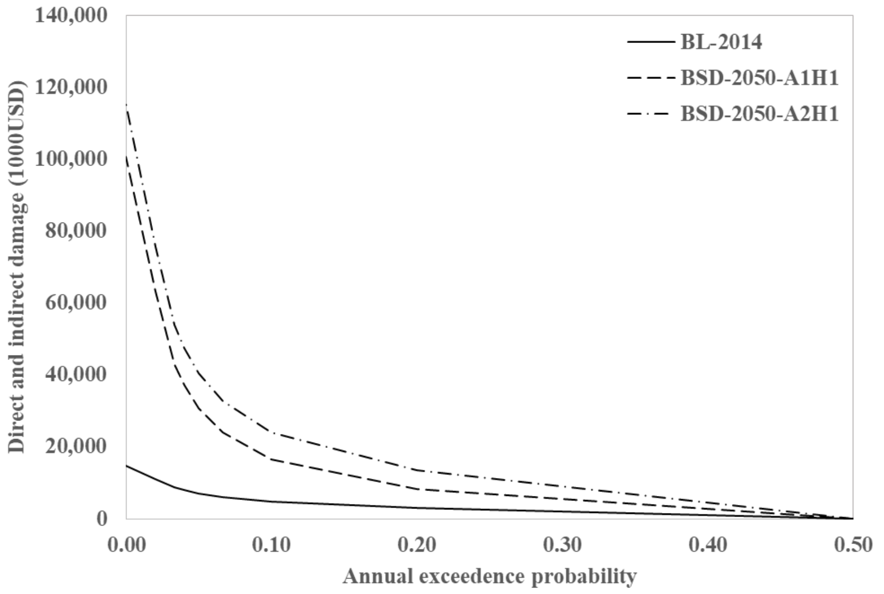

Figure 5.56: Damage Probability Curve: Total damage for Bakan and Phnom Kravanh districts

Average Annual Damage (AAD) in 2030 and 2050 in All Sectors

The average annual damage (AAD) of flood damage in all sectors in each scenario and each year:

- BL-2014
- 2030: BSD-2030-A1H1, BSD-2030-A2H1
- 2050: BSD-2050-A1H1, BSD-2050-A2H1

BSD-2030-A2H1

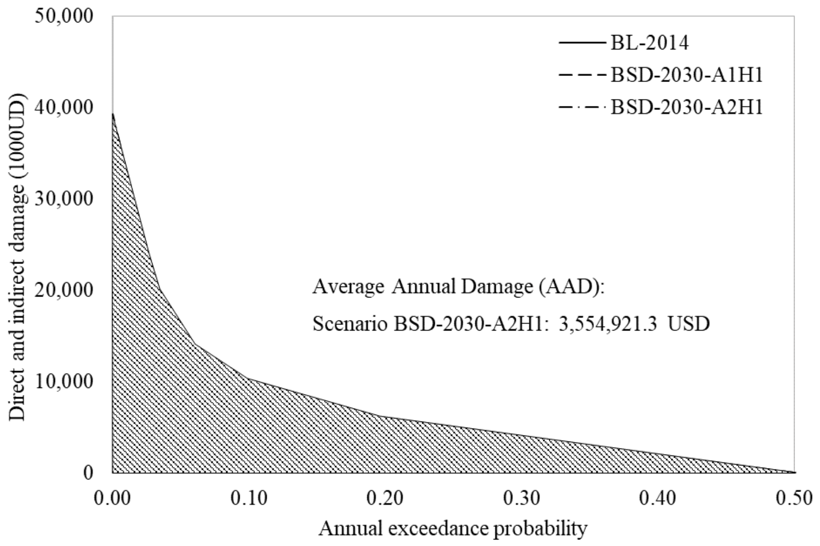

BSD-2050-A2H1

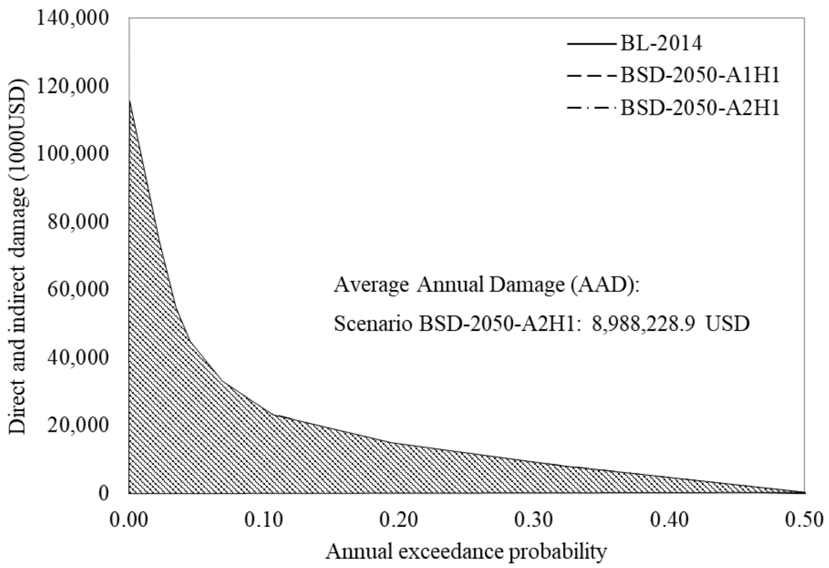

Figure 5.57: Average Annual Damage (ADD): Total damage in Bakan and Phnom Kravanh districts

Figure 5.57 visualizes an example of total average annual damage in all sectors of the second scenario (A2H1) in 2030 and 2050. The estimated average annual damage in all sectors in 2030 is around 3.55 million USD, while the estimated average annual damage in all sectors in 2050 is around 5.25 million USD. The average annual damage of TDPC in other scenarios of each sector is summarized in Table 5-20.

Table 5-20: NPV of AAD in each development scenario in each sector

	Sector	BL-2014	BSD-2030-A1H1	BSD-2030-A2H1
Market price	A	1,446,693.9	2,068,692.7	2,525,005.9
	H	219,046.1	1,029,915.3	1,029,915.3
	All	1,665,739.9	3,098,608.1	3,554,921.3
	Sector	**BL-2014**	**BSD-2050-A1H1**	**BSD-2050-A2H1**
Market price	A	1,446,693.9	2,802,707.8	5,255,391.2
	H	219,046.1	3,732,837.7	3,732,837.7
	All	1,665,739.9	6,535,545.5	8,988,228.9

Note: A is Agriculture; H is Affected people; and All is All Sectors

5.4.3 Flood Mitigation: 2030 and 2050

The second scenario (A2H1) in 2030 and 2050 are considered for the mitigation plan because the expected average annual damage is high compared with the first scenario. The potential damage in the second scenario in 2030 and 2050 is considered as risk once flood hazard occurs as estimated by annual exceedance probability. In this aspect, risk reduction is considerably implemented. Flood risk reduction refers to any mitigation measures implemented to reduce flood damage. In practice, flood damages cannot be 100% mitigated since the greatest magnitude of flood cannot be estimated. For example, even though the damage caused by 100-year return period of flood have been mitigated, a 500-year return period of floods could possibly occur in 2030 or 2050 and produces greater damages. Hence, it is usual that there are still some risks remained (Residual Risk) after a part of risks has been reduced (Risk Reduction). Risk reduction can be evaluated in monetary terms and this amount of money should be economical balance with the cost invested in mitigation measures.

It is true that different sectors need different mitigation measures due to the level of vulnerability, exposure and coping capacity of elements at risk. Moreover, disaster mitigations and planning are also needed to be prioritized due to the limitation of the budgets allocated to protect the areas at risk. Besides, inappropriate mitigation measures can lead to another risk later. Basically, life safety is the first priority in all risk mitigation and planning. Based on the experiences of flood in the previous years, people leave their properties behind during flooding and move to another safe place just for their own safety. In this case, the first priority is placed at the residential area basically referred to life of the people at risk. Agriculture is considered as the second priority. In order to reduce the risk from flood, it is assumed that only the damage causing by the 5-year return period of flood is needed to be mitigated in agriculture, while flood damage caused by 10-year return period of flood in residential area have to be protected. Based on this assumption, if the risks are the same between agriculture and affected people, the budget will be invested in mitigation measure in residential area. It is also noted that residual risk still can be existed when the 15-year return period of flood occurs in both sectors since the mitigation is prepared to reduce only 5 and 10-year return period of flood magnitude.

Based on section 2.5.5, it is possible to build a dike to prevent agricultural area from a 5-year return period of flood, while the non-mitigation measure should be implemented in residential area to increase the coping capacity and to protect the people from 10-year return period of flood, for example flood warning and evacuation systems and flood proofing. Besides the value of the elements at risk that we already assessed, the real situation of the area should also be carefully examined so that the selection of the mitigation measure is suitable and economical, and no further risks caused by the selected mitigation measures. For example, in case of Phnom Penh City the capital of Cambodia, the Royal Government of Cambodia built floodwalls to protect the area from flood from Mekong River since the city is the center of country economy including service, industry and luxurious residential area. Looking back to Bakan and Phnom Kravanh districts, the area mostly covers by agricultural area, where floodwall is very high-cost structural measure to be considered comparing with the risk reduction.

From the previous information, the Damage Probability Curve in Agriculture (ADPC), Affected people (HDPC) and Total damage (TDPC) in each scenario and each year is indicated in the abbreviation below:

- BL-2014: Baseline scenario in 2014 (ADPC2014)
- BSD-2030-A1H1: ADPC2030 Based Development Scenario 1 in 2030
- BSD-2030-A2H1: ADPC2030 Based Development Scenario 2 in 2030

- BSD-2030-A2H1-MIT: ADPC2030 Based Development Scenario 2 with Mitigation in 2030
- BSD-2050-A1H1: ADPC2050 Based Development Scenario 1 in 2050
- BSD-2050-A2H1: ADPC2050 Based Development Scenario 2 in 2050
- BSD-2050-A2H1-MIT: ADPC2050 Based Development Scenario 2 with Mitigation in 2050

2030	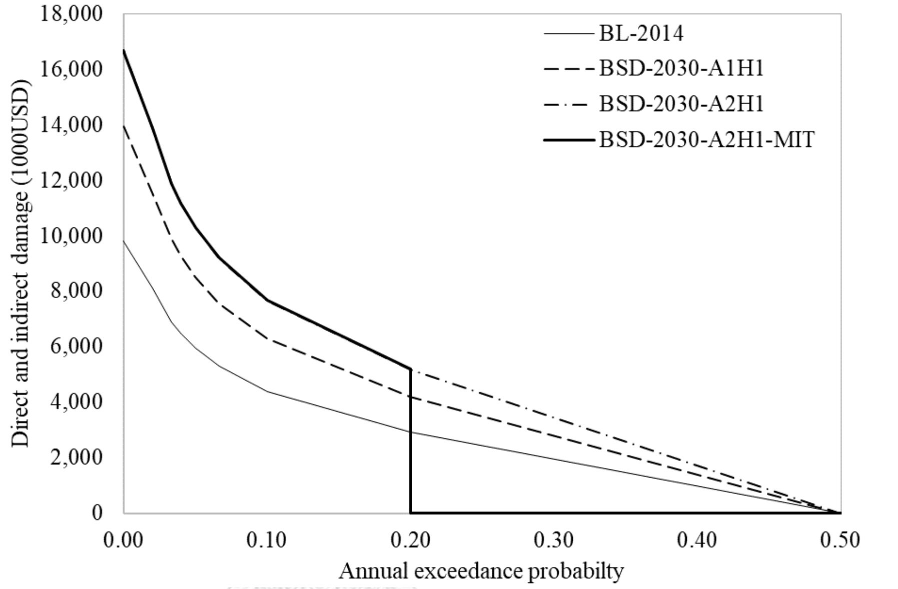
2050	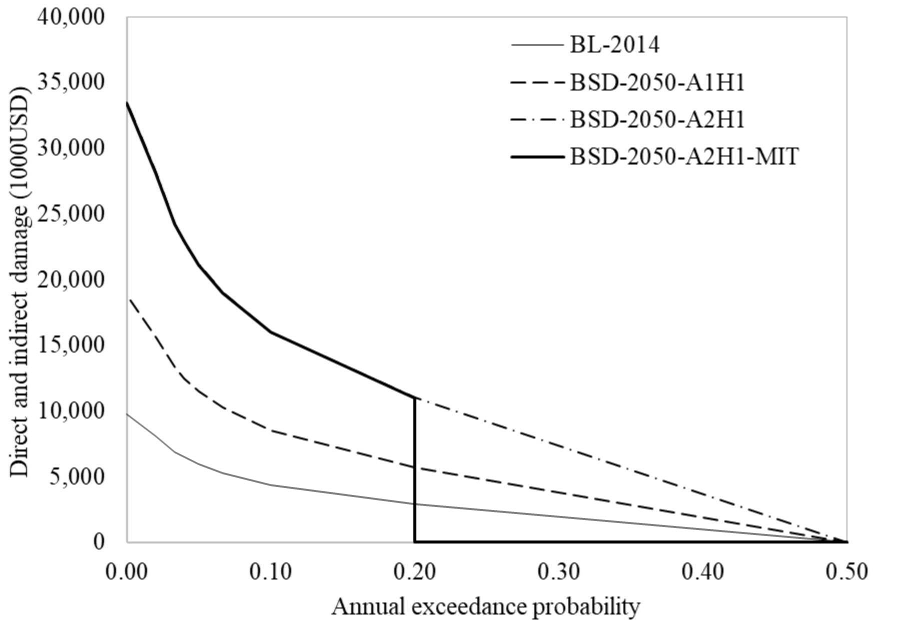

Figure 5.58: Damage Probability Curve: Agriculture damage with mitigation for Bakan and Phnom Kravanh districts

Figure 5.58, Figure 5.59, and Figure 5.60 indicate the damage probability curve in Agriculture, Affected people and All Sectors respectively with mitigation plan in the second scenario (A2H1) in 2030 and 2050. The dark solid curve represents the mitigation line in the second scenario (A2H1). The area above the dark curve represents the risk reduction, while the area under the dark curve represents the residual risk.

2030

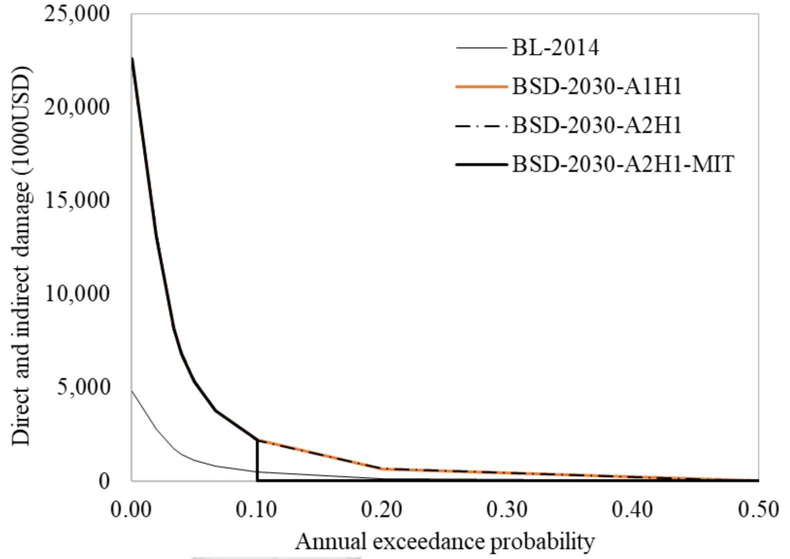

2050

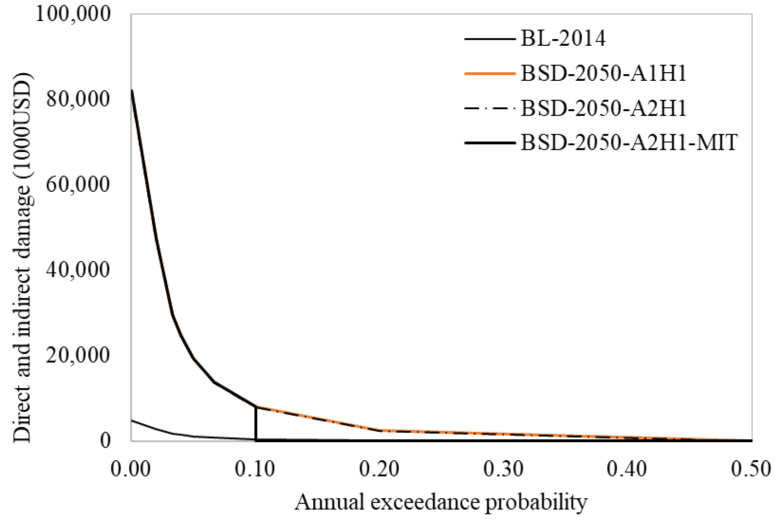

Figure 5.59: Damage Probability Curve: Affected people damage with mitigation for Bakan and Phnom Kravanh districts

In Figure 5.58, the damage under the ADPC2030 and ADPC2050 (BSD-2030-A2H1 and BSD-2050-A2H1) is removed when the annual exceedance probability is equal or greater than 0.2 meaning that only the damage in agriculture caused by 5-year return period of flood is protected. In Figure 5.59, the damage under the

HDPC2030 and HDPC2050 (BSD-2030-A2H1 and BSD-2050-A2H1) is removed when the annual exceedance probability is equal or greater than 0.1 meaning that the damage of the affected people caused by 10-year return period of flood is protected. Figure 5.60 indicates the total damage in agriculture and affected people with mitigation in the second scenario (A2H1). Similar to agriculture and affected people, the area above the dark solid curve represent the risk reduction, while the area under the curve represents the residual risk.

2030

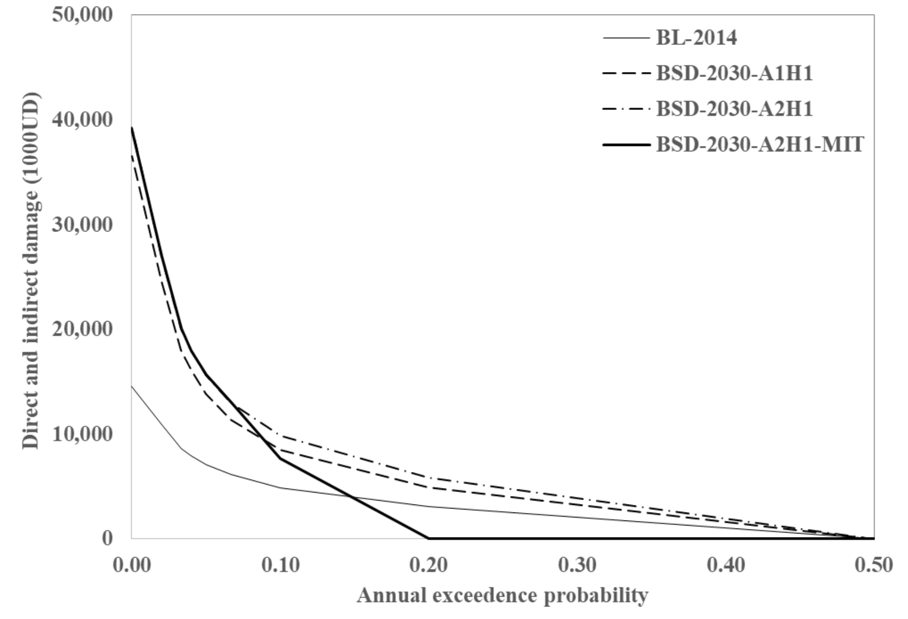

2050

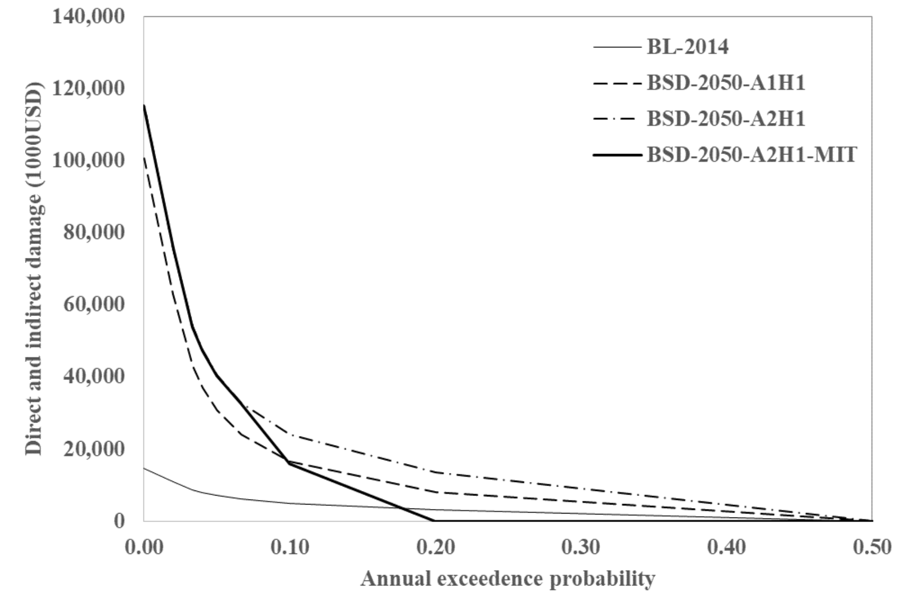

Figure 5.60: Damage Probability Curve: Total damage with mitigation for Bakan and Phnom Kravanh districts

Average Annual Damage (AAD) of Annual Risk Reduction and Residual Risk

As indicated in the previous section, risk reduction refers to the amount of risk that is removed using the mitigation measure, while the residual risk is the amount of risk remaining after a part of risk has been reduced. In this case, the residual risk can be estimated by the integration of the area under the curve after a part of risk is removed following the assumption of risk reduction in agriculture and affected people. Risk reduction is the result of the subtraction between the average annual damage (ADD) and the residual risk.

Figure 5.61 indicates the annual risk reduction and residual risk of the total damage probability curve in the second scenario (A2H1) in 2030 and 2050. The average annual damage of the TDPC2030 in the second scenario (A2H1) is found to be 3.55 million USD or 773,654.4 USD (price in 2014), while residual risk of the TDPC2030 after risk reduction in both Agriculture and Affected people is estimated to be 486,907.7 USD (price in 2014). Hence, the annual risk reduction in TDPC2030 (A2H1) is expected to be 286,746.7 USD, where 225,436.2 USD is the reduction in Agriculture and 61,310.6 USD is the reduction in Affected people.

The average annual damage of the TDPC2050 in the second scenario (A2H1) is estimated to be 8.98 million USD (price in 2050) or 290,761.9 USD (price in 2014); the residual risk of TDPC2050 after risk reduction in both Agriculture and Affected people is estimated to be 5.76 million USD (price in 2014) or 186,618.6 USD (price in 2014). Hence, the annual risk reduction in TDPC2050 (A2H1) is expected to be 3.22 million USD (price in 2030) or 104,143.3 USD (price in 2014), where 71,112.4 USD comes from the reduction in Agriculture and 33,030.8 USD comes from the reduction in Affected people. The summary of net present value (NPV) of average annual damage (AAD) with mitigation in each development scenario in each sector is indicated in Table 5-21.

BSD-2030-A2H1-MIT	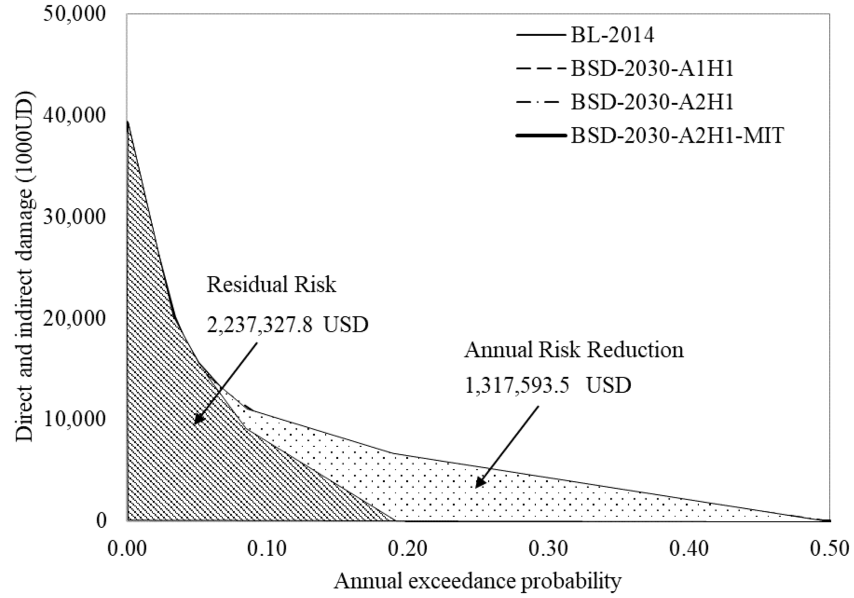
BSD-2050-A2H1-MIT	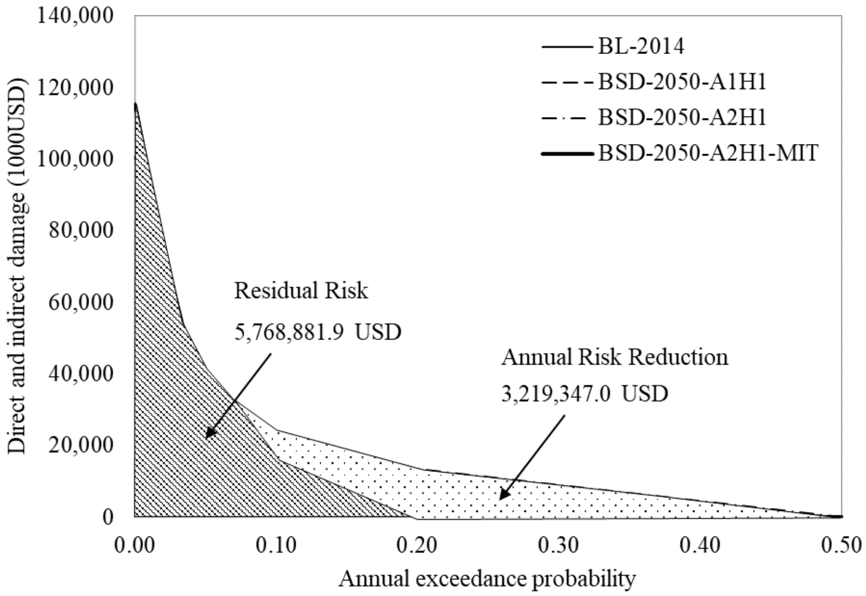

Figure 5.61: Annual Risk Reduction and Residual Risk: Total damage for Bakan and Phnom Kravanh districts

Table 5-21: AAD with mitigation in each development scenario in each sector (USD)

	Sector	BL-2014	BSD-2030-A1H1	BSD-2030-A2H1	BSD-2030-A2H1-MIT	Risk Reduction
Market price	A	1,446,693.9	2,068,692.7	2,525,005.9	1,489,132.8	1,035,873.1
	H	219,046.1	1,029,915.3	1,029,915.3	748,195.0	281,720.3
	All	1,665,739.9	3,098,608.1	3,554,921.3	2,237,327.8	1,317,593.5
	Sector	**BL-2014**	**BSD-2050-A1H1**	**BSD-2050-A2H1**	**BSD-2050-A2H1-MIT**	**Risk Reduction**
Market price	A	1,446,693.9	2,802,707.8	5,255,391.2	3,057,114.8	2,198,276.4
	H	219,046.1	3,732,837.7	3,732,837.7	2,711,767.1	1,021,070.6
	All	1,665,739.9	6,535,545.5	8,988,228.9	5,768,881.9	3,219,347.0

Note: A is Agriculture; H is Affected people; and All is All Sectors

5.4.4 Summary

The third objective of the research is to estimate the potential flood damage in Agriculture and Affected people in Bakan and Phnom Kravanh districts in 2030 and 2050 associated with socio-economic development including mitigation plan.

Socio-economic development scenario in 2030 and 2050 is estimated based on the government policy, the perception of local experts and the development trend in the past. The damage probability curve in 2030 and 2050 is the multiplication between the degree of expansion in each sector and the damage probability curve in 2014 (Baseline scenario). The average annual damage in each scenario and each sector is the result of the integration of the area under the damage probability curve. Annual risk reduction is the result of the subtraction between the average annual damage and the annual residual risk.

The result indicates that:

1) **Agriculture**: the average annual damage in 2030 in the first and the second scenario is estimated to be around 2,068,692.7 USD and 2,525,005.9 USD respectively, while the average annual damage in 2050 in the first and the second scenario is 2,802,707.8 USD and 5,255,391.2 USD respectively. The residual risk in the second scenario (A2H1) after the damage caused by 5-year return period of flood being protected is estimated to be 1,489,132.8 USD in 2030 and 3,057,114.8 USD in 2050, while the annual risk reduction is projected to be 1,035,873.1 USD in 2030 and 2,198,276.4 USD in 2050.
2) **Affected people:** the average annual damage in 2030 and 2050 is expected to be 1,029,915.3 USD and 3,732,837.7 USD respectively. The annual residual risk after the damage caused by 10-year return period of flood being protected is estimated to be 748,195.0 USD in 2030 and 2,711,767.1 USD in 2050 respectively, while the annual risk reduction is estimated to be 281,720.3 USD and 1,021,070.6 USD respectively.
3) **All Sectors:** the total damage probability curve (TDPC) is the combination between damage probability curve in Agriculture (ADPC) and damage probability curve in Affected people (HDPC). The average annual damage in 2030 for the first and the second scenario is estimated to be 3,098,608.1 USD

and 3,554,921.3 USD respectively, while the average annual damage in 2050 in both scenarios is estimated to be 6,535,545.5 USD and 8,988,228.9 USD respectively. The annual residual risk in the second scenario (A2H1) after risk reduction in Agriculture and Affected people is estimated to be 2,237,327.8 USD in 2030 and 5,768,881.9 USD in 2050, while the annual risk reduction is estimated to be 1,317,593.5 USD in 2030 and 3,219,347.0 USD in 2050.

CHAPTER 6
CONCLUSIONS AND RECOMMENDATIONS

6.1 Conclusions

This research is attempt to 1) assess flood damages in Agriculture and Affected people from 2000 to 2014 by using Google Earth Engine; 2) develop damage probability curve in 2014; and 3) estimate the potential flood damages in Agriculture and Affected people in Bakan and Phnom Kravanh districts in 2030 and 2050 associated with socio-economic development including mitigation plan.

Flood extent is derived from Monthly Water History, v1.0. The affected area in Agriculture between 2000 and 2014 is confirmed to be damaged by flood by using the Normalized Difference Vegetation Index (NDVI) and Leaf Area Index (LAI), while the affected people by flood is the result from the integration between flood map and Nighttime Light Index. Flood frequency curve is developed using the annual maximum discharge from Bak Trakoun flow station between 1994 and 2018. The average annual damage in 2014 is the integration of the area under the damage probability curve in each sector. Socio-economic development scenario in 2030 and 2050 is estimated based on the government policy, the perception of local experts and the development trend in the past. Annual risk reduction is the result of the subtraction between the average annual damage and the annual residual risk

The result followed the first objectives indicates that the Coefficient of Determination (R^2) between maximum monthly water level and maximum monthly water extent is equal to 0.57. The unexplained variation is likely to be the effect of the flood extent from the Tonle Sap Lake at downstream of Pursat River Basin, rainfall in the river basin and the reduction of water pixels on the map by no observation data. The total damage area in Agriculture from 2000 to 2014 is around 43,745 Ha including Rice (5,327 Ha) and Cropland (38,418 Ha). The highest damage in Agriculture is found to be 8,328 Ha in 2013, while the lowest damage is around 328 Ha in 2008. The total number of affected people predicted from 2000 to 2014 is around 44,860 persons. The highest number of people affected by flood is 18,194 persons in 2013 and the lowest number of people affected by floods is 786 people in 2006.

The result followed the second objective indicates that Log-Pearson Type III is the best fitted distribution to the maximum observed discharges at Bak Trakoun flow station. The highest return period to be considered in this study is 100-year return period, where the corresponding predicted discharge is estimated to be 1485 m^3/s. The coefficient of determination (R^2) in logarithm scale of the discharge-damage curve for Agriculture and Affected people is found to be 0.65 and 0.83 respectively, while the significant level (α) taking into account the 95% confidence level is 0.000503 in Agriculture and 0.000006 in Affected people. These significant levels are smaller than 0.05 meaning that the regression analysis is acceptable, or those variables are correlated. The average annual damage (AAD) in 2014 is estimated to be 1.66 million USD, almost 90% of the damage is in Agriculture, and 10% is in Affected people implying that the affected area in Bakan and Phnom Kravanh districts is rural area where agriculture is the main sector.

The result followed the third objective indicates that the average annual damage in all sectors in 2030 is estimated to be 3.09 million USD in scenario A1H1 and 3.55 million USD in scenario A2H1, while the average annual damage in 2050 in both scenarios estimated to be 6.53 million USD and 8.98 million USD respectively. The damage in scenario A2H1 is higher than that of A1H1 in both 2030 and 2050 due to the different price of normal and organic rice. The annual residual risk in scenario A2H1 after the risk reduction in Agriculture and Affected people is estimated to be 2.24 million USD in 2030 and 5.77 million USD in 2050, while the annual risk reduction is estimated to be 1.32 million USD in 2030 and 3.22 million USD in 2050.

This result can be used as the basic information to support the government policy in the future regarding the mitigation plans to reduce flood damages to ensure the sustainable socio-economic development and better quality of living in the rural area following the national strategic development plan of the Royal Government of Cambodia. The methodology applied in this research can be implemented as a feasibility study not only in Bakan and Phnom Kravanh districts, but also in other river basins in other countries, where the same condition exist since the satellite data is available globally.

6.2 Recommendations

6.2.1 First Objective

1) The good quality of the observed flood damage is needed for flood damage assessment. Moreover, one flow station (Bak Trakoun flow station) cannot be well-represented the effect of flood in the whole River Basin so more flow stations need to be installed in both the upstream and downstream part of the Pursat River Basin.
2) The datasets in Google Earth Engine should be further examined since it can be used to solve the problem in Water Resources Engineering in term of the initial planning in case that there is no ground observed data.
3) However, the ground observed data is still the first priority. If observed data are available, the data from Google Earth Engine will be used the second priority to support the method.
4) The discharge at the downstream of Pursat River Basin near the Tonle Sap Lake should be taken into account in this analysis.

6.2.2 Third Objective

1) Climate change scenarios should be considered and combined with socio-economic development scenario so that the whole picture of potential flood damages in 2030 and 2050 is more comprehended.
2) Water level at the downstream of Pursat River Basin near the Tonle Sap Lake should be examined for multiple regression analysis since back water from the Tonle Sap Lake can affect the water extent downstream.
3) The degree of expansion is the most critical factor for socio-economic development in the future. Hence, the accurate development policy is basically needed in order to obtain the better and more reliable findings of flood damages in the future.
4) It is true that life safety is the first priority for flood mitigation plan. However, in case of Bakan and Phnom Kravanh districts, for instance, around 85% of flood damage is estimated to be in Agriculture, where the majority of people incomes is constantly located. Hence, the proper mitigation measures should

be implemented in the agricultural sector in order to reduce the damage from floods and to ensure the sustainable socio-economic development in the future for the local farmers.

5) Since the negative value of NDVI refers to surface water, it is possible to assess the area of flood extent with 8-day record without disturbance from no observation pixels by using NDVI. The results from this assessment can be used to compare with flood map from Monthly Water History, v1.0.
6) Since NDVI is sensitive to both flood and drought, the use of NDVI to confirm flood damage much be carefully examined and differentiated between the value of NDVI affected by flood and the value of NDVI affected by drought. Based on the report from MOWRAM, drought possibly occurs in some places within a short period of time in rainy season.

REFERENCES

An, L. H. (2014). "COUNTRY REPORT OF CAMBODIA DISASTER MANAGEMENT." National Committee for Disaster Management (NCDM).

Australia, E. M. (2002). "Disaster loss assessment guidelines." AUSTRALIAN EMERGENCY MANUALS SERIES **Volume 3**.

Bank, W. (2012). "Flood in Thailand 2011_World Bank Report."

Büchele, B., H. Kreibich, A. Kron, A. Thieken, J. Ihringer, P. Oberle, B. Merz and F. Nestmann (2006). "Flood-risk mapping: contributions towards an enhanced assessment of extreme events and associated risks." Natural Hazards and Earth System Science **6**(4): 485-503.

Chaiwat, T. (2016). "Growth Dispersion of Asean Countries: Evidence from Night Lights." Southeast Asian Journal of Economics 5(1), January - June 2017: 21 - 39.

Chow, V. T., D. R. Maidment and L. W. Mays (1988). "Applied Hydrology."

Dutta, D., S. Herath and K. Musiake (2003). "A mathematical model for flood loss estimation." Journal of Hydrology **277**(1-2): 24-49.

Elvidge, C. D., K. E. Baugh, S. J. Anderson, P. C. Sutton and T. Ghosh (2012). "The Night Light Development Index (NLDI): a spatially explicit measure of human development from satellite data." Social Geography **7**(1): 23-35.

Forster, S., B. Kuhlmann, K.-E. Lindenschmidt and A. Bronstert (2008). "Assessing flood risk for a rural detention area." Nat. Hazards Earth Syst. Sci.,8: 311–322.

Gorelick, N., M. Hancher, M. Dixon, S. Ilyushchenko, D. Thau and R. Moore (2017). "Google Earth Engine: Planetary-scale geospatial analysis for everyone." Remote Sensing of Environment **202**: 18-27.

Grünthal, G., A. H. Thieken, J. Schwarz, K. S. Radtke, A. Smolka and B. Merz (2006). "Comparative Risk Assessments for the City of Cologne – Storms, Floods, Earthquakes." Natural Hazards **38**(1-2): 21-44.

H. de Moel, J., van Alphen2 and J. C. J. H. Aerts (2009). "Flood maps in Europe – methods, availability and use." Nat. Hazards Earth Syst. Sci., 9: 289–301.

Handmer, J., J. Abrahams, R. Betts and M. Dawson (2005). "Australian Journal of Emergency Management." **Vol. 20**(No. 1).

Hansen, M. C., P. V. Potapov, R. Moore, M. Hancher, S. A. Turubanova, A. Tyukavina, D. Thau, S. V. Stehman, S. J. Goetz, T. R. Loveland, A. Kommareddy, A. Egorov, L. Chini, C. O. Justice and J. R. Townshend (2013). "High-resolution global maps of 21st-century forest cover change." Science **342**(6160): 850-853.

Joshi, A. R., E. Dinerstein, E. Wikramanayake, M. L. Anderson, D. Olson, B. S. Jones, J. Seidensticker, S. Lumpkin, M. C. Hansen, N. C. Sizer, C. L. Davis, S. Palminteri and N. R. Hahn (2016). "Tracking changes and preventing loss in critical tiger habitat." Sci Adv **2**(4): e1501675.

Karamouz, M., F. Szidarovszky and B. Zahraie (2003). "Water Resource System Analysis." **ISBN 1-56670-642-4**.

Keola, S., M. Andersson and O. Hall (2015). "Monitoring Economic Development from Space: Using Nighttime Light and Land Cover Data to Measure Economic Growth." World Development **66**: 322-334.

Kreibich, H. and A. H. Thieken (2008). "Coping with floods in the city of Dresden, Germany." Natural Hazards **51**(3): 423-436.

Markantonis, V., V. Meyer and R. Schwarze (2012). "Review Article "Valuating the intangible effects of natural hazards – review and analysis of the costing methods&quot." Natural Hazards and Earth System Sciences **12**(5): 1633-1640.

Merz, B., J. Hall, M. Disse and A. Schumann (2010). "Fluvial flood risk management in a changing world." Nat. Hazards Earth Syst. Sci., 10: 509–527.

Merz, B., H. Kreibich, R. Schwarze and A. Thieken (2010). "Review article "Assessment of economic flood damage"." Natural Hazards and Earth System Science **10**(8): 1697-1724.

Moser, D. A. (1994). "Economics of selection of flood mitigation measures." 585-596.

MRC (2009). "Flood Damages, Benefits and Flood Risk in Focal Areas." The Flood Management and Mitigation Programme,

Component 2: Structural Measures & Flood Proofing

in the Lower Mekong Basin **Draft Final Report, Volume 2C**.

Pekel, J. F., A. Cottam, N. Gorelick and A. S. Belward (2016). "High-resolution mapping of global surface water and its long-term changes." Nature **540**(7633): 418-422.

Pistrika, A. K. and S. N. Jonkman (2010). "Damage to residential buildings due to flooding of New Orleans after hurricane Katrina." Natural Hazards **54**(2): 413-434.

Prakash, M., K. Rothauge and P. W. Cleary (2014). "Modelling the impact of dam failure scenarios on flood inundation using SPH." Applied Mathematical Modelling **38**(23): 5515-5534.

Puttanapong, N., S. Chantarat, P. Rakwatin and T. Tanompongphandh (2014). "The Study of Agricultural Risk Management Mechanism for Preparation toward Extreme Weather Conditions using Crop Insurance: The Case Study of Thailand’s Rice Cultivation." Thailand’s Research Fund **Grant No. RDG5530013**.

Reinhardt-Imjela, C., R. Imjela, J. Bölscher and A. Schulte (2018). "The impact of late medieval deforestation and 20th century forest decline on extreme flood magnitudes in the Ore Mountains (Southeastern Germany)." Quaternary International **475**: 42-53.

RGC (2014). "National Strategic Development Plan 2014-2018 of The Royal Government of Cambodia."

Rodríguez, S. L. (2013). "The Economic Opportunity Cost of Capital for Mexico – A Revised Empirical Update."

Romali, N. S., M. S. A. K. Sulaiman, Z. Yusop and Z. Ismail (2015). "Flood Damage Assessment: A Review of Flood Stage–Damage Function Curve." 147-159.

ROS Bansok, N. Phirun and C. Chhun (2011). "Agricultural Development and Climate Change: The Case of Cambodia." CDRI Publication **Working Paper Series No. 65**.

Shrestha, S. and W. Lohpaisankrit (2017). "Flood hazard assessment under climate change scenarios in the Yang River Basin, Thailand." International Journal of Sustainable Built Environment **6**(2): 285-298.

Smith, D. (1994). "Flood damage estimation - A review of urban stage-damage curves and loss functions." Water SA **Vol. 20** (No. 3).

Suriya, S. and B. V. Mudgal (2012). "Impact of urbanization on flooding: The Thirusoolam sub watershed – A case study." Journal of Hydrology **412-413**:

210-219.

Thieken, A. H., H. Kreibich, M. MüLler and B. Merz (2007). "Coping with floods: preparedness, response and recovery of flood-affected residents in Germany in 2002." Hydrological Sciences Journal **52**(5): 1016-1037.

Thieken, A. H., M. Müller, H. Kreibich and B. Merz (2005). "Flood damage and influencing factors: New insights from the August 2002 flood in Germany." Water Resources Research **41**(12).

Thomas, T. S., T. Ponlok, R. Bansok, T. D. Lopez, C. Chiang, N. Phirun and C. Chhun (2013). "Cambodian Agriculture: Adaptation to Climate Change Impact." Environment and Production Technology Division **IFPRI Discussion Paper 01285**.

Vu, T. T. and R. Ranzi (2017). "Flood risk assessment and coping capacity of floods in central Vietnam." Journal of Hydro-environment Research **14**: 44-60.

Yue, S., T. B. M. J. Ouarda, B. Bobée, P. Legendre and P. Bruneau (1999). "The Gumbel mixed model for flood frequency analysis." Journal of Hydrology **226**(1): 88-100.

APPENDIX

APPENDIX A: Earth Engine Codes

APPENDIX A1: Monthly Water History, v1.0

```
// Monthly Water History, v1.0
//*****************************************

// Country Selection
var countries = ee.FeatureCollection('USDOS/LSIB_SIMPLE/2017');
var Country_array = ['Cambodia'];
Country_array.forEach(function(c) {
  print(c);
  var sel = countries.filter(ee.Filter.eq('country_na', c));
//*****************************************

// Image collections
// Source: https://developers.google.com/earth-engine/ic_filtering
var collection2000 = ee.ImageCollection('JRC/GSW1_0/MonthlyHistory')
.filter(ee.Filter.date('2010-09-01', '2010-10-30'));

//Clip to Specified Region
var clipped2000 = collection2000.max().clip(sel);
//*****************************************

// Image visualization
// Source: https://developers.google.com/earth-engine/image_visualization
Map.setCenter(103.86, 12.47, 9);
Map.addLayer(clipped2000, {min: 0.0, max: 2.0,
palette: ['ffffff', 'fffcb8', '0905ff']}, 'Water');
//*****************************************

// Export.image.toDrive
// Criteria: image, description, folder, fileNamePrefix,dimensions,
// region, scale, crs, crsTransform, maxPixels, shardSize,fileDimension,
// skipEmptyTiles, fileFormat, formatOptions
// Source: https://developers.google.com/earth-engine/exporting
Export.image.toDrive({
     image : clipped2000,
     description: 'image'.concat('_', c),
     folder: 'GEE DATA',
     maxPixels: 3784216672400,
     scale: 30,
     crs : 'EPSG:4326',
     fileFormat: 'GeoTIFF',
```

```
    region: sel.geometry().bounds()
    });
});

// ************************************************
// Author: Chhunleang Rorm
// Date  : 01st March 2019
// ************************************************
```

APPENDIX A2: Time-Series Nighttime Light Index (NLI)

```
// Time-series Nighttime Light Index
//************************************************

// Define a FeatureCollection: Bakan and Phnom Kravanh districts
var regions = ee.FeatureCollection([
   ee.Feature(  // Study Area
   study_area, {label: 'Study Area'),
  ee.Feature(  // Phnom Penh City
   Phnom_Penh, label: 'Phnom Penh'),
  ee.Feature(  // Siem Reap City
   Siem_Reap, label: 'Siem Reap'),
]);
//************************************************

// Image collections
// Source: https://developers.google.com/earth-engine/ic_filtering
var collection2014 = ee.ImageCollection('NOAA/DMSP-
OLS/NIGHTTIME_LIGHTS')
.filter(ee.Filter.date('1992-01-01', '2014-01-01')).select('avg_vis');

//Clip to Specified Region
var clipped2014 = collection2014.max().clip(regions);
//************************************************

// Charts
// Long-Term Time Series
// Source: https://developers.google.com/earth-engine/charts_image_series_by_region
var TS_NTL = ui.Chart.image.seriesByRegion(
   collection2014, regions, ee.Reducer.mean(), 'avg_vis', 500, 'system:time_start',
'label')
      .setChartType('ScatterChart')
      .setOptions({
        title: ' Annual Average Nighttime Light 1992-2014',
        vAxis: {title: 'NLT (3-60)'},
        hAxis: {title: 'Time'},
        lineWidth: 1,
        pointSize: 4,
```

```
        series: {
          0 : {color: 'FF0000'}, // Study Area
          1 : {color: '00FF00'}, // Phnom Penh
          2 : {color: '0000FF'}  // Siem Reap
}});
//**************************************************

// Display.
print(TS_NTL);

// Image visualization
// Source: https://developers.google.com/earth-engine/image_visualization
Map.setCenter(105, 11.5, 7);
Map.addLayer(clipped2014, {min: 3.0, max: 60.0}, 'avg_vis');

// ***********************************************
// Author: Chhunleang Rorm
// Date  : 01st March 2019
// ***********************************************
```

APPENDIX A3: MODIS Normalized Difference Vegetation Index (NDVI)

```
// MODIS Normalized Difference Vegetation Index (NDVI)
//*****************************************************

// Country Selection
var countries = ee.FeatureCollection('USDOS/LSIB_SIMPLE/2017');
var Country_array = ['Cambodia'];
Country_array.forEach(function(c) {
  print(c);
  var sel = countries.filter(ee.Filter.eq('country_na', c));
//*****************************************************

// Image collections
// Source: https://developers.google.com/earth-engine/ic_filtering
var collection2014 = ee.ImageCollection('MODIS/MCD43A4_NDVI').select('NDVI')
.filter(ee.Filter.date('2000-07-01', '2000-07-30'));

//Clip to Specified Region
var clipped2014 = collection2014.max().clip(sel);
//****************************************************

// Image visualization
// Source: https://developers.google.com/earth-engine/image_visualization
Map.setCenter(105, 11.5, 7);
Map.addLayer (clipped2014, {min: 0.0, max: 1,
palette: ['FFFFFF','CC9966','CC9900', '996600',
'33CC00', '009900','006600','000000']}, 'NDVI');
```

```
//*****************************************************

// Export.image.toDrive
// Criteria: image, description, folder, fileNamePrefix,dimensions,
// region, scale, crs, crsTransform, maxPixels, shardSize,fileDimension,
// skipEmptyTiles, fileFormat, formatOptions
// Source: https://developers.google.com/earth-engine/exporting
Export.image.toDrive({
     image : clipped2014,
     description: 'image'.concat('_', c),
     folder: 'GEE NDVI',
     maxPixels: 3784216672400,
     scale: 30,
     crs : 'EPSG:4326',
     fileFormat: 'GeoTIFF',
     region: sel.geometry().bounds()
     });
});

// ************************************************
// Author: Chhunleang Rorm
// Date  : 01st March 2019
// ************************************************
```

APPENDIX A4: MODIS Leaf Area Index (LAI)

```
// MODIS Leaf Area Index (LAI)
//************************************************

// Country Selection
var countries = ee.FeatureCollection('USDOS/LSIB_SIMPLE/2017');
var Country_array = ['Cambodia'];
Country_array.forEach(function(c) {
  print(c);
  var sel = countries.filter(ee.Filter.eq('country_na', c));
//************************************************

// Image collections
// Source: https://developers.google.com/earth-engine/ic_filtering
var collection2014 = ee.ImageCollection('MODIS/006/MCD15A3H').select('Lai')
.filter(ee.Filter.date('2015-10-01', '2015-10-30'));

//Clip to Specified Region
var clipped2014 = collection2014.max().clip(sel);
//************************************************

// Image visualization
// Source: https://developers.google.com/earth-engine/image_visualization
```

```
Map.setCenter(105, 11.5, 7);
Map.addLayer (clipped2014, {min: 0.0, max: 25,
palette: ['e1e4b4', '999d60', '2ec409', '0a4b06']}, 'LAI');
//***********************************************

// Export.image.toDrive
// Criteria: image, description, folder, fileNamePrefix,dimensions,
// region, scale, crs, crsTransform, maxPixels, shardSize,fileDimension,
// skipEmptyTiles, fileFormat, formatOptions
// Source: https://developers.google.com/earth-engine/exporting
Export.image.toDrive({
     image : clipped2014,
     description: 'image'.concat('_', c),
     folder: 'GEE LAI',
     maxPixels: 3784216672400,
     scale: 30,
     crs : 'EPSG:4326',
     fileFormat: 'GeoTIFF',
     region: sel.geometry().bounds()
     });
});

// ***********************************************
// Author: Chhunleang Rorm
// Date  : 01st March 2019
// ***********************************************
```

APPENDIX A5: Average-Light of Nighttime-Light Index (NLI)

```
// Average Light of Nighttime Light Index (NLI)
//************************************************************
```



```
// Country Selection
var countries = ee.FeatureCollection('USDOS/LSIB_SIMPLE/2017');
var Country_array = ['Cambodia'];
Country_array.forEach(function(c) {
  print(c);
  var sel = countries.filter(ee.Filter.eq('country_na', c));
//************************************************************

// Image collections
// Source: https://developers.google.com/earth-engine/ic_filtering
var collection2014 = ee.ImageCollection('NOAA/DMSP-
OLS/NIGHTTIME_LIGHTS')
.select('avg_vis').filter(ee.Filter.date('2011-01-01', '2011-12-31'));

//Clip to Specified Region
var clipped2014 = collection2014.max().clip(sel);
```

```
//************************************************************

// Image visualization
// Source: https://developers.google.com/earth-engine/image_visualization
Map.setCenter(105, 11.5, 7);
Map.addLayer(clipped2014, {min: 0.0, max: 60.0}, 'Nighttime Lights');
//************************************************************

// Export.image.toDrive
// Criteria: image, description, folder, fileNamePrefix,dimensions,
// region, scale, crs, crsTransform, maxPixels, shardSize,fileDimension,
// skipEmptyTiles, fileFormat, formatOptions
// Source: https://developers.google.com/earth-engine/exporting
Export.image.toDrive({
    image : clipped2014,
    description: 'image'.concat('_', c),
    folder: 'GEE NTL',
    maxPixels: 3784216672400,
    scale: 30,
    crs : 'EPSG:4326',
    fileFormat: 'GeoTIFF',
    region: sel.geometry().bounds()
    });
});

// ***********************************************
// Author: Chhunleang Rorm
// Date  : 01st March 2019
// ***********************************************
```

APPENDIX B: Monthly Water Extent Map in 2013

January	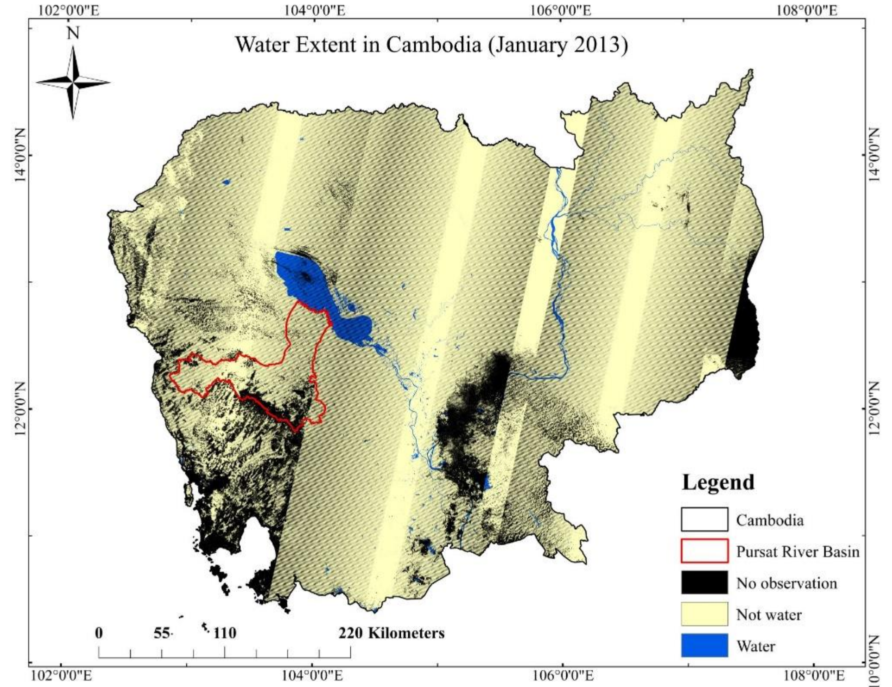
February	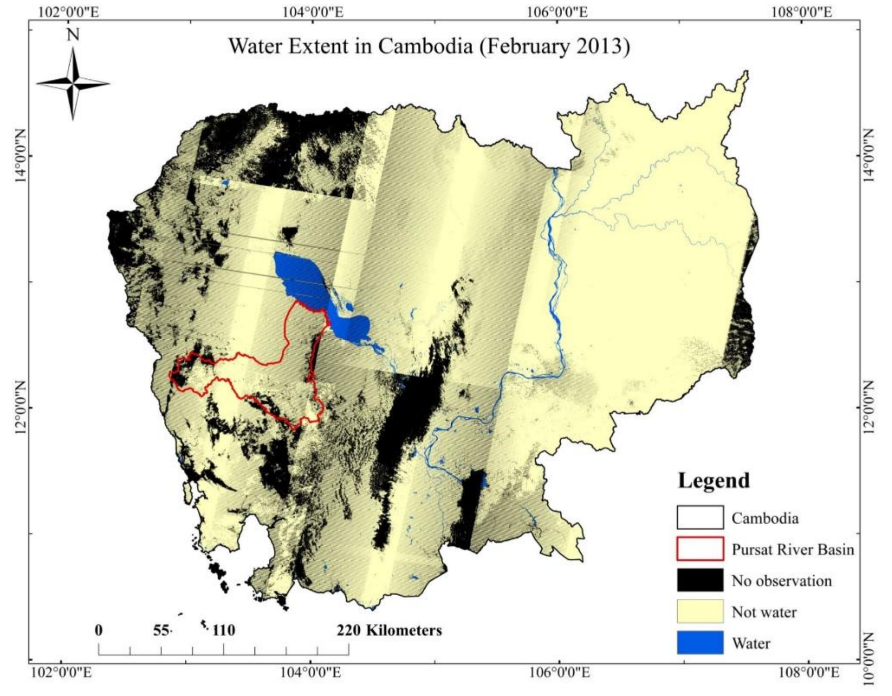

<table>
<tr>
<td>March</td>
<td>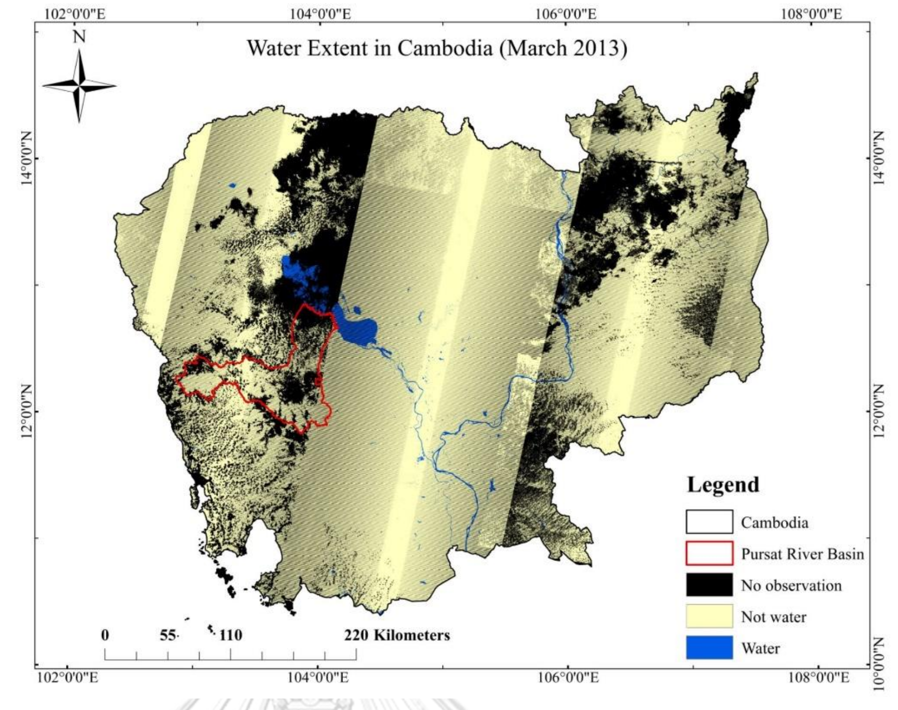
</td>
</tr>
<tr>
<td>April</td>
<td>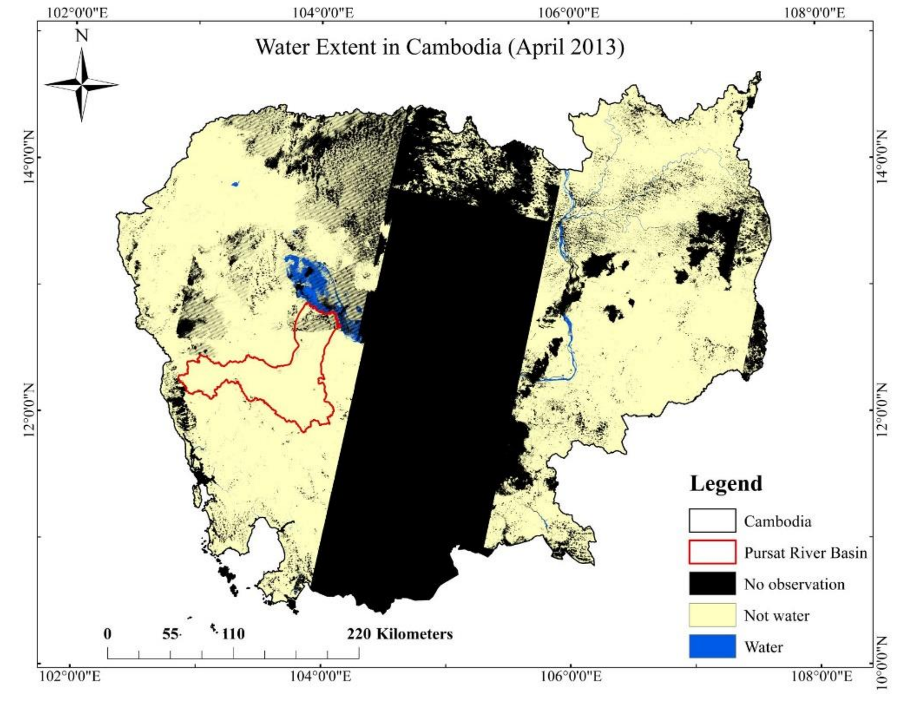
</td>
</tr>
</table>

May	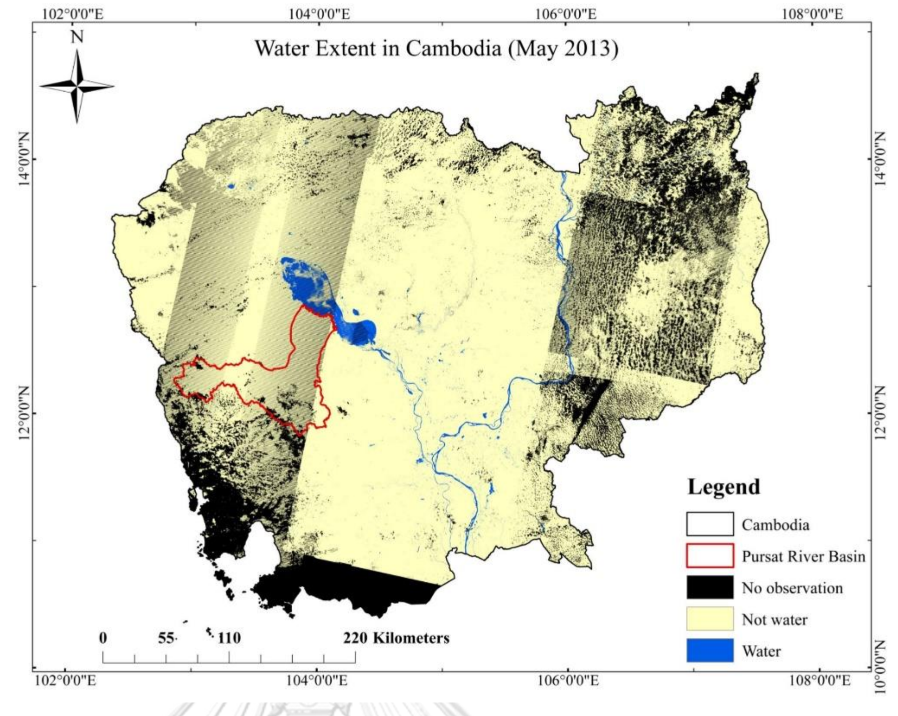 Water Extent in Cambodia (May 2013) N 102°0'0"E 104°0'0"E 106°0'0"E 108°0'0"E 14°0'0"N 12°0'0"N 10°0'0"N Legend Cambodia Pursat River Basin No observation Not water Water 0 55 110 220 Kilometers
June	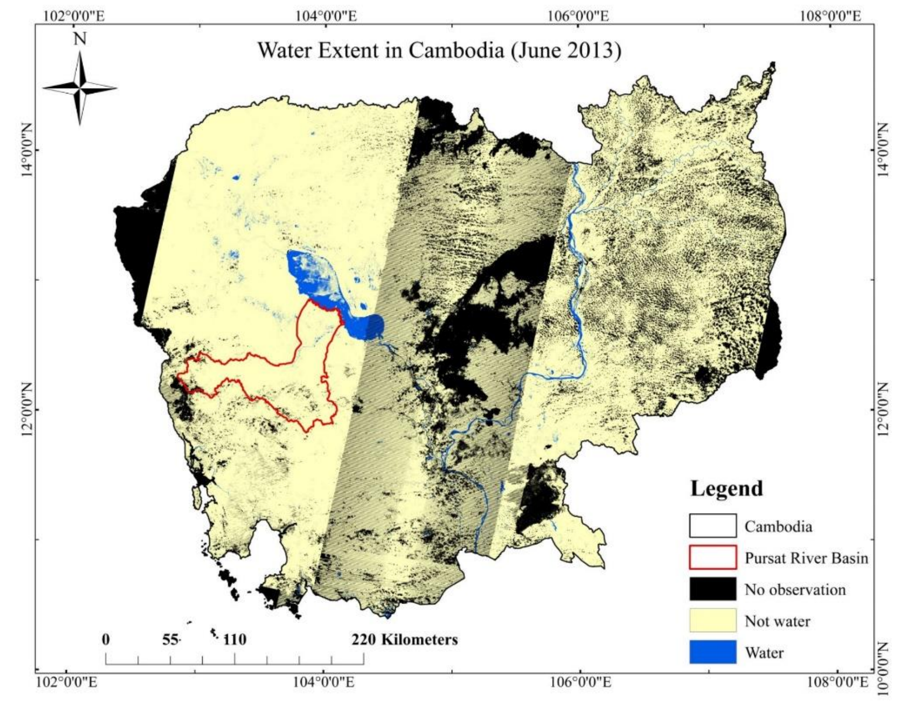 Water Extent in Cambodia (June 2013) N 102°0'0"E 104°0'0"E 106°0'0"E 108°0'0"E 14°0'0"N 12°0'0"N 10°0'0"N Legend Cambodia Pursat River Basin No observation Not water Water 0 55 110 220 Kilometers

July	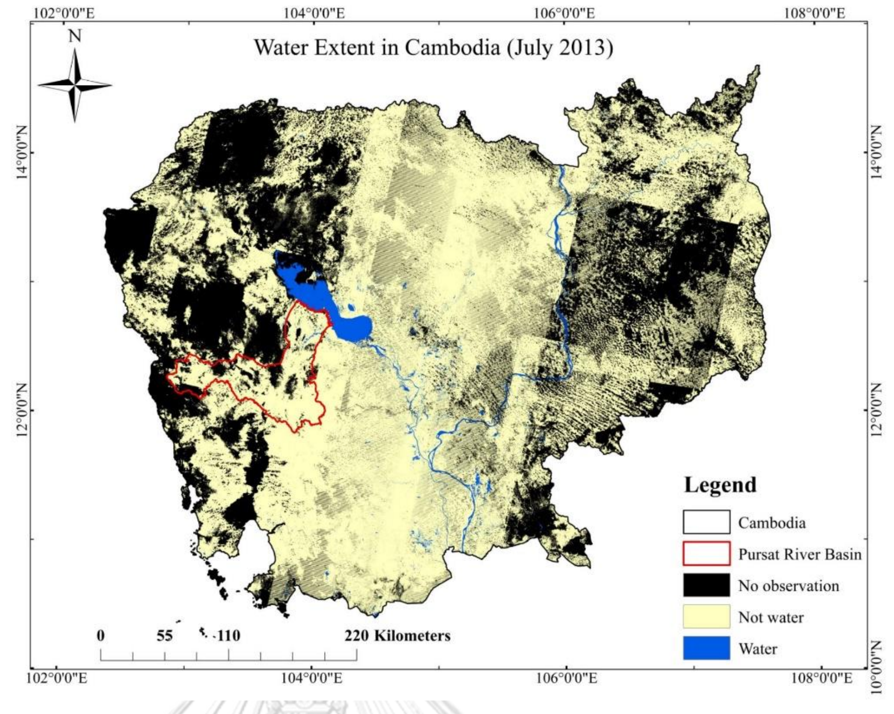Water Extent in Cambodia (July 2013) N 102°0'0"E 104°0'0"E 106°0'0"E 108°0'0"E 14°0'0"N 12°0'0"N 10°0'0"N Legend Cambodia Pursat River Basin No observation Not water Water 0 55 110 220 Kilometers
August	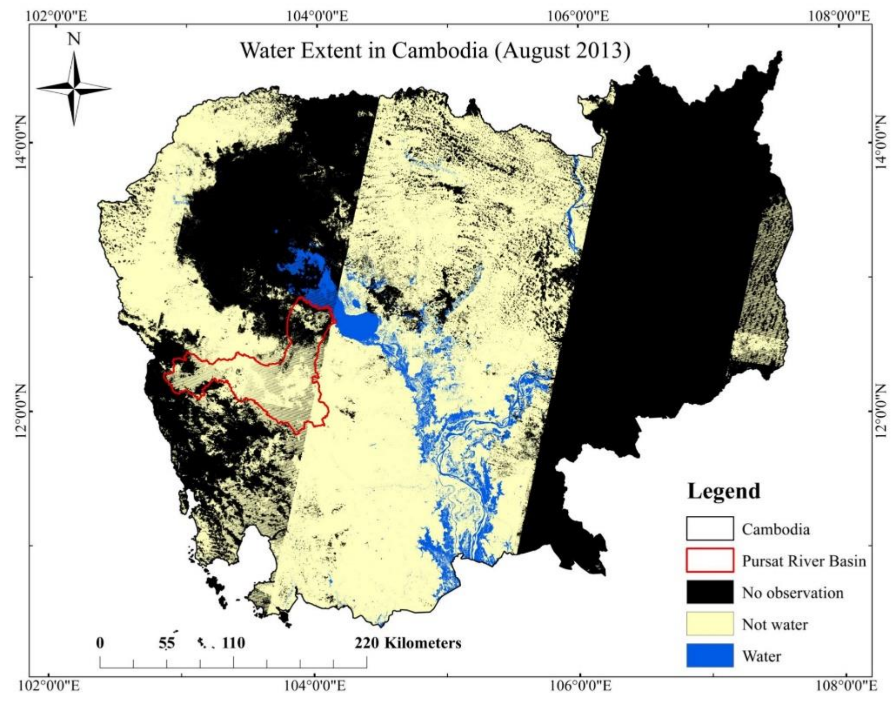Water Extent in Cambodia (August 2013) N 102°0'0"E 104°0'0"E 106°0'0"E 108°0'0"E 14°0'0"N 12°0'0"N Legend Cambodia Pursat River Basin No observation Not water Water 0 55 110 220 Kilometers

September	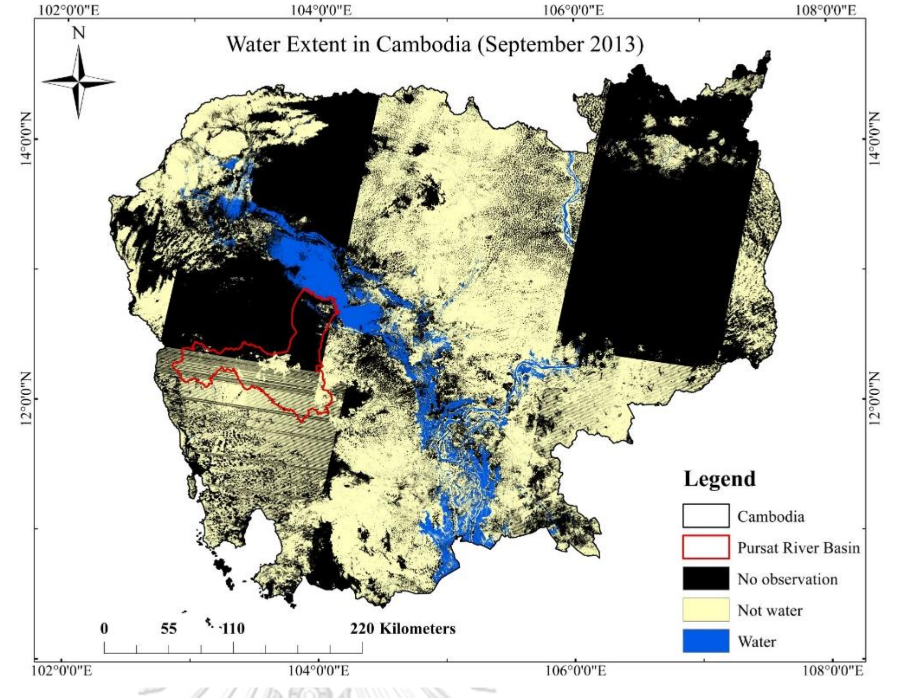
October	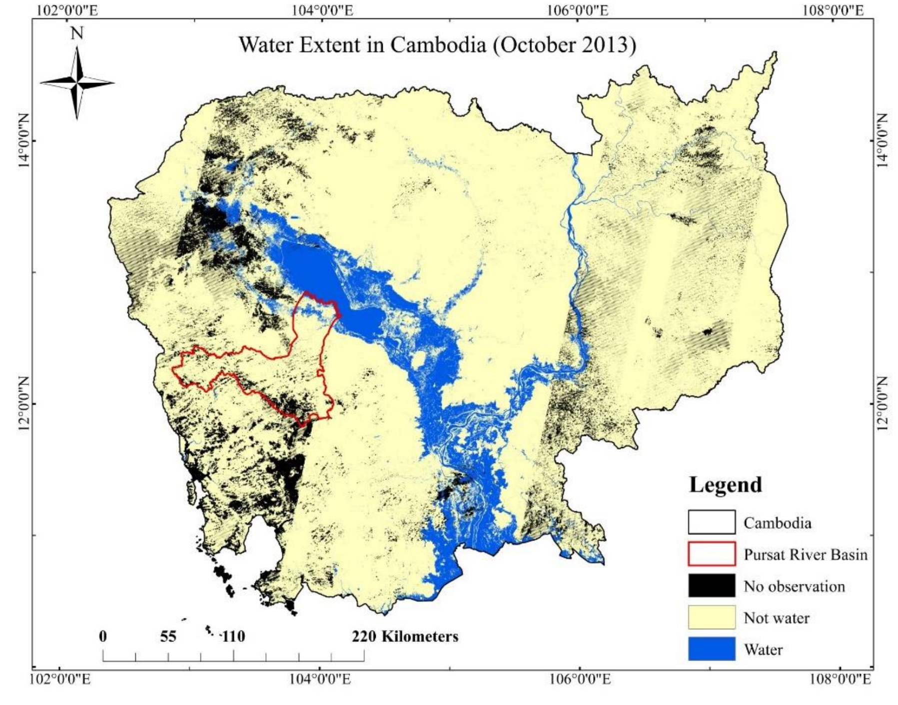

November	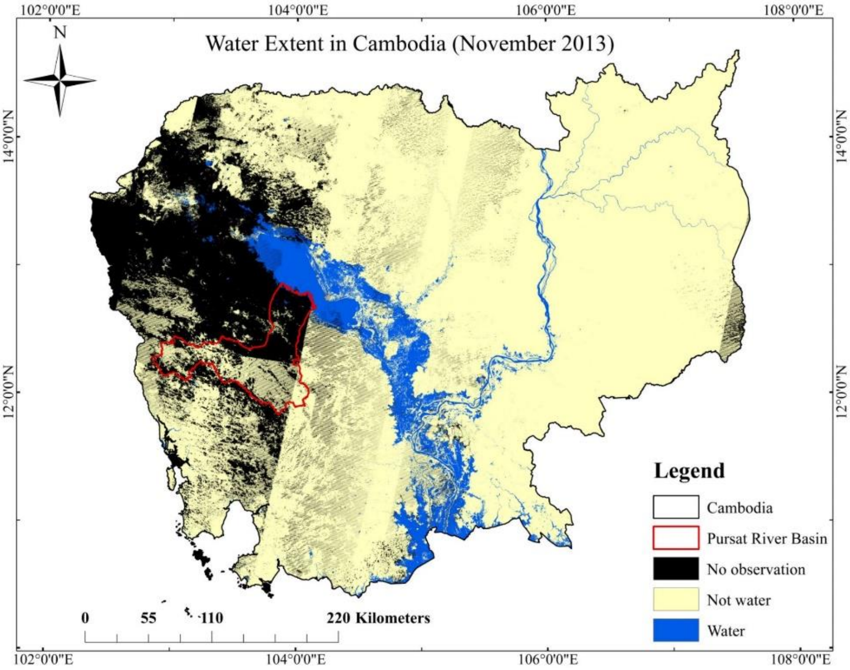
December	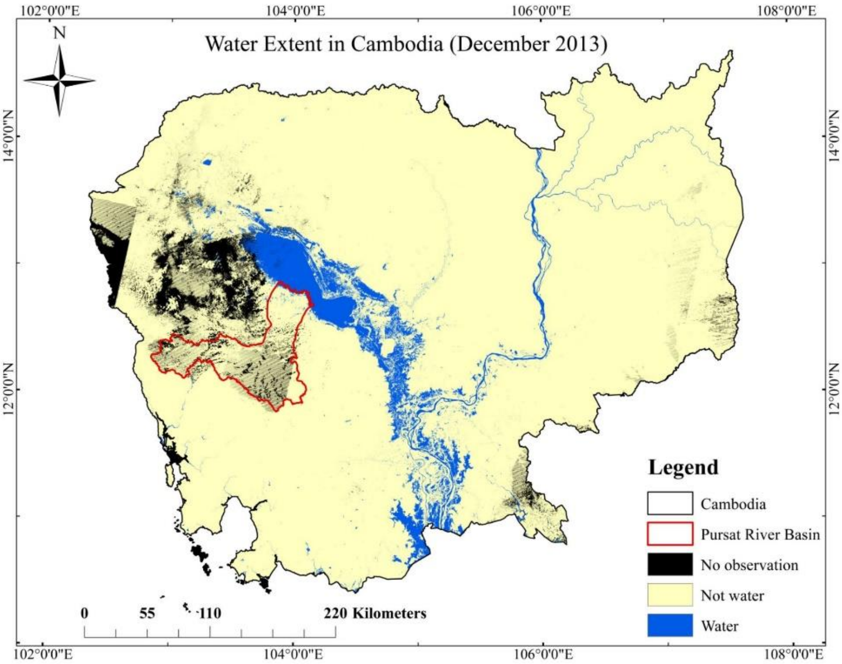

APPENDIX C: Water Extent Area

APPENDIX C1: Water Extent Area in Pursat River Basin

N	Image ID	Maximum Monthly Water Level (m.AMSL)	Water Extent Area (km^2)
1	IC_200003	21.75	1.87
2	IC_200008	24.19	188.27
3	IC_200011	24.53	171.32
4	IC_200012	22.51	57.30
5	IC_200201	21.56	25.54
6	IC_200203	21.32	1.78
7	IC_200204	21.75	1.74
8	IC_200209	23.38	194.51
9	IC_200211	23.24	148.90
10	IC_200212	22.05	58.21
11	IC_200301	21.71	18.47
12	IC_200302	22.24	2.28
13	IC_200303	22.25	2.74
14	IC_200304	22.10	12.86
15	IC_200308	25.08	15.35
16	IC_200310	27.18	66.30
17	IC_200311	22.88	44.35
18	IC_200312	21.78	25.37
22	IC_200504	21.26	1.24
23	IC_200505	22.03	1.63
24	IC_200506	22.57	4.39
25	IC_200508	25.53	67.90
26	IC_200509	23.95	125.27
27	IC_200511	24.21	126.51
28	IC_200512	21.95	40.09
29	IC_200601	21.47	36.92
30	IC_200602	21.15	19.82
31	IC_200604	22.85	5.66
32	IC_200605	23.15	3.37
33	IC_200606	23.02	8.08
34	IC_200607	25.70	30.99
35	IC_200609	24.79	97.10
36	IC_200610	24.63	192.08
37	IC_200611	21.99	113.51
38	IC_200612	21.48	56.44
39	IC_200701	21.30	30.83
40	IC_200702	21.17	21.16
41	IC_200703	21.35	8.32
42	IC_200704	21.40	3.22
43	IC_200705	23.26	30.80
44	IC_200706	24.73	19.70
45	IC_200707	25.42	9.77
46	IC_200708	23.70	16.83
47	IC_200711	23.22	101.41
48	IC_200712	21.81	25.51

49	IC_200801	21.41	23.30
50	IC_200802	21.00	5.56
51	IC_200803	22.73	2.63
52	IC_200804	24.14	2.63
53	IC_200805	25.37	17.25
54	IC_200807	23.68	11.24
55	IC_200808	24.75	56.87
56	IC_200812	22.56	55.14
57	IC_200901	22.28	30.78
58	IC_200902	21.13	12.40
59	IC_200903	21.09	9.20
60	IC_200904	23.67	0.38
61	IC_200905	24.21	14.31
62	IC_200906	23.99	11.79
63	IC_200911	22.82	127.41
64	IC_200912	21.30	33.01
65	IC_201001	21.31	7.96
66	IC_201002	21.12	13.97
67	IC_201003	21.60	3.85
68	IC_201004	21.36	3.66
69	IC_201005	21.44	1.91
70	IC_201007	22.88	10.80
71	IC_201009	26.04	65.04
72	IC_201010	26.73	56.04
73	IC_201012	21.74	23.21
74	IC_201101	21.34	12.76
75	IC_201102	21.12	7.31
76	IC_201103	21.95	8.04
77	IC_201107	22.87	5.20
78	IC_201108	23.95	82.92
79	IC_201110	26.44	190.84
80	IC_201111	22.55	263.34
81	IC_201201	21.41	52.75
82	IC_201207	22.84	12.45
83	IC_201210	26.75	79.44
84	IC_201211	24.14	54.86
85	IC_201301	21.21	4.08
86	IC_201306	24.43	24.97
87	IC_201307	23.96	32.93
88	IC_201309	24.19	66.44
89	IC_201310	26.73	244.71
90	IC_201312	22.17	109.57
91	IC_201401	21.38	59.96
92	IC_201403	20.97	6.27
93	IC_201404	21.35	7.18
94	IC_201405	23.12	5.70
95	IC_201406	23.36	5.04
96	IC_201410	24.96	80.75
97	IC_201412	22.02	4.53

Note: IC_201412 means Image Cambodia in December 2014

APPENDIX C2: Water Extent in Bakan and Phnom Kravanh districts

N	Image ID	Maximum Monthly Water Level (m.AMSL)	Water Extent Area (km^2)
1	IC_200003	21.75	0.39
2	IC_200008	24.19	166.22
3	IC_200011	24.53	150.75
4	IC_200012	22.51	79.43
5	IC_200201	21.93	45.84
6	IC_200203	22.79	0.45
7	IC_200204	21.84	0.69
8	IC_200209	24.16	181.64
9	IC_200211	23.38	135.00
10	IC_200212	21.86	80.07
11	IC_200301	21.71	39.09
12	IC_200302	22.24	5.13
13	IC_200304	22.10	3.89
14	IC_200308	25.08	8.24
15	IC_200310	27.18	98.81
16	IC_200311	22.88	64.14
17	IC_200312	21.78	44.09
21	IC_200504	21.26	0.32
22	IC_200505	22.03	0.45
23	IC_200506	22.57	5.55
24	IC_200508	25.53	85.03
25	IC_200509	23.95	130.88
26	IC_200511	24.21	124.02
27	IC_200512	21.95	54.35
28	IC_200601	21.47	27.54
29	IC_200603	21.66	6.26
30	IC_200604	22.85	2.35
31	IC_200605	23.15	1.18
32	IC_200606	23.02	14.51
33	IC_200607	25.70	3.22
34	IC_200609	24.79	102.26
35	IC_200610	24.63	172.07
36	IC_200611	21.99	130.50
37	IC_200612	21.48	65.04
38	IC_200701	21.30	15.60
39	IC_200702	21.17	10.15
40	IC_200703	21.35	4.20
41	IC_200704	21.40	1.36
42	IC_200705	23.26	22.04
43	IC_200706	24.73	21.47
44	IC_200707	25.42	3.71
45	IC_200708	23.70	6.12
46	IC_200711	23.22	116.21
47	IC_200712	21.81	18.53
48	IC_200801	21.41	23.23
49	IC_200802	21.00	3.77
50	IC_200803	22.73	2.60

51	IC_200804	24.14	1.35
52	IC_200805	25.37	7.45
53	IC_200807	23.68	7.25
54	IC_200808	24.75	52.68
55	IC_200812	22.56	14.15
56	IC_200901	22.28	32.05
57	IC_200902	21.13	6.85
58	IC_200903	21.09	7.91
59	IC_200905	24.21	14.42
60	IC_200906	23.99	8.89
61	IC_200911	22.82	150.61
62	IC_200912	21.30	55.10
63	IC_201001	21.31	5.18
64	IC_201002	21.12	7.14
65	IC_201003	21.60	1.49
66	IC_201004	21.36	1.59
67	IC_201005	21.44	0.59
68	IC_201006	22.01	3.44
69	IC_201007	22.88	4.46
70	IC_201009	26.04	56.08
71	IC_201010	26.73	82.81
72	IC_201012	21.74	21.11
73	IC_201101	21.34	6.42
74	IC_201102	21.12	4.68
75	IC_201106	22.85	7.59
76	IC_201107	22.87	2.91
77	IC_201108	23.95	64.73
78	IC_201110	26.44	177.30
79	IC_201111	22.55	266.62
80	IC_201201	21.41	59.19
81	IC_201202	21.20	11.10
82	IC_201204	21.46	0.83
83	IC_201207	22.84	7.90
84	IC_201208	23.08	11.16
85	IC_201210	26.75	114.45
86	IC_201211	24.14	75.22
87	IC_201301	21.21	1.58
88	IC_201302	21.03	0.92
89	IC_201304	22.53	1.65
90	IC_201305	21.63	0.93
91	IC_201306	24.43	23.04
92	IC_201308	24.08	6.92
93	IC_201309	24.19	62.81
94	IC_201310	26.73	237.20
95	IC_201311	26.51	37.98
96	IC_201312	22.17	110.91
97	IC_201401	21.38	64.67
98	IC_201402	21.08	8.43
99	IC_201403	20.97	1.63
100	IC_201404	21.35	3.54
101	IC_201405	23.12	3.33
102	IC_201406	23.36	2.06

103	IC_201410	24.96	121.93
104	IC_201412	22.02	1.84
105	IC_201501	21.05	5.91
106	IC_201502	20.86	0.58
107	IC_201503	20.85	0.83
108	IC_201504	20.99	1.65
109	IC_201505	21.13	1.83
110	IC_201506	23.99	0.51
111	IC_201507	21.88	2.65
112	IC_201508	22.19	15.18
113	IC_201509	25.85	44.88

Note: IC_201509 means Image Cambodia in September 2015

APPENDIX D: Normalized Difference Vegetation Index (NDVI)

APPENDIX D1: Monthly Average of NDVI (Raw Data)

Month	NDVI_2000	NDVI_2003	NDVI_2005	NDVI_2009	NDVI_2008	NDVI_2010	NDVI_2011	NDVI_2012	NDVI_2013	NDVI_2014	NDVI_2015
January		0.48	0.43	0.46	0.48	0.45	0.47	0.55	0.51	0.47	0.49
February	0.68	0.57	0.41	0.58	0.50	0.44	0.55	0.58	0.49	0.44	0.52
March	0.65	0.67	0.53	0.69	0.64	0.56	0.67	0.63	0.59	0.62	0.57
April	0.72	0.66	0.62	0.69	0.66	0.64	0.70	0.69	0.63	0.64	0.62
May	0.77	0.67	0.73	0.71	0.67	0.71	0.76	0.74	0.68	0.72	0.64
June	0.73	0.67	0.70	0.64	0.71	0.73	0.73	0.72	0.63	0.68	0.68
July	0.55	0.67	0.72	0.61	0.70	0.68	0.59	0.67	0.68	0.63	0.66
August		0.59	0.12	0.51	0.60	0.67	0.46	0.59	0.70	0.58	0.69
September	0.53	0.50	0.52	0.60	0.63	0.60	0.39	0.55	0.44	0.67	0.70
October	0.66	0.54	0.56	0.59	0.62	0.54	0.57	0.59	0.56	0.62	0.61
November	0.62	0.59	0.60	0.56	0.59	0.60	0.51	0.57	0.53	0.56	0.56
December	0.56	0.53	0.56	0.48	0.51	0.51	0.49	0.55	0.50	0.56	0.55

APPENDIX D2: Z-score of NDVI

Month	NDVI_2000	NDVI_2003	NDVI_2005	NDVI_2009	NDVI_2008	NDVI_2010	NDVI_2011	NDVI_2012	NDVI_2013	NDVI_2014	NDVI_2015
January		0.12	-1.45	-0.70	-0.05	-0.97	-0.21	2.05	1.04	-0.15	0.32
February	2.02	0.64	-1.41	0.70	-0.30	-1.07	0.27	0.69	-0.40	-1.04	-0.11
March	0.58	0.95	-1.78	1.40	0.41	-1.18	0.96	0.17	-0.58	-0.04	-0.89
April	1.68	-0.04	-1.18	0.71	-0.02	-0.49	1.19	0.94	-0.92	-0.66	-1.21
May	1.51	-1.08	0.56	0.10	-0.88	-0.01	1.19	0.69	-0.64	0.30	-1.74
June	1.06	-0.78	0.17	-1.40	0.37	1.08	1.00	0.86	-1.75	-0.32	-0.29
July	-2.01	0.39	1.36	-0.81	0.92	0.68	-1.16	0.38	0.51	-0.44	0.20
August		0.25	-2.54	-0.26	0.31	0.69	-0.55	0.23	0.87	0.15	0.85
September	-0.30	-0.60	-0.40	0.50	0.74	0.42	-1.73	-0.06	-1.28	1.18	1.54
October	1.96	-1.24	-0.74	0.01	0.80	-1.21	-0.44	0.08	-0.74	0.93	0.59
November	1.35	0.67	0.90	-0.50	0.61	0.96	-1.86	-0.09	-1.26	-0.28	-0.50
December	0.96	0.03	1.08	-1.51	-0.58	-0.63	-1.23	0.67	-0.86	1.20	0.87

APPENDIX E: Leaf Area Index (LAI)

APPENDIX E1: Monthly Average of NDVI (Raw Data)

Month	LAI_2003	LAI_2006	LAI_2007	LAI_2008	LAI_2009	LAI_2010	LAI_2011	LAI_2012	LAI_2013
January	14.91	13.64	13.83	13.27	13.25	13.19	14.24	12.88	14.65
February	15.01	14.92	15.03	12.59	14.44	14.58	13.99	14.11	15.46
March	16.89	14.25	15.47	14.47	14.06	15.48	14.16	15.92	14.55
April	18.71	16.38	13.33	14.62	15.19	13.47	13.64	15.49	10.11
May	14.42	13.88	15.39	15.48	14.22	12.34	16.33	16.69	12.44
June	15.59	12.43	16.51	11.99	17.25	14.24	12.59	11.98	13.88
July	14.65	12.03	15.61	15.22	11.32	13.21	13.10	16.90	11.27
August	14.76	10.65	11.72	14.29	13.41	12.58	12.78	14.44	14.53
September	11.31	9.92	13.64	11.25	10.97	13.41	10.09	12.18	12.33
October	11.68	14.07	10.52	13.54	11.68	13.38	10.80	14.49	13.01
November	17.04	16.72	13.92	13.42	14.64	14.65	10.97	13.84	12.03
December	15.87	14.67	13.44	11.99	13.75	12.55	10.80	16.67	10.90

APPENDIX E2: Z-Score of LAI

Month	LAI_2003	LAI_2006	LAI_2007	LAI_2008	LAI_2009	LAI_2010	LAI_2011	LAI_2012	LAI_2013
January	1.63	-0.17	0.10	-0.70	-0.73	-0.82	0.68	-1.25	1.26
February	0.65	0.55	0.68	-2.21	-0.03	0.15	-0.56	-0.41	1.18
March	1.93	-0.80	0.46	-0.58	-1.00	0.46	-0.90	0.92	-0.49
April	1.75	0.77	-0.51	0.03	0.27	-0.46	-0.38	0.40	-1.87
May	-0.10	-0.45	0.53	0.58	-0.23	-1.44	1.13	1.36	-1.38
June	0.77	-0.81	1.23	-1.03	1.60	0.09	-0.73	-1.04	-0.08
July	0.47	-0.83	0.96	0.76	-1.19	-0.25	-0.30	1.60	-1.21
August	1.07	-1.82	-1.07	0.74	0.12	-0.46	-0.32	0.84	0.90
September	-0.27	-1.33	1.49	-0.32	-0.53	1.31	-1.20	0.38	0.50
October	-0.62	1.04	-1.43	0.67	-0.62	0.56	-1.23	1.33	0.30
November	1.48	1.32	-0.11	-0.36	0.26	0.26	-1.62	-0.15	-1.08
December	1.19	0.61	0.01	-0.68	0.17	-0.41	-1.26	1.58	-1.21

APPENDIX F: Cambodia Nighttime Light Index in 2013

FID	Province	Area (km^2)	Population (head)	Population Density	Area_NLI (km^2)	Area*NLI (km^2)	Average NLI	Average DN
0	Banteay Mean Chey	6679	776051	116	6233	27666	4.44	6.62
1	Battambang	11702	1170748	100	12211	53457	4.38	6.08
2	Kompot	4873	618851	127	4776	21322	4.46	6.01
3	Kampong Cham	4549	990579	218	4558	19557	4.29	6.29
4	Kampong Chhnang	5521	527991	96	5445	21339	3.92	4.17
5	Kampong Speu	7017	783333	112	6892	34248	4.97	6.07
6	Kampong Thom	13814	677340	49	12934	54277	4.20	5.67
7	Kandal	3568	1443102	404	3647	22909	6.28	11.88
8	Koh Kong	11160	141110	13	12372	47773	3.86	4.84
9	Kep	336	42838	127	151	674	4.46	6.69
10	Kratie	11094	363883	33	12186	73102	6.00	8.98
11	Krong Pailin	803	97360	121	1105	4843	4.38	6.21
12	Krong Preah Sihanouk	868	260034	300	1423	7219	5.07	11.31
13	Mondol Kiri	14288	75615	5	13856	78372	5.66	6.57
14	Oddar Mean Chey	6158	235897	38	5241	25127	4.79	5.80
15	Phnom Penh	678	1704071	2513	419	15226	36.34	31.05
16	Pursat	12692	436202	34	12543	52626	4.20	4.99
17	Preah Vihear	13788	191104	14	14143	64841	4.58	6.13
18	Prey Veng	4883	981199	201	4789	19627	4.10	4.64
19	Ratanakiri	10782	172901	16	11956	66098	5.53	7.68
20	Siem Reap	10299	1048281	102	13067	62687	4.80	8.76
21	Steung Treng	11092	127681	12	12112	56416	4.66	6.04
22	Svay Rieng	2966	502287	169	2890	13589	4.70	7.60
23	Takeo	3563	881157	247	3519	15060	4.28	5.83
24	Tbong Khmum	4928	754000	153	4989	21827	4.38	5.07

APPENDIX G: Extreme Value Distributions at Bak Trakoun Flow Station

Year	Rank (m)	Plotting Position	Tr	Observed	Gumbel	Frechet	Log Pearson III
1999	1	0.04	24.00	1394	1365	1696	1356
1996	2	0.08	12.00	1263	1198	1328	1222
2000	3	0.13	8.00	1091	1098	1146	1134
2012	4	0.17	6.00	1007	1025	1030	1066
2013	5	0.21	4.80	1002	967	946	1010
2010	6	0.25	4.00	1001	918	881	960
2003	7	0.29	3.43	981	876	828	916
2016	8	0.33	3.00	961	838	783	875
2011	9	0.38	2.67	911	804	745	837
1995	10	0.42	2.40	908	772	710	801
2017	11	0.46	2.18	753	741	680	767
2015	12	0.50	2.00	739	713	652	734
2006	13	0.54	1.85	696	685	626	701
2009	14	0.58	1.71	608	658	602	669
2005	15	0.63	1.60	598	632	579	637
2001	16	0.67	1.50	537	605	557	605
2007	17	0.71	1.41	526	578	535	573
2008	18	0.75	1.33	515	551	514	539
2014	19	0.79	1.26	513	522	493	505
2002	20	0.83	1.20	508	491	471	467
1998	21	0.88	1.14	435	456	447	427
2018	22	0.92	1.09	354	414	421	380
1994	23	0.96	1.04	224	357	387	320

VITA

NAME	Mr. Chhunleang Rorm
DATE OF BIRTH	05 April 1993
PLACE OF BIRTH	Banteay Meanchey Province, Cambodia
INSTITUTIONS ATTENDED	Institute of Technology of Cambodia (ITC)
HOME ADDRESS	Mongkulborey District, Banteay Meanchey Province, Cambodia